

University of Southampton Research Repository ePrints Soton

Copyright © and Moral Rights for this thesis are retained by the author and/or other copyright owners. A copy can be downloaded for personal non-commercial research or study, without prior permission or charge. This thesis cannot be reproduced or quoted extensively from without first obtaining permission in writing from the copyright holder/s. The content must not be changed in any way or sold commercially in any format or medium without the formal permission of the copyright holders.

When referring to this work, full bibliographic details including the author, title, awarding institution and date of the thesis must be given e.g.

AUTHOR (year of submission) "Full thesis title", University of Southampton, name of the University School or Department, PhD Thesis, pagination

UNIVERSITY OF SOUTHAMPTON

FACULTY OF NATURAL AND ENVIRONMENTAL SCIENCES

Centre for Biological Sciences

**Delineation of a gut brain axis that regulates context-dependent
feeding behaviour of the nematode *Caenorhabditis elegans***

by

Nicolas Dallièrè

Thesis for the degree of Doctor of Philosophy

December 2015

UNIVERSITY OF SOUTHAMPTON

ABSTRACT

FACULTY OF NATURAL AND ENVIRONMENTAL SCIENCE

Centre for Biological Science

Thesis for the degree of Doctor of Philosophy

DELINEATION OF A GUT BRAIN AXIS THAT REGULATES CONTEXT-DEPENDENT FEEDING BEHAVIOUR OF THE NEMATODE

CAENORHABDITIS ELEGANS

Nicolas Dallièrè

Food directed behaviours execute key aspects of an animal's ability to maintain a balanced energy intake. This homeostasis needs to integrate external cues that define the source and suitability of food and metabolic states that define requirements for food. In a human context, impairments in the mechanisms underlying feeding behaviours may result in maladapted responses that eventually lead to obesity and other metabolic diseases (e.g. bulimia and anorexia nervosa). Given the fundamental nature of this animal behaviour, simple invertebrate models can provide a route to facilitate understanding in higher animals and humans.

In this study, the adaptive behavioural response of the nematode *C. elegans* to food is used to investigate the fundamental mechanisms underlying feeding behaviour. This utilized the behavioural transition of the worm's feeding organ, the pharynx, during presentation and removal of food. Feeding behaviour was assayed in intact worms by counting the contraction-relaxation cycles of the pharynx. On food this shows a high pumping rate of around 250 pump.min⁻¹ (ppm). In contrast, when transferred onto a no food arena, the pumping rate is reduced to almost zero. Subsequently, in the absence of food, the worms display a two phase adaptive pumping behaviour. The first 'early phase' has a slow increase of pumping rate up to ~30-40 ppm followed by a 'late phase' where the pumping rate becomes highly variable, fluctuating from very low (0-10 ppm) to high (100-150 ppm) values, and lasts at least up to 8 hours following the initial removal of food.

Using this paradigm, I demonstrated that pumping behaviours were more than a simple ON/OFF switch but instead actively modulated by distinct neuronal circuits depending on the food context. Both non-peptidergic transmitters and neuropeptides are involved in the control of this adaptive response in a complex manner with the manner of regulation depending on the food context. For example, glutamate signalling stimulates pumping 'on' food while acting to reduce pumping in its absence. On food, the neurons M3 are known to increase the pumping rate via the release of glutamate. In this thesis, I have shown that a significant part of the glutamate associated with glutamatergic inhibitory tone in response to food removal is released from the pharyngeal neurons I2 and acts through the AVR-14 glutamate-gated chloride channel. In keeping with this, RIP ablation, the sole physical link between the

pharyngeal and central nervous system, shows no aberrant pumping behaviours, suggesting an important role for the worm's enteric system.

Genetic and environmental manipulation of sensory structures was used to address the modalities mediating the pumping behaviours. This analysis revealed that specific sensory structures and pathways are utilized in the distinct 'on' and 'off' food context. Strikingly, perception of odours from food by chemosensory neurons of the central nervous system does not contribute to the pumping rate as mutants in which the sensory functions of these neurons are deficient show no aberrant pumping behaviour in the presence of food. Rather mechanical cues seem important. The same chemosensory mutants show pumping rates off food that indicate they do not perceive food removal. This contrasts with the observation highlighted by RIP ablation and indicates that extrapharyngeal structures are involved but must be utilizing volume transmission.

Investigation of the role of neurohormonal signalling was assessed by analysis of neuropeptide deficient and synaptic protein mutants. In *egl-3* the pumping rate is totally abolished during food-deprivation. In contrast, *unc-31* showed an elevated pumping rate 'off' food. These results suggest that neuropeptide signalling is required both to maintain the low level of pumping and to reduce it in the absence of food. Investigation of the role of individual neuropeptides supports the above. Interestingly both pharyngeally and extrapharyngeally expressed peptides support these phenotypes, consistent with a model in which food signals, involving discrete enteric and central nervous system, regulate the worm's feeding behaviours.

Overall, this thesis provides new insight into the neural substrates of behavioural plasticity in *C. elegans*. It shows that even a simple nematode with a nervous system of 302 neurons can show complex regulation of feeding behaviours, involving multiple pathways, which conceptually resonates with higher organisms' organisation.

Table of Contents

ABSTRACT.....	i
Table of Contents.....	iii
List of tables	xiii
List of figures	xv
DECLARATION OF AUTHORSHIP.....	xxi
Acknowledgements.....	xxiii
Definitions and Abbreviations	xxv
Chapter 1: General Introduction	1
1.1. <i>Caenorhabditis elegans</i> a model organism to study feeding behaviour.....	1
1.1.1. Introduction to <i>C. elegans</i>	1
1.1.2 Nervous system.....	6
1.2 Feeding behaviours	24
1.2.1 Locomotion.....	26
1.2.2 Pharyngeal pumping.....	33
1.3 Neuronal regulation of the feeding behaviours.....	40
1.3.1 Neurotransmitter.....	40
1.3.2 Neuropeptides/neurohormonal regulation of feeding behaviours	51
1.3.3 Neuropeptide receptors' role in feeding behaviours	54
1.4 Energy storage, metabolism and nutritional status	60
1.4.1 Energy metabolism.....	60
1.4.2 Regulation of fat stores in <i>C. elegans</i>	70
1.4.3 Nutritional status and feeding behaviour	80
Aims	84

Chapter 2: Materials and Methods	85
2.1 Strains used	85
2.2 <i>C. elegans</i> maintenance	87
2.2.1 Culturing <i>C. elegans</i>	87
2.2.2 Longer storage of <i>C. elegans</i>	87
2.3 Solution recipes	88
2.3.1 NGM (Nematode Growth Medium)	88
2.3.2 M9 Buffer	88
2.3.3 Freezing Buffer	88
2.3.4 Lysis buffer	89
2.3.5 S-basal	89
2.3.6 LB (Luria-Bertani) broth and agar	89
2.3.7 PBS (Phosphate Buffered Saline)	90
2.4 Behavioural assays	90
2.4.1 Measuring pharyngeal pumping in the presence and absence of food	90
2.4.2 Local Search Area assay	91
2.4.3 Re-entry on food	91
2.4.4 Pumping behaviour in the presence of polystyrene microspheres	91
2.4.5 Statistical analysis	92
2.5 Microinjection of <i>C. elegans</i>	93
2.6 Laser microsurgery of <i>C. elegans</i>	94
2.6.1 Microsurgery equipment	94
2.6.2 Worm preparation	94
2.6.3 Ablation	94
2.6.4 Confirmation of the ablation	95
2.7 Optogenetics	95
2.7.1 Retinal plates preparation	95

2.7.2	Pharyngeal pumping under the influence of optogenetic stimulation of glutamatergic neurons	95
2.8	Calcium Imaging	96
2.9	Pharynx dissection	96
2.10	Dil staining.....	97
2.11	Sudan Black staining.....	97
2.12	Solid-state Nuclear Magnetic Resonance (NMR).....	98
2.12.1	Sample preparation:	99
2.12.2	Sample processing and data analysis	100
2.13	Coherent Anti-stokes Raman Spectroscopy (CARS) microscopy	100
2.13.1	Sample preparation	100
2.13.2	Mounting	101
2.13.3	CARS imaging methodology.....	101
2.13.4	Imaging and data analysis	102
2.13.5	Statistical analysis	103
2.14	<i>eat-4 (ky5); Ex[Pflp-15::ChR2;YFP]</i> mutant strain generation by crossing	103
2.14.1	Male generation	103
2.14.2	Cross	104
2.14.3	Genotyping by single worm PCR	104
2.15	Molecular Biology	106
2.15.1	Generation of the construct <i>Peat-4::eat-4</i>	106
2.15.2	Generation of the <i>Pmyo-2::npr-3</i> expression construct	113
Chapter 3:	Development of “on” and “off” food paradigms to identify complex regulation of feeding behaviour in <i>C. elegans</i>.....	121
3.1	Introduction	121
3.2	Results	123
3.2.1	Food deprivation leads to reduction of the pharyngeal pumping rate in two distinct phases	123

3.2.2	ACh, glutamate and 5-HT food-dependent modulation of the pumping behaviour	125
3.2.3	GABA and dopamine promote pumping during food deprivation	128
3.2.4	<i>unc-31</i> pumps constitutively throughout food deprivation	131
3.2.5	Neuropeptide signalling acts to maintain a slow pumping rate in the absence of food.....	132
3.2.6	Two parallel pathways fine-tune feeding behaviour in the absence of food	135
3.2.7	Laser ablation that disconnects the pharyngeal nervous system from the extrapharyngeal nervous system does not affect pharyngeal pumping.....	139
3.3	Discussion	141
3.3.1	An adaptive pumping behaviour in the absence of food	141
3.3.2	Inhibitory and excitatory pathways fine tune the pumping behaviour off food	142
3.3.3	UNC-31 and EAT-4 are the main determinants of the reduction of the pumping rate observed in absence of food.....	144
3.3.4	Neuropeptide-dependent maintenance of a basal pumping rate in absence of food.....	145
3.3.5	Role of the transmitters ACh, 5-HT, GABA and dopamine in the control of the pumping behaviour both on and off food.....	145
3.3.6	Biogenic amine transmitters tyramine and octopamine do not regulate the pumping behaviour in this paradigm. 147	
3.4	Conclusion.....	148

Chapter 4: Revealing and characterising the context-dependent regulation of pharyngeal pumping by the enteric glutamatergic neurons I2	151
4.1 Introduction	151
4.1.1 Ionotropic receptors (iGluR)	152
4.1.2 Glutamate-gated chloride channels (GluCl)	153
4.1.3 Metabotropic glutamate receptors (MGL)	154
4.2 Results	157
4.2.1 Pharyngeal response to food removal is dependent on glutamate signalling	157
4.2.2 Light induced glutamatergic neurons activity decrease the pumping rate in the presence but not in the absence of food	160
4.2.3 Glutamate released upon food removal does not act directly onto the pharynx muscles	164
4.2.4 Ionotropic glutamate-gated receptors (iGluRs) do not modulate the pumping behaviour	167
4.2.5 Investigation of metabotropic glutamate receptors (MGLs) revealed a role for MGL-2 in the control of the pumping rate on food	168
4.2.6 Glutamate-gated chloride-channel <i>avr-14</i> acts to reduce the pumping rate in response to food removal	170
4.2.7 <i>avr-14</i> expression pattern investigation reveals expression in the pharyngeal nervous system	172
4.2.8 M3 motorneurons modulate the pumping rate in presence of food but not in its absence	175
4.2.9 Pharyngeal glutamatergic neuron I2 is a major determinant of the pumping behaviour off food but is not involved in the pumping regulation on food	177

4.2.10	I2 acts to reduce the pumping rate in an off food context via both glutamate- dependent and independent pathways	182
4.2.11	Gap junction communication between neurons appears to play a role in the regulation of the pumping rate in the absence of food	183
4.3	Discussion	185
4.3.1	M3 and I2 neurons are selectively recruited depending on the food context	185
4.3.2	Glutamate receptors drive the food context dependent pumping behaviours	186
4.3.3	Wider roles of I2 and downstream mediators	188
4.4	Conclusion	189
Chapter 5: Neuropeptide modulation of context-dependent pharyngeal behaviour		193
5.1	Introduction	193
5.2	Results	195
5.2.1	Approach 1: the proprotein (<i>kpc</i>) convertase family	195
5.2.2	Approach 2: neuropeptide receptor mutants screen....	199
5.2.3	Approach 3: selection of peptides inducing stimulation when exogenously added	207
5.2.4	Individual candidate neuropeptides appear to have opposite roles on the pumping behaviour.....	209
5.2.5	<i>npr-3</i> rescue in pharyngeal muscle	215
5.3	Discussion	216
5.3.1	Neuropeptides exhibiting a stimulatory effect on the pumping rate off food	221
5.3.2	Neuropeptides mediating the reduction of the pumping rate in absence of food.....	226

5.3.3	Neuropeptides modulating the high pumping rate in response to food	228
5.4	Conclusion	229
Chapter 6:	Investigation of the sensory modalities that modulate the food-dependence of pumping behaviour	231
6.1	Introduction	231
6.2	Results	233
6.2.1	The role of ciliated sensory neurons in the regulation of pumping off food suggests central integration of the response to the absence of food	233
6.2.2	No ciliated neurons are observed in the pharyngeal nervous system	236
6.2.3	Cell specific restoration of glutamate transmission in the AWC sensory neurons is not sufficient to rescue the <i>eat-4</i> mutant aberrant pumping behaviour off food	238
6.2.4	Glutamatergic thermo/CO ₂ sensory neuron AFD modulates the pumping behaviour off food	241
6.2.5	Physical contact with food is required to increase the pumping rate	244
6.2.6	Dopaminergic signalling is not required for the high pumping rate observed upon contact with food	246
6.2.7	Mechanosensory cues trigger a burst in pumping rate	246
6.2.8	Prolonged exposure to beads increases the pumping rate	251
6.2.9	Increase of pumping rate in response to prolonged exposure to beads is dependent on 5-HT signalling	253
6.3	Discussion.....	253
6.3.1	Pharyngeal pumping rate is reduced in response to the absence of bacterially derived chemosensory stimulation	253

6.3.2	The rate of pumping as the worm enters a bacterial lawn	255
6.3.3	Glutamate transmission from AWC neurons is not sufficient to modulate the pumping rate.....	255
6.3.4	Glutamate signalling in the central nervous system from AFD sensory neurons modulates pumping behaviour on and off food.....	256
6.3.5	Physical contact with food increases the pharyngeal pumping rate in a dopamine-independent fashion	257
6.3.6	Mechanosensory cues in the pharynx increase the pumping rate in a 5-HT-dependent fashion	258
6.4	Conclusion.....	261
Chapter 7: Nutritional status and pumping behaviour in response to food-deprivation.....		263
7.1	Introduction.....	263
7.2	Results.....	265
7.2.1	Lipids consumption during food deprivation.....	265
7.2.2	Metabolomic approach in <i>C. elegans</i> by Nuclear Magnetic Resonance showed a marked reduction of lipid stores after 2hours of food deprivation.....	268
7.2.3	Coherent anti-Stokes Raman scattering (CARS) imaging of <i>C. elegans</i> lipid stores	272
7.3	Discussion	277
7.3.1	NMR-based metabolomic analysis revealed potential reduction of carbohydrates and lipids during the first 2 hours of food-deprivation.....	277
7.3.2	CARS-based lipid imaging validates and refines previous findings to show significant reduction of lipid stores after 30 min off food.....	279
7.3.3	Correlation between timing of changes in nutritional status and adaptive feeding behaviours	280

7.4 Conclusion	281
Chapter 8: General discussion	285
8.1 Conceptually conserved mechanisms regulating feeding behaviours	286
8.2 Evidence for an autonomic regulation of the pumping behaviours	289
8.3 Pumping behaviours are polymodal	292
8.4 Chain of event: Transition from no food to food.....	295
List of References	299

List of tables

Table 1: Enzymatic digestion using EcoRI and Aval.	117
Table 2: <i>Pmyo-2::npr-3</i> digestion with Aval.....	119
Table 3: Expression pattern and known ligands of neuropeptides Y-like receptors involved in the regulation of the pumping phenotype.	207
Table 4: Summary of the effects of exogenously added neuropeptides on the pumping rate of isolated pharynxes.....	208
Table 5: Comparison of the effects of neuropeptides on the pharyngeal pumping activity of isolated pharynxes and their role on pumping behaviours.	220
Table 6: Expression pattern and pumping phenotypes of the candidate <i>flp</i> mutants assessed.	222

List of figures

Figure 1: <i>Caenorhabditis elegans</i> lifecycle at 20° C.	3
Figure 2: Schematic representation of the main characteristics of the <i>C. elegans</i> nervous system.....	8
Figure 3: Sensory neurons in <i>C. elegans</i>	10
Figure 4: Cartoon representation of the main classical neurotransmitter pathways found in <i>C. elegans</i>	13
Figure 5: The coelomocytes take up neuropeptides from the pseudocoelomic fluid by phagocytosis.....	15
Figure 6: Structural representation of the kex-2/subtilisin-like proprotein convertase (kpc) family.	18
Figure 7: <i>Caenorhabditis elegans</i> neuropeptide processing pathway.....	20
Figure 8: Simplified cartoon of postsynaptic signal transduction.	24
Figure 9: <i>C. elegans</i> reversals, omega turn and head oscillations patterns.	27
Figure 10: Schematic model illustrating the disinhibitory and stimulatory circuits.	29
Figure 11: Adaptive locomotory behaviour in response to food withdrawal....	31
Figure 12: Food motion during pharyngeal pumping.	35
Figure 13: The main neural components of the pharyngeal nervous system...	38
Figure 14: Simplified summary of GPCR type receptors found in <i>C. elegans</i> organised according to the GRAFS classification.....	56
Figure 15: Summary of metabolism and ATP production.....	63
Figure 16: Cartoons of the major conserved pathways of intermediary metabolism in <i>C. elegans</i> and of the Glyoxylate cycle.....	67
Figure 17: DAF-7/TGF- β ligand regulates feeding, development and fat storage via distinct pathways.....	76
Figure 18: Unprocessed CARS image of the head region of a well-fed adult worm (A) and the same image with adjusted threshold to highlight lipid stores (B).....	103
Figure 19: Restriction mapping of possible <i>eat-4</i> insert orientations.....	109
Figure 20: Restriction mapping of the <i>peat-4::eat-4</i> following recombination.112	
Figure 21: Gel electrophoresis of the amplified <i>npr-3</i> cDNA prior excision...	114
Figure 22: Verification of the <i>npr-3</i> cDNA insertion in the TOPO vector by gel electrophoresis:	116

Figure 23: Restriction mapping of possible <i>npr-3</i> insert orientations	117
Figure 24: Restriction mapping of the pENTR_ <i>npr-3</i> following TOPO ligation.	118
Figure 25: Restriction mapping of the <i>pmyo-2::npr-3</i> following recombination.	120
Figure 26: Modulation of pharyngeal pumping on and off an <i>E. coli</i> OP50 food source.....	124
Figure 27: Comparison of the role played by major pharyngeal transmitters acetylcholine, glutamate and 5-HT to the pharyngeal pumping rate on and off food.....	127
Figure 28: Modulation of pharyngeal pumping by major neurotransmitters that are synthesized extrinsically to the pharynx: GABA and dopamine.....	129
Figure 29: Modulation of pharyngeal pumping by major neurotransmitters that are synthesized extrinsically to the pharynx: octopamine and tyramine.	130
Figure 30: UNC-31 mediates the reduction of pumping rate observed in absence of food.	132
Figure 31: Mutants deficient in neuropeptide synthesis show a reduced pumping rate in absence of food.....	134
Figure 32: Epistatic analysis revealed <i>unc-31</i> and <i>egl-3</i> act in the same genetic pathway.	136
Figure 33: <i>eat-4(ky-5); unc-31(e169)</i> double mutant pumped at a similar rate in the presence or in the absence of food.....	138
Figure 34: Pharyngeal pumping in the presence and absence of food in RIP ablated worms.	140
Figure 35: A summary of the multiple excitatory and inhibitory neural signals that regulate feeding behaviour in the presence of food and fictive feeding during food deprivation.....	150
Figure 36: Glutamate receptors in <i>C. elegans</i>	156
Figure 37: <i>eat-4</i> -dependence of on and off food pharyngeal pumping behaviours reveals distinct context dependent regulation by glutamatergic transmission.....	159
Figure 38: Artificial activation of a glutamatergic inhibitory tone by optogenetics.....	162
Figure 39: Artificial light-activation of glutamatergic neurons can reduce the pumping rate in a glutamate-independent fashion.	163

Figure 40: A comparison of pumping behaviours on and off food in N2 and mutants deficient in pharyngeal muscle glutamate receptors.	166
Figure 41: Ionotropic glutamate receptors do not act in the modulation of the pumping behaviour.	168
Figure 42: Metabotropic glutamate receptor MGL-2 modulates the high pumping rate observed on food.	169
Figure 43: Glutamate-gated chloride channels <i>avr-14</i> mediates the reduction of the pumping rate in absence of food.	171
Figure 44: <i>avr-14</i> is widely expressed in <i>C. elegans</i> nervous system but revealed as being integral to the pharyngeal microcircuit in the isolated pharynx.	174
Figure 45: Genetic disruption of pharyngeal glutamatergic neuron M3 reveals that M3 modulates the pumping rate in presence but not in absence of food.	176
Figure 46: 12 pharyngeal neurons modulate the off food pumping behaviour via glutamate release.	178
Figure 47: Light activation of pharyngeal neurons 12 reduces the pumping rate.	180
Figure 48: Increase calcium activity observed in 12 neurons in absence of food.	182
Figure 49: UNC-7 and UNC-9 innexins mediates the reduction of the pumping rate in absence of food.	184
Figure 50: Schematic representation of the context dependent glutamate dependence of the pumping behaviour.	191
Figure 51: Schematic representation of the strategy used to narrow down the neuropeptide candidates that can modulate the worm's pumping phenotype.	195
Figure 52: Pumping off food phenotype of the <i>kpc</i> family members.	197
Figure 53: <i>flp-18</i> encoded peptides profile of the <i>kpc</i> -family mutants. Modified from <i>Husson et al. 2006</i>	199
Figure 54: Screen of neuropeptide receptor mutants for their pumping on food phenotype.	200
Figure 55: Screen of neuropeptide receptors mutants for their pumping off food phenotype.	202
Figure 56: Pumping off food phenotype of <i>npr-3</i> , <i>npr-4</i> and <i>npr-5</i> mutants.	204
Figure 57: <i>npr-1(ky13)</i> and <i>npr-9(1562)</i> mutation did not affect the PoffF phenotype.	205

Figure 58: Venn diagram representing the neuropeptide genes selected for further investigation for their role in the control of the worm's pumping behaviour.	210
Figure 59: Neuropeptide mutant strains candidate analysis of on and off food pumping phenotype.	212
Figure 60: Screen of individual neuropeptides	214
Figure 61: Specific expression of <i>npr-3</i> cDNA in the pharynx muscle.	216
Figure 62: Hypothetical model of I2 modulating both the reduction of the pumping rate and the maintenance of the basal pumping rate in absence of food.	224
Figure 63: Model of the modulation of the pumping phenotype on and off food by individual neuropeptides.	230
Figure 64: Mutations affecting cilia of sensory neurons selectively affect the pumping behaviour in absence of food.	235
Figure 65: Dil staining does not stain pharyngeal neurons.	237
Figure 66: Rescue of <i>eat-4</i> in AWC sensory neurons does not restore glutamatergic dependent regulation of pharyngeal pumping 'on' and 'off' food.	240
Figure 67: Glutamatergic neuron AFD has an opposite effect on the pumping rate in presence and in absence of food.	243
Figure 68: Pumping increase following contact with food appears not to require dopamine signalling.	245
Figure 69: Physical contact with beads triggers a transient increase of the pumping rate.	248
Figure 70: Epi-florescence microscopy images of worm fed with 0.5 μ m beads for 10 min.	250
Figure 71: High pumping rate observed after an hour in the presence of bead is 5-HT-dependent	252
Figure 72: Cartoon representation of the pharyngeal neuron NSM.	260
Figure 73: Schematic representation of the context-dependent involvement of sensory modalities in the control of the pumping behaviour.	262
Figure 74: Sudan black staining of wild type well-fed or starved worms' lipid stores.	267
Figure 75: 1H high resolution magic angle spinning whole-organism nuclear magnetic resonance (¹ H HRMAS-NMR) of wild type worms, well-fed or food deprived for 4 and 24 hours.	269

Figure 76: ¹ H high resolution magic angle spinning whole-organism nuclear magnetic resonance (¹ H HRMAS-NMR) of <i>egl-3 (ok979)</i> worms, well-fed or food deprived for 2, 4 and 24 hours.	271
Figure 77: Illustration of the 3 regions of the worm imaged with CARS.	274
Figure 78: Analysis of lipid stores in <i>C. elegans</i> during food deprivation using CARS shows significant decrease over time.	276
Figure 79: Model representing the correlation between lipid stores consumption and the switch of pumping phases in response to prolonged food-deprivation.	282
Figure 80: Schematic model of the regulation of the pumping behaviour in the presence of food.	287
Figure 81: Schematic model of the pumping off food behaviour regulation.	291
Figure 82: Simplistic representation of the quantitative effects of the main pathways modulating the reduction of the pumping rate observed in response to food removal.	294

DECLARATION OF AUTHORSHIP

I, Nicolas Dallièrè declare that this thesis and the work presented in it are my own and has been generated by me as the result of my own original research.

Delineation of a gut brain axis that regulates context-dependent feeding behaviour of the nematode *Caenorhabditis elegans*

I confirm that:

1. This work was done wholly or mainly while in candidature for a research degree at this University;
2. Where any part of this thesis has previously been submitted for a degree or any other qualification at this University or any other institution, this has been clearly stated;
3. Where I have consulted the published work of others, this is always clearly attributed;
4. Where I have quoted from the work of others, the source is always given. With the exception of such quotations, this thesis is entirely my own work;
5. I have acknowledged all main sources of help;
6. Where the thesis is based on work done by myself jointly with others, I have made clear exactly what was done by others and what I have contributed myself;
7. None of this work has been published before submission

Signed:.....

Date:.....

Acknowledgements

First, I'd like to thank Prof. Lindy Holden-Dye, Vincent O'Connor and Robert Walker for their determined supervision and support throughout my PhD, for helping directing my research on the right track, and for making these 4 years a lot easier. Thanks to Dr. Ben Mulcahy, Dr. James Dillon and Dr. Anna Crisford for sharing their valuable knowledge and helping in the lab.

Thanks to Dr. Nikhil Bhatla and to Prof. Robert Horvitz and all his lab members for welcoming me and sharing their laser ablation and calcium imaging techniques with me.

I'd like to acknowledge The Gerald Kerkut Trust for funding, making this project possible and providing their support. Thanks to the Caenorhabditis elegans Genetics Centre and the National Bioresource Project of Japan for providing worm strains.

Thanks to Lorraine Prout and the rest of the administrative staff who facilitate our research efforts.

An immense thank you to Elodie and David Stafford who kindly accommodated me during the production of this thesis.

Thanks to all my family and friends for their support and for refraining from enquiring too frequently about the advancement of this thesis. Thanks for the 'MCC' and its members for making my adaptation easier and maintaining my cheese and wine consumption to a decent level. A big thank you to the two other 'three musketeers' for everything!

Lastly, thank you to Carte Noire and Lavazza for their coffee which played a crucial part in the completion of this thesis. Thanks to Vangelis, Thom Yorke and others for their music which helped me focus on my writing.

Definitions and Abbreviations

5-HT: 5-Hydroxytryptamine

ACh: acetylcholine

AChE: ACh esterase

AChR: ACh receptor

AGRP: agouti-related peptides

ATP: adenosine tri-phosphate

BSA: bovine serum albumin

C. elegans: *Caenorhabditis elegans*

CGC: *Caenorhabditis elegans* genetics centre

DCV: dense core vesicle

DIC: differential interference contrast

DNA: deoxyribonucleic acid

E. coli: *Escherichia coli*

EM: electron microscopy

EPG: electrophoreneogram

GABA: γ -aminobutyric acid

GFP: green fluorescent protein

IGF: insulin-like growth factor

NGM: nematode growth medium

NMDA: N-methyl-D-aspartate

NMJ: neuromuscular junction

NPY: neuropeptide Y

PCR: polymerase chain reaction

POMC: pro-opiomelanocortin

PPM: pump per min

RNA: ribonucleic acid

TCA : tricarboxylic acid

UV: ultra violet

YFP: yellow fluorescent protein

Chapter 1: General Introduction

1.1. *Caenorhabditis elegans* a model organism to study feeding behaviour

Animals must balance energy intake against energy expenditure in order to thrive. To achieve this balance animals respond appropriately to changes in food availability and their nutritional status (Friedman, 2010). In mammals, distinct hypothalamic circuits respond to multiple converging signals to either increase or decrease food intake (Aponte et al., 2011). In humans, where this behaviour is influenced by complex motivational states and higher cognitive processing, there is strong evidence for a dominant role of subconscious fundamental biological processes that control eating (Friedman, 2009), and understanding these has relevance to understanding eating disorders and obesity. The complexity of the mammalian nervous system makes the deciphering of neuronal circuits involved in the regulation of behaviours extremely complicated.

In contrast to the human brain which has an estimated 86 billion neurons (Herculano-Houzel, 2012), the free living nematode *Caenorhabditis elegans* has just 302 (White *et al.*, 1986). As further detailed below, *C. elegans* displays a range of adaptive behaviours, including feeding behaviours, controlled by a relatively simple nervous system. Therefore, this animal provides a highly tractable experimental platform for temporal analysis of the neurobiological processes that control the response to food and food deprivation (Greer et al., 2008).

1.1.1. Introduction to *C. elegans*

Caenorhabditis elegans is a transparent free-living soil nematode, a roundworm, found world-wide in rotten fruit or compost (Brenner, 1974; Felix and Duvéau, 2012). Newly hatched larvae are 0.25 mm long and develop through 4 larval stages to reach 1 mm at the adult stage. The worm's life-cycle

Chapter 1

is relatively short as it takes approximately 3 days from egg to egg-laying adult (**Figure 1**). *C. elegans* is easily maintained in the laboratory using Petri dishes containing a modified agar medium, the Nematode Growth Medium (NGM), seeded with OP50 *E. coli* serving as a source of food. Moreover, *C. elegans* are self-fertilizing hermaphrodites, i.e. they possess male and female reproductive organs, and one worm can lay up to 300 genetically identical progeny in its adult life, permitting an easy conservation of a genotype. However, a small fraction of males can also be found to permit the exchange of genetic material, they usually arise at a frequency less than 0.2% due to a mis-segregation of the sexual chromosomes as they only possess one chromosome X. Males notably differ from hermaphrodites in their morphology, displaying a specialised tail for mating with a distinct shape to hermaphrodites. Furthermore, the adult male possesses 1031 somatic nuclei compared to 959 in the adult hermaphrodite (Sulston *et al.*, 1980).

1.1.1.1 Life cycle

The nematode undergoes four larval stages to reach adulthood, L1 to L4. A sleep-like period of inactivity, called lethargus (Raizen *et al.*, 2008), is observed at the end of each stage where the nematode generates a new cuticle, a protective outer collagenous layer (Johnstone, 1994; Kramer, 1994). Behavioural activity is resumed after the moulting of the old cuticle marking the entry into the new stage. Each stage last approximately 12 hours at 20 °C except for the first one which is slightly longer lasting 16 hours (**Figure 1**).

Interestingly, when environmental conditions are unfavourable, such as the absence of food, *C. elegans* L2 larvae can enter an alternative stage called the dauer stage, promoting survival (Hu, 2007). This is a non-feeding stage in which the moult generates an enhanced cuticle, more resistant to chemicals, that completely surrounds the worm and plugs the mouth. In this form, the nematode can survive harsh conditions and subsist on its pre-formed energy stores, such as glycogen and lipids (O'Riordan and Burnell, 1990; Kimura *et al.*, 1997). Dauer larvae are characterised by fat accumulation and a shift in their metabolism to help them survive the lack of ingested food (Wadsworth and Riddle, 1989; Kimura *et al.*, 1997). In this state they are true anhydrobiotes as they can resist severe desiccation involving up to 98% removal of the

organism's water. This ability is conferred by a high concentration of trehalose (Erkut et al., 2011).

Eventually, when dauer larvae encounter a favourable environment, they start feeding again and moult to directly enter the L4 stage.

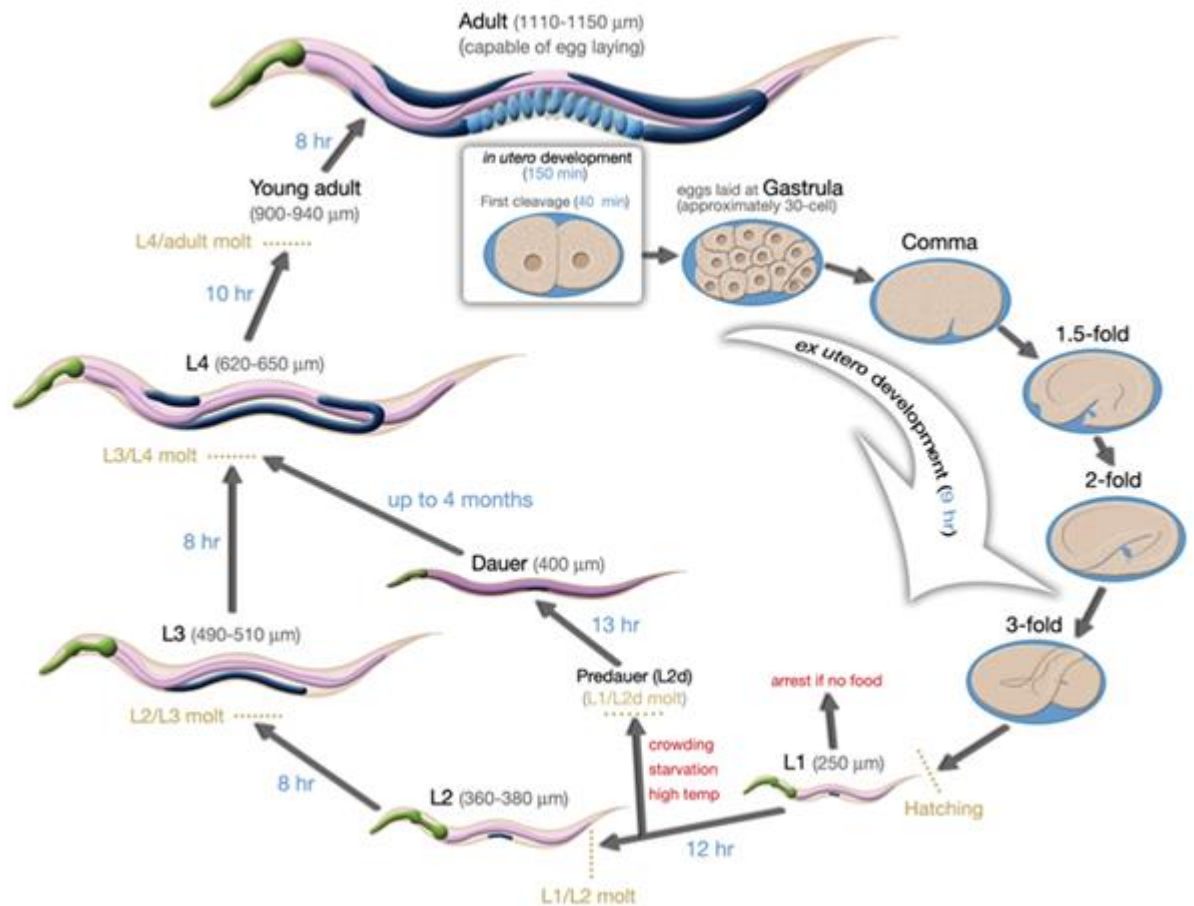


Figure 1: *Caenorhabditis elegans* lifecycle at 20°C.

C. elegans hermaphrodite goes through 4 larval stages (L1 to L4) before reaching the adult stage. It takes up to 3 days from egg to adult. Under unfavourable conditions, L2 larvae enter an alternative survival stage called dauer and can survive up to several months in this state. Upon favourable conditions, worms can resume the life cycle by entering the stage L4.

Cartoon taken from WormAtlas.

1.1.1.2 *C. elegans*; its advantages as a model organism

As a model organism, *C. elegans* possesses a number of advantages in addition to those described above. Firstly, it is a powerful model for genetics, it was the first multicellular organism with a complete genome sequence (Consortium, 1998), and ~38% of the protein coding genes have predicted orthologs in human (Shaye and Greenwald, 2011). Furthermore, the percentage of human genes to have an ortholog in the *C. elegans* genome is estimated around 60-80% (Kaletta and Hengartner, 2006) and around 40% of the genes associated with human disease have a clear ortholog in the nematode (Culetto and Sattelle, 2000). A particular advantage is the ease with which mutants may be generated and their availability from stock centres; the 'Caenorhabditis Genetics Center' and the 'National BioResource Project'. Moreover, the worm's transparency is a useful tool to investigate gene and protein expression patterns as it allows direct observation of fluorescent markers throughout the nervous system (Kim and Li, 2004). The ease of making transgenic animals by direct microinjection of genetic materials (Mello *et al.*, 1991) and the possible use of cell specific promoters for reporting gene expression make these techniques easier to perform in *C. elegans* than in mammalian systems. Finally, gene expression can also be selectively silenced by RNAi (Fire *et al.*, 1998; Timmons and Fire, 1998) or CRISPR system (Kim *et al.*, 2014). The availability of database resources for *C. elegans* greatly facilitates these techniques (Kamath and Ahringer, 2003; Qu *et al.*, 2011).

1.1.1.2.1 Advantages as a model for developmental biology

Given these experimental advantages *C. elegans* has served as a model to study development and its mechanisms. Because of its transparency and its fixed number of somatic cells, the lineage of each individual cell in the adult nematode has been tracked (Sulston and Horvitz, 1977; Sulston *et al.*, 1983). Notably, these studies permitted the discovery of apoptosis, and its molecular mechanisms (Horvitz, 2003). Indeed, during embryogenesis, 671 cells are generated, however, 113 undergo apoptosis, and the first larval stage hatches with 558 cells (Sulston *et al.*, 1983).

1.1.1.2.2 Advantages as a model for neurobiology

C. elegans has been increasingly used for neuroscience. The *C. elegans* connectome, a wiring map of the 302 neurons of the adult hermaphrodite nervous system, is available (White *et al.*, 1986). Indeed, the positions of the 302 neurons have been identified as well as their chemical and electrical (gap junctions) synapses using serial section electron micrographs (Albertson and Thomson, 1976; White *et al.*, 1986). However, the existing connectome has been shown to be incomplete as some functional synapses are not found in the original connectome (Bhatla *et al.*, 2015). Efforts are constantly ongoing to rework and reconstruct the worm's connectome with more modern technologies and comparing with the wiring map of other nematodes (Varshney *et al.*, 2011; Bumbarger *et al.*, 2013).

Despite the numerical simplicity of the *C. elegans* nervous system the fundamentals of nerve transmission are similar to higher organisms. The neurons communicate with each other and with muscle cells through an estimated 6400 chemical synapses, 900 gap junctions and 1500 neuromuscular junctions (Durbin, 1987). *C. elegans* displays a range of innate or learnt (Giles *et al.*, 2006) adaptive behaviours involving modulation of locomotion, foraging (Gray *et al.*, 2005; Boender *et al.*, 2011), feeding, defecation (de Bono and Maricq, 2005; Avery and You, 2012), and mating (Lipton *et al.*, 2004) or learning and memory. *C. elegans* has therefore been adopted as a model to investigate neural substrates of adaptive behaviour. It is possible to follow the calcium activity of a neuron or a subset of neurons, using a calcium sensor GCaMP (Chalasani *et al.*, 2007; Akerboom *et al.*, 2012) in fixed and freely moving live animals, an approach made possible by the transparency of the worm (Chalasani *et al.*, 2007; Flavell *et al.*, 2013; Bhatla and Horvitz, 2015). This permits the study of neuronal and circuit activity in parallel to behaviour. Finally, the transparency allied with selective expression of fluorescent reporters allows neuronal identification and single neuron ablation in the live animal (Fang-Yen *et al.*, 2012a).

Chapter 1

1.1.2 Nervous system

C. elegans hermaphrodites have a nervous system composed of exactly 302 neurons, with 383 neurons in the male worms. Neuron cell bodies are usually grouped in a few ganglia in the head, tail and ventral cord, and although the nematode does not have a brain-like organ per se the majority of the neurons have their cell bodies localised in the nerve ring in the head (White *et al.*, 1986) (Figure 2). Most neurons mainly display simple monopolar or bipolar morphologies with mostly unbranched processes and, with the exception of some sensory neurons, it is usually hard to tell the dendrite from the axon as both can receive and give synapses (White *et al.*, 1986). Indeed, it has been shown that both pre and post synaptic zone could be found in the same neurite (Rongo *et al.*, 1998), indicating that the polarity usually defining neurons can be mixed on individual processes. Most of the synapse connections in *C. elegans* are made 'en passant' (side by side as neurites pass each other) (White *et al.*, 1986).

The main difference between *C. elegans* and mammalian neurons is in how they utilize electrical potentials. There are no classical sodium-dependent action potentials in the nematode's neurons (Goodman *et al.*, 1998). Moreover, although voltage-gated K⁺ and Ca²⁺ channels are present, genes encoding classic voltage-gated sodium channels have not been found in the worm's genome (Bargmann, 1998), but a large variety of ion channels are expressed in neurons (Hobert, 2013), including a large number of potassium channels (Salkoff *et al.*, 2005). In contrast there is clear evidence for muscle action potentials in both the body wall and pharyngeal muscle, indicating the lack of molecularly identifiable sodium channels does not prevent electrical signalling acting in the worm's nervous system (Raizen and Avery, 1994; Gao and Zhen, 2011).

Because of their high membrane resistance (2.0 to 8.4 GΩ) and the short distance of their projections (a few hundred micrometres) it has been suggested that many neurons are isopotential, i.e. any change in voltage is instantaneously experienced by the entire cell (Goodman *et al.*, 1998; Dittman, 2009). Although there are no action potentials, neurons recorded using *in situ* patch-clamp recording techniques have been shown to respond to injected

currents with a quasi-stable plateau-like graded potential (Goodman *et al.*, 1998; Lockery and Goodman, 2009). For instance, the motor neurons RMD, appear to have two resting potentials at -70mV and -35mV, and a positive injected current pulse induced a depolarisation response followed by a third, higher, plateau (Mellem *et al.*, 2002). Unlike the 'all or none' response observed in mammalian neurons, *C. elegans* neurons can display graded responses, for instance, graded potentials have been observed between ASH and AVA neurons (Lindsay *et al.*, 2011). Consistently, *C. elegans* release neurotransmitters in a graded manner where the level of neurotransmitters released depends on the level of depolarisation (Liu *et al.*, 2009). Interestingly, plateau potentials like those described above are also found in other vertebrates and invertebrates, such as, rats and moths (Scroggs and Anderson, 1989; Di Prisco *et al.*, 1997; Derjean *et al.*, 2005; Mercer *et al.*, 2005). Therefore, synaptically evoked currents are likely to be graded depending on transmitter receptor activation, depolarising the membrane without driving the neuron to a threshold. This is similar to ribbon synapses found in the mammalian retina and auditory hair cells which specialise in rapid and continuous release of neurotransmitters in response to very specific changes in light or sound intensity (von Gersdorff, 2001; Sterling and Matthews, 2005).

In contrast, the nematode's body wall muscles exhibit all-or-none calcium-dependent action potentials in response to injected voltage. These action potentials at the NMJ are mediated by the worm homologue of mammalian L-type voltage-gated calcium and Kv1 voltage-dependent potassium channels mediating the depolarisation and repolarisation phase of these action potentials, respectively (Byerly and Masuda, 1979; Gao and Zhen, 2011).

1.1.2.1 The sensory organs

The detection and the processing of external and internal environmental cues by sensory neurons are two important functions underpinned by defined neuronal structures (Crook and Walters, 2011). In *C. elegans*, 32 presumed sensory neurons are found in sensilla, sensory organs, localised in the head (amphids), the inner labia, and the tail (phasmids and deirids) (Ward *et al.*, 1975; Perkins *et al.*, 1986). Amphids, are innervated invaginations of cuticle localised in the head region and are the main chemosensory organs with 12 sensory neurons (ADF, ADL, AFD, ASE, ASG, ASH, ASI, ASJ, ASK, AWA, AWB, AWC) found in each of them (see **Figure 3**). Interestingly, most sensory neurons possess a single non-motile cilium at their dendritic terminal end allowing contact with the environment. Indeed, these cilia go through openings in the cuticle generated by glial cells called the socket and sheath cell (Perkins *et al.*, 1986). However, some sensory functions are performed in absence of cilia or with no direct contact with the environment, for instance mechanosensation with CEP, ADE and PDE (Sawin *et al.*, 2000), or thermosensation by AFD neurons (Mori and Ohshima, 1995). Sensory neurons are usually organised as bilateral pairs. Although each neuron from each pair is morphologically similar, their sensory function may differ. For instance, in the gustatory ASE pair of neurons, the ASEL (left) detects increase in NaCl while ASER (right) respond to decrease in NaCl (Suzuki *et al.*, 2008). Similarly, the two olfactory AWC neurons, named AWC^{ON} and AWC^{OFF} both display an odour-OFF response, i.e. increased activity upon odour removal, to the odorant benzaldehyde and isoamyl alcohol, but only AWC^{OFF} exhibits an odour-OFF response to the removal of 2,3-pentanedione (Wes and Bargmann, 2001; Chalasani *et al.*, 2007).

Chapter 1

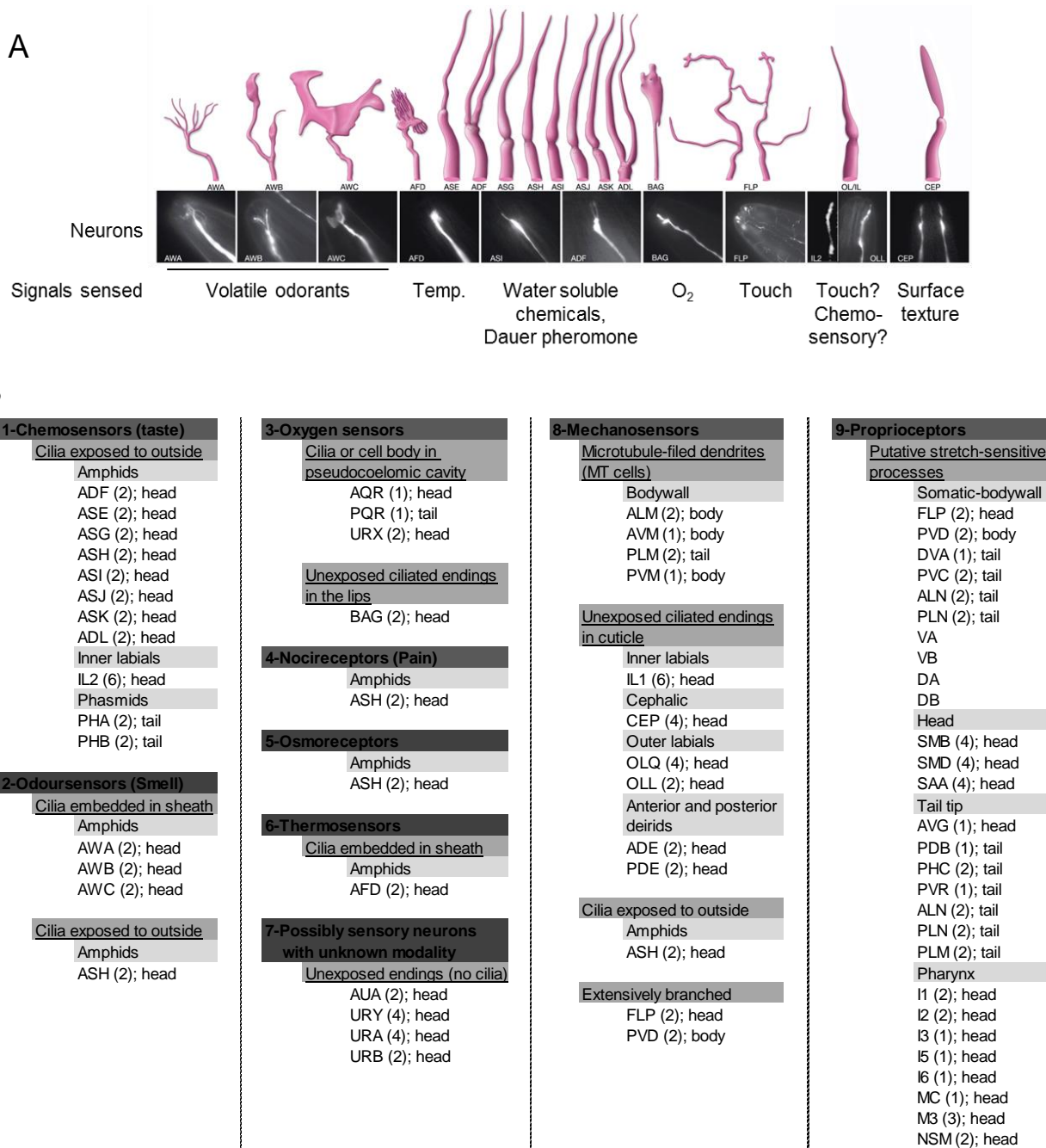


Figure 3: Sensory neurons in *C. elegans*.

A. Illustration and epifluorescent microscope images of cilia morphology of some sensory neurons representing the main different types, and signals sensed. Modified from Wormatlas. **B.** List of *C. elegans* sensory neurons sorted by sensory modality and position. Numbers in brackets indicate the number of cells per type of neuron. Information taken from Wormatlas.

1.1.2.2 Classical small molecule neurotransmitters

The *C. elegans* nervous system possesses similar nerve signalling in terms of neurochemistry to higher animals. Indeed, a similar suite of genes encoding key components underlying the nervous system of mammals is found in the worm genome (Bargmann, 1998; Hobert, 2013). This includes the two kinds of molecules allowing the transmission of information; the classical small molecule neurotransmitters and the neuropeptides.

C. elegans uses the common neurotransmitters utilized across phyla including, acetylcholine, 5-Hydroxytryptamine (5-HT or serotonin), glutamate, γ -amino butyric acid (GABA) and dopamine (Hobert, 2013). However, the signalling amines noradrenaline and adrenaline are not found in *C. elegans* (Sanyal *et al.*, 2004) but their functions are believed to be fulfilled by their invertebrate counterparts, octopamine and tyramine (Roeder *et al.*, 2003; Sanyal *et al.*, 2004; Alkema *et al.*, 2005).

1.1.2.3 Chemical neurotransmission

Pre-stored transmitters are accumulated in synaptic vesicles and undergo a co-ordinated series of steps in which they are translocated and docked at specific sites of the presynaptic plasma membrane that act as transmitter release sites (**Figure 4A**). The docked vesicles are then subjected to priming, the event that leads to the vesicle fusion competence, involving a complex molecular cascade. Priming involves the controlled modulation of the SNARE (soluble NSF attachment protein receptors) complex made up of the predominantly localised plasma membrane proteins syntaxin (*unc-64*) and SNAP-25 (*ric-4*) and the synaptic vesicle protein synaptobrevin (*snb-1*) (Chen and Scheller, 2001). These proteins are orchestrated by priming molecules including UNC-13 to ensure they are arranged in a juxtaposed configuration that bridges the synaptic vesicle and plasma membrane. *unc-13*, ortholog of the mammalian Munc13-1, is known to promote neurotransmission release (Betz *et al.*, 1998). Similarly in *C. elegans*, a study showed *unc-13* promotes the open configuration of syntaxin required to allow its trans membrane interaction with SNAP25 and synaptobrevin (Richmond *et al.*, 2001). This configuration allows the helical structures that underpin the SNARE complex to

Chapter 1

become increasingly associated and drive the two membranes to be increasingly drawn together. This configuration is clamped as a super-primed state and likely hemi-fused state that arrests vesicle fusion until it is triggered by rapid increases in intracellular Ca^{2+} at the transmitter release site (Richmond *et al.*, 2001). This Ca^{2+} is sensed by the synaptic vesicle protein synaptotagmin protein which contains two calcium-binding domains, C_2 (Nonet *et al.*, 1993; Sudhof, 2013). The timing of neurotransmitter release following Ca^{2+} influx, within 0.2 msec, suggests that most of the steps that lead to the arrested super-primed state occur before the rise of Ca^{2+} . After fusion the SNARE proteins are found in the same membrane in a post fusion conformation.

The rise in Ca^{2+} occurs via the opening of the voltage-gated calcium channels that are activated by neuronal depolarisation. In *C. elegans*, the Ca^{2+} channel subunits contributing to the synaptic Ca^{2+} signalling include UNC-2 (Richmond *et al.*, 2001), EGL-19 (Lee *et al.*, 1997) and UNC-36 (Schaffer and Lodish, 1994) and NCA-1 and NCA-2 (Yeh *et al.*, 2008).

Neurotransmitter reuptake and/or degradation occur after release in order to carefully control the strength of the signalling. This rapid termination of the signal is important to ensure a local signal has a good response to the next neuronal impulse. Acetylcholine in cholinergic synapses is broken down by acetylcholinesterase enzymes, and the use of a cholinesterase inhibitor, such as, aldicarb leads to an overstimulation of muscles and to the spastic paralysis of nematodes (Miller *et al.*, 1996).

The worm's genome contains orthologs of the mammalian SLC transporter family permitting reuptake of released neurotransmitters (He *et al.*, 2009). For instance, *cho-1* (SLC5 family) transports choline, the breakdown product of acetylcholine, *mod-5* (SLC6 family) 5-HT, *snf-11* (SLC6 family) GABA, *dat-1* (SLC6 family) dopamine while 6 transporter genes, the *glt* (SLC1 family) reuptake glutamate (**Figure 4B**) (Hobert, 2013). These transporters are mostly found expressed on neurons producing the transported neurotransmitter, however, glutamate transporters are also expressed in muscles and excitatory canal cells (cells contributing to excretion and electrolyte balance) (Mano *et al.*, 2007). Furthermore, some neurons, called 5-HT-absorbing neurons, do not synthesize 5-HT but express the 5-HT transporter *mod-5* and transport 5-HT

from the extracellular space to subsequently release it as a neurotransmitter (e.g. AIM and RIH) (Jafari *et al.*, 2011).

The specific molecular and cellular determinants acting in the biosynthesis, transport, release and reuptake of the different individual neurotransmitters are indicated on the diagram of the **Figure 4B**.

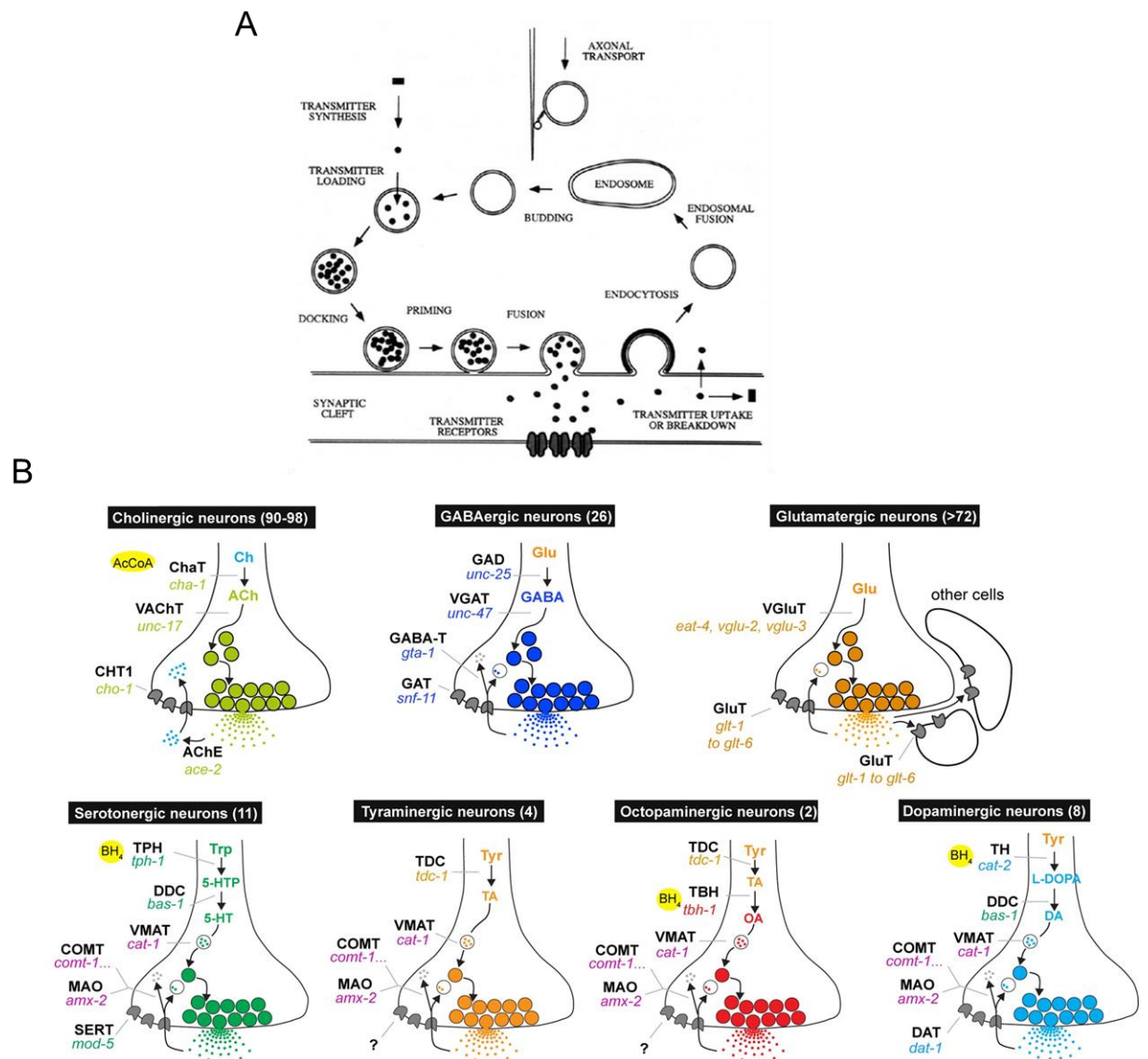


Figure 4: Cartoon representation of the main classical neurotransmitter pathways found in *C. elegans*.

A. Neurotransmitters are loaded inside synaptic vesicles via neurotransmitter transporters and stored. Vesicles are then mobilized within the synapse to the

Chapter 1

active zone where they dock. Following docking, a priming step occurs where vesicles become fusion competent. Then, upon neuron excitation, the increased intracellular Ca^{2+} triggers fusion of the vesicles with the plasma membrane releasing the neurotransmitters into the synaptic cleft. Finally, vesicle proteins are retrieved by clathrin-mediated endocytosis and recycled back to allow subsequent rounds of vesicle mediated transmitter release. Taken from *C. elegans* II. 2nd edition. **B.** Each cartoon represents the steps of synthesis, vesicular loading and reuptake of individual fast neurotransmitters/neuromodulators. Estimated number of neurons expressing each neurotransmitter is indicated between brackets. Taken from Hobert *et al.* 2013, WormBook.

1.1.2.4 Neuropeptides in *C. elegans*

Besides the small classical transmitters, neuropeptides are the other major type of transmitter found in neurons. These neuropeptides are not specifically released at the neuron active zones (Salio *et al.*, 2006) and their signalling is not restricted to juxtaposed synapses. They are also widely discussed as underpinning important neuromodulatory volume, or wireless, transmission. Neuropeptides and low-molecular-weight neurotransmitters coexist in neurons, however, neuropeptides appear not to be mainly localised at synaptic zones, like classical neurotransmitters, but more scattered along the nerve terminal (Salio *et al.*, 2006). This differential subcellular site of storage and the coexistence of both transmitter types allow fast (3-5 ms) and slow (100-500 ms) synaptic connections to take place.

In the case of *C. elegans* this distal diffusion can involve the pseudocoelom, a fluid-filled body cavity lying inside the external body wall of the nematode that bathes the internal organs (Wood, 1988), allowing a more indirect signalling. This mode of signalling is assumed based on observations that released peptides can be detected in the three pairs of coelomocytes which are positioned in the pseudocoelomic cavity on the ventral side close to

the head and near the mid-body, and dorsally in the posterior body, at some distance from released peptides (**Figure 5**). These are endocytotic scavenger cells which are proposed to have an immune role, support detoxification, have hepatic functions, and act as useful reporters of pseudocoelom contents (Fares and Greenwald, 2001; Sieburth *et al.*, 2007)

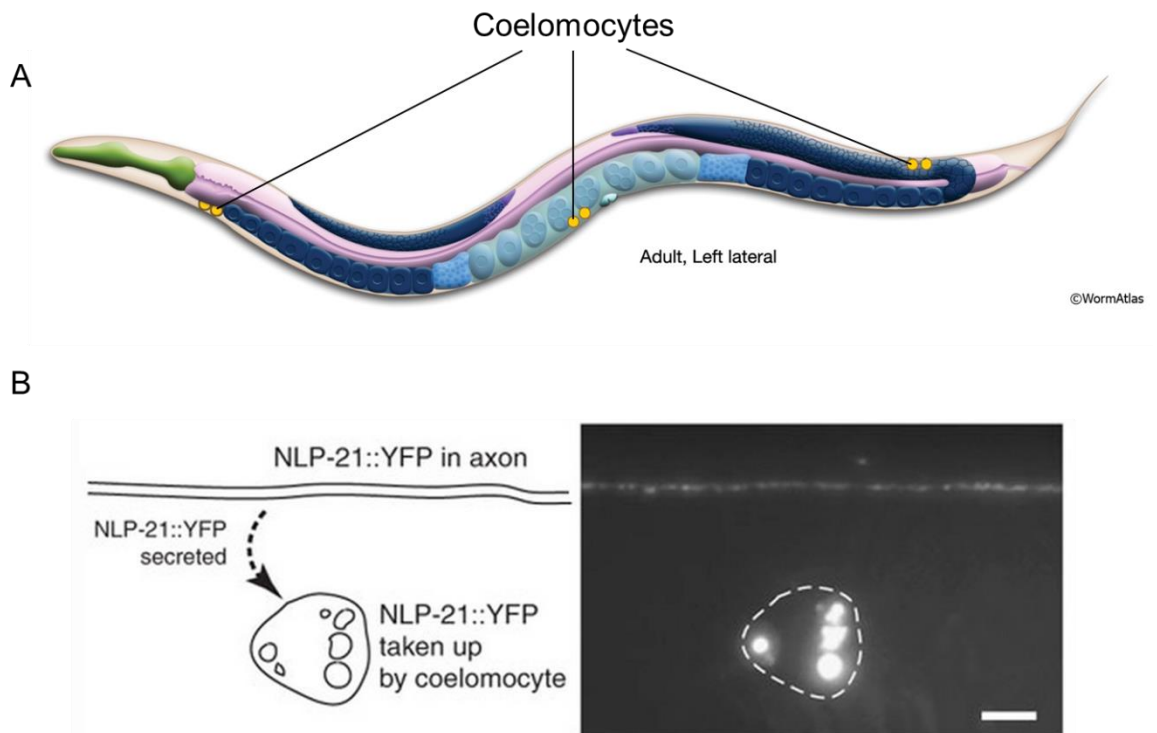


Figure 5: The coelomocytes take up neuropeptides from the pseudocoelomic fluid by phagocytosis.

A. Cartoon representing the localisation of the coelomocytes. There are 6 coelomocyte cells forming 3 pairs in total. Coelomocytes are represented by yellow circles. Two pairs are positioned ventrally with two cells (ccPR and ccAR) close to the head and the other two (ccPL and ccAL) close to the midbody. The last pair is positioned dorsally in the posterior part of the body.

B. Example of neuropeptide uptake with the tagged NLP-21::YFP expressed in cholinergic neurons. Fluorescence can be observed in both the axon and the coelomocyte despite its selective expression in the motorneuron, indicating release from the motorneuron and uptake by coelomocytes. Taken from Sieburth, D. *et al.* 2007.

1.1.2.4.1 Classes of neuropeptides

The *C. elegans* genome has around 122 genes encoding for around 250 neuropeptides (Li and Kim, 2010; Holden-Dye and Walker, 2013). Neuropeptides are divided into three categories: the FMRFamide-related peptides (FLPs), the insulin-like peptides (INSs) and the neuropeptide-like peptides (NLPs). There are 80 FLPs encoded by 32 genes encoding from 1 to 9 discrete peptides (Li and Kim, 2010). FLPs have been found expressed in all neuronal cell types and in more than 150 of the 302 neurons (Kim and Li, 2004). 40 genes (39 *ins* genes and one *daf* gene) encode an estimated 42 INS peptides. They seem to be less widely expressed than FLPs, and are largely restricted to amphidal neurons (Pierce *et al.*, 2001). NLP peptides are described as non-insulin and non-FLP peptides, and thus form a heterogeneous family. There are 51 genes encoding 125 peptides classified as NLPs (Husson *et al.*, 2009; Li and Kim, 2010). Many of these NLPs are found in amphid neurons, some in the pharyngeal nervous system and interestingly some can be expressed outside the nervous system and could act as anti-microbial agents (Couillault *et al.*, 2004; Li and Kim, 2008).

Recently, a vasopressin and oxytocin (VP/OT)-related signalling system has been identified in *C. elegans* (Garrison *et al.*, 2012). A single VP/OT-like peptide, NTC-1 for nematocin, has been identified along with two receptors, NTR-1 and NTR-2 (Beets *et al.*, 2012; Garrison *et al.*, 2012).

1.1.2.4.2 Neuropeptide biogenesis

Neuropeptide synthesis mechanisms are very similar to those found in mammals. Neuropeptide genes synthesize large inactive precursor molecules, called proproteins or propeptides, typically containing more than one peptide. Processing of these precursors occurs in dense core vesicles (DCV) where neuropeptides are stored, together with processing enzymes, and transported along the axon. Propeptides are firstly processed by proprotein convertases (Figure 6).

1.1.2.4.3 The *kex2*/subtilisin-like proprotein convertase (*kpc*) family

Proprotein convertase enzymes are found in every eukaryote and are responsible for the cleavage of large inactive polypeptide precursors including neuropeptides and other structural and signalling proteins (**Figure 7**). The furin enzyme, encoded by the gene *fur*, was the first proprotein convertase discovered in mammals (Fuller *et al.*, 1989). The endoprotease activity of furin processes a wide range of precursor proteins (Nakayama, 1997).

In *C. elegans*, the *kex2*/subtilisin-like proprotein convertases (*kpc*) family is composed of 4 genes encoding enzymes: *kpc-1*; *egl-3/kpc-2*; *aex-5/kpc-3* and *bli-4/kpc-4*, all acting in neuropeptide processing by cleaving propeptides into individual peptides (Husson *et al.*, 2006). Interestingly, 3 of those *kpc* genes are found in chromosome I, however, genetic studies, loci location and coding sequences, showed they do not come from the duplication of the same gene. The structure of the *kpc* family members is described in **Figure 6**. There are two main domains characterising the KPCs; the subtilisin-like catalytic domain bearing the endopeptidase function, and immediately following a highly-conserved sequence unique to KPCs named the P domain. The P domain is required for folding and maintaining the catalytic domain and to regulate its calcium and acidic pH dependence of its endopeptidase activity (Zhou *et al.*, 1998).

kpc-1, originally named CelfurPC for *C. elegans* furin proprotein convertase, was first isolated in the nematode in 1997 and identified as a member of the Kex2 family of serine endoproteases, with strong structural homology to the furin/PACE4 family (Gomez-Saladin *et al.*, 1997), PC5/6, PACE4 and *C. elegans* BLI-4/KPC-4 (Thacker and Rose, 2000). *kpc-1* encodes two isoforms, KPC-1A/B, with KPC-1A possessing an additional 64 amino acids in its P domain. EGL-3/KPC-2 is the orthologue to the mammalian protein convertase 2 (PC2) and is responsible for the processing of most NLP and FLP neuropeptides. Expression pattern analysis revealed neuronal expression in many, but not all, neurons (Kass *et al.*, 2001). *egl-3* was first identified in a screen for mutants defective in egg-laying (*egl*) phenotype, hence its name (Trent *et al.*, 1983). *aex-5/kpc-3* regulates the anterior body contraction and the worm's defecation cycle (Thomas, 1990) and is expressed in all muscles, except pharyngeal muscles (Thacker and Rose, 2000). *aex-5/kpc-3* is also

believed to process a neuropeptide involved in a retrograde signal to regulate exocytosis, together with the human BAP3 orthologue *aex-1* (Doi and Iwasaki, 2002). Finally, *bli-4/kpc-4*, a complex gene producing nine different isoforms generated by alternate splicing, is mainly known for its function in the maintenance of cuticle integrity by cleaving procollagen into collagen (Thacker *et al.*, 1995; Thacker and Rose, 2000). As for KPC-1, BLI-4/KPC-4 shares similarities with human furin, PC5/6 and PACE4 (Thacker and Rose, 2000). *bli-4/kpc-4* is expressed in hypodermal tissue but also in neural tissue although no specific expression in individual neurons has been clarified (Thacker and Rose, 2000).

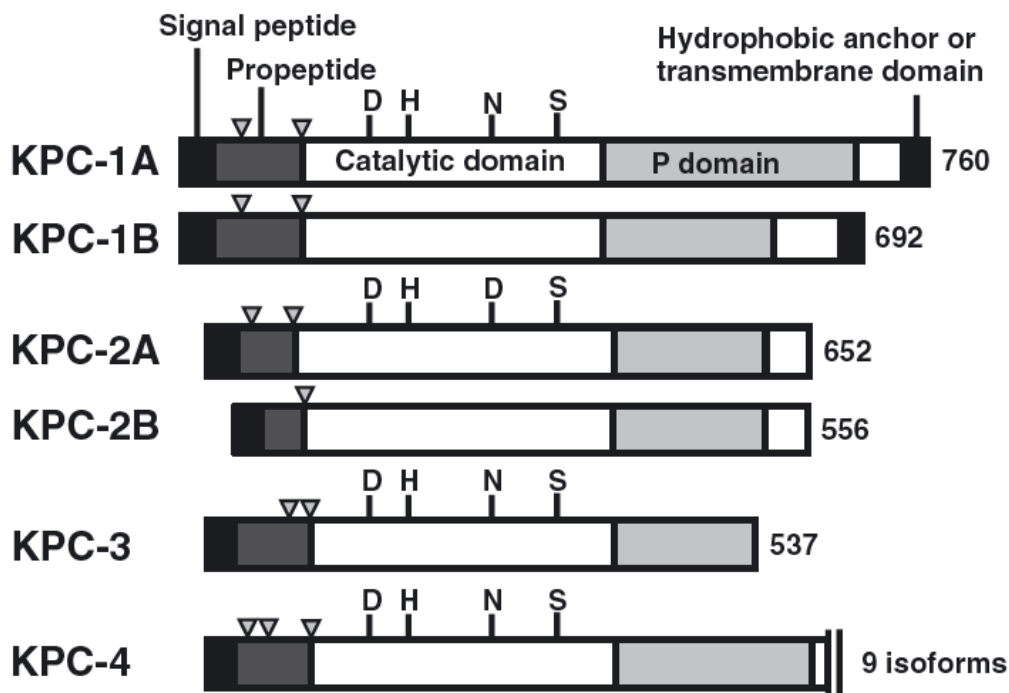


Figure 6: Structural representation of the *kex-2*/subtilisin-like proprotein convertase (*kpc*) family.

The KPCs are synthesised as inactive precursors and auto-cleavage removes the amino-terminal propeptides at sites indicated by inverted triangles to allow activation of the enzyme. The signal peptide permits localisation of the KPC in the dense core vesicle. The subtilisin-related catalytic domain is conserved throughout the *kpc* family. The three amino acids aspartic acid (D), histidine

(H) and serine (S) are absolutely required for the KPC's enzymatic activity. Immediately downstream of the catalytic domain is the P domain, a region conserved only among the *kpc* family and required for the maintenance and activity of the catalytic domain. The carboxyl-terminal region is the least conserved and appears different for each enzyme. Taken from Husson *et al.* 2006.

Husson *et al.* published in 2006 the peptide profile of mutants for *kpc* family members, using a mass spectrometry based method, to better determine the role of each *kpc* in the processing of neuropeptides. They have shown that only a few of the 100 neuropeptides detected by this peptidomic approach were present in *egl-3* mutants (from zero to 13 depending on the allele) while a majority of them remain detectable in other *kpc* mutants (Husson *et al.*, 2006). Interestingly, some NLP and FLP peptides were still processed in the different *kpc-2/egl-3* alleles tested, indicating an *egl-3*-independent pathway for the processing of these peptides. However, INS peptides were not investigated in this study. Nonetheless, genetic studies have shown that individual INS peptides could be processed by *kpc* convertases, which is notably the case for INS-6 which can be cleaved by BLI-4 or EGL-3 (Hung *et al.*, 2013; Leinwand and Chalasani, 2013)

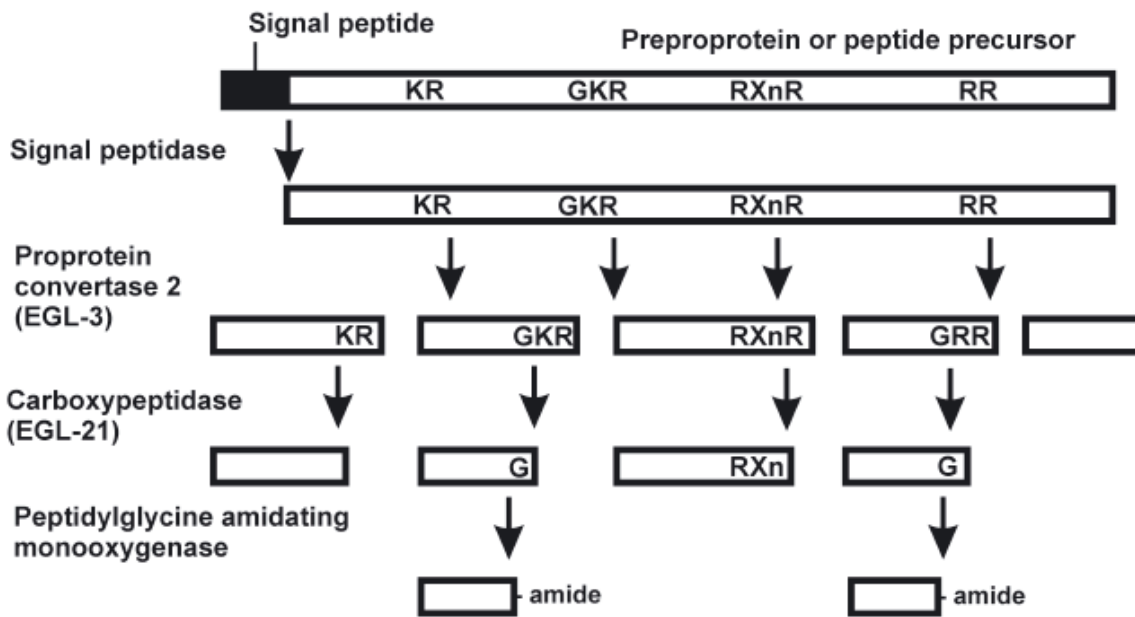


Figure 7: *Caenorhabditis elegans* neuropeptide processing pathway.

Neuropeptide genes encode large pre-proteins often containing several peptides. When entering the secretory pathway (Dense Core Vesicles) the signal peptide of the preproprotein is cleaved off. The proprotein convertase EGL-3/KPC-2 then cleaves the propeptides at specific dibasic (KR, RR, RK and KK) or monobasic (K and R) sites. Basic residues can be separated by two to eight other residues as indicated by (RXnR). Some individual peptides are further processed by the carboxypeptidase EGL-21. Finally, following the activity of EGL-21, the C-terminal basic amino acids are removed to permit the transformation of a Glycine (G) residue, when present, into an amide by amidation enzymes. *Taken from Husson et al. 2007.*

1.1.2.4.4 Further modification of cleaved individual peptides

Following cleavage by the proprotein convertases, carboxypeptidase processing removes basic amino acids in the carboxy-terminal region of individual neuropeptides. EGL-21, the ortholog of the mammalian carboxypeptidase E, plays the role of the main carboxypeptidase in *C. elegans* (Husson et al., 2007). Similarly to *egl-3* mutant strains, peptide profile analysis

showed that the *egl-21(n476)* mutant is deficient in bioactive peptides, although less neuropeptides are affected by this mutation than by *egl-3* mutation (Husson *et al.*, 2007). Mass spectrometry indeed revealed 24 fully processed neuropeptides (NLP-7, -8, -11, -11, FLP-3, -3, -9, -11, -14, -15, -18, -18, -18, -19, -22, -24, -25, -26, -26) in *egl-21(n611)* and the *egl-21(n476)* strains. It is likely there are additional carboxypeptidases in *C. elegans*. Indeed, the yet uncharacterised F59A3.1 and T27A8.1 genes were shown as orthologs of the mammalian carboxypeptidase D family (*cpd-1* and *cpd-2*) (Dong *et al.*, 1999; Husson *et al.*, 2007).

Finally, an amidation step may occur on peptides with a C-terminal glycine. Indeed, some bioactive peptides require amidation for full function. However, unlike proprotein convertases and carboxypeptidases, less is known about this process in *C. elegans*. In other organisms, the amidation process is performed by a mono oxygenase PHM (peptidylglycine- α -hydroxylating), which hydroxylates glycine (Mueller *et al.*, 1993), and the enzyme PAL (peptidyl- α -hydroxyglycine α -amidating lyase) which cleaves the hydroxyglycine to produce the peptide-amide (Prigge *et al.*, 2000). In higher organisms, including human, these two activities are performed by a single bi-functional enzyme, PAM (peptidylglycine α -amidating monooxygenase) (Prigge *et al.*, 2000), which is not the case in *Drosophila* where the two activities are split (PHM and PAL) (Kolhekar *et al.*, 1997). Interestingly, preliminary studies revealed the *C. elegans*' genome contains orthologs for both, split and unsplit, versions. Indeed, based on protein domains, *pamn-1* is predicted to encode for an ortholog of the multi-enzyme PAM, while *pghm-1* and *pgal-1* encode for PHM and PAL orthologs, respectively (Wormbase).

A summary of the different steps of neuropeptide processing can be found in **Figure 7**.

1.1.2.4.5 Neuropeptides release

Neuropeptides are stored in DCVs and UNC-31, the homologue of the mammalian Ca^{2+} activated proteins for secretion (CAPS) (Grishanin *et al.*, 2004), contributes to the release of neuropeptides by exocytosis (Ann *et al.*, 1997). Release of neuropeptides from DCVs appears dependent on an increase of

Chapter 1

intracellular Ca^{2+} throughout the nerve terminal rather than a localised increase at the synaptic zone like neurotransmitters (Salio *et al.*, 2006).

While in mammals CAPS has been shown to regulate the vesicular-mediated release of glutamate (Jockusch *et al.*, 2007), a study in *C. elegans* revealed that *unc-31* was not involved in the release of classical neurotransmitter (Speese *et al.*, 2007). However, using a method for recording synaptic currents and potentials in the command neuron AVA, Lindsay *et al.* recorded activity in AVA when its presynaptic glutamatergic neurons ASH were artificially stimulated by optogenetics (Lindsay *et al.*, 2011). The evoked currents observed in AVA upon activation of ASH were abolished in an *unc-13* mutant, indicating communication driven by a fast neurotransmitter, glutamate in the case of ASH. Evoked currents in a mutant for *unc-31* were also tested, and although the results are non-significant, there is a clear trend toward a reduction of evoked currents in AVA (Lindsay *et al.*, 2011). Therefore, it would be interesting to further assess the role of *unc-31* in the vesicular-mediated release of 'fast' transmitter, e.g. glutamate.

The basic mechanisms of DCVs-mediated release utilised the same related molecules in core functions as for small vesicles, involving docking, priming and Ca^{2+} dependent release. This is notably the case of UNC-13 which is required to prime both types of vesicles (Richmond *et al.*, 2001; Sieburth *et al.*, 2007). However, the specificity of UNC-31, although controversial, suggests some distinct mechanisms between DCV and small vesicle-mediated release.

1.1.2.5 Post synaptic signal reception and transduction

The effect of a neurotransmitter released onto the postsynaptic neuron depends on the transmitter receptors expressed post synaptically. There are two main types of receptors a transmitter can bind to, ligand-gated ion channels (LGIC), also called ionotropic receptors, and GPCRs (G-protein coupled receptors), or metabotropic receptors (**Figure 8**). Neurotransmitters can act in fast transmission via the activity of LGICs that can be either excitatory or inhibitory receptors, i.e. leading to depolarisation or hyperpolarisation of the targeted neuron respectively. LGICs are transmembrane ion channels which open upon binding of its ligands to allow anions, such as Cl^- , or cations, Na^+ , K^+

and Ca^{2+} , to pass through the membrane. In general, binding to cation channels is associated with excitatory events, for instance the ACh nicotinic receptors (nAChRs) or ionotropic glutamate receptors (iGluRs) (McKay *et al.*, 2004; Brockie and Maricq, 2006). Conversely, activation of ligand-gated chloride channels, for instance glutamate-gated chloride channels (GluCl) and GABA_A receptors, mostly leads to inhibition (Schofield *et al.*, 1987; Brockie and Maricq, 2006). Alternatively, neurotransmitters can also act as neuromodulators via the more slow acting GPCR receptors, acting through more distant sites and affecting multiples neurons. At synaptic sites, released neurotransmitters are rapidly taken up/degraded. However, neurotransmitters can be released at synaptic terminals that do not form junctional complexes with another neuron and therefore the neurotransmitters can escape degradation and act onto non-junctional receptors (Sarter *et al.*, 2009).

The same neurotransmitter can act as both excitatory and inhibitory fast transmitter and modulatory transmitter. For instance, glutamate can act on both glutamate-gated cations channels, GLR-1 to GLR-8, and anion channels, e.g. AVR-14 and AVR-15 (detailed in **section 4.1**) (Dent *et al.*, 1997; Brockie and Maricq, 2003). In addition, three glutamate metabotropic receptors are found in the *C. elegans* genome (Dillon *et al.*, 2006). Similarly, 5-HT can act through MOD-1, a serotonin-gated chloride channel, or the metabotropic receptors SER-4, SER-5 and SER-7 (Komuniecki *et al.*, 2004).

There are examples of these phenomena in relation to food-dependent behaviours in *C. elegans*. In the presence of food, 5-HT released from the pharyngeal neuron NSM modulates locomotion in response to food by acting on neurons localised in the nerve ring and thus not in direct contact with NSM, via MOD-1 (Flavell *et al.*, 2013) while 5-HT released from ADF acts at a distance via the SER-5 receptor on AVJ neurons to regulate the pharyngeal pumping rate (Cunningham *et al.*, 2012) (see **section 1.3.1.1**). Further evidence for the activation of non-junctional receptors by neurotransmitters comes from tyramine and octopamine. Indeed, although not released in the pharyngeal nervous system, receptors are found expressed in it, and exogenous addition of tyramine or octopamine lead to a reduction of feeding (see **sections 1.3.1.6 and 1.3.1.7**) (Horvitz *et al.*, 1982; Rex *et al.*, 2004).

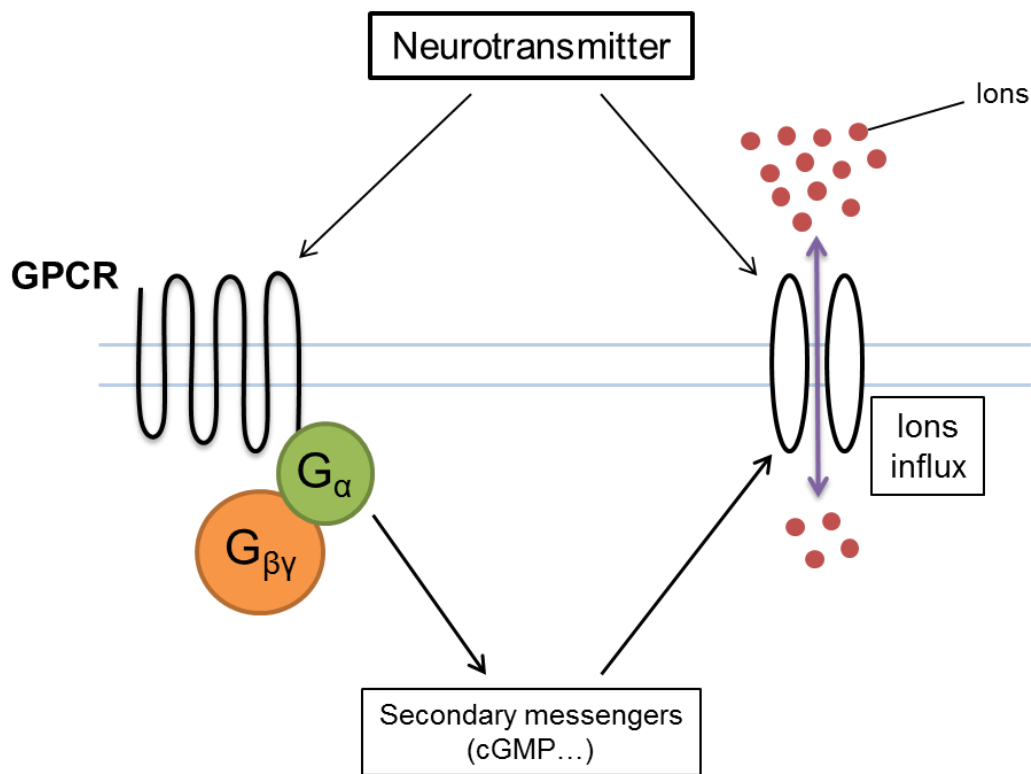


Figure 8: Simplified cartoon of postsynaptic signal transduction.

Neurotransmitters can act through metabotropic GPCR receptors and ionotropic receptors, ligand-gated ion channels (LGIC). Upon neurotransmitter binding, the ion channel opens allowing influx of ions, cations or anions leading to the activation or inhibition of the cell, respectively. Following activation of a GPCR receptor, conformational changes occur and the receptor catalyses the release of GDP and binding of GTP by the G_{α} subunit. The activated G_{α} -GTP subunit dissociates from the receptor and acts directly or indirectly via intracellular secondary messengers such as cGMP, to trigger the open conformation of a LGIC.

1.2 Feeding behaviours

Feeding behaviours designate all the actions of an organism related to the presence or the absence of food. By their nature, they are conserved throughout evolution, as they confer advantages to grow, develop and breed

(Wang *et al.*, 2006). Historically, Hetherington and Ransom showed that feeding behaviours are mediated inside the nervous system (Hetherington and Ransom, 1940). Indeed, appetite appeared neuronally controlled as removing one part of the rat hypothalamus resulted in an increase of food intake (hyperphagia) and body weight while removing another part led to the opposite result, a decrease of food intake (hypophagia) and starvation to death (Hetherington and Ransom, 1940). More recently, more precise location within the hypothalamus of specific neuronal types has been associated with appetite, such as, the neuropeptide Y/agouti related protein (NPY/AgRP)-expressing neurons promoting food intake and the pro-opiomelanocortin (POMC)-expressing neurons of the ventromedial hypothalamus reducing food intake (Aponte *et al.*, 2011).

In *C. elegans*, feeding behaviours are mainly linked to the regulation of locomotion and pharyngeal pumping. The regulation of locomotion patterns permits the worms to explore their environment to find food and eventually to stay on this source of food. Interestingly, *C. elegans* dauer larvae, are able to initiate a nictation behaviour characterised by the larvae standing up on their tail so they can use flying insects as carriers to reach further sources of food (Lee *et al.*, 2012). The pharyngeal pumping is the worm's natural way of feeding and therefore the regulation of behaviours involving pharyngeal pumping are directly linked to food intake. Detection of food is an important part in feeding behaviours and the decision-making process. Indeed, it is crucial for worms, and other animals, to properly perceive their environment and to be able to discern whether an environment is favourable or not. The *C. elegans* nervous system is able to detect food, or its absence, by different means, for instance volatile chemicals (Bargmann, 2006), oxygen levels (Gray *et al.*, 2004; Reddy *et al.*, 2009), temperature or physical presence (Sawin *et al.*, 2000). The neuronal control of these behaviours is discussed in this section.

1.2.1 Locomotion

1.2.1.1 Basics of *C. elegans* locomotion

Worms explore their environment by “crawling” on solid surfaces (or by swimming in liquid). The regulation of its locomotion is very important for the worm in order to adapt to environmental changes, to find food or to escape unfavourable and noxious conditions (Hilliard *et al.*, 2002; Gray *et al.*, 2005; Milward *et al.*, 2011).

C. elegans locomotion is described as a biased random walk as it is often interrupted by reversals (backward movement) and turns that allow change of direction (de Bono and Maricq, 2005). Reversals are characterised by the number of head swings occurring before reorientation with reversals considered short with 2 or less head swings and long with at least 3 head swings (Gray *et al.*, 2005) (**Figure 9A**). The largest reorientation of the worm’s direction is named “omega” turns because of the shape taken by the worm during the turning event that resembles the Greek letter Ω (**Figure 9A**). Periods of rapid direction change are called “pirouettes”, and the frequency of these pirouettes changes in relation to food availability, or the detection of an attractant chemical. Pirouettes indeed become more frequent when the environment is turning unfavourable and vice versa (Pierce-Shimomura *et al.*, 1999).

In parallel to the pirouettes model, another strategy, called the weathervane strategy, has been shown to direct the worm during chemotaxis toward an attractant (Iino and Yoshida, 2009). During forward locomotion in a salt gradient, worms were observed to curve toward the highest salt or odorant concentration without using pirouettes. Therefore, worms direct themselves during chemotaxis using pirouettes in response to temporal changes in chemoattractant concentration while responding to spatial gradient, perpendicular to the direction of locomotion, triggers a gradual curving to the side in the direction to the attractant (Iino and Yoshida, 2009).

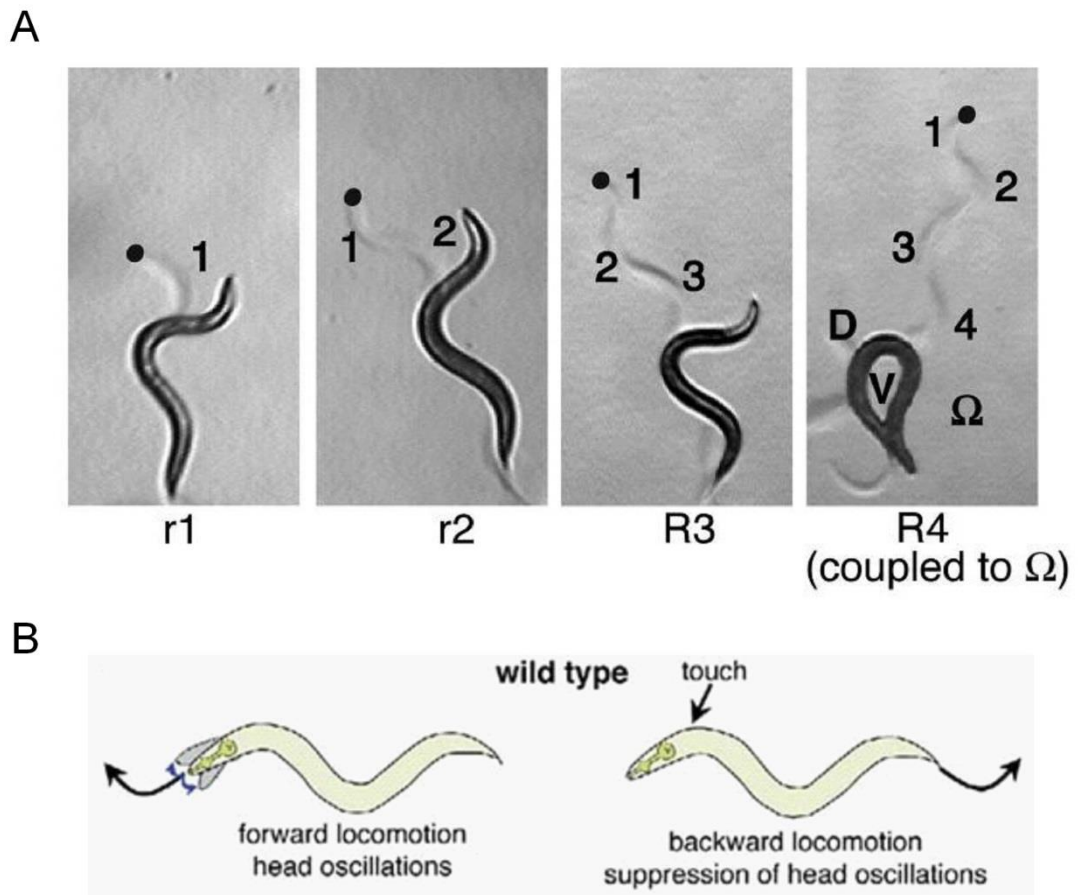


Figure 9: *C. elegans* reversals, omega turn and head oscillations patterns.

A. Turning behaviours interrupting forward movement. Pictures show different reversal strategies allowing the nematode to explore its environment. Turning behaviours can be produced either by a reversal followed by a reorientation and the resumption of forward movement in a new direction, or by omega turns. Tracks left by nematodes observed in these pictures served as indication regarding their previous position. Reversal with (r1) a single head swing and a 40° change of direction, (r2) two head swings and a 70° change of direction, (R3) three head swings and a 90° change of direction (R4) four head swings follow by an omega turn (170° change of direction). In picture (R4) V stands for Ventral side of the animal during omega turn, D for dorsal side. Picture taken from Gray *et al.* 2005.

B. Schematic representation of head oscillations during *C. elegans* locomotion. Forward locomotion of wild-type animals is accompanied by oscillatory head movements. Anterior touch of wild-type animals with an eyelash induces backward movement during which head oscillations are suppressed. Modified from Alkema *et al.* 2005.

Chapter 1

Head oscillations occur during forward locomotion, supposedly to enhance the efficiency of immediate environment exploration since the tip of the nose possessed sensory neurons (amphids) (Croll, 1975). These head oscillations are suppressed during touch-induced backward movement by the activity of the pair of motoneurons RIM (Alkema *et al.*, 2005). Interestingly, RIM neurons also regulate the frequency of spontaneous reversals (**Figure 10**) that occur during locomotion, as RIMs' activity represses these spontaneous reversals (Piggott *et al.*, 2011).

In addition to spontaneous reversals, reversals can also be triggered by light touch in the head or tail region (Chalfie *et al.*, 1985) where *C. elegans* possesses touch receptors (Chalfie and Sulston, 1981). If the touch occurs in the head region a backward movement (reversal motion) is initiated. Conversely when touch occurs near the tail, a forward movement is observed. This behaviour has been shown to be driven by the "escape circuit", a neuronal circuit composed of six mechanosensory neurons (ALM, AVM, LUA, PLM, ASH, FLP) which upon detection of stimuli establish synaptic connections with command interneurons (AVA, AVD and AVE) which in turn modulate the motoneurons involved either in forward or backward movements (A, B, AS) (Chalfie *et al.*, 1985; Kaplan and Horvitz, 1993). However, Piggott *et al.* have more recently shown that AVA has a more important role in triggering reversals than AVD and AVE, but also that the ablation of the three neurons together only reduced the frequency of reversals without stopping them completely (Piggott *et al.*, 2011). This result indicates that AVA, AVE and AVD command interneurons are not essential for the control of the frequency of both spontaneous and touch-induced reversals.

Thanks to a multidisciplinary approach, Piggott *et al.* have shown that a disinhibitory and stimulatory circuits are working in parallel to regulate the frequency of reversals (Piggott *et al.*, 2011) (**Figure 10**). Indeed, though the role of AVA in the control of reversals was known, they were the first to show that the circuit ASH-AVA is not the only one regulating backward locomotion. On the contrary, they have identified an additional circuit acting in parallel to this stimulatory circuit. RIM neuron activity suppresses reversals independently of AVA, and they have found that RIM activity is modulated by AIB. Indeed AIB

represses RIM activity, which in turn suppresses the inhibitory effect of RIM and enhances reversals. This circuit has thus been named disinhibitory. It is interesting to notice that both circuits may be modulated by the same sensory neuron, namely ASH, a pair of nociceptive neurons involved in social feeding behaviour (see **section 1.2.1.2**).

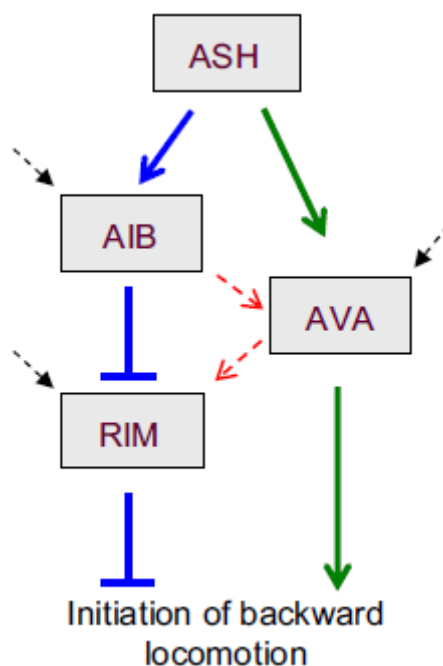


Figure 10: Schematic model illustrating the disinhibitory and stimulatory circuits.

ASH sensory neuron activation activates AIB and AVA interneurons.

Subsequently, AIB activation suppresses RIM activity, which normally acts to repress reversals. Thus AIB promotes reversals by suppressing the inhibitory activity of RIM, hence the “disinhibitory” circuit. In parallel, in the stimulatory circuit, the activation of command interneuron AVA promotes reversals.

Arrows in black indicate that other sensory neurons may regulate the two circuits. Arrows in red indicate possible crosstalk between the two circuits. Taken from Piggott *et al.* 2011.

1.2.1.2 The availability of food plays a crucial role in locomotion behaviours

In the presence of food, *C. elegans* spontaneously switches between two locomotion behaviours called dwelling and roaming (Ben Arous *et al.*, 2009). The dwelling state corresponds to a reduced speed and an increase of turn frequency permitting the worm to remain on a small area on food. Conversely, roaming is characterised by a higher speed but with fewer turning events allowing exploration of the food patch (**Figure 11A**). These behaviours are believed to reflect an exploration-exploitation decision about the value of the local environment (decision-making) as the worms spend less time dwelling and more time roaming in the presence of low-quality food or when there is no food (Ben Arous *et al.*, 2009) and conversely more time dwelling on food (Flavell *et al.*, 2013). *C. elegans* responds to the presence of food by displaying a slowing response, represented by a decreased body bends frequency, so they can spend more time on food (Sawin *et al.*, 2000). The physical presence of bacteria is detected by mechanosensory neurons which in turns triggers this slowing response. Interestingly, worms that have been food-deprived for 30 min showed an enhanced slowing response with a further reduction of body bends per minute. This experience-dependent enhanced response is distinctly regulated compared to the basal slowing response, and involves the serotonergic pharyngeal neurons NSM (Sawin *et al.*, 2000).

In absence of food, *C. elegans* displays an exploratory behaviour that can be divided in two phases; an early phase called local search area (LSA), also called area restricted search (ARS), and a late phase where nematodes exhibit long range dispersal (Hills *et al.*, 2004; Gray *et al.*, 2005) (**Figure 11B**).

The LSA behaviour is defined by a burst of turn and reversal frequencies during the 15 first minutes; following removal of food, corresponding to worms searching for food in a restricted area. This food-seeking behaviour depends on the pair of amphid wing sensory neurons AWCs (Chalasani *et al.*, 2007). Finally, after ~12 minutes, *C. elegans* switches behaviours from LSA to foraging. Worms undertake straight forward runs, correlated with a marked decrease of reversal frequency, in order to explore further areas and find a more favourable environment (**Figure 11B**).

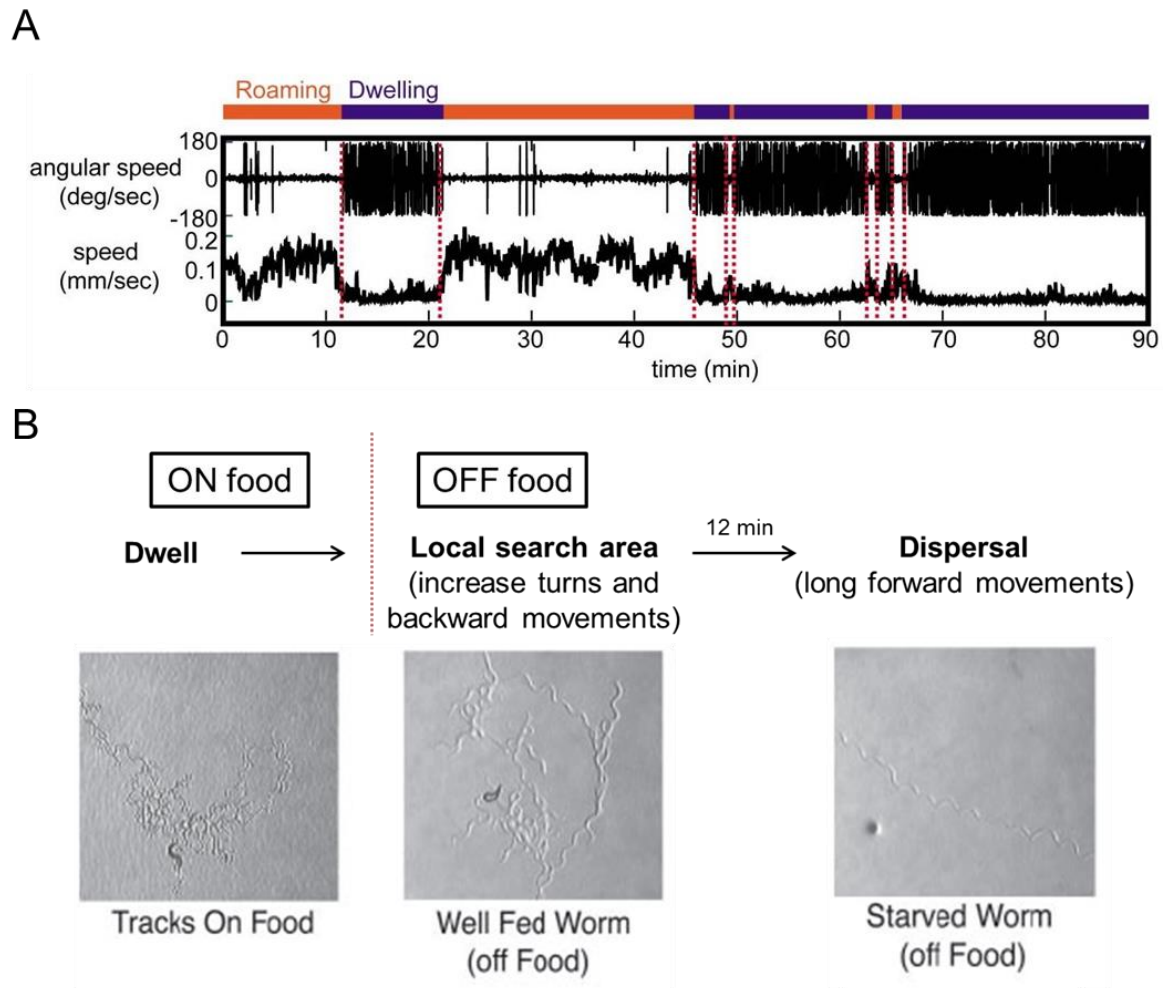


Figure 11: Adaptive locomotory behaviour in response to food withdrawal.

A. Locomotion patterns of *C. elegans* in the presence of food. Turning events and speed are modified to give two distinct behaviours; dwelling (low speed and high turning rate) and roaming (high speed and low turning rate).

B. Tracks of an individual worm on food and removed from food for 1 and 12 minutes. A wild type worm keep on food dwells.

After food removal, the worm changes its locomotion pattern and displays a Local Search Area behaviour. An increase in turn and backward movement frequencies is observed during locomotion permitting exploration of a restricted area.

Chapter 1

12 min following removal of food, the worm displays a behavioural shift to a dispersal phase. Long forward movements (runs) are observed permitting to explore further area in hope to find food. Modified from Gray *et al.* 2005.

Worms constantly assess the quality of food. *C. elegans* sometimes leaves its food patch in search for 'better' food. For instance, food patch leaving probability is higher from bacteria scored as poor quality food (DA837) compared to those with high-quality (HB101) based on their growth promoting potential (Shtonda and Avery, 2006).

In 2011, Milward *et al.* observed that the probability of seeing worms leave food increases when the food becomes depleted over time (i.e. when the food becomes depleted) and they have underlined several sensory neurons involved in the regulation of this adaptive food-leaving behaviour (Milward *et al.*, 2011). Among them, the neurons expressing the cGMP-gated ion channel subunits TAX-2/TAX-4, which are important for the modulation of chemosensory transduction (Komatsu *et al.*, 1996), promote food-leaving as *tax-2* and *tax-4* mutants show a marked reduction of food-leaving probability. Specific rescue of *tax-2* expression in sensory neurons indeed revealed that the CO₂-sensing neurons ASE and BAG (Bretscher *et al.*, 2008; Bretscher *et al.*, 2011), as well as one or more of the O₂ sensing neurons AQR, PQR and URX increase food-leaving events. The perception of CO₂ by ASE, AFD and/or BAG neurons plays a role in food leaving behaviour since worms lacking these neurons display a reduced food-leaving phenotype induced by an increase of CO₂ (Milward *et al.*, 2011). Conversely, OCR-2 (transient receptor potential V-like channel associated subunit) acts in ADF neuron to inhibit food-leaving.

AFD neurons appear to be able to both promote and inhibit food-leaving depending on the context. Indeed, when ASE and BAG neurons are defective, AFDs promote food leaving, while in contrast, AFDs act to suppress food-leaving when ASE and BAG neurons are functional (Milward *et al.*, 2011). This is similar to the role of AFD in CO₂ avoidance, in which AFD can both promote and suppress avoidance (Bretscher *et al.*, 2011).

Behavioural comparison between the N2 strain and other wild-type isolates, including the Hawaiian CB4856 strain or the German strain RC301, revealed two distinct feeding behaviours on food. When entering food, N2 worms slow their locomotion rate and disperse on the food lawn. In contrast, the CB4856 and RC301 strains maintain a high locomotion rate and aggregate on the border of the lawn forming clumps of worms (de Bono and Bargmann, 1998). The N2 dispersion behaviour is referred as solitary feeding in contrast to the aggregation behaviour referred as social feeding. Remarkably, this difference in social feeding behaviour is associated with a polymorphism in the neuropeptide Y-like receptor (NPR) encoding gene *npr-1* (see **section 1.3.3.2**) (de Bono and Bargmann, 1998).

Aggregation and bordering is promoted by the O₂-sensing neurons URX, AQR and PQR in response to hyperoxic condition (high O₂ concentration) (Gray *et al.*, 2004). URX, AQR and PQR promote hyperoxia avoidance. Because of the highest concentration of bacteria in the border of a bacterial lawn, O₂ concentration is reduced relative to the centre of the lawn or outside the lawn (Gray *et al.*, 2004). Therefore, URX, AQR and PQR may promote aggregation and bordering via their hyperoxia avoidance role, leading the worm towards the border of the bacterial lawn where the O₂ concentration is lower.

The nociceptive ASH and ADL neurons promote social feeding behaviour as their simultaneous ablation, but not individual ablation, suppress social feeding behaviour displayed by *npr-1(ad609)* mutants (de Bono *et al.*, 2002).

1.2.2 Pharyngeal pumping

1.2.2.1 The Pharynx

Worms feed almost continuously through their life cycle, except during moult or dauer stage (Wormatlas), although there is a clear age dependent decline in pharyngeal pumping (Mulcahy *et al.*, 2013). Bacteria, their main source of food, are taken up and transported from the mouth to the intestine by the pharynx. The pivotal role of the pharynx in mediating *C. elegans* feeding makes investigation of the control of the pharyngeal pumping an explicit route to probe feeding behaviour.

Chapter 1

The pharynx organ is a muscular pump 100 μm long structure with a diameter of 20 μm , isolated from the rest of the body by a basement membrane. Its anatomy has been investigated by the reconstruction of serial section electron micrographs in 1976 by Albertson and Thomson (Albertson and Thomson, 1976). It is composed of 20 muscle cells, among them some are syncytial, forming eight muscle layers, pm1-8 (Franks *et al.*, 2006). These muscles finally form the three main compartments of the pharynx: the corpus, the isthmus and the terminal bulb (**Figure 12**) (Avery and Shtonda, 2003).

The pharynx acts as a pump and transports ingested bacteria by coordinated peristalsis. It generates pressure to force bacteria into the intestine by contracting. Furthermore, the pharynx also concentrates bacteria before ingestion. Bacteria are suspended in liquid, and when pumped into the pharynx, most of the liquid is expelled through the mouth concentrating food prior to transport into the intestine (**Figure 12C**). Furthermore, isthmus peristalsis allows for the transport of food particles to the terminal bulb and occurs once for every four pumps a mechanism that further concentrates the bacteria (Avery and Horvitz, 1989; Avery and Shtonda, 2003). This is believed to facilitate the action of digestive enzymes that breakdown the bacteria and thus enhances nutrient transfer (Avery and Shtonda, 2003).

C. elegans is a filter-feeder and utilizes the radially orientated (a tri-radial symmetry) muscles of the pharynx (corpus and anterior isthmus) to open the lumen when they contract. By following blue-dyed 0.8 μm latex beads through the pharynx during pumping, food transport in the pharynx has been detailed (Avery and Shtonda, 2003). A summary can be found in **Figure 12C**.

The pharyngeal muscles of the worm are electrically coupled by gap junctions. This is similar to the vertebrate cardiac muscle cells and plays an important role in synchronizing contractility (Starich *et al.*, 1996). The *C. elegans* genome does not contain genes encoding connexins, found in most of the vertebrate gap junctions, but instead possesses a family of gap junction-forming proteins called innexins (Phelan *et al.*, 1998). In the innexin *eat-5(ad464)* mutant, the corpus and terminal bulb contractions are

desynchronized (Starich *et al.*, 1996). This network is thought to play an important role in coordinating the muscle response which despite an intrinsic myogenic activity is largely co-ordinated by the overlying pharyngeal nervous system (Li *et al.*, 2003; Starich *et al.*, 2003).

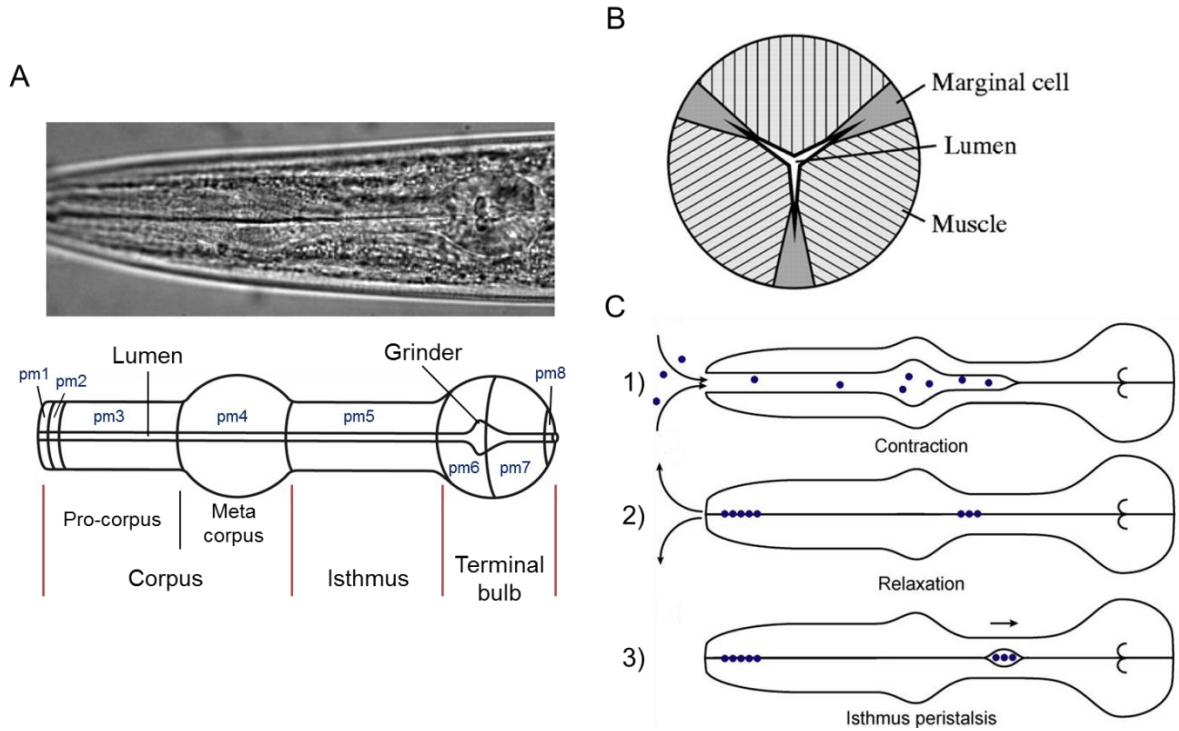


Figure 12: Food motion during pharyngeal pumping.

A. DIC 63X image of a N2 pharynx and schematic representation of *C. elegans* pharynx. The pharynx is made-up of three distinct specializations. The corpus, composed of the procorpus in its anterior part and the metacarpus in its posterior part. The terminal bulb is the most posterior compartment. The Grinder, a muscle specialising in smashing the food, is localised in the terminal bulb. Finally, the Isthmus is the link between the Corpus and the Terminal Bulb. pm = pharyngeal muscle. **B.** Schematic representation of a cross-section in the pharynx. Lumen is closed due to the relaxation of radially orientated muscles. Orientation of actin-myosin filaments is represented by hatching. Apices are anchored by three intermediate-filament-containing marginal cells. Taken from Avery *et al.* 2012. **C.** Pharyngeal pumping. (1) Food enters into the corpus which contracts (altogether with the anterior isthmus) when the pump

Chapter 1

begins leading to the opening of the lumen, allowing the fluids to rush in at the mouth. (2) The corpus relaxes, closing the lumen, and the fluids are then expelled while the bacteria are trapped and transported posteriorly. Simultaneous with the corpus contraction, the terminal bulb contracts, leading to the rotation of the plates of the Grinder in order to smash the bacteria and to push the debris into the intestine. (3) Between those two compartments, the isthmus also plays an important role. During pumping, the posterior isthmus remains closed and isolates the corpus from the terminal bulb. Bacteria are transported in the terminal bulb only during isthmus peristalsis, an event occurring approximately every four pumps (Avery and Horvitz, 1987, 1989). This allows bacteria to be concentrated in the isthmus before they can reach the terminal bulb where they will be subsequently smashed by the grinder and transported through the intestine. Taken from Fang-Yen *et al.* 2009.

The pharyngeal pump rate can be easily assessed by direct observation utilizing a dissection microscope at 40X magnification. The number of pharyngeal contractions is assessed by observation of the grinder's movement, considering that a forward-backward movement counts as a pump. In the presence of food, wild type worms usually show a pumping rate around 250 ppm (pump.min⁻¹) (Walker *et al.*, 2002) which is much reduced in the absence of food (Sze *et al.*, 2000; Hobson *et al.*, 2006; You *et al.*, 2006).

1.2.2.2 The pharyngeal nervous system

The pharynx possesses its own nervous system composed of 20 neurons (Albertson and Thomson, 1976) (**Figure 13**). The pharyngeal nervous system is isolated from the rest of the body by a basement membrane, and is linked to the extra-pharyngeal nervous-system by a sole pair of RIP neurons (White *et al.*, 1986). RIPs interact with the pharyngeal nervous system via a gap junction with the pharyngeal neurons I1 (Albertson and Thomson, 1976) (**Figure 13A**). There is no known chemical post-synaptic interaction between RIP and the pharyngeal neurons (White *et al.*, 1986).

The 20 pharyngeal neurons are divided in 14 distinct types, with 6 bilaterally paired and 8 single neurons. Most pharyngeal neurons are unbranched, unipolar or bipolar (Albertson and Thomson, 1976), and their processes form “en passant” synapses with their targets. The pharyngeal neurons release three types of classical fast neurotransmitters: glutamate, acetylcholine and 5-HT (**Figure 13B**). However, the pharyngeal nervous system expresses receptors for neurotransmitters which it does not synthesise, for instance dopamine DOP-4 receptor on I1, I2 and NSM (Sugiura *et al.*, 2005), indicating these transmitters can act on the pharynx by volume transmission (see **Section 1.1.2.5**).

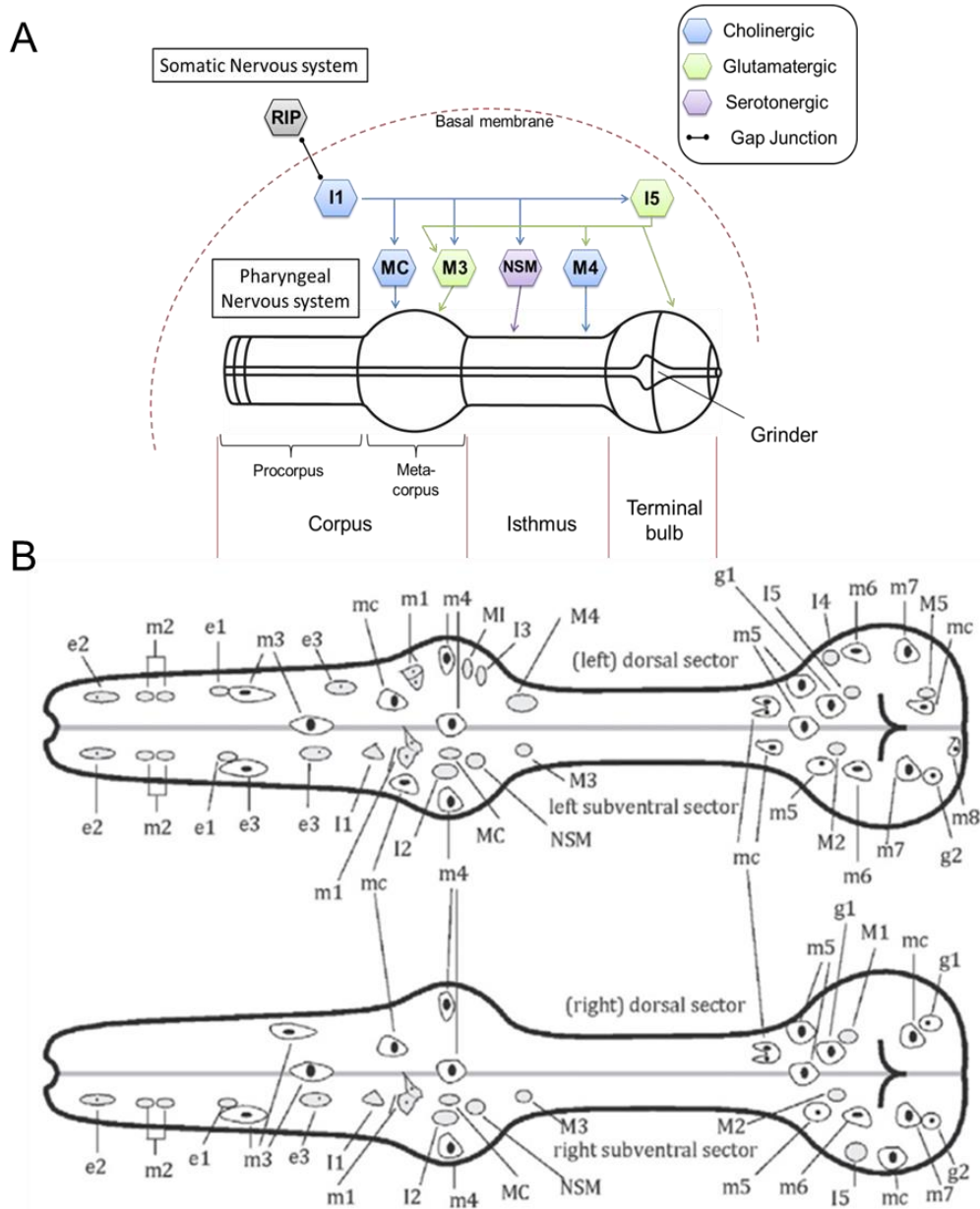


Figure 13: The main neural components of the pharyngeal nervous system.

A. The pharynx (composed of a corpus, isthmus and terminal bulb) and its embedded nervous system are isolated from the rest of the body by a basal membrane, and only physically linked to the somatic nervous system by the RIP-I1 gap junction. MC (cholinergic), M3 (glutamatergic) and NSM (serotonergic) are the main pharyngeal neurons known to control pharyngeal pumping rate in the presence of food. **B.** Map of the pharyngeal neuron somas.

Taken from *Fang-Yen et al. 2012*

Complete pharyngeal neurons list: Motorneurons: M1, M2L/R, M3L/R, M4, M5. Interneurons: I1L/R, I2L/R, I3, I4, I5, I6. Other neurons: MI, NSML/R, MCL/R.

1.2.2.3 Cellular basis of pharyngeal pumping

Among pharyngeal neurons, three motorneurons play a key role in the regulation of the pharyngeal pumping: MC, M3 and M4. M4, which synapses with the posterior part of pm5, is known to be essential for growth and viability. Indeed, M4 ablation has been shown to stop growth as worms cannot ingest food since the posterior part of the isthmus remains relaxed and the lumen closed (Avery and Horvitz, 1989). It appears that worms lacking M4 would be viable on smaller bacteria. However data supporting this result have not been published yet (Avery, 2010).

The M3 motorneurons, synapsing with pm4, control the pumping duration by triggering the end of a pump motion by initiating pharyngeal relaxation (Avery, 1993). In this regard, M3 ablation increases the pharyngeal contraction duration and therefore reducing the pumping rate (Raizen *et al.*, 1995). This is driven by glutamate signalling acting on the glutamate gated chloride channel AVR-15 expressed on pm4 and pm5 (Dent *et al.*, 1997).

Finally, the MC motorneurons synapse with pm4 (metacorpus) and are responsible for the fast pharyngeal pumping rate. MC ablation indeed reduces significantly the pharyngeal pumping (~ 5 fold slower) reducing food intake and therefore slowing growth and conferring a starved phenotype to ablated worms (Avery and Horvitz, 1989). Moreover, it is believed that MCs may act as mechanosensory neurons due to their free subcuticular endings between pm3 and pm4 which could physically detect the presence of bacteria in the pharynx (White *et al.*, 1986; Franks *et al.*, 2006).

Strikingly, after total laser ablation of the pharyngeal nervous system, the pharynx continues to pump slowly (Avery and Horvitz, 1989). This result implies there is an underlying myogenic activity of the pharynx. However the neurons, for instance MC, M3, and M4, play a critical role in modulating the pumping rate.

1.3 Neuronal regulation of the feeding behaviours

Feeding behaviours are mediated by the nervous system. In order to better understand the fundamental mechanisms underlying feeding behaviours, many studies in *C. elegans* aimed to investigate the molecular and cellular determinants involved in the control of both locomotion and pharyngeal pumping. The following section describes the role of individual transmitters on the regulation of these feeding behaviours.

1.3.1 Neurotransmitter

The product of the gene *unc-13* is essential for proper classical neurotransmitter release at synaptic clefts (see **section 1.1.2.3**) (Kohn *et al.*, 2000). Mutants for *unc-13(s69)* show defects in both pumping and locomotion (Richmond *et al.*, 2001). The *unc-13(s69)* mutants indeed displayed uncoordinated locomotion, as indicated by the 'unc', almost paralysing the worms with a greatly reduced pumping rate on food to around 70 ppm (Richmond *et al.*, 2001). Given the role of *unc-13*, these results indicate an important role for classical neurotransmitters in the control of feeding behaviours.

Conceptually, the classical neurotransmitters represent the synapse to synapse regulation of feeding behaviours. Moreover, together with the description and availability of the worm's connectome (see **section 1.1.2**), the roles of individual neurotransmitters have been increasingly studied to allow researchers to build an understanding of the neuronal circuit underpinnings the control of specific behaviours in response to specific cues.

1.3.1.1 5-HT

1.3.1.1.1 5-HT and pumping behaviours

The biogenic-amine transmitter 5-HT (serotonin) is made in 2 types of pharyngeal neurons (NSM and I5) in addition to 6 other serotonergic neurons in *C. elegans* nervous system (Chase and Koelle, 2007). Different studies have shown that exogenous addition of 5-HT in the presence of food increases the pumping rate by around 40 ppm (Avery and Horvitz, 1990; Niacaris, 2003). In the absence of food, exogenous addition of 5-HT triggers a marked elevation of pumping rate mimicking the rate observed in the presence of food (Sze *et al.*, 2000).

In contrast to the above, *tph-1* mutants deficient in the tryptophan hydroxylase enzyme required for 5-HT synthesis, show a marked reduction in the pump rate in the presence of food (Sze *et al.*, 2000). However, the *tph-1* mutation failed to decrease the pumping rate of worms that have been food-deprived. In the presence of food, 5-HT acts on pharyngeal pumping via the activation of two pharyngeal neurons, M3 and MC (Niacaris, 2003). MC neurons provide the major excitatory drive underpinning elevated pumping rates on food. 5-HT leads to an increase in MC acetylcholine release and also increases the excitability of the pharyngeal muscle (Avery and Horvitz, 1989). In parallel, 5-HT stimulates glutamate release from M3 neurons that controls the pump duration by speeding up the relaxation phase (Avery, 1993). Therefore, 5-HT increases the pumping rate in response to food by stimulating distinct arms of the contraction-relaxation cycle of the pharynx, enhancing the activity of both MC and M3 neurons in response to food and thus shortening the pump duration (Niacaris, 2003). 5-HT also modulates the activity of the pharyngeal neuron M4 to facilitate isthmus peristalsis (Song and Avery, 2012). The physiological source of 5-HT was initially discussed as being NSM-mediated stimulation of the pharyngeal circuit. However more recent data makes a case for the extrapharyngeal neurons ADF primarily contributing to the physiological increase in pumping in response to food. However, it is currently under debate as to whether NSM or ADF are the primary determinants that mediate the 5-HT modulation of the sustained high frequency of pumping in the presence of bacteria (Cunningham *et al.*, 2012; Li *et al.*, 2012).

1.3.1.1.2 5-HT and locomotion behaviours

5-HT signalling also plays an important role in the control of the worm's locomotion. *tph-1(mg280)* mutants display a dwelling-like behaviour off food with an increase in short reversals frequency relative to N2 during both local search area (LSA) and following dispersion (Gray *et al.*, 2005). Ablation of the serotonergic neurons ADF leads to a reduction of forward movement duration correlating with an increase of reversals (Wakabayashi *et al.*, 2004). Therefore 5-HT from ADF modulates both pumping and locomotory behaviours (Cunningham *et al.*, 2012).

In the presence of food, NSMs promote dwelling behaviour and NSMs were proposed as potential sensory neurons that may detect the presence of food, in the pharynx, and in response release 5-HT to modulate locomotion so the worm does not leave the food (Flavell *et al.*, 2013). Overall, these observations indicate that 5-HT in response to food promotes feeding by enhancing the pumping rate and reducing locomotion.

Furthermore, 5-HT released from NSM is also responsible for the enhanced slowing response exhibited by food-deprived worms reintroduced on food (Sawin *et al.*, 2000). Interestingly, this specific role of 5-HT in the control of this state dependent behaviour can be correlated with the control of hyperactive pumping, another state-dependent feeding behaviour (see **section 1.4.3**). These results indeed show that 5-HT not only is a major determinant of the worm's feeding behaviours, but is also crucial in the modulation of the behavioural response to food following a period of fasting.

1.3.1.1.3 Receptors mediating 5-HT regulation of feeding behaviours

The serotonin receptor SER-7 has been shown to control the increase of pumping rate and the regulation of isthmus peristalsis (Song and Avery, 2012). SER-7 is localised on both MC and M4 pharyngeal neurons (Hobson *et al.*, 2003; Hobson *et al.*, 2006). SER-1 5-HT receptor is also found in the pharyngeal muscles and nervous system while SER-4 expression is restricted to neurons (Tsalik *et al.*, 2003). SER-1, similar to SER-7, is required for the

increased feeding rate observed in response to exogenous addition of 5-HT (Srinivasan *et al.*, 2008). Finally, SER-4 (Komuniecki *et al.*, 2004) and MOD-1, a 5-HT gated chloride channel, control the 5-HT dependent reduction of locomotion (Ranganathan *et al.*, 2000), MOD-1 notably has been shown to promote dwelling locomotion on food (Flavell *et al.*, 2013).

1.3.1.2 Glutamate

1.3.1.2.1 Glutamate and pumping behaviours

Glutamate is one of the three classical neurotransmitters expressed in the pharyngeal nervous system (**Figure 13A**) (Serrano-Saiz *et al.*, 2013). In the presence of food, glutamate signalling is involved in the maintenance of the high pumping rate. Mutants for *eat-4*, encoding for a vesicular glutamate transporter (Lee *et al.*, 1999), exhibit a reduced pumping rate in the presence of food (Greer *et al.*, 2008; Lee *et al.*, 2008). As mentioned above, 5-HT released in response to food triggers the activity of the glutamatergic pharyngeal neurons M3 (Niacaris, 2003). The fast inhibitory glutamatergic transmission is mediated by a glutamate-gated chloride channel encoded by *avr-15* expressed on the pharynx muscles pm4 and pm5 (Dent *et al.*, 1997). The action of glutamate via AVR-15 leads to chloride dependent relaxation that speeds up pump termination (Avery, 1993). Therefore, the glutamate inhibitory tone, which generates fast inhibitory postsynaptic potentials (IPSPs) in the contracted pharyngeal muscle, shortens the pump duration which leads to an increase in pumping frequency. In consequence, mutants deficient for glutamate signalling such as the *eat-4* mutants show a reduced pumping rate (Greer *et al.*, 2008; Lee *et al.*, 2008; Li *et al.*, 2012).

Mechanosensory inputs have been shown to slow down pumping. Tapping the tail of adult worms for instance, reduces the pumping rate by around 6 fold (Keane and Avery, 2003). This phenotype requires glutamate signalling as the *eat-4(ky5)* mutant, deficient in glutamate release, showed a marked resistance to the tap tail effect on pumping. Moreover, this glutamate signalling acts through both glutamate-gated chloride channels AVR-14 and AVR-15 (Keane and Avery, 2003).

1.3.1.2.2 Glutamate and foraging behaviours

Glutamate signalling has also been shown as an important determinant for foraging behaviour. In the presence of food, N2 worms reduce their foraging by decreasing their speed and body bend frequency. *eat-4(n2474)* mutants show a hyperactive foraging behaviour defined by a marked increase of the their body bends' frequency (Lee *et al.*, 2008).

Glutamate signalling is necessary for the high turn rate observed during the first minutes spent off food as the *eat-4(ky5)* mutant shows the same high-angle turn (Hills *et al.*, 2004) and reversal followed by omega turn (Chalasani *et al.*, 2007) frequencies after 5 min off food as after 35 min (see **section 1.2.1.2**). The glutamate signalling from the olfactory neurons AWC is directly involved in this although AWC activity cannot account for the entire behaviour as the restoration of glutamate signalling uniquely in AWCs only partially rescued *eat-4* mutants' LSA defect (Chalasani *et al.*, 2007). It is noteworthy that AWC neurons respond to the removal of odours rather than their presence (Chalasani *et al.*, 2007). The glutamatergic gustatory neurons ASK were also shown to promote reversals and to reduce forward locomotion in the absence of food (Wakabayashi *et al.*, 2004; Gray *et al.*, 2005). Both AWC and ASK act through the interneuron AIB to modulate the LSA (Gray *et al.*, 2005). Both ionotropic glutamate receptors GLR-1 and GLR-2 and glutamate-gated chloride channel GLC-3 are required for the high-angle turn and omega turn frequency in response to the removal of food (Hills *et al.*, 2004; Chalasani *et al.*, 2007). Notably, AWCs release glutamate onto AIY, AIA and AIB neurons which have opposite effects depending on the receptor. Indeed, glutamate activates AIB via the GLR-1 receptor while inhibiting the activity of AIY and AIA by binding GLC-3.

1.3.1.3 Acetylcholine

1.3.1.3.1 Acetylcholine in pumping behaviours

In *C. elegans*, acetylcholine (ACh) is the major neurotransmitter at excitatory neuromuscular junctions. ACh is crucial for development and null

mutants for the synaptic vesicle acetylcholine transporter (VACHT) *unc-17* are lethal (Alfonso *et al.*, 1993), hence the necessity to use hypomorphic mutations to investigate adult behaviours. The pharynx has at least 6 cholinergic neurons of which MC is best studied and known to play an important role in the high frequency pump rate observed in the presence of food (see **section 1.2.2.3**). Indeed, subsequent to 5-HT stimulation in response to food, MCs release ACh on nicotinic receptors at the pharyngeal muscle neuromuscular junctions (Raizen *et al.*, 1995; Niacaris, 2003). ACh released from MCs acts on pm4 via the nicotinic cholinergic receptor EAT-2 (McKay *et al.*, 2004). Both the *eat-2(ad465)* mutant and MC ablated worms show a reduced pumping rate in the presence of food (Raizen *et al.*, 1995; McKay *et al.*, 2004).

In addition, a muscarinic subtype of cholinergic receptors GAR-3 has been shown to control the membrane potential and excitation-contraction coupling of the pharyngeal muscle. In worms in which GAR-3 signalling is enhanced, by overexpression of *gar-3* or mutation of *gpb-2*, a G-protein normally acting to reduce GAR-3 signalling, addition of the muscarinic agonist arecoline inhibits pharynx muscle relaxation, keeping the pharynx in an 'open' configuration therefore impairing feeding (Steger and Avery, 2004). In the presence of food, *gar-3(lg1201)* mutants show a reduced pump duration, and thus an increased pumping rate relative to N2, exhibiting abnormally brief contractions of the terminal bulb due to shortened action potentials specifically in the terminal bulb (Steger and Avery, 2004). These results indicate that loss of *gar-3* function speeds up terminal bulb repolarization. In the absence of food, *gar-3(lg1201)* loss-of-function mutation reduces the pumping rate while *gpb-2* mutants show an increased pumping rate off food (You *et al.*, 2006).

Overall, these results indicate a food context-dependent modulation of the pumping rate by GAR-3 signalling. In the presence of food, an enhanced GAR-3 signalling leads to a reduction of the pump rate. In contrast, an enhanced GAR-3 signalling in the absence of food leads to an increased pumping rate while a reduced signalling decreases the pump rate.

1.3.1.3.2 Acetylcholine in locomotory behaviours

ACh is crucial for normal movement such as body bends as shown by the uncoordinated phenotype of *unc-17* mutants (Brenner, 1974; Rand and Russell, 1984), thus unpicking the role of cholinergic transmission on the basis of ACh transmitter nulls is of limited use. However, investigating the contribution made by different cholinergic receptors does reveal insight into roles of food mediated effects.

Interestingly, *eat-2(ad465)* mutants show an enhanced probability of leaving the food patch relative to N2 when placed onto low-quality food such as DA837 (Shtonda and Avery, 2006). Therefore, given the pumping defect of *eat-2(ad465)* mutant, it is possible that the higher leaving probability on low quality-food is due to the lower feeding rate of the mutant as potentially less nutrient are taken from food. This would make the case for a coupling between feeding or nutritional intake and the locomotory circuits. Consistent with this hypothesis, no differences in leaving probability are observed between *eat-2(ad465)* and N2 when placed onto the high-quality food *Comamonas sp.* (Shtonda and Avery, 2006).

1.3.1.4 Dopamine

1.3.1.4.1 Dopamine and pumping behaviours

Dopamine is an important context dependent modulator in both *C. elegans* and higher organisms. In mammals, dopamine modulates the reward system, acting in positive behavioural reinforcement (Di Chiara and Bassareo, 2007).

Currently, there is no evidence that exogenous application of dopamine (up to 30mM) modulates the pumping rate on food (Barros et al., 2014). However, the dopamine receptor DOP-4 is expressed in the pharyngeal nervous system in I1, I2 and NSM (Sugiura et al., 2005), and therefore could potentially impact pharyngeal functions and future work will need to consider a possible role for dopamine in pumping.

1.3.1.4.2 Dopamine and locomotory behaviours

In a way that mimics aspects of the localisation of this biogenic amine in higher organism, dopamine is restricted to a distinct set of neurons. The hermaphrodite worm's nervous system contains three types of dopaminergic neurons ADE, PDE and CEP, all found outside of the pharynx (Franks *et al.*, 2006). ADE and CEP neurons are localised in the head sensilla while PDE is found in the posterior part of the worm (Lints and Emmons, 1999). Interestingly, these three types of neurons are mechanosensory and were shown to have a redundant role in the control of the basal slowing response. Dopamine is indeed required to induce the slowing response on food as the *cat-2(e1112)* mutant, deficient in the tyrosine hydroxylase required for the biosynthesis of dopamine, shows no reduced locomotion in response to food (Sawin *et al.*, 2000). However, dopamine is not involved in the modulation of the enhanced slowing response as *cat-2(e1112)* worms food-deprived for 30 min showed a similar response to food as food-deprived N2. The enhanced slowing response is indeed rather dependent on 5-HT signalling (see **section 1.3.1.1**) (Sawin *et al.*, 2000). Individual ablation of ADE, CEP and PDE have modest effects on the basal slowing response to food, however, ablation of the three types of neurons completely abolished this behaviour (Sawin *et al.*, 2000). This indicates a largely redundant role between the different pathways.

Dopamine signalling is also involved in the control of the LSA. Exogenous application of dopamine increases the high-angled turn frequency (details in **section 1.2.1.2**). Furthermore, dopaminergic CEP and PDE neuron simultaneous ablation, or *cat-2* mutants abolished the LSA adaptive behaviour (Hills *et al.*, 2004). The ability of exogenous dopamine to rescue the LSA deficiency in dopamine deficient mutants is not observed in a glutamate transmission deficient background. This indicates that dopamine modulates the LSA via activation of glutamate signalling (Hills *et al.*, 2004). It is possible that a steady decay in dopaminergic transmission over time during food-deprivation, due to the absence of food cues, may account for the behavioural switch from LSA to dispersion, although no evidence have been shown to reinforce this hypothesis.

Nonetheless, dopamine plays important roles in two distinct locomotory behaviours, both ensuring the worms stay on a restricted area, either to keep

Chapter 1

feeding when food is present or to explore in priority local area when seeking for food.

1.3.1.5 GABA

There is no observation for GABA release or for the presence of GABA receptors in the pharynx (Jorgensen, 2005). Moreover, there is no direct evidence for a GABAergic role in pumping behaviours (Franks *et al.*, 2006).

1.3.1.5.1 GABA in locomotory behaviours

GABA signalling plays the counterpart of ACh in the control of normal locomotion in *C. elegans*. Indeed, GABA is notably expressed in VD and DD neurons required for body bends. For a body bend to happen, muscles must contract on one side while simultaneously be relaxed on the opposite side (**Figure 2**) (Schuske *et al.*, 2004; Donnelly *et al.*, 2013). Therefore, while one muscle is stimulated by ACh, the muscle on the opposite side is relaxed by the inhibitory action of GABA signalling.

Moreover, GABA also mediates foraging behaviour. While exploring its environment, the tip of the worm oscillates from side to side within a narrow range, supposedly to enhance the chances that its chemosensory neurons perceive environmental cues (Jorgensen, 2005). Interestingly, following ablation of the four GABAergic RME neurons, the arc movement appeared exaggerated with a marked increase in the angles range, indicating RMEs limit the range of head swings during foraging.

1.3.1.6 Tyramine

1.3.1.6.1 Tyramine in pumping behaviours

Tyramine via the action of the tyramine β -hydroxylase TBH-1, is converted to the biogenic amine octopamine but is also a bona fide neurotransmitter in its own right (Alkema *et al.*, 2005). The tyrosine decarboxylase 1 (TDC-1) enzyme responsible for the biosynthesis of tyramine is found in three cell

types, RIM, RIC and the uv1 neuroendocrine cells (Alkema et al., 2005). However, since *tbh-1* is expressed in RIM, only RIC and uv1 cells are thought to release tyramine. Furthermore, potential effects of a *tdc-1* mutation may reflect either the role of tyramine or octopamine, and it is therefore necessary to compare with the effect of a *tbh-1* mutation to determine whether the phenotype result from tyramine or octopamine deficiency.

tdc-1(ok914) and *tdc-1(n3419)* mutants show no aberrant pumping behaviour in the presence of food (Greer et al., 2008; Li et al., 2012). However, exogenous application of tyramine inhibits the 5-HT induced high pumping rate of isolated pharynx preparations (Packham et al., 2010) and whole worms (2mM) (Rex et al., 2004; Li et al., 2012). This reduction, up to 60% decrease, is dependent on the tyramine receptor SER-2 (Rex et al., 2004; Li et al., 2012). The SER-2 receptor is found in the pharynx on NSM neurons and the pm1 and pm6 muscles (Tsalik et al., 2003; Rex et al., 2004). Another tyramine receptor, TYRA-2, has been identified (Rex et al., 2005). No role for TYRA-2 has been defined yet, however, analysis of its expression pattern reveals expression in the pharyngeal neurons MC and NSM (Rex et al., 2005). Therefore, TYRA-2 could potentially be a determinant in the modulation of the worm's feeding behaviours.

Tyramine, along with octopamine, was proposed to be released in response to bad/repellent smells in order to reduce feeding (Li et al., 2012).

1.3.1.6.2 Tyramine in locomotory behaviours

Different roles for tyramine in the regulation of locomotion have been demonstrated. For instance, tyramine induces immobilisation in a dose dependent manner (Donnelly et al., 2013), an effect dependent on the receptor SER-2. SER-2 is expressed in a subset of GABAergic neurons, including VD motoneurons (Donnelly et al., 2013). Furthermore, *tdc-1(n3419)* mutant shows no suppression of head oscillations during touch-induced backward movements in worms outside of the bacterial lawn (Alkema et al., 2005). Moreover, no phenotype is observed in *tbh-1(n3247)* mutant, indicating that the effect observed is due to tyramine rather than octopamine. Similarly, *tdc-1(n3419)*, but not *tbh-1(3247)*, shows an increase in spontaneous reversals

Chapter 1

(Alkema et al., 2005). Furthermore, ablation of the primary octopamine releasing neuron, RIC, causes no defect while RIM ablation also leads to an increase of spontaneous reversals.

The tyramine receptor TYRA-3 acts to suppress food-leaving probability. Indeed, a polymorphism between the N2 and Hawaiian strain CB4856 *tyra-3* gene has been shown to underpin the difference in food-leaving frequency between the strains. A N2 worm leaves food on average once every 100 min while the CB4856 leaves food once every 5-6 min (Bendesky *et al.*, 2011). Injection of the N2 *tyra-3* or high quantity of CB4856 *tyra-3* genomic DNA rescues the high leaving frequency of the CB4856 strain, indicating the N2 *tyra-3* is more active than the CB4856 one in suppressing the frequency of the leaving event. Moreover, specific expression of *tyra-3* in the sensory neurons BAG or ASK partially rescues the leaving rate of CB4856 (Bendesky *et al.*, 2011).

tyra-3 inactivation by RNAi leads to an increased locomotion rate (body bends per min) in the absence of food, but has no effect in the presence of 5-HT (Carre-Pierrat *et al.*, 2006).

1.3.1.7 Octopamine

1.3.1.7.1 Octopamine in pumping behaviours

Octopamine is only synthesised by TBH-1 from tyramine in the RIC interneurons and the gonadal sheath cells (Alkema *et al.*, 2005). Since the TBH-1 enzyme produces octopamine from tyramine, only octopamine is reduced by *tbh-1* mutations. Little is known about the effect of *tbh-1* mutation. For instance, *tbh-1(n3247)* and *tbh-1(ok1196)* mutants do not show aberrant pumping in the presence of food (Greer *et al.*, 2008; Li *et al.*, 2012). However, exogenous addition of octopamine, similarly to tyramine, reduces the pumping rate of whole worms (Horvitz *et al.*, 1982). Moreover, octopamine also reduces the 5-HT induced high pumping rate of cut pharynx preparations (Rogers *et al.*, 2001; Packham *et al.*, 2010). Notably, octopamine has the opposite effect to 5-HT, increasing the pharynx action potential duration, observed by EPG, by

suppressing M3 activity (Niacaris, 2003), therefore reducing the pumping rate (Rogers *et al.*, 2001).

While octopamine is not synthesised in the pharyngeal nervous system, the octopamine receptor SER-3 is found in the pharynx muscle (Carre-Pierrat *et al.*, 2006), suggesting octopamine can act as a neurohormone to regulate pharyngeal pumping. The *ser-3(ad1774)* mutant displays a slightly lower pumping rate in the absence of food, after 2 hours of food deprivation, or in presence of 5-HT (~15 ppm less relative to N2) (Carre-Pierrat *et al.*, 2006). Furthermore, SER-3 receptor is expressed on the cholinergic SIA neurons, and is required for the SIAs activation upon food-deprivation triggered by octopamine release from RIC neurons (Suo *et al.*, 2006). However, the role of SIA neurons on feeding behaviours is not known.

1.3.1.7.2 Octopamine in locomotory behaviours

SER-3's role on locomotion rate appears dependent on the 5-HT context. *ser-3(ad1774)* mutants show an enhanced body bends frequency in the absence of food and 5-HT (Carre-Pierrat *et al.*, 2006). In contrast, in the presence of 5-HT, *ser-3(ad1774)* mutants show a further reduction of the locomotion rate relative to N2.

1.3.2 Neuropeptides/neurohormonal regulation of feeding behaviours

1.3.2.1 The net effect of neurohormonal signalling in feeding behaviours

Different methods have been used to genetically investigate the role of global neuropeptide signalling in *C. elegans*. In general, they involved mutants deficient in the processing or the release of neuropeptides.

Chapter 1

For instance, both the proprotein convertase *egl-3/pc2(nu349)* mutants, and the carboxypeptidase *egl-21/cpe(n476)* mutants (see **section 1.1.2.4**) are defective in mechanosensation and locomotion (Kass *et al.*, 2001; Jacob and Kaplan, 2003). More specifically, mutants for *egl-3* show insensitivity to gentle body touch with only 20% of the *egl-3(nr2090)* mutant tested responding relative to almost 100% of N2 (Kass *et al.*, 2001). Furthermore, an *egl-3(nr2090)* mutant shows a reduced locomotion rate (body bends per min) (Edwards *et al.*, 2009). In addition, peptides processed by EGL-3/KPC-2 act to stimulate the pumping rate in the absence of food as *egl-3/kpc-2* mutants display a reduced pumping rate after 1 hour in the absence of food (Cheong *et al.*, 2015).

Among the other proprotein convertases (see **section 1.1.2.4**), little is known about the role of *kpc-1*, however, a *kpc-1* deletion mutant displays mild locomotory defects, uncoordinated movements, and slow growth, indicating a requirement for KPC-1 processed peptides for normal movement and growth (Thacker and Rose, 2000). *aex-5/kpc-3* regulates the worm's defecation cycle (Thomas, 1990). More recently, *aex-5/kpc-3* has been proposed to regulate the secretion of an intestinal signal controlling defecation behaviours via activation of the GPCR *aex-2* on AVL and DVB neurons (Mahoney *et al.*, 2008). Finally, *kpc-4/bli-4* was involved in the modulation of chemotaxis to salt by cleaving the insulin peptide INS-6 in the ASEL gustatory neuron (Leinwand and Chalasani, 2013).

The worm's CAPS ortholog, *unc-31*, is also required for a proper chemotaxis to high salt concentrations, suggesting an UNC-31-dependent release of the INS-6 peptide to modulate locomotion in response to high salt concentrations (Leinwand and Chalasani, 2013). Moreover, *unc-31* mutants display an uncoordinated locomotory behaviour and show slow movements on food (Brenner, 1974; Edwards *et al.*, 2009). UNC-31 is required in the inhibition of repetitive turning behaviour (Liu *et al.*, 2007). Finally, UNC-31 was also involved in the reduction of the pumping rate observed off food as *unc-31* mutants show a higher constitutive pumping rate during food deprivation (Avery *et al.*, 1993).

An *unc-108/Rab-2* mutation has been shown to impair the dense core vesicles function and accounts for a defect of locomotion rate (body bends

frequency) on food (Edwards *et al.*, 2009) and backing movement (Mangahas *et al.*, 2008). The effect of *unc-108/Rab-2* on neuropeptide is reinforced by the fact that *unc-108/rab-2* mutation does not further decrease the *unc-31(e928)* reduced locomotion (Edwards *et al.*, 2009).

Overall these data demonstrate that neuropeptides play a key role in the regulation of feeding behaviours.

1.3.2.2 Role of individual neuropeptides in the control of feeding behaviours

1.3.2.2.1 Role in pumping behaviours

Little is known about the role of neuropeptides in the regulation of the worm's pumping behaviour. In 2005, a study investigating the role of FLP neuropeptides was published (Papaioannou *et al.*, 2005). At least one FLP peptide encoded by each of the 26 *flp* genes tested was exogenously applied to semi-intact pharyngeal preparations and the effect on the pumping rate assessed by electropharyngeogram (EPG). Nine FLPs had an excitatory effect in absence of 5-HT stimulation, in which FLP-17A, FLP-17B and FLP-8(AF1) were more potent than FLP-2A, FLP-4A, FLP-5A, FLP-6(AF8) and FLP-22. In contrast, 12 FLP peptides induced an inhibitory effect, viz, FLP-11A and FLP-13A for the most potent effect in the presence of 5-HT relative to FLP-1A1, FLP-1A2, FLP-3A, FLP-9A and FLP-19A. FLP-14B, FLP-15A, FLP-16A(AF15), FLP-18A and FLP-21(AF9) also induced inhibition but in the absence of 5-HT. The peptides FLP-7A, FLP-10A, FLP-12A, FLP-14C, FLP-20 and FLP-23 showed no effect using this preparation.

In 2008, a similar study was conducted using 6 NLP peptides encoded by 5 *nlp* genes (Papaioannou *et al.*, 2008a). Four of those NLPs triggered an excitation of the pump rate; NLP-1A, NLP-2A, NLP-3 and NLP-10A with the latter leading to the most potent excitation. NLP-8 application led to a weak inhibition while NLP-2B had no effect. The effects of those neuropeptides are summarized in **Table 5 (Chapter 5)**.

Although NLP-24 appears not to be involved in the regulation of the pumping rate in the presence of food, an *nlp-24(tm2105)* mutant shows a

Chapter 1

reduced pumping rate off food after 1 hour of food deprivation, indicating a context-dependent effect of NLP-24 (Cheong *et al.*, 2015). Furthermore, NLP-24 stimulates pumping off food via the receptor NPR-17.

1.3.2.2.2 Role in foraging behaviours

Some neuropeptides have previously been shown to be involved in the regulation of foraging behaviours. PDF-1 was recently shown to promote long roaming states as oppose to dwelling (Flavell *et al.*, 2013). Overall these data demonstrate that neuropeptides play a key role in the regulation of foraging behaviours.

In 2009, Cohen *et al.* showed that *flp-18* mutants are defective in olfactory behaviour and in adaptive response to food deprivation: 15 min after the withdrawal of food (local search behaviour), worms failed to enter the dispersal phase. The reintroduction of a wild-type copy of *flp-18* cDNA in AIY alone was sufficient to rescue this phenotype (Cohen *et al.*, 2009). AIY is thus important in the decision-making event which allows the worm to switch its behaviour from local search to dispersal (see **section 1.2.1.2**). Finally the authors also demonstrated that FLP-18s are able to activate NPR-4 receptors on AVA and RIV interneurons involved in the regulation of foraging behaviour by acting on reversals and turns, respectively (Chalfie *et al.*, 1985; Gray *et al.*, 2005). FLP-18 and FLP-21 have both been shown to bind NPR-1 receptors and regulate social feeding (Boender *et al.*, 2011).

Finally, the neuropeptides encoded by *flp-1* act to reduce the worm's locomotion. Mutants for *flp-1* are indeed hyperactive while conversely, overexpression of those peptides reduced worm mobility (Nelson, 1998).

1.3.3 Neuropeptide receptors' role in feeding behaviours

1.3.3.1 General overview

In 1998, one of the first analyses of the *C. elegans* genome showed that more than 5% of the worm's genes, around 1300, encoded for GPCR receptors

(Bargmann, 1998). Around 100 were found to share clear sequence homology with identified receptor genes in other animals, while 1000 were referred as 'orphan', indicating worm-specific receptors. To date, only few of the worm-specific GPCR have been 'deorphanized', i.e. for which ligand(s) have been identified, and functionally characterized as neuropeptide GPCRs (**Figure 14**). Identification of ligands ('deorphanization') for individual GPCR has been undertaken in many studies investigating the role of those GPCRs. A reverse pharmacology approach is usually used, by expressing the orphan GPCR in Chinese hamster ovary (CHO) or human embryonic kidney (HEK) cells and testing the effects of a library, or candidate, neuropeptides on them (Szekeres, 2002; Beets *et al.*, 2011).

In 2010, Janssen and colleagues used a Multiple Expectation Maximization for Motif Elicitation/Motif Alignment and Search Tool (MEME/MAST) analysis to predict neuropeptide GPCRs, and the method has been enhanced in 2012 to increase the number of 'deorphanized' neuropeptide GPCRs from 6 to 23 (Janssen *et al.*, 2010; Frooninckx *et al.*, 2012). GPCR receptors can be classified according to the GRAFS classification (Glutamate, Rhodopsin, Adhesion, Frizzled, and Secretin families) proposed by Fredriksson and Schiöth, who showed these main families arose before the split of nematodes from the chordate lineage (Fredriksson and Schiöth, 2005) (**Figure 14**). Predicted neuropeptide GPCRs are part of the Rhodopsin and Secretin family, the former being subdivided into distinct groups based on their homology with insect and mammalian receptors. The best known and most studied, being the neuropeptide Y (NPY)/RFamide-like receptor family. Found in the mammalian brain, Neuropeptide Y (NPY) is one the most potent orexigenic peptides to induce food intake (Stanley and Leibowitz, 1984; Morley *et al.*, 1987). Furthermore, NPY has been shown to induce carbohydrate preference (Stanley *et al.*, 1989) and is related to hyperphagia and obesity (Beck *et al.*, 1990; Beck *et al.*, 1993; Sahu *et al.*, 1997).

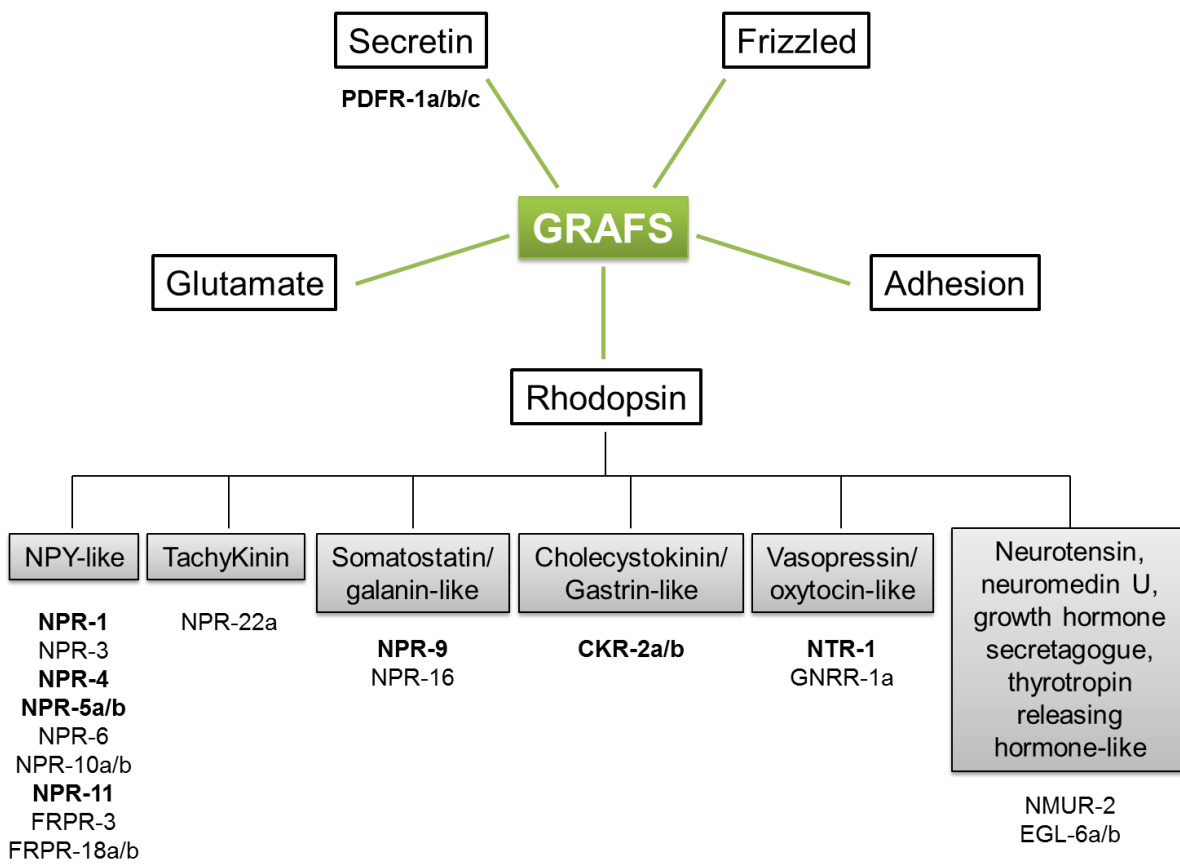


Figure 14: Simplified summary of GPCR type receptors found in *C. elegans* organised according to the GRAFS classification.

GRAFS classification stands for Glutamate, Rhodopsin, Adhesion, Frizzled, and Secretin families. Only deorphanised neuropeptide receptors are indicated. Receptors annotated in bold have a known role in the control of feeding behaviours.

1.3.3.2 NPY-like receptors

In *C. elegans*, 12 of the 41 members (Frooninckx *et al.*, 2012) have been ‘deorphanised’; NPR-1 (FLP-18, FLP-21), NPR-3 (FLP-15), NPR-4 (FLP-4, FLP-18), NPR-5a/b (FLP-18), NPR-6 (FLP-18), NPR-10a/b (FLP-3), NPR-11 (FLP-11), FRPR-3 (FLP-7, FLP-11), and FRPR-18a/b (FLP-2) with the main cognate peptide ligand in brackets. Studies over the years revealed various functions for those receptors. Inactivation by RNAi of the following neuropeptide receptor genes, *npr-4*, *npr-*

6, *npr-11* and *frpr-3* led to a defect in brood size while inactivation of *npr-2* and *npr-3* induced locomotion defects (Keating *et al.*, 2003).

NPR-1, one of the most studied neuropeptide receptors, is a key determinant of the social feeding behaviour. N2 worms are solitary feeders, dispersing on food, while other wild-type isolates are social feeders, characterised by the formation of clumps on the border of the bacterial lawn and an increased locomotion speed on food relative to N2 (see **section 1.2.1.2**) (de Bono and Bargmann, 1998; Rogers *et al.*, 2003). A single nucleotide polymorphism at the residue 215 of the *npr-1* gene is responsible for the distinct behaviours. The valine found in the NPR-1 of the N2 strain (NPR-1 215V) is substituted with a phenylalanine (NPR-1 215F) in the social feeder strains. Since the *npr-1* mutant strains show a social feeding behaviour, it was proposed that *npr-1* 215F is a less active form than *npr-1* 215V. Indeed, a 3 to 10 fold overexpression of the *npr-1* 215F form relative to the *npr-1* 215V is required to rescue the social feeding behaviour in an *npr-1* mutant (de Bono and Bargmann, 1998), indicating that both NPR-1 forms are able to suppress the social feeding behaviour but with different efficiency. Interestingly, NPR-1 antagonised the hyperoxia avoidance mediated by URX, AQR and PQR neurons that lead to bordering and aggregation (see **section 1.2.1.2**) (Coates and de Bono, 2002; Cheung *et al.*, 2004). Furthermore, an *npr-1(ad609)* mutant shows an increase in food leaving probability and locomotion speed (Bendesky *et al.*, 2011; Milward *et al.*, 2011). NPR-1 has also been associated with foraging behaviour, with social feeders *npr-1* exhibiting an increased dispersal propensity from one food patch to another relative to solitary feeders N2 (Gloria-Soria and Azevedo, 2008).

NPR-4 and NPR-5 have been implicated in the regulation of distinct behaviours (Cohen *et al.*, 2009). For instance, an *npr-4(tm1782)* mutant exhibits a defect of chemotaxis towards a diluted concentration of benzaldehyde but normal chemotaxis towards higher concentrations. NPR-4 also modulates adaptive foraging behaviours as *npr-4(tm1782)* mutants fail to switch from LSA to the dispersal phase. In contrast, an *npr-5(ok1583)* mutant shows wild-type olfaction and adaptive foraging behaviour. However,

Chapter 1

overexpression of the neuropeptide FLP-18 triggers a marked reduction of locomotion rate by acting on both NPR-4 and NPR-5. Notably, an *npr-5(ok1583)* mutation markedly suppresses the *flp-18* overexpression locomotion defect while *npr-4(tm1782)* shows a weaker but significant rescue, consistent with the interpretation that NPR-5 is a cognate receptor for FLP-18. In addition, both NPR-4 and NPR-5 have been shown to play a role in a distinct food related phenomenon, namely the regulation of fat storage (Cohen *et al.*, 2009).

NPR-11, and its ligand NLP-1, regulate olfactory adaptation and off food search behaviour via a feedback signal to AWC olfactory neurons, limiting their activity and effect on locomotion (Chalasani *et al.*, 2010).

1.3.3.3 Other Rhodopsin family members

Besides the NPY-like receptors, the roles of GPCRs from other sub-divisions of the Rhodopsin family have also been identified. *tkr-3* (tachykinin receptor family) inactivation by RNAi led to slowing locomotion (Keating *et al.*, 2003) and embryo development defects (Simmer *et al.*, 2003). The allatostatin/galanin-like receptor NPR-9 that is selectively expressed in AIB neurons, is implicated in fat storage and the promotion of roaming behaviour on food (Bendena *et al.*, 2008), while RNAi targeting the somatostatin-like receptor *npr-16* induced an increased accumulation of fat (Ashrafi *et al.*, 2003).

Cholecystokinin/gastrin-like receptor CKR-1 plays a role in reproduction as RNAi inactivation leads to decreased brood size and embryonic lethality (Rual *et al.*, 2004). CKR-2 enhances the locomotion rate via a mechanical feedback loop by potentiating transmission at cholinergic neuromuscular junctions (Hu *et al.*, 2011). CKR-2 also acts to modulate fat storage and the stimulation of amylase secretion in the intestine (Janssen *et al.*, 2008), similar to the known CCK/gastrin signalling functions in mammals (e.g. the stimulation of digestive enzyme production) (Konturek *et al.*, 2003).

In 2012, vasopressin/oxytocin (VP/OT)-like receptor NTR-1, for nematocin receptor-1, was shown to affect experience-driven modulation of salt chemotaxis (Beets *et al.*, 2012). Interestingly, this role in gustatory associative learning resonates with one of the roles of the VP/OT signalling system in mammals where it functions in the central nervous system as a neuromodulator of memory and learning (Meyer-Lindenberg *et al.*, 2011).

1.3.3.4 Neurotensin

3 of the 17 known GPCRs of neurotensin, namely, neuromedin U (NMU), growth hormone secretagogue, and thyrotropin releasing hormone (TRH)-like receptors group, have been orphanised: NMUR-2 and EGL-6a/b (Ringstad and Horvitz, 2008; Lindemans *et al.*, 2009). While the role of NMUR-2 is unknown, EGL-6 is believed to have a function in reproduction as the gain-of-function mutant *egl-6(n592)* displays slower egg-laying rate and longer retention of the embryos (Ringstad and Horvitz, 2008).

1.3.3.5 Secretin

Potential roles of two GPCR receptors from the secretin family have been identified recently. SEB-3, an orphan GPCR, has been identified as part of the CRF (corticotropin-releasing factor) system. This includes food related behaviours in which mutants have suppressed dwelling behaviour (Jee *et al.*, 2013). The *pdf-1* gene, orthologous to the *Drosophila* pigment dispersing factor, encodes 3 receptors of the secretin family. A *pdf-1(lst34)* mutant shows locomotion defects with a reduced speed and increased reversal frequency (Meelkop *et al.*, 2012). More recently, signalling through *pdf-1* has been shown to initiate and extend roaming states in the worms in response to food (Flavell *et al.*, 2013).

1.3.3.6 Other peptidergic signalling

Insulin-related peptides (see **section 1.1.2.4**), and in particular the roles of INS-1 and INS-6 peptides described above (see **section 1.3.2.1**), indicate a role

for insulin signalling in the control of the worm feeding behaviours. The insulin/IGF receptor DAF-2 has been implicated in the control of feeding behaviours. For instance, *daf-2* mutants were shown defective in the slow increase of pumping rate normally observed over time in the absence of food (Dwyer and Aamodt, 2013). A mutant for the insulin/IGF receptor *daf-2* shows a reduced mobility and feeding rate on food relative to N2 when maintained at 22.5 °C (Gems *et al.*, 1998).

The DAF-7/TGF- β signalling modulates the high pumping rate observed on food as indicated by the reduced pumping rate exhibited by both *daf-7* and its receptor *daf-1* mutants (Greer *et al.*, 2008). Signalling from *daf-7/daf-1* regulates the pumping rate by blocking the inhibitory tyraminerpic and octopaminergic signalling from RIM and RIC neurons (Greer *et al.*, 2008). No aberrant pumping behaviour was observed in the absence of food. Furthermore, DAF-7/TGF- β signalling also acts to promote roaming behaviours in the presence of food (Ben Arous *et al.*, 2009). Finally, DAF-7 is involved in the control of social feeding behaviour, acting in a parallel pathway to *npr-1* (de Bono *et al.*, 2002).

1.4 Energy storage, metabolism and nutritional status

1.4.1 Energy metabolism

In the preceding sections, locomotory and pumping behaviours have been discussed with the intention of covering food-dependent behaviours. Feeding behaviours are by definition strongly linked to energy homeostasis and therefore impairment in the mechanisms regulating these behaviours may trigger maladapted responses and eventually lead to obesity or metabolic diseases, such as, bulimia nervosa and anorexia nervosa (Jimerson *et al.*, 2010). Because of the occurrence of obesity as a consequence of Western diet (O'Rahilly and Farooqi, 2008), there are an increasing number of studies aiming to shed light on the mechanisms regulating food intake and appetite,

fat storage and metabolism. Model organisms have been extensively used including those like *C. elegans* which have excellent genetic tractability (Belkhou *et al.*, 1991; Jones and Ashrafi, 2009; Mullaney and Ashrafi, 2009). The previous section has focussed on the behavioural response and some of the signalling underpinning food intake, the pharyngeal pumping, and foraging and food related locomotory changes. However, an additional key consideration is how this behaviour is regulated in the context of the internal metabolic and nutritional status of the animal.

Adenosine triphosphate (ATP) is the universal molecule carrying energy. ATP indeed transports chemical energy within cells to fuel metabolism and cellular processes (Knowles, 1980). The production of ATP from the ingested food is therefore crucial for life.

Carbohydrates, fatty acids and proteins are the three key nutrients supplying energy to the organism and are obtained from food (**Figure 15**). Part of this energy, carbohydrates and fat, is stored (Wang *et al.*, 2006). Energy is then obtained by three main metabolic pathways: glycolysis for the use of carbohydrates, fatty acids metabolism (beta-oxidation), and amino-acid metabolism (proteolysis to fuel gluconeogenesis). These pathways provide the major part of the energy needed for maintenance and growth (**Figure 15**). In mammals, most of the carbohydrates are digested and broken down into monosaccharides then mostly transported as glucose. The remaining are transported as fructose and galactose (Alvarado *et al.*, 1984; Drozdowski and Thomson, 2006) and subsequently transformed into glucose and glycogen in the liver (Gannon *et al.*, 2001; Tappy and Le, 2010).

In mammals, carbohydrates are the primary source of energy and are usually used directly without intermediary metabolism to generate the substrates for energy. Alternatively they are used in anabolic metabolism where they are stored as glycogen in muscle cells for their own use as muscle do not release glucose back into the bloodstream (Berg *et al.*, 2002).

Lipids are stored as triglycerides (TAG, also called fats), formed by one glycerol anchoring three fatty acids (FA), in adipose tissues (Wolins *et al.*, 2006; Gross and Silver, 2014). Excess carbohydrate is converted to lipid in the liver (Owen

Chapter 1

et al., 1979). Finally, amino acids can be transformed into glucose through gluconeogenesis or ketone bodies through ketogenesis (Brosnan, 2003; Glew, 2010).

These metabolic routes can lead to the formation of acetyl-CoA which enters the tricarboxylic acid (TCA) cycle and generates NAD(P)H which subsequently enters the electron transport chain pathway to produce energy, ATP, by oxidative phosphorylation (Figure 15).

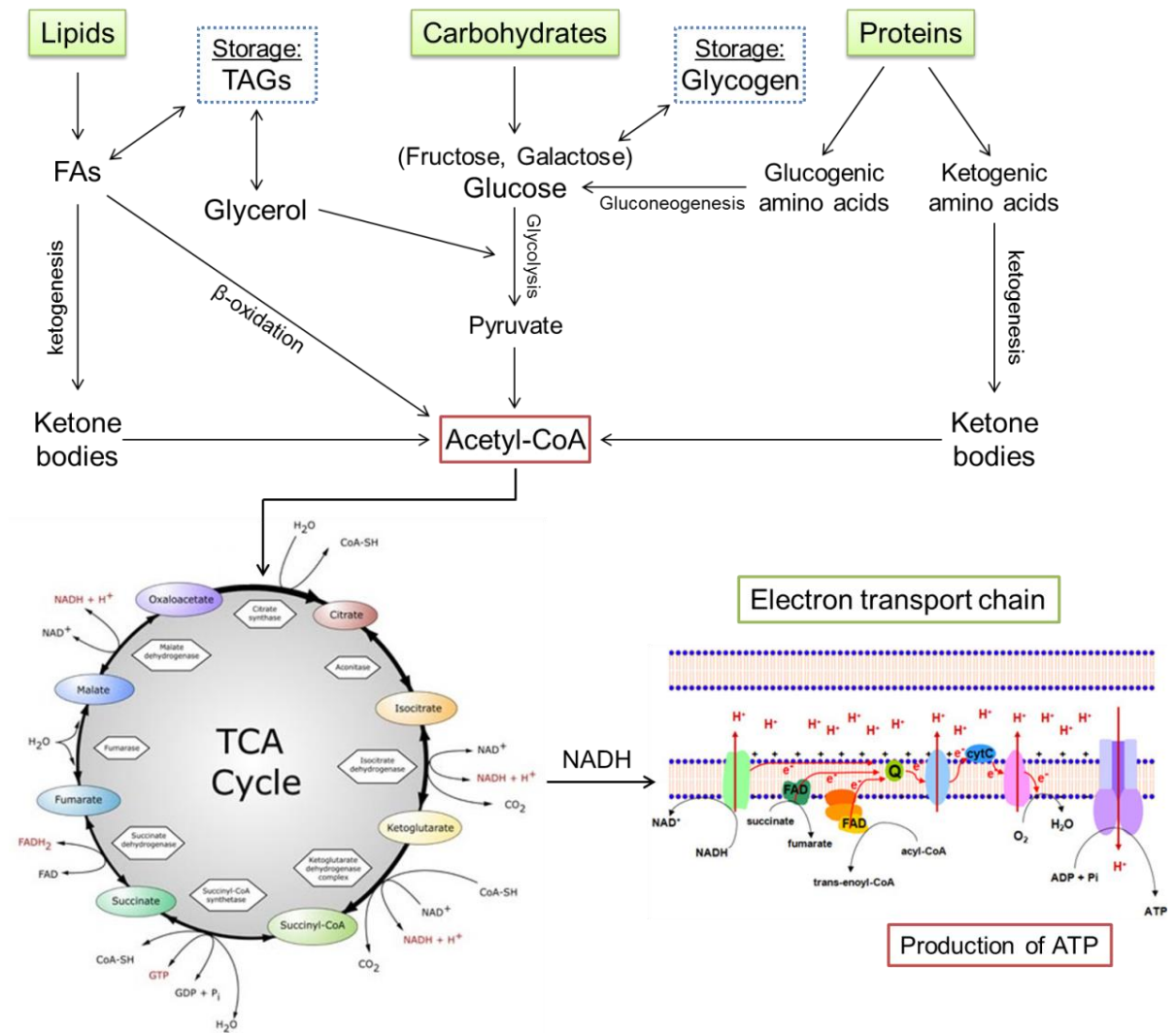


Figure 15: Summary of metabolism and ATP production.

Lipid, carbohydrate and protein metabolic pathways lead to the formation of acetyl-CoA. Fatty acids (FA) from the diet or the breakdown of triglycerides (TAG) are transformed into acetyl-CoA by β-oxidation. FA can also be transformed in ketone bodies that will subsequently be transformed into acetyl-CoA in other tissues. Dietary glucose or from the breakdown of glycogen is converted to pyruvate by glycolysis then further transformed into acetyl-CoA. Amino acids from the breakdown of proteins are divided in two categories. The ketogenic amino acids (e.g. leucine) are converted to ketone bodies while glucogenic amino acids are used for gluconeogenesis in order to produce acetyl-CoA. Acetyl-CoA enters the tricarboxylic (TCA) cycle which generates NADH through different enzymatic reactions. The formed NADH subsequently enters the electron transport chain to fuel ATP production via oxidative phosphorylation. TCA cycle diagram modified from Champe, P.C. *et al.* 1994.

Electron transport chain diagram modified from

<http://www.nature.com/scitable>

1.4.1.1 Food deprivation in 3 phases

It is crucial animals adapt when food becomes scarce. Animals react to food deprivation by switching their metabolism. These metabolic responses are part of an integrated biological response and may have important and evolutionary sound consequences on behaviour (Lutter and Nestler, 2009; Keen-Rhinehart *et al.*, 2013). When no food is available, animals must draw on their internal stores to fuel the energetic requirements for basal energy expenditure (metabolism, physical activity, growth, and reproduction). During food deprivation, both mammals and birds go through three different metabolism phases defined by the progressive metabolic changes occurring over time. These phases are characterised by the difference in energy stores used to fuel vital functions and the associated changes in overall body mass (Cahill *et al.*, 1966; Cahill, 1976; Robin *et al.*, 1988; Andriamampandry *et al.*, 1996; Thouzeau *et al.*, 1999; Bertile *et al.*, 2003).

The initial phase or post-absorptive phase starts immediately after the last meal has been absorbed by the gastrointestinal track and usually lasts for hours (Wang *et al.*, 2006). During this first phase, energy is mainly provided by carbohydrates. Glycogen stores are transformed into glucose by glycogenolysis, and used during the first hours of food deprivation. In parallel, lipid stores start to breakdown TAG and release glycerol and fatty acids allowing tissues, such as, skeletal muscle to use an alternative source of energy and save glucose (Belkhou *et al.*, 1991).

The second phase of food deprivation begins when the glycogen stores in the liver are depleted and when gluconeogenesis, the synthesis of glucose, starts. Indeed, some organs, such as the brain, require glucose to properly function (Nehlig, 2004; Wang *et al.*, 2006). Initially, amino acids obtained from muscle protein proteolysis are used to fuel the gluconeogenesis, however, the consumption of amino acids falls markedly when more glycerol is freed by TAG break down and released by adipose tissues. Indeed, during phase II, most of

the energy (80-90%) is provided by fat oxidation whilst protein degradation is slow and only accounts for the remaining energy expenditure (10-20%) in order to spare the breakdown of vitally needed proteins (Robin *et al.*, 1988; Belkhou *et al.*, 1991; Thouzeau *et al.*, 1999). In addition to glycerol, free fatty acids (FA) are released from the breakdown of TAG and are transformed to acetyl-CoA through β -oxidation to be either directly used to make energy via the TCA (TriCarboxylic Acid) cycle or to produce ketone bodies (in the liver) which will be taken up by other organs and converted back to acetyl-CoA (Laffel, 1999). There is an elevated production of ketone bodies during periods of glucose deficiency, an important process as some organs including the brain cannot use FA but can produce energy from ketone bodies which therefore play a key role in sparing glucose utilization (Randle *et al.*, 1964; Nehlig, 2004) and reducing the proteolysis required to produce glucose (Sherwin *et al.*, 1975). Alternatively, some organs in mammals can directly take up and use FA for energy such as heart or kidneys (Cahill, 1971). In human, this phase can be maintained for several weeks (Wang *et al.*, 2006) but for only around 3 days in rats (Bertile *et al.*, 2003).

Phase III corresponds to longer periods of food-deprivation when adipose lipid stores are progressively depleted and protein degradation progressively rises (Robin *et al.*, 1988). Although the beginning of this phase does not correspond to the complete depletion of adipose stores (Belkhou *et al.*, 1991), muscle proteins are then rapidly degraded to produce glucose via gluconeogenesis which corresponds to a loss in body mass (Bertile *et al.*, 2003; Wang *et al.*, 2006). Unlike phase II, this third phase cannot be sustained for long and rapidly causes animal death (Wang *et al.*, 2006).

Starvation can be defined at the end of phase II or beginning of phase III, i.e. the moment when a shift from protein sparing (phase II) to protein breakdown (Phase III) occurs. Non-essential proteins are used first, muscles are notably broken down first, and the body wastes away. Essential proteins will eventually be used until cell functions ceases.

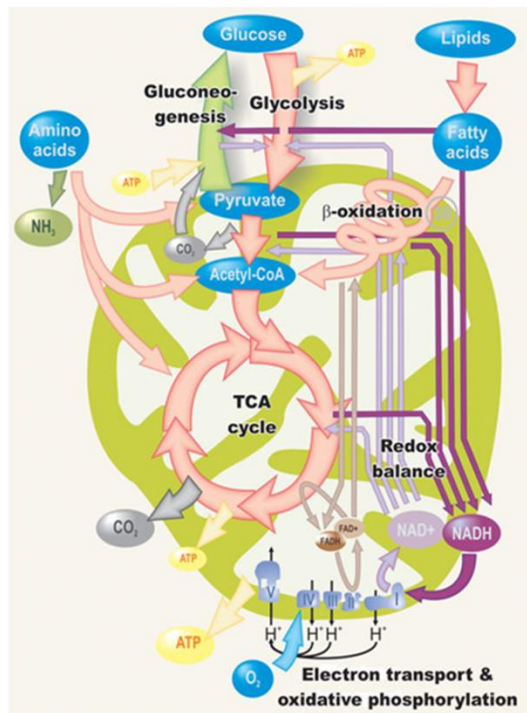
1.4.1.2 Energy metabolism in *C. elegans* and differences with mammals

The main metabolic pathways, providing energy from the three key nutrients, described above, are well conserved in *C. elegans* where orthologs for most of the key enzymes involved in metabolism are found (McElwee *et al.*, 2006; Ashrafi, 2007) (**Figure 16A**). In *C. elegans*, lipids represent the major source of energy for the worms and are obtained as 90% from the bacterial diet whilst the remaining 10% are synthesised internally (Perez and Van Gilst, 2008).

Less is known about carbohydrate metabolism in *C. elegans*. Carbohydrates are also stored as glycogen (found near the pharyngeal terminal bulb, in the tail near the dorsorectal ganglion, in oocytes and gonad arm) (Frazier and Roth, 2009), but can also be stored as trehalose (Behm, 1997; McElwee *et al.*, 2006). Trehalose is a nonreducing disaccharide of glucose present in significant quantities in all stages of the worm (2.3% of dry weight) (Pellerone *et al.*, 2003). Trehalose is important to protect the worm from desiccation, a state of extreme dryness, and is therefore crucial for dauer larvae viability (Erkut *et al.*, 2011). Furthermore, trehalose is also important in energy storage as it can be transformed into glucose by the action of trehalase (Pellerone *et al.*, 2003). Furthermore, trehalose has been detected in all tissues in the nematode *Ascaris suum* (Behm, 1997).

An early study performed on *Caenorhabditis* species (undescribed species) showed that glycogen stores were rapidly used prior to lipids during food deprivation (Cooper and Van Gundy, 1970).

A



B

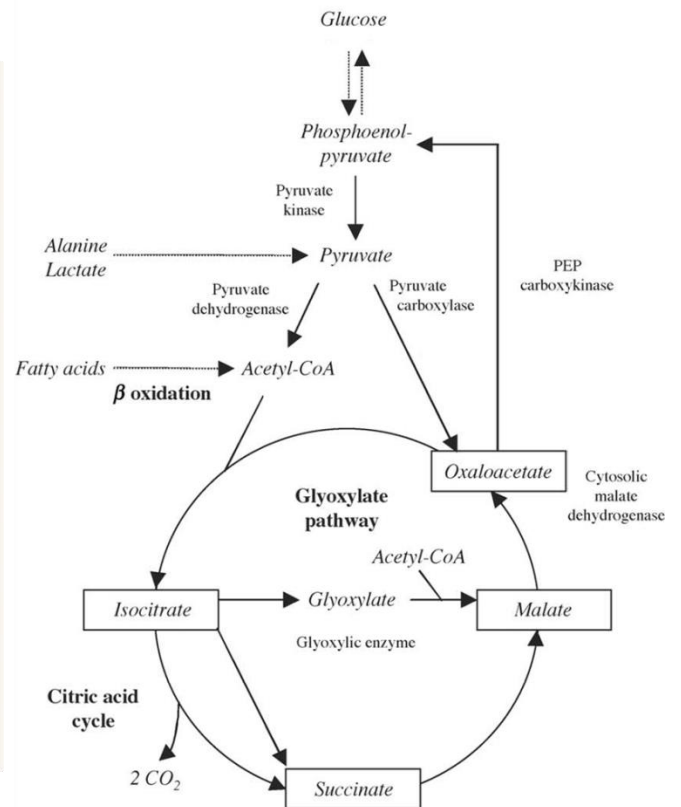


Figure 16: Cartoons of the major conserved pathways of intermediary metabolism in *C. elegans* and of the Glyoxylate cycle.

A. The cartoon depicts the cytosolic and mitochondrial pathways that generate NADH and FADH as key ATP generating intermediates. Briefly, glucose through glycolysis and formation of pyruvate, fatty acids via β -oxidation and amino acids via transformation into pyruvate or ketone bodies lead to the formation of acetyl-CoA. This then enters the TCA cycle (tricarboxylic acid cycle) and generates NADH and FADH that are subsequently transformed into ATP (energy) via the electron transport chain and oxidative phosphorylation. Alternatively glycolysis builds up ATP while β -oxidation and the conversion of pyruvate into Acetyl-CoA also lead to the formation of NADH and FADH by themselves. *Taken from the wormatlas.*

B. The Glyoxylate cycle, not found in mammals, permits the conversion of acetyl-CoA into phosphoenolpyruvate for gluconeogenesis. Modified from McElwee *et al.* 2006.

Chapter 1

However, some differences with mammalian systems exist. *C. elegans* possesses two genes encoding two enzymes, isocitrate lyase and malate synthase. These enzymes are not found in mammals, and in the nematode they permit acetyl-CoA to be used as a substrate for gluconeogenesis via the glyoxylate pathway (**Figure 16B**) (Liu *et al.*, 1995) converting acetyl-CoA into oxaloacetate which is subsequently converted into phosphoenolpyruvate (McElwee *et al.*, 2006). An early study showed that activity of the glyoxylate cycle was linked to a decline in TAG and conversely to an increase in carbohydrates in embryos (Kahn and McFadden, 1980). Furthermore, fasting during development has been shown to increase the expression of the glyoxylate enzyme (Liu *et al.*, 1997). Therefore, one hypothesis is that nematodes use this specific pathway to synthesise carbohydrates from stored lipids in the gut during periods of food deprivation to supply muscle and neurons which may use predominantly glycolysis.

1.4.1.2.1 Lipid storage

In the worm, and similar to mammals, lipids are mainly stored as TAG, although diglycerides and monoglycerides can also be found (Srinivasan, 2014). However, unlike adipose cells in mammals, there are no cells dedicated specifically for fat storage in *C. elegans*. Instead, lipids are stored in two types of subcellular organelles primarily found in the intestine, but also in the worm's epithelial system, the hypodermis (the worm's equivalent of the epidermis), and in the oocytes (Mullaney and Ashrafi, 2009). Therefore in worms, the intestine is a multitask organ, as it not only plays a role of epithelial barrier, but also has the fat storage role of mammalian adipocytes. In addition, the intestine is known to carry out drug detoxification activity which is undertaken by hepatocytes in mammals (An and Blackwell, 2003) and to be an important insulin signalling centre (Murphy *et al.*, 2007).

The two subcellular organelles storing fat were first discovered using transmission electron micrographs. Most fat in the intestine is stored in neutral lipid droplets (LDs) (Zhang *et al.*, 2010b) which are encapsulated by a phospholipid monolayer (Zhang *et al.*, 2010a). The other organelle storing fat is the lysosome-related organelles (LROs), or gut granules (Schroeder *et al.*,

2007). This organelle is related to endosomes and lysosomes (Marks et al., 2013).

1.4.1.2.2 *C. elegans* specializations in lipid metabolism

C. elegans have to obtain cholesterol from their diet which is in contrast to mammals which utilize an established cholesterol biosynthesis pathway. The lack of this pathway makes worms auxotrophic for cholesterol (Hieb and Rothstein, 1968). They take in and modify yeast, plant or mammalian externally added sterols (Chitwood, 1999). There is a limited sterol content of the worm's cell membrane structure but small quantities are absolutely required for viability and growth (Kurzchalia and Ward, 2003; Merris *et al.*, 2003), similarly to that observed in insects (Svoboda *et al.*, 1975). Most bacteria, including *Escherichia coli* (and thus the OP50 strain) do not contain sterols (Volkman, 2003). Therefore, *C. elegans* must obtain its dietary sterols from another source of food which one would hypothesise as being yeast (Zinser *et al.*, 1993).

In contrast with cholesterol, *C. elegans* is able to synthesise essential polyunsaturated fatty acids (PUFAs) and are therefore not dependent on dietary supplies for these lipids (Watts and Browse, 2002) whilst mammals, for instance, must obtain linoleic acid (18:2n6) and linolenic acid (18:3n3), two essential PUFAs, in their diet. The worm's genome encodes desaturases and elongases necessary for the *de novo* synthesis of these lipids (Beaudoin *et al.*, 2000; Watts and Browse, 2002).

1.4.1.2.3 Regulation of fat metabolism

Lipid metabolism is a critical juncture in the starvation response (see **section 1.4.1.1**). *C. elegans* lack certain key mammalian fat regulatory mechanisms. For instance, no clear ortholog for leptin, a cytokine-like hormone secreted from white adipose-tissue promoting energy expenditure pathways and suppressing food intake (Friedman, 2002), is found in the *C. elegans* genome (Mullaney and Ashrafi, 2009).

Chapter 1

While in mammals starvation is defined as the moment when more proteins start to be consumed than lipids to provide energy, there is no clear definition in *C. elegans*. In 1990, Avery and Horvitz used in their experiment ‘starved’ worms that have been food deprived for between 6 and 12 hours (Avery and Horvitz, 1990), or more recently You *et al.* used ‘starved’ worms food deprived for 1 to 6 hours (You *et al.*, 2006). However, starvation is not based on metabolic status, as most of the authors define a worm as starved at the moment it is removed from food, without considering its metabolic status (Sze *et al.*, 2000; Suo *et al.*, 2006; Tan *et al.*, 2011). Therefore, defining a clear metabolic definition of starvation in *C. elegans* remains to be done.

1.4.2 Regulation of fat stores in *C. elegans*

1.4.2.1 Visualisation of fat stores

Observation of fat stores is widely used as a surrogate to investigate metabolic state. Lipids were mainly studied in *C. elegans* compared to proteins and carbohydrates as they are more difficult to study. Distinct methods were used in *C. elegans* to visualise fat stores.

In *C. elegans*, fat stores were historically imaged by EM microscopy, then quantified using a dye-labelled assay for lipid stores (Mullaney and Ashrafi, 2009). The most common fat soluble dyes used for staining assay have been Sudan Black, staining lipids in black (Kimura *et al.*, 1997; McKay *et al.*, 2003a), and Nile Red (Ashrafi *et al.*, 2003). Sudan Black was first used to stain lipids in bacteria (Burdon *et al.*, 1942), and showed to stain in the intestine, hypodermis and gonad of *C. elegans*. However, the experimental procedure requires fixation of the animals. To improve throughput for those interested in defining genetic modulation of fat storage, Nile Red and BODIPY-conjugated fatty acids were developed as markers of lipid stores in the worm. Both were initially introduced to investigate lipid storage and dynamics in mammalian cells (Greenspan *et al.*, 1985; Schaffer and Lodish, 1994). Nile Red or BODIPY-conjugated fatty acids are ingested together with bacteria that have been grown in the presence of these dyes on agar plates and cross the intestinal

epithelium to accumulate in fat storage (Ashrafi *et al.*, 2003), but the mechanism of absorption is unknown.

Although these techniques provide a convenient route to rapidly observe lipid stores in worms, they are not without limitations which are increasingly appreciated and considered. For instance, Sudan Black was reported highly variable in adult animals due to the destaining step of its protocol and variation in the destaining time led to significant changes in the final Sudan Black intensity (O'Rourke *et al.*, 2009). In the case of Nile Red, it appeared to more efficiently indicate fat stores in fixed (dye is added post fixation) rather than live animals (Brooks *et al.*, 2009). Furthermore, studies pointed out that dye-labelled assays in live animals do not always correlate with standard biochemical assays for fat quantification (Brooks *et al.*, 2009) such as thin layer chromatography (TLC) (Watts and Browse, 2006) followed by Gas Chromatography (GC) (Watts and Browse, 2002). More importantly, O'Rourke *et al.* demonstrated that the use of Nile Red in live animals only stained lysosome-related organelles (LROs) but not LDs fat stores (O'Rourke *et al.*, 2009), the organelle that stores most of the lipids in *C. elegans* (Zhang *et al.*, 2010b). Nile red staining in live animals mainly stains the intestine but is less efficient for the germline, oocytes, and hypodermis. More importantly, Nile red staining does not decrease upon fasting, even after 24 hours of food-deprivation, surprisingly showing a slight increase (O'Rourke *et al.*, 2009). Although previous studies showed a reduced Nile red signal following food-deprivation (Ashrafi *et al.*, 2003; Jo *et al.*, 2009), it is important to note that in these studies, the no food arena used to food-deprive the worms was not supplemented with Nile red unlike in O'Rourke's protocol and therefore the previously described decrease in Nile red signal may correspond to a Nile red turnover rather than an actual effect due to lipid consumption.

Overall, these findings indicate that results observed with Nile red staining in live animal should be taken with caution. For instance, the insulin-receptor-like mutant *daf-2* was shown to accumulate more fat than N2 worms using Sudan Black staining (Kimura *et al.*, 1997) or biochemical assays (Perez and Van Gilst, 2008), but Nile red staining and BODIPY-labelled fatty acids assays gave an opposite result with a decreased staining in worms with reduced *daf-2* activity (Wang *et al.*, 2008; Soukas *et al.*, 2009).

Chapter 1

In contrast, O'Rourke *et al.* presented oil red O as a good dye-labelled staining alternative for fat stores visualisation (O'Rourke *et al.*, 2009). Indeed, oil red O appeared to stain the major lipid stores in all the worm's organs able to store fat. Furthermore, analysis of metabolic mutants stained with oil red O correlates with the trends in fat stores observed using biochemical measurement of triglycerides and wild-type worms food-deprived for 6 hours showed a reduced oil red O staining relative to well-fed worms (O'Rourke *et al.*, 2009). However, the changes observed using oil red O still appeared quantitatively less important relative to those observed using biochemical techniques.

1.4.2.2 Improved routes to lipid measurement

More recently, label-free techniques have been developed to visualise/quantify fat storage in *C. elegans*. The coherent anti-Stokes Raman scattering (CARS) microscopy is a non-invasive imaging technique utilizing vibrational frequency of molecular bonds. Each molecule has a distinct spectrum and CARS takes advantage of the vibrational C-H bond signature of molecules (when excited by two lasers) to permit direct visualisation of lipid organelles (LDs) rich in CH₂ groups (Hellerer *et al.*, 2007; Klapper *et al.*, 2011). CARS has been shown to permit the relatively specific visualisation of LDs. Further investigation of these LDs using confocal Raman spectral analyses revealed strong content of TAG (Le *et al.*, 2010). Given the CARS principle based on the vibration of C-H bonds, the CARS signal arises from both fat stores and membrane phospholipids. However, the signal from fat stores is much stronger and therefore a threshold can be applied to avoid visualising lipids from phospholipid membranes and other cellular structures (Yen *et al.*, 2010). Using this label-free method an increase in CARS signal has been observed in the *daf-2* mutant. Furthermore, this increase in CARS signal correlates with an increase in TAG in *daf-2* mutant observed using biochemical methods (Yen *et al.*, 2010).

1.4.2.3 Genetic regulation of fat stores

Fat storage can be influenced by different factors such as the quantity of fatty acids ingested from food, the conversion of nutrients into fat (*de novo* lipogenesis) and conversely the quantity of FA used for β -oxidation. Taking advantage of the aforementioned techniques, important regulators of *C. elegans* fat storage have been identified.

1.4.2.3.1 Insulin

Insulin signalling modulates fat storage as elevated fat stores were observed in worms deficient in the insulin/IGF receptor *daf-2* signalling using distinct methods (Kimura *et al.*, 1997; Perez and Van Gilst, 2008; Yen *et al.*, 2010) (see **section 1.4.2.2**). Using a temperature sensitive *daf-2(e1370)* mutant (nonpermissive at 25 °C), Kimura *et al.* observed accumulation of fat stained with Sudan Black in the intestine and hypodermis of both worm larvae arrested in dauer stage and worms at the L4 or adult stage obtained by switching the *daf-2* mutant allele after development using the nonpermissive temperature (Kimura *et al.*, 1997). Similarly, increased fat stores were observed using oil red O or the label-free CARS technique in L3/L4 *daf-2(e1370)* worms (Yen *et al.*, 2010), and an increase in TAGs observed by TLC/GC has been described (Brooks *et al.*, 2009).

daf-2 is known to play a key role in modulating longevity with deficient mutants showing an extended lifespan dependent on the downstream *daf-16*/FoxO transcription factor. DAF-2 signalling normally acts to inhibit DAF-16 activity, therefore in *daf-2* mutant DAF-16/FoxO can be relocated in the nucleus and activate target genes (Lee *et al.*, 2001). *daf-2* mutant's long-life phenotype is suppressed by *daf-16* mutation (Kenyon *et al.*, 1993). Similarly, *daf-16(mgDf47)* or *daf-16(mgDf50)* null mutations also suppress *daf-2* increased fat accumulation whilst *daf-16* single mutant shows no abnormal fat storage phenotype (Ogg *et al.*, 1997).

Using a ^{13}C isotope assay Van Gilst *et al.* showed that membrane phospholipids (PLs) and TAGs have the same ratio of newly synthesised/dietary FAs, indicating that both sources of lipids come equally from the same pool of

Chapter 1

FAs and are used to form PLs and TAGs (Perez and Van Gilst, 2008). With this method, they observed an increase of around 80% TAGs in *daf-2(e1370)* mutants relative to N2 and showed that the majority of this increase was due to an increase of newly synthesised FAs. In addition, *daf-16(m26)* mutation was shown to suppress the elevated FA synthesis of *daf-2(e1370)* mutant with the double mutant, similar to the single *daf-16(m26)* mutant, displaying a slightly reduced FA synthesis. *daf-2(e1370)* also has an increased fraction of dietary FAs in their TAGs (Perez and Van Gilst, 2008). One possibility for this is that due to the increased fraction of synthesised FAs in the pool of available free FAs, more synthesised FAs are available to make PL membranes and therefore freeing more dietary FAs to form TAGs fat storage. Alternatively, it is possible that β -oxidation is reduced in *daf-2(e1370)* (Perez and Van Gilst, 2008).

Fat accumulation is not always related to increased lifespan. Mutations in *nhr-49*, an ortholog of the mammalian nuclear hormone receptor (NHR) HNF-4 (hepatocyte nuclear factor 4), leads to a reduced lifespan but an increased fat accumulation (vital Nile red) (Van Gilst *et al.*, 2005). qRT-PCR analysis revealed that the *nhr-49* mutation has dramatic effects on the expression of genes acting in two metabolic pathways; mitochondrial β -oxidation (e.g. *acs-2*) and fatty acid desaturation (e.g. *fat-5*), indicating *nhr-49* is a key regulator of the pathways controlling fat consumption and maintaining a normal balance of FAs. This also confirms that fat accumulation can be caused by a reduction of β -oxidation.

1.4.2.3.2 TGF- β signalling

The TGF- β -like ligand DAF-7 pathway regulates the entry into the dauer stage by acting as a sensor of environmental conditions. The absence of food reduces *daf-7* expression which leads to dauer formation. Conversely, *daf-7* mutants show an increased percentage of dauer formation (Ren *et al.*, 1996). Greer *et al.* showed the role of *daf-7* was not restricted to development but also acts as a sensory gauge of environmental conditions in order to regulate energy homeostasis pathways in the adult (Greer *et al.*, 2008). For instance, a *daf-7* mutation induces an increase of fat storage, observed by Sudan Black staining, and supported by reported additional TLC-GC (Brooks *et al.*, 2009)

and BODIPY 493/503 on fixed animals (Klapper *et al.*, 2011). This change is sustained despite an apparent 20% reduction in the pumping rate in the presence of food (Greer *et al.*, 2008). The reduction of pumping rate in *daf-7* mutant could be perceived by the worm as an increase of population density or a depletion of the source of food, and this is consistent with the build-up of fat reservoir observed in unfavourable conditions, similar to that observed before entry into dauer stage (Kimura *et al.*, 1997).

The DAF-7 ligand can bind both type I and type II TGF- β receptors DAF-1 and DAF-4 (Georgi *et al.*, 1990; Estevez *et al.*, 1993). DAF-7 is uniquely expressed in a pair of interneurons, ASI (Schackwitz *et al.*, 1996). This contrasts with DAF-1 and DAF-4 which are widely expressed in ciliated neurons, pharyngeal neurons, interneurons, ventral nerve cord neurons, and in distal tip cells of the gonad (Gunther *et al.*, 2000). Greer *et al.*, however, showed that under favourable environmental conditions, DAF-7 ligand is released from ASI and acts through DAF-1/4 receptors localised in interneurons RIG and RIM (Greer *et al.*, 2008). This triggers the inhibition of DAF-3 co-SMAD signalling leading to the inhibition of dauer formation (see **section 1.1.1.1**) via the nuclear hormone receptor DAF-12's activity and the disinhibition of the pharyngeal pumping via the absence of tyramine and octopamine signalling (see **section 1.3.1.6** and **1.3.1.7**). Interestingly, DAF-7 regulates fat storage through glutamate signalling via two metabotropic receptors; MGL-1 and MGL-3 (**Figure 17**) (see **section 4.1.3**). Although no direct connections are shown, this metabotropic glutamate signalling is thought to act to promote *de novo* fat synthesis as, similar to *daf-2* mutant (Perez and Van Gilst, 2008), *daf-7* mutants were shown to have an increased fraction of newly synthesised FAs.

This increase does not act through the insulin/IGS signalling as a *daf-16* mutation does not suppress *daf-7* mutant's fat accumulation phenotype (Ogg *et al.*, 1997). In contrast, mutation in the tryptophan hydroxylase *tph-1* gene down regulates DAF-7::GFP fusion gene expression (~6 fold decrease), suggesting a 5-HT regulation of DAF-7 ligand expression (Sze *et al.*, 2000). A *tph-1* mutant shows an excess fat accumulation (Sudan Black) while a *daf-3(mgDf90)* mutation suppresses it. Exogenous 5-HT application markedly

reduces fat stores observed with Nile red staining (Srinivasan et al., 2008). Overall, these findings strongly suggest that 5-HT signalling acts to promote DAF-7 release and subsequent inhibition of co-SMAD DAF-3 to regulate fat storage (Figure 17).

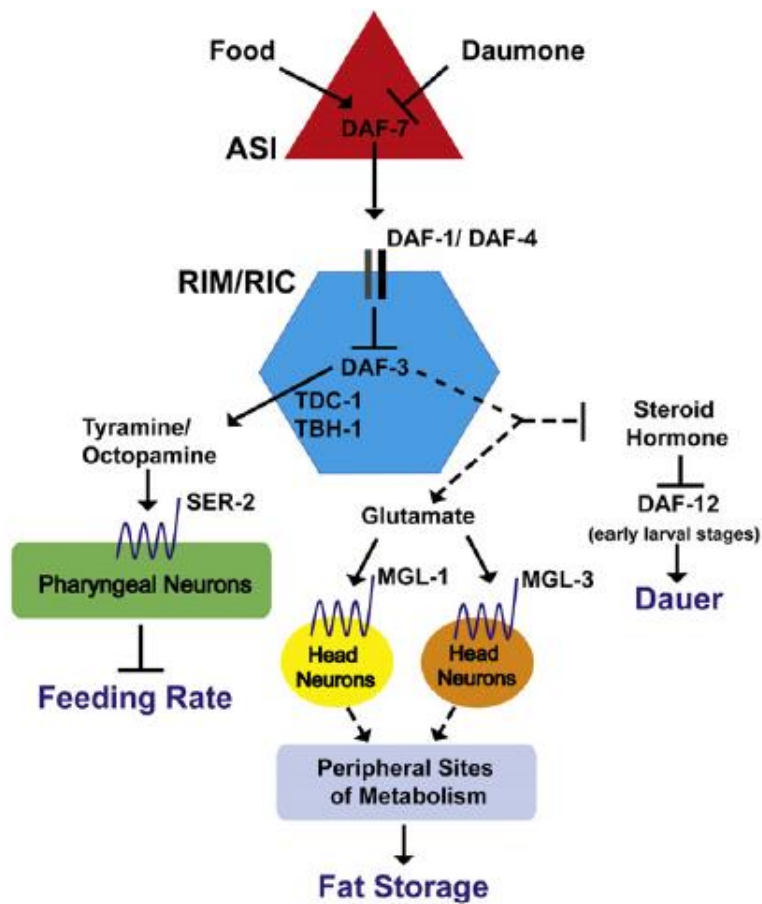


Figure 17: DAF-7/TGF-β ligand regulates feeding, development and fat storage via distinct pathways.

Released DAF-7 from ASI in favourable conditions acts through DAF-1 and DAF-4 receptors localised on RIG and RIM interneurons to inhibit the co-SMAD DAF-3 activity. Under unfavourable conditions, DAF-3 activity leads to the activation of the nuclear hormone receptor DAF-12 which in turn promotes entry into dauer stage. In parallel, DAF-3 stimulates the release of tyramine and octopamine to reduce the pharyngeal pumping rate. Finally, DAF-3 activity triggers a metabotropic glutamate signalling, via MGL-1 and MGL-3, leading to an increased fat accumulation. Model taken from Greer *et al.* 2008.

1.4.2.3.3 Krüppel family

The Krüppel-like factors, KLF, are a family of 17 mammalian zinc finger transcription factors involved in a wide range of physiological processes including adipogenesis and lipogenesis (Wu and Wang, 2013). *C. elegans* genome encodes for three KLF members, *klf-1*, *klf-2*, and *klf-3* (Hashmi *et al.*, 2011). *klf-1* and *klf-3* are both essential regulators of lipid metabolism, and mutants for *klf-1* and *klf-3* displayed an increased fat accumulation phenotype observed using Sudan Black (Hashmi *et al.*, 2008; Zhang *et al.*, 2009). Interestingly, expression of genes regulating FA desaturation and β -oxidation pathways were deregulated in *klf-3(ok1915)* mutant (Zhang *et al.*, 2009), resulting in aberrant ratio of saturated to monounsaturated FAs as supported by the FA composition analysis of *klf* mutant by gas chromatography. This aberrant ratio could be the cause of the increased fat accumulation observed in *klf-3(ok1915)* mutant. A marked increased expression of genes involved in monounsaturated lipid synthesis, such as *fat-1* and *fat-3*, is observed in *klf-3(ok1915)*. Furthermore, there is a reduced expression of *acs-2*, which promotes FA metabolism via β -oxidation, similar to that observed in *nhr-49* mutant (Van Gilst *et al.*, 2005). Overall, these observations indicate that *klf-3* acts to balance lipid composition by promoting lipid metabolism and in parallel reducing the synthesis of monounsaturated FAs.

A *kfl-3* mutant has a reduced *daf-2* and *daf-16* expression indicating KLF-3 may regulate fat storage via an insulin/IGF signalling pathway (Hashmi *et al.*, 2013). In contrast, *daf-7* expression is increased in the *kfl-3(ok1975)* mutant while *daf-7* mutants, as *kfl-3*, showed accumulation of fat (Mukhopadhyay *et al.*, 2005; Zhang *et al.*, 2009). Therefore this suggests that *klf-3* does not act through *tub-1* or *daf-7/TGF- β* pathway to regulate fat storage.

1.4.2.3.4 C/EBP and SREBP

Other transcription factors acting in the regulation of fat storage are the homologs of the mammalian C/EBP (CCAAT/enhancer binding protein) and SREBP (sterol regulatory element binding protein), known to regulate adipocyte differentiation and fat formation (Rosen *et al.*, 2000). In *C. elegans*, inactivation by RNAi of orthologs for either SREBP (*lpd-1* for lipid depleted 1 also called *sbp-*

Chapter 1

1) or C/EBP (*lpd-2*) leads to a reduction of fat stores observed by Sudan Black (McKay *et al.*, 2003a). Consistent with this, TLC/GC assay revealed decreased levels of TAGs upon *lpd-1* RNAi (Yang *et al.*, 2006). EM microscopy observation of *lpd-1(gf1)* mutant showed an overall normal physiology with the exception of the dark storage granules which are missing in the mutant, indicating a defect in fat stores. Moreover, *lpd-1* and *lpd-2* RNAi leads to the reduced expression of lipogenic enzyme genes, suggesting a conserved role for SREBP and C/EBP from nematodes to mammals. Furthermore, McKay *et al.* discovered a new protein, named *lpd-3*, which is similar to SREBP and appeared conserved from worm to mammals (McKay *et al.*, 2003a). Indeed, *lpd-3* is expressed in the worm's intestine while the putative mammalian ortholog, *mlpd-3*, is expressed in mouse and human fat stores. *mlpd-3* expression reduced by RNAi leads to the abrogation of lipid accumulation in adipocytes cell cultures (McKay *et al.*, 2003a).

1.4.2.3.5 Neuropeptides/neurohormonal signalling role in fat regulation

Neuropeptides also play a role in the regulation of fat storage in *C. elegans*. For instance, *egl-3(gk238)* and *egl-21(n611)* mutants have a reduced fat content relative to wild type animals (Husson *et al.*, 2007), suggesting an overall role for neuropeptides. FLP-18 neuropeptides are released by AIY and RIG interneurons and act on NPR-5 receptors localised on a small subset of sensory neurons, including ASI and ADF, to regulate fat storage (Cohen *et al.*, 2009). Furthermore, FLP-18 peptides also act on the intestine through the NPR-4 receptor to regulate fat accumulation. However, FLP-18s and their receptors NPR-4 and NPR-5 have opposite effects to EGL-3 as *flp-18*, *npr-3* and *npr-4* mutants (and also *npr-2* and *npr-7*) all show elevated fat accumulation (Cohen *et al.*, 2009), indicating a more complex role for general neuropeptide signalling in the control of fat storage.

The conserved cholecystokinin (CCK)/gastrin signalling in *C. elegans* displays similar biological activities with respect to digestive enzyme secretion and fat storage (Janssen *et al.*, 2008; Janssen *et al.*, 2009). Indeed, *nlp-12* and its receptor *ckr-2* mutants both showed increased fat accumulation (Janssen *et al.*, 2008), indicating CCK signalling acts to control fat storage in *C. elegans*.

1.4.2.3.6 Diet and fat storage

Input of diet is an additional important facet of fat storage. The impact of the type of food on modulation of behaviour, life span and fecundity are increasingly studied and discussed (Shtonda and Avery, 2006; MacNeil *et al.*, 2013).

One study investigated the effect of different types of food on the worm's fat stores. *E. coli* strains have differences in carbohydrates and FAs composition. Nile red staining on fixed animals showed differences in fat accumulation depending on the source of food worms have been raised on (Brooks *et al.*, 2009), in accordance with lipid analysis by biochemical assays. Worms fed with OP50 and the lower quality food DA837 (You *et al.*, 2008) showed larger lipid droplets and increased Nile red staining relative to those fed with the high-quality food HB101 (You *et al.*, 2008) or HT115. The specific FA composition of the different *E. coli* strains was reflected in the FA composition of worms that have been raised on them. However, these changes in FA composition do not correlate with the worm's fat stores. For instance, worms raised on OP50 and HT115 show similar FA composition but different levels of fat stores. Furthermore, carbohydrate content does not correlate with fat content, indicating that both lipid and carbohydrate composition do not dictate fat storage. Given that high-quality food leads to less fat accumulation than low-quality food, it is possible this reflects the time spent actively feeding on these bacteria and may be a consequence of the quiescence behaviour, i.e. periods of time when worms stop feeding (You *et al.*, 2008) (see below **section 1.4.3.2**).

This differential fat accumulation still occurs in neuroendocrine mutants known to regulate fat storage, such as, *daf-7/TGF- β* or *daf-2*, indicating that these pathways are not required for differential fat storage (Brooks *et al.*, 2009). However, the authors found one gene, *pept-1*, encoding for an intestinal peptide transporter, where the mutation leads to no differences between worms raised on OP50 and HT115. Indeed, a *pept-1* mutant stores high levels of fat (~65% of the lipids are TAGs against 40% in N2) regardless of its dietary bacteria (only OP50 and HT115 were tested). This study suggests that fat metabolism and fat storage levels can be regulated by specific peptides or

Chapter 1

amino acids, providing evidence for nutritional signals distinct to neuroendocrine cues.

1.4.2.3.7 Conclusion

Overall, these studies indicate the regulation of fat storage in *C. elegans* involves a complex signalling network exemplified by the kind of integrated interactions shown in Figure 15 (Jeong *et al.*, 2005; Greer *et al.*, 2008; Perez and Van Gilst, 2008), with uptake and transport through *pept-1* (Ashrafi *et al.*, 2003; Brooks *et al.*, 2009) and storage through SREBP and C/EBP (McKay *et al.*, 2003a).

1.4.3 Nutritional status and feeding behaviour

As mentioned previously, *C. elegans* displays behavioural adaptations in response to food deprivation (see **section 1.2**). Both locomotion and pumping behaviour are modified upon food removal and there exists a temporal aspect to these adaptive behaviours, for instance, the transition from LSA to long run after 15 min of food deprivation (see **section 1.2.1.2**). Therefore, this suggests a link between nutritional status and feeding behaviours.

The behavioural response to food depends on the worm's feeding history. For instance, starved animals (6 to 12 hours of food deprivation) transferred back onto food show an enhanced pumping rate, proportional to the time spent off food, relative to the "normal" rate displayed by well-fed worms raised on food (Avery and Horvitz, 1990). This enhanced pumping rate upon refeeding, or hyperactive feeding, is dependent on 5-HT signalling acting through the SER-5 receptor (Lemieux *et al.*, 2015). Furthermore, worms that have been starved will display increased pumping rate in response to a much lower concentration of food than a well-fed worm would do, indicating that the period of starvation sensitized *C. elegans* to nutrient levels (Avery and Horvitz, 1990). Moreover, You *et al.* suggested that activation of the muscarinic pathway upon starvation leads to the phosphorylation of MAPK and triggers changes in the pharyngeal pumping physiology, permitting an enhanced

response when food is available (You *et al.*, 2006). Similarly, when re-introduced to food, worms reduce their speed in order to stay on food, called the slowing response. Worms which have undertaken a period of food-deprivation show an enhanced slowing response, which, as the enhanced pumping response, is proportional to the time spent off food (Sawin *et al.*, 2000). In addition, well-fed animals placed in absence of food immediately increase their turning rate and try exploring the near environment whilst in contrast worms starved for several hours transferred onto a non-seeded plate displayed almost no reversals and immediately start to escape from this unfavourable environment (Tsalik and Hobert, 2003). Intriguingly, worms appear to have a memory of their starved condition as worms that were starved while maintained at a specific temperature will avoid this temperature in the future (Mori and Ohshima, 1995).

These behaviours are regulated by a homeostatic system, similar to mammals, allowing the animal to balance its food intake to match its energy expenditure and recover from a period of fasting by motivating an animal to eat more following depletion of energy stores (Lutter and Nestler, 2009). Lemieux *et al.* recently showed that kynurenic acid (KynA), a metabolite derived from tryptophan degradation via the kynurenine pathway (KP), was used in the worm as a gauge of internal nutrient availability and was a key modulator of the hyperactive feeding post-fast (Lemieux *et al.*, 2015). In well-fed worms, KynA levels are high (derived from ingested food) and act through the glutamate receptor *nmr-2* on AVA neurons to attenuate the release of FLP-18 neuropeptides while the presence of food cues triggers a release of 5-HT. In contrast, upon fasting, reduced levels of KynA lead to the enhanced activity of AVA neurons increasing the release of FLP-18 peptides which, upon binding to their receptors NPR-5, increase the activity in the serotonergic neurons ADF. However, the absence of cues from the food prevent the release of 5-HT. Finally, when reintroduced to food, the activated FLP-18/NPR-5 signalling state triggers an enhanced release of 5-HT from ADFs leading to the hyperactive feeding observed immediately post-fast. With time and increased food intake, the KynA pool is re-built, leading to the inhibition of AVAs through NMDA receptor and the reduction of FLP-18 release leading to the restoration of a normal feeding rate (Lemieux *et al.*, 2015).

1.4.3.1 The mammalian complexity: overriding basic feeding cues?

In mammals there is another system modulating feeding behaviour; the hedonic system. The hedonic system, or reward-based feeding, can override the homeostatic system, allowing an animal to eat more than it needs to match its energy balance which permits it to store energy (Lutter and Nestler, 2009). In this regards, the hedonic system will promote the uptake of highly palatable food, usually rich in fat and carbohydrates, by creating the hunger feeling independently of the nutritional status and by releasing dopamine. Release of dopamine on the nucleus accumbens has been associated with the reward mechanisms (Kalivas and Nakamura, 1999), and studies have shown that it is the expectation of a reward that triggers the release of dopamine in the nucleus accumbens (de la Fuente-Fernandez *et al.*, 2002). Dopamine drives animals to obtain food rewards, such as increased arousal, psychomotor activation, and conditioned learning (Wise, 2006). Animals remember rich food-associated stimuli promoting intake in a similar manner to that observed with addiction (Nestler, 2001). Neuropeptides play a part in this system with orexin, a neuropeptide involved in arousal, wakefulness, and appetite (Davis *et al.*, 2011), released upon feeding and stimulating dopamine neurons (Zheng *et al.*, 2007).

Although it is not as clearly defined in *C. elegans*, some specific behaviours suggest a hedonic-like system that can impose regulation of feeding in the worm. For instance, the worm's innate preference to high quality food, defined as food which will best promote growth, such as *Pseudomonas sp.* B7 and W11, *Comamonas sp.* H3 and *E. coli* HB101 (Avery and Shtonda, 2003), supports this hypothesis. After a first exposure to high quality food, *C. elegans* seeks similar food in binary dietary choice assays (Shtonda and Avery, 2006). Furthermore, a quiescence behaviour was observed in *C. elegans* (see below) in which worms cease feeding and moving after feeding on high quality food (You *et al.*, 2008).

1.4.3.2 Quiescence behaviour

In mammals, satiety occurs to prevent animals feeding after copious amounts have been eaten and is characterised by the meal termination, reduction of locomotion, rest and sleep (Antin *et al.*, 1975; Schwartz *et al.*, 2000). In *C. elegans*, You *et al.* have described quiescence behaviour in which worms become immobile and display a cessation of pumping which is thought to be the equivalent of satiety in mammals, showing in both cases a gradual reduction of food intake and locomotion (Antin *et al.*, 1975; You *et al.*, 2008). A worm is considered as quiescent when no movement or pumping motion is observed for at least 10 seconds. The quiescence behaviour is almost never observed in worms feeding on low quality food such as DA837, where less than 5% of observed worms entered quiescence, while more than 90% of the assessed worms entered quiescence after feeding on high quality food (HB101). The quiescence state lasts an average of 15 seconds after 3 hours of feeding and ~25 seconds after 6 hours.

This quiescence behaviour is regulated by nutritional status as well as feeding history. Indeed, in *eat-2* mutants, displaying a reduced pumping rate on food, only 10% of the mutant worms showed quiescence when fed with the high quality food HB101. Similarly, *act-5* mutants, deficient for a microvillus-specific actin required for absorbing nutrients from the intestine, the fraction of worms entering quiescence is reduced by half compared to that displayed by wild-type. Furthermore, after a 12 hours fasting period, worms refed with high quality food display increased quiescence compared to fasted worms refed with low quality food (You *et al.*, 2008). This increase quiescence can be correlated to the hyperactive feeding observed after fasting (Lemieux *et al.*, 2015).

Overall, these observations indicate the important role of nutritional signals from the intestine in the regulation of this behaviour. Indeed, both *daf-7/TGF- β* , insulin/IGF (*daf-2*) and cGMP (*tax-2/4*) pathways are required for quiescence entry upon refeeding with all three mediated by PKG/EGL-4.

Aims

This introduction discussed the advantages of the nematode *Caenorhabditis elegans* as a model to inform on the molecular, cellular and behavioural regulation of feeding. The efforts made to investigate the mechanisms underlying feeding behaviours have been particularly strong in regard to locomotory behaviours modulation in response to different food-contexts and environmental cues.

In this thesis, I would like to build on this and focus on the pharyngeal response as a surrogate of feeding behaviour. In particular, I aim to develop an assay to investigate the nematode's pumping behaviours on food as well as the pumping response to food removal. This assay will be utilised to better characterise the adaptive response to prolonged food-deprivation, an aspect that has been less studied.

The new pumping assay will serve to resolve the cellular and molecular determinants mediating pumping behaviours depending on the food-context. In addition, the sensory modalities perceiving the cues from food will be investigated.

Finally, in contrast to mammals, the evolution of the nutritional status of *C. elegans* during food-deprivation is ill-defined. I will therefore investigate the adaptations in nutritional status following protracted food-deprivation and attempt to build correlations with adaptations in pumping behaviour.

Chapter 2: Materials and Methods

2.1 Strains used

The Bristol isolate N2 has been used as the wild-type strain. The following mutants strains were used in this study:

Strain name	Gene	Allele	Supplier
VC671	<i>egl-3</i>	<i>ok979</i>	CGC
MT150	<i>egl-3</i>	<i>n150</i>	CGC
KP2018	<i>egl-21</i>	<i>n476</i>	CGC
MT13113	<i>tdc-1</i>	<i>n3419</i>	CGC
CB113	<i>unc-17</i>	<i>e113</i>	CGC
	<i>unc-17</i>	<i>e245</i>	CGC
GR1321	<i>tph-1</i>	<i>mg280</i>	CGC
CB156	<i>unc-25</i>	<i>e156</i>	CGC
CB1112	<i>cat-2</i>	<i>e1112</i>	CGC
RB1161	<i>tbh-1</i>	<i>ok1196</i>	CGC
MT6318	<i>eat-4</i>	<i>n2474</i>	CGC
MT6308	<i>eat-4</i>	<i>ky5</i>	CGC
DA1371	<i>avr-14</i>	<i>ad1302</i>	CGC
DA1051	<i>avr-15</i>	<i>ad1051</i>	CGC
VM4314	<i>glr-1</i>	<i>kyl76</i>	
VM487	<i>nmr-1</i>	<i>ak4</i>	CGC
RB1808	<i>glr-2</i>	<i>ok2342</i>	CGC
	<i>glr-7</i>	<i>tm2877</i>	NBRP
	<i>glc-1</i>	<i>pk54::Tc1</i>	Avery's lab (Virginia Commonwealth University)
VC722	<i>glc-2</i>	<i>ok1047</i>	CGC
RB594	<i>glc-3</i>	<i>ok321</i>	CGC
RB658	<i>glc-4</i>	<i>ok212</i>	CGC
??	<i>mgl-1</i>	<i>tm1811</i>	NBRP
??	<i>mgl-2</i>	<i>tm355</i>	NBRP
??	<i>mgl-3</i>	<i>tm1766</i>	NBRP
CB5	<i>unc-7</i>	<i>e5</i>	CGC
CB101	<i>unc-9</i>	<i>e101</i>	CGC
RWK102	<i>eat-4; egl-3</i>	<i>n2474; n150</i>	Komuniecki Lab (University of Toledo)
DA509	<i>unc-31</i>	<i>e928</i>	CGC
	<i>unc-31</i>	<i>u280</i>	Horvitz's lab (MIT)
CB169	<i>unc-31</i>	<i>e169</i>	CGC
NY7	<i>flp-1</i>	<i>yn2</i>	Chris Li
VC2497	<i>flp-3</i>	<i>ok3265</i>	CGC
VC2504	<i>flp-15</i>	<i>gk1186</i>	CGC

Chapter 2

VC2016	<i>flp-18</i>	<i>gk3063</i>	CGC
RB982	<i>flp-21</i>	<i>ok889</i>	CGC
CX4148	<i>npr-1</i>	<i>ky13</i>	CGC
	<i>npr-2</i>	<i>ok419</i>	CGC
XA3722	<i>npr-3</i>	<i>tm1583</i>	NBRP
XA3740	C16D6.2/ <i>npr-4</i>	<i>tm1782</i>	NBRP
XA3728	Y58G8A.4/ <i>npr-5</i>	<i>ok1583</i>	CGC
	F41E7.3/ <i>npr-6</i>	<i>tm1497</i>	NBRP
XA3701	F35G8.1/ <i>npr-7</i>	<i>ok527</i>	CGC
IC683	<i>npr-9</i>	<i>tm1652</i>	CGC
XA3711	C53C7.1/ <i>npr-10</i>	<i>tm1568</i>	NBRP
XA3700	C25G6.5/ <i>npr-11</i>	<i>ok594</i>	CGC
	T22D1.12/ <i>npr-12</i>	<i>tm1498</i>	NBRP
	ZC412.1/ <i>npr-13</i>	<i>tm1504</i>	NBRP
RB1321	C56G3.1	<i>ok1439</i>	CGC
VC48	<i>kcp-1</i>	<i>gk8</i>	CGC
JT23	<i>kpc-3/aex-5</i>	<i>sa23</i>	CGC
CB937	<i>kpc-4/bli-4</i>	<i>e937</i>	CGC
	<i>unc-31; egl-3</i>	<i>e928; ok979</i>	Generated by Sarah Luedtke
	<i>eat-4; unc-31</i>	<i>ky5; e169</i>	Generated by Sarah Luedtke
PR767	<i>ttx-1</i>	<i>p767</i>	CGC
MT3600	<i>osm-3</i>	<i>p802</i>	Horvitz's lab (MIT)
PR811	<i>osm-6</i>	<i>p811</i>	Horvitz's lab (MIT)
CB1124	<i>che-3</i>	<i>e1124</i>	Horvitz's lab (MIT)
CB3332	<i>che-12</i>	<i>p1812</i>	Horvitz's lab (MIT)
CB3323	<i>che-13</i>	<i>e1804</i>	Horvitz's lab (MIT)
TB200	<i>ceh-2</i>	<i>ch4</i>	Horvitz's lab (MIT)
PR767	<i>ttx-1</i>	<i>p767</i>	Horvitz's lab (MIT)
FG58	<i>dop-4</i>	<i>tm1392</i>	CGC
nEx1997	<i>N2; Ex[Pgpa-16::GFP]</i>		Horvitz's lab (MIT)
MT21421	<i>N2; Is[Pflp-1::Csp-1b]</i>		Horvitz's lab (MIT)
MT21212	<i>eat-4(ky5); Is[Pflp-15::eat-4; lin-15(+); lin-15 (n765)]</i>		Horvitz's lab (MIT)
	<i>N2; Ex[Pflp-15::ChR2;YFP]</i>		Horvitz's lab (MIT)
	<i>eat-4(ky5); Ex[Pflp-15::ChR2;YFP]</i>		Generated by crossing
	<i>N2; Is[Peat-4::ChR2::mRFP]</i>		Generated by Catriona Murray
	<i>eat-4(ky5); Is[Peat-4::ChR2::mRFP]</i>		Generated by Catriona Murray
	<i>N2; Is[Pflp-15::GCaMP3]</i>		Horvitz's lab (MIT)
	<i>eat-4(n2474); Ex[PAWC::eat-4]</i>		Generated by Microinjection

2.2 *C. elegans* maintenance

2.2.1 Culturing *C. elegans*

C. elegans were maintained according to Brenner (Brenner, 1974). Briefly, worms were kept at 20°C on nematode growth medium (NGM) agar plates. Single colonies of *E. coli* OP50 were grown at 37°C overnight in around 15 mL of LB (Luria Bertani) and unless otherwise stated striated cultures were used to seed plates with bacteria.

Plates were seeded with 50µL of the overnight culture of *Escherichia coli* (OP50) at least 2-3 days before use. These seeded plates were stored for between 2 and 20 days at 20 °C before use.

General husbandry

Plates containing worms were sealed with parafilm to prevent cross-contamination between strains during routine passaging. Worms (usually L4s) were transferred to a fresh plate every 3 days.

2.2.2 Longer storage of *C. elegans*

Populations of worms were frozen for storage purposes. A worm population of mixed ages and close to starvation was washed off a NGM plate with two 600µL volumes of M9 solution before transfer to a 15mL Falcon tube. 1.2 mL of freezing buffer (see **section 2.3.3**) was added (1:1 M9/freezing buffer proportion) and around 650µL of the mix was transferred into each cryovial before storage at -80°C.

2.3 Solution recipes

2.3.1 NGM (Nematode Growth Medium)

For 5L

NaCl	15g
Bactopectone	12.5g
Agar	85g
Cholesterol (5mg/mL in EtOH)	5mL
dH ₂ O	q.s. 5L

A large magnetic stirrer bar was added in bottle. Following autoclaving, the following were added:

CaCl ₂ 1M	5mL
MgSO ₄ 1M	5mL
K Phosphate 1M pH6	125mL

2.3.2 M9 Buffer

KH ₂ PO ₄	3g
Na ₂ HPO ₄	6g
NaCl	5g
MgSO ₄ 1M	1mL
dH ₂ O	q.s. 1L

2.3.3 Freezing Buffer

NaCl	5.85g
KH ₂ PO ₄	6.8g
Glycerol	300g
NaOH 1M	5.6mL
dH ₂ O	q.s. 1L

Following autoclaving, the following were added 3mL of 0.1M of MgSO₄

2.3.4 Lysis buffer

Tris HCl 1M pH8.3	1mL
KCl 1M in dH ₂ O	5mL
MgCl ₂ 1M	0.25mL
NP40 45% (v/v)	1mL
Tween 20 45% (v/v)	1mL
Gelatin 0.1% (w/v)	10mL
dH ₂ O	q.s. 100mL

2.3.5 S-basal

Tris HCl 1M pH8.3	1mL
KCl 1M in dH ₂ O	5mL
MgCl ₂ 1M	0.25mL
NP40 45% (v/v)	1mL
Tween 20 45% (v/v)	1mL
Gelatin 0.1% (w/v)	10mL
dH ₂ O	q.s. 100mL

2.3.6 LB (Luria-Bertani) broth and agar

dH ₂ O	950 mL
Tryptone	10 g
NaCl	10 g
Yeast extract	5 g

pH was adjusted to 7.0 with 5 N NaOH (~0.2 mL). Sterilised by autoclaving.

For LB agar, 15g/L of agar was added before autoclave.

2.3.7 PBS (Phosphate Buffered Saline)

NaCl	8g
KCl	0.2g
Na ₂ HPO ₄	1.44g
KH ₂ PO ₄	0.24g
dH ₂ O	q.s. 1L

pH was adjusted to 7.4. Sterilised by autoclaving.

2.4 Behavioural assays

2.4.1 Measuring pharyngeal pumping in the presence and absence of food

Pumping may be scored by direct visual observation of movements of the grinder in the terminal bulb of the pharynx in intact freely moving worms. One anterior and posterior movement of the grinder is scored as a single pharyngeal pump. Experiments were performed on age-synchronised young adult worms (L4 plus one day old) and mutant experimental groups were paired with a wild-type N2 control group on each day of assay. The pumping of each worm was counted for one min on the food-containing plates used to cultivate them from an L4 stage overnight. The worms were then transferred onto a non-food plate and left for one minute to clean themselves of attached bacteria before being transferred onto the assay plate. The plates in which pharyngeal pumping off food was observed were 9 cm diameter plates containing 30 ml of NGM (not less than 3 days old and not more than two weeks old). After transfer to the assay plate, pumping rate was recorded at periodic intervals as indicated up to a maximum of eight hours. Depending on the experiment, worms were then placed back onto a fresh food plate and a final score made. During all off food experiments there was an unavoidable attrition rate in the worms as some of each experimental group were lost because they dried out after migrating off the edge of the agar plate.

2.4.2 Local Search Area assay

Synchronised L4 + 1 day worms were used for this assay. Animals were scored for reversals followed by Omega turns (turns in which the head nearly touched the tail) 1 min after removal from food to allow recovery from the picking stress. Two periods of 5 min were then scored: from 1 to 6 min; and from 7 to 12 min following food removal. Plates were covered with their lid during the entire observation period. Omega turns were defined as those that followed a reversal were counted.

2.4.3 Re-entry on food

To assess the pumping behaviour of worms encountering food, three L4+1 synchronised worms were transferred onto a 'cleaning' plate for 1 min prior to transfer onto the non-seeded edge of a bacteria lawn containing plate, at a distance of around 2 cm from food. Pump frequency was assessed using an online counter (<http://wormweb.org/countdown>) as soon as the top of the nose of one worm touched the bacteria lawn. Pumping rate off food, during chemotaxis, was not recorded in this experiment but direct observation was made to ensure the pump rate was as low as expected in absence of food.

2.4.4 Pumping behaviour in the presence of polystyrene microspheres

In order to assess the effect of mechanical stimuli on the pumping rate of food-deprived worms, a 3.64×10^{11} particles/ml in DI water stock solution of Fluoresbrite® YG Carboxylate Microspheres 0.50 μ m (Polysciences, Inc.), was used in these assays.

2.4.4.1 10 min assay

A dilution of the stock solution was performed to obtain a concentration of 10^9 particles per mL. 363 μ L of S-basal solution (see **section 2.3.5**) was added to each μ L of stock solution.

Chapter 2

Plates used for the assay were seeded with 200 μ L of 10^9 /mL beads in S-basal solution ($2 \cdot 10^8$ beads per plate in total). Beads were spread all over the plate so the worms were always in contact with them. Synchronised L4 + 1 worms were transferred onto a cleaning plates prior to further transfer onto the bead-seeded assay plate. The pumping rate was assessed every min for 10 min in total.

2.4.4.2 30-60 min assay

In this assay, unlike the 10min assay, plates were seeded with 300 μ L of 10^9 /mL beads in S-basal solution ($3 \cdot 10^8$ beads per plate) and control plates were supplemented with 300 μ L of S-basal solution. Synchronised L4 + 1 worms underwent a 1 min cleaning step on a non-seeded plate prior to transfer onto the assay plate. The pumping rate was assessed for 1 min after 30 and 60 min after transfer onto the beads-seeded plate.

2.4.5 Statistical analysis

Statistical analyses were made using GraphPad Prism (GraphPad Software, Inc.). One-way ANOVA with Bonferoni post-test was used to test for significant difference between strains' pumping rate on food and omega turns following reversal. Two-way ANOVA with Bonferoni post-test was used to test for significant difference between strains, wild-type compared to mutant, over time following removal from food. For protracted assays, the time periods of the behavioural adaptation to food deprivation were divided into an early phase (from 0 to 120 min post food withdrawal) and a late phase (from 150 min until transfer back on food) and these periods were analysed for statistical significance between wild-type and mutant separately. Statistical significance was set at $p < 0.05$. Similarly, a two-way ANOVA statistical test was used for the 45 min off food pumping assay. A Bonferoni post-test was used to compare the average pumping rate over 45 min of each strain simultaneously.

A two-way ANOVA with Bonferoni post-test was used to compare the entry-on food phenotypes of assessed mutants to the paired N2 control.

2.5 Microinjection of *C. elegans*

Transgenic strains were created by introducing plasmid DNA by microinjection. This technique was used to rescue a mutant by introducing a wild type copy of the defective gene or to create expression constructs to analyse a gene expression pattern. The plasmid of interest was co-injected with a plasmid marker containing a fluorescent TAG, allowing rapid selection of the offspring carrying the transgenes. *Pmyo-2::GFP*, expressing GFP in the pharyngeal muscle, or *Pmyo-3::GFP* (L3785) expressing GFP in the body wall muscle lining the worm, were used.

The injection mix contained 40ng/μL of the plasmid of interest and 30ng/μL of the marker plasmid in a final volume of 50μL. The injection mix was centrifuged prior to injection for 30 min at 14k rpm.min⁻¹ and 40μL of the supernatant was transferred into another tube.

Agarose pads used for injection were prepared by pipetting 1 or 2 droplets of 2% agarose solution on a microscope slide and then covering this immediately with another slide to flatten the molten agarose. The second slide was removed and the pad 'baked' in the oven (110 °C) for at least 1 hour. L4 worms were picked the evening before injection in order to obtain staged gravid young adult worms. Needles made from aluminosilicate glass capillaries (1 mm diameter) were pulled on a P-2000 Sutter Instrument electrode puller (program 99), and the injections were carried out according to Michael Koelle's microinjection protocol

(<http://medicine.yale.edu/lab/koelle/protocols/index.aspx>). Briefly, the non-sharp part of the needle was put in contact with the injection mix for at least 5 minutes in order to allow capillary action to fill the needle. The needle was then fixed to the injection arm and moved into position using a micro-manipulator (Eppendorf TransferMan NK2). The needle was broken at its tip by gently brushing it against a broken cover slip immersed in Halocarbon oil.

Worms were dipped into a sufficient volume (covering the worm) of Halocarbon oil to prevent drying and then placed onto the agarose pad. The DNA was injected inside the worm's gonads using the microinjection system: an Eppendorf TransferMan NK2 manipulator attached to the eppendorf FemtoJet pressure system. The needle was visualised under NikonEclipse

Chapter 2

TE200 microscope (Japan) X40 magnification. After injection, individual worms were transferred onto a fresh seeded plate.

The progeny was observed and fluorescent worms (carrying the GFP co-marker) were individually selected. Each green worm was placed onto separated plates to ensure the transmission of the extra-chromosomal arrays.

2.6 Laser microsurgery of *C. elegans*

2.6.1 Microsurgery equipment

Laser beam ablation was performed using a MicroPoint laser (Laser Science inc. LSI, VSL-337; output 337nm, 142μJ) mounted on an epi-fluorescent microscope with Nomarski DIC optics according to the previously described method (Fang-Yen *et al.*, 2012b). A dye cell containing Coumarin 440 (5mM in methanol) was added to sharpen the laser wavelength to 435nm. A dichroic, or beam splitter, was also included to the system to allow both the laser and the UV light to reach the eyepiece.

2.6.2 Worm preparation

L1/L2 larvae, expressing GFP in the desired neurons, RIPs, were mounted on a freshly made NGM agar pad and immobilized with 10mM sodium azide (NaN₃). A coverslip was placed on the top of the pad. Sham-ablated controls were performed at the same time.

2.6.3 Ablation

The RIP neurons, expressing GFP, were first identified under an epi-fluorescent microscope. Optics were switched to Nomarski to conduct the laser ablation. The laser-induced GFP disappearance was confirmed under UV light. Only half of the worms present on the pad were ablated and the other half served as sham-ablated control worms. Following ablation, the coverslip was

carefully removed by sliding it off and each worm picked onto individual plates.

2.6.4 Confirmation of the ablation

To score ablation relative to GFP disappearance due to bleaching, worms were mounted the following day again as described above. The absence of signal and the presence of neurons' 'corpses' viewed by Nomarski were used to authenticate neuronal ablation. The ablated worms were picked back onto individual plates and incubated at 20 °C for behavioural analysis.

2.7 Optogenetics

2.7.1 Retinal plates preparation

200µL of overnight OP50 culture was supplemented with 2µL of 250µM All trans retinal (Sigma Aldrich) and vortexed. Then ~200µL was spread to cover the entire surface of each plate. The retinal laced bacteria plates were used the following day after being seeded.

2.7.2 Pharyngeal pumping under the influence of optogenetic stimulation of glutamatergic neurons

Channelrhodopsin-2 (ChR2) cDNA was integrated in the genome of both N2 and *eat-4(ky5)* strains by Catriona Murray to generate the transgenic strains N2; *Is[Peat-4::ChR2;mRFP]* and *eat-4(ky5); Is[Peat-4::ChR2;mRFP]*. Worms were picked onto the retinal plates at least 3 hours prior to the experiment. The transgenic strain N2; *Ex[Pflp-15::ChR2;YFP]* was made by Dr. Nikhil Bhatla and crossed with *eat-4(ky5)* mutant (see **section 2.14**) to generate the strain *eat-4(ky5); Ex[Pflp-15::ChR2;YFP]*.

For the pumping on food assay, worms were simply kept on the retinal laced bacterial plates and the pumping rate of each worm was assessed within a 5min window as described. The UV light was turned on 1 min after the

beginning of the assay, the first minute serving as the unstimulated control. The UV light (excitation wavelength: 480/40nm) was then turned on and maintained for 2 min, so that the whole worm was illuminated. After 2 min, the light was turned off and measurement of pumping made for a further 2 minutes.

The same protocol was used to assess the pumping rate off food, except that the worm first underwent a 1 min cleaning step (see **section 2.4.1**) prior to transfer onto a 90mm non-seeded plate. Light-activation was conducted 30 min after the initial removal from food.

2.8 Calcium Imaging

Calcium activity was assessed using the genetically encoded calcium indicator GCaMP3 (Tian *et al.*, 2009). The transgenic strain N2; *Is[Pflp-15::GCaMP3]* expressing GCaMP3 under the control of *flp-15* promoter was used to observe calcium activity in the pharyngeal neurons I2 (Bhatla and Horvitz, 2015). Synchronised well-fed or food-deprived for 30min L4 + 1 worms were mounted on 10% agarose pads under a coverslip, using polystyrene beads for immobilization (Kim *et al.*, 2013). An inverted microscope with a 40x air objective served to image and stimulate neurons using 26 mW/mm² 485 nm light. Videos were recorded using an EMCCD camera and analysed using a custom Matlab software coded by Dr. Nikhil Bhatla (available at <http://www.wormweb.org>). Because I2 activity increases in response to light, a lower power (2 mW/mm²) and reduced exposure time (100–200 ms, 1fps) were used for imaging to minimise this activation.

2.9 Pharynx dissection

Around 10 L4+1 worms were transferred into a 3cm Petri dish containing 2mL of M9 supplemented with an undefined amount of BSA, and incubated for 1 hour at 4 °C to anaesthetise the worms. Worms were viewed under a normal dissection microscope (40x magnifications). An incision was made with a razor blade at the tip of the worm, near the lips. The internal pressure of the

pharynx forces it to pop out of the cuticle after several minutes depending on the size of the initial incision. Addition of a couple of drops of 10mM levamisole were used to help in removing the pharynx from the cuticle.

Once exposed, the pharynx is separated from the rest of the body by cutting the connection with the intestine. Pharynxes coiled around the intestine were subjected to further dissection to remove obstructing structures. The isolated pharynxes were pipetted onto a 2% agarose pad and covered with a cover slip prior to experimental observation.

2.10 Dil staining

A Dil (2 mg/ml) in dimethylformamide (100%) stock solution was stored at -20 °C wrapped in foil.

A 1:200 dilution of the stock dilution was prepared in M9 and 150µL of the dilution transferred to a 1.5mL tube.

L4+1 worms crawling out of food were picked and dropped into the tube containing the dye. The worms were then incubated 3 hours at room temperature with gentle rolling.

Three wash-cycles were performed with 500µL of M9.

For this assay, worms subjected to this staining were either kept intact or the pharynx was isolated as described (see **section 2.9**).

Stained worms were transferred onto a 2% agarose pad immobilized with levamisole and visualized by fluorescence using a Nikon eclipse E800 fluorescence microscope (63X and 100X magnifications).

2.11 Sudan Black staining

L4 worms were picked 32 hours prior to staining to obtain a synchronised population of adults. Worms for the well-fed control group were kept on food the entire 32 hours. Worms for the food-deprived groups were transferred onto

Chapter 2

non-seeded plates after 30 hours (2 hours food-deprived), 27 hours (5 hours food-deprived), 22 hours (10 hours food-deprived) and 8 hours (24 hours food-deprived). Worms of all groups were maintained at 20 °C.

Worms were harvested from the plates using 500µL of 1X PBS (see **section 2.3.7**) and transferred into a non-stick 500µL Eppendorf tube. Two more wash-cycles were performed before fixation with 1% Paraformaldehyde (PFA v/v) for 15min at room temperature.

These PFA fixed worms were subjected to three freeze-thaw cycles involving plunging the Eppendorf into liquid nitrogen and heat-block before worms were incubated for a further 5 min at room temperature. After a further 10 min incubation on ice, pelleted worms underwent three further wash-cycles with 500µL 1X PBS.

The worms were dehydrated by sequential exposure to increasing concentrations of EtOH (25%, 50% and 70%). Between each step, worms were incubated with rolling movements for 3min in EtOH. As much EtOH as possible was then removed, and the worms were incubated over night with 50% saturated Sudan Black (Fluka) in 70% EtOH. Sudan black was prepared beforehand in 70% EtOH then filtered using 0.22µm filter.

Worms were pelleted by a brief spin and re-hydrated by three washing steps with decreasing concentration of EtOH (70%, 50% and 25%). Two final wash-cycles were then conducted with 1% PBS. As much supernatant as possible was removed. Stained worms were transferred onto a 2% agarose pad for observation.

2.12 Solid-state Nuclear Magnetic Resonance (NMR)

¹H high-resolution magic angle spinning NMR spectroscopy (¹H HRMAS-NMR) provides a route to follow changing levels of metabolites in the whole worm (Pontoizeau *et al.*, 2014). This methodology was extended to look at changes in response to increasing time off food (see **section 7.3.1**)

2.12.1 Sample preparation:

For this experiment, it is preferable to use well-seeded plates, *i.e.* seeded with 150 μL of OP50 bacteria instead of 50 μL , to ensure there is enough food on the plate throughout the different phases and that worms do not undergo food-deprivation during the process.

2.12.1.1 Worm synchronization

10 gravid adults were picked per plate for a total of 35 plates. The plates were stored at 20°C for at least 3 hours to allow the worms to lay between 80 and 100 eggs per plate. The worms were then removed from the plates and the plates stored at 20°C for 3 days.

2.12.1.2 Food-deprivation step

After 3 days, the relatively synchronized adult worms were harvested by washing the plates twice with 600 μL of M9, and worms containing M9 were recovered with a glass Pasteur pipette. Worms were allowed to settle by gravity and the total cohort of worms pooled in a 15 mL Falcon tube.

Around 100 worms from this pooled cohort were placed on 24 OP50 seeded-plates and 8 non-seeded plates, the latter were destined to be the food-deprived worms for the 24 hours condition. Finally, 8 plates were washed, using the same protocol as above, and 20 hours and 22 hours later worms were placed on non-seeded plates to obtain the 4 hours and 2 hours food-deprived condition, respectively.

2.12.1.3 Fixation step

24 hours after the first washing step, worms from all conditions were collected by washing (see **section 2.12.1.2**). After discarding the supernatant, each condition were transferred to a 1.5mL Eppendorf tube, and subjected to 5 pellet-resuspension wash-cycles (PRWC) using 500 μL of M9.

Chapter 2

Supernatant was discarded and worms were fixed by added 120 μ L of Formalin 4%. Tubes were incubated at room temperature for 30 min and 3 PRWC using 600 μ L of ddH₂O followed by 3 further washes with D₂O were performed. Samples were kept in 100 μ L of D₂O and stored at 4°C before further processing.

A similar protocol was used for the mutant strain *egl-3(ok979)*, but the number of worms required to obtain enough eggs differed from wild-type N2 worms. Indeed, at least 30 gravid *egl-3(ok979)* adults per plate are required to obtain 80-100 eggs after at least 4 hours.

2.12.2 Sample processing and data analysis

The *C. elegans* were loaded into a 4mm Bruker magic-angle spinning (MAS) rotor and 5 μ L of D₂O added to provide a lock signal. Spectra were acquired on a Bruker 400 MHz Avance NMR spectrometer equipped with double resonance MAS probe. The sample was maintained at 25°C and rotated at 4kHz about the magic-angle to remove residual anisotropic interactions and susceptibility broadening. Proton spectra were acquired using a 4 μ s $\pi/2$ pulse for excitation, followed by 2 seconds acquisition with a dwell time of 120 μ s. The resulting free induction decay was processed in matNMR (van Beek, 2007), applying 1 Hz line broadening prior to Fourier Transform. Signal intensities were obtained by integration of the corresponding peak regions in Matlab (Mathworks).

Data analysis conducted by Dr Phillip Williamson using a custom script.

2.13 Coherent Anti-stokes Raman Spectroscopy (CARS) microscopy

2.13.1 Sample preparation

The sample preparation was similar to that used for NMR. L4 worms were picked 16-18h prior to the beginning of the experiment. 7 different conditions

were used: N2 worms well-fed or food deprived for 0.5, 1, 1.5, 2, 4 and 24h. In the following, t₀ (time 0) corresponds to the moment when all conditions were harvested just before the fixation step.

At t-24h a plate containing around 45 L4 + 1 worms was washed twice with 600 μ L of M9 and worms containing M9 transferred into a 1.5mL Eppendorf tube. 3 PRWC with 500 μ L of M9 were performed before the worms were dropped onto a non-seeded plate.

The same protocol was applied at t-4h, t-2h, t-1.5h, t-1h and t-0.5h to obtain the 7 different conditions of food deprived worms ready at the same time at t₀.

All plates were washed twice with 600 μ L at t₀ and worms from each condition were transferred into a 1.5mL Eppendorf tube. 3 wash-cycles with 500 μ L of M9 were performed, then as much supernatant as possible was discarded trying not to pipette up worms. 150 μ L of formalin 4% was added under a chemical hood. 45min at room temperature was allowed for the fixation step to occur. Finally, 3 wash-cycles with 500 μ L of ddH₂O were applied and the samples kept at 4°C until the mounting step.

2.13.2 Mounting

Fixed samples were mounted between 2 cover slips (22x50 and 22x22 mm). A small square of parafilm was cut with scissors to produce a round-shape well and placed on the large coverslip to act as a spacer to avoid deforming the worms prior to imaging. A small droplet containing the fixed worms was placed in the well and then covered with the second cover slip.

2.13.3 CARS imaging methodology

CARS is a 4-photon process that requires excitation by two laser beams at two different wavelengths. A Chameleon Ultra Titanium Sapphire (Ti : Sa) pulsed femtosecond laser (Coherent Inc.) was used and split into two beams: A pump beam (835 nm) with 100 fs pulse duration and 80 MHz repetition rate and a second, Stokes beam, generated by optical parametric generation. The

Chapter 2

optical parametric oscillator (OPO) (Semi-Automatic, APE GmbH, Berlin) generated photons between 1080 nm and 1600 nm. For imaging lipids the CH₂ stretching frequency at 2845 cm⁻¹ was targeted as it is the CARS frequency for neutral lipids. The OPO was tuned to 1097 nm and both the beams were overlaid by a delay stage (LTS203, Thorlabs). For spatial overlap and scanning, a home-built galvanometer scanner was used. CARS emission was optimized by alignment of spatial and temporal overlay. Pixel dwell times were < 30 μs. The beams were coupled into an inverted microscope (Nikon Ti-U) for imaging the specimen. The resulting blue shifted CARS signals were read out in the Epi (back scattering) configuration. This minimized the CARS background. A Nikon 20x objective (0.75 NA) was used for imaging. The total power applied was less than 20 mW during imaging.

2.13.4 Imaging and data analysis

A series of images was taken for each time point and each individual sample. An area of 125 x 125 μm was scanned to generate highly resolved images at the optical diffraction limit with 1024 x 1024 pixels. For each time point, 3 worms were imaged. On each image, an area of interest has been drawn and the number of pixels corresponding to the area has been determined in ImageJ (U. S. National Institutes of Health, Bethesda, Maryland, USA, <http://imagej.nih.gov/ij/>). PMT (Photomultiplier tube) shot noise (electric noise) occurring in the images was smoothed out using average filtering. Images have been further processed by adjusting threshold so that lipid stores have been shown in white while the rest of the image remained black (**Figure 18**). ImageJ calculated the area count of lipid stores for each image. The ratio between pixel number that corresponds to distinct regions of interest and pixel number that corresponds to lipid stores area was used to determine lipid content in the worms.

Microscopy and images processing were performed by Justyna Smus.

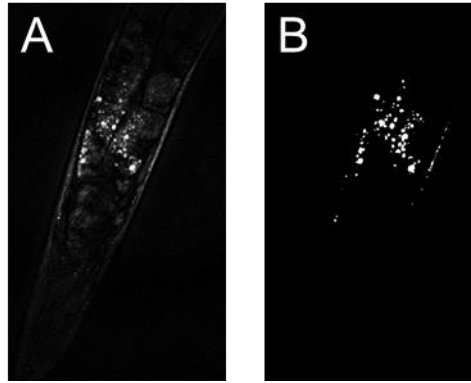


Figure 18: Unprocessed CARS image of the head region of a well-fed adult worm (A) and the same image with adjusted threshold to highlight lipid stores (B).

2.13.5 Statistical analysis

On the data sets obtained from image evaluation, one-way ANOVA and paired t-test were carried out in GraphPad Prism to determine overall and pair-wise significance

2.14 *eat-4(ky5); Ex[Pf1p-15::ChR2;YFP]* mutant strain generation by crossing

Cross between N2; *Ex[Pf1p-15::ChR2;YFP]* and *eat-4(ky5)*.

2.14.1 Male generation

10 plates where 5 N2; *Ex[Pf1p-15::ChR2;YFP]* L4 were picked, sealed with parafilm and sunk into a water bath at 33°C for 45 min. The plates were then stored for 3 days at 20°C.

2.14.2 Cross

12 males N2; *Ex[Pflp-15::ChR2;YFP]* positively selected for YFP expression were picked onto a plate with 4 *eat-4(ky5)* L4.

Three YFP positive worms of the F1 generation were picked onto 3 fresh plates.

30 individual F2 YFP positive worms were picked and maintained for 1-2 days to allow them to lay eggs (F3). The F2 parents were genotyped by single-worm PCR.

2.14.3 Genotyping by single worm PCR

2.14.3.1 Lysis step:

5 μ L of proteinase K containing lysis buffer (1 μ L of proteinase K for 100 μ L of lysis buffer) was placed per 0.2 μ L PCR tube. Each worm was then delicately picked inside each tube and lysed in the heating block (PCR machine model) using the following program.

60°C	1 hour
95°C	15 min
4°C	∞

After lysis the residual reagent was supplemented with Oligo (MWG Eurofins) and PCR reagents as indicated below.

2.14.3.2 Single worm PCR:

The PCR reaction was done using a Taq DNA Polymerase (1 U/ μ l), dNTPack (Roche Diagnostics GmbH, Germany, product no. 04738225001). Recipes were designed following the manufacturer's instructions.

Primers:

Forward	eat-4_gen0_Fwd	5' TCAACTTGCTTTTTCCTTCCTC 3'
Reverse	eat-4_gen0_Rev	5' AAGAAAACCAGCCGGAATCT 3'

Reaction:

	Stock unit	Final unit	Volume (μ L) 1 tube
dH ₂ O			11.75
Taq buffer	10 X	1 X	2.50
dNTP PCR grade	10 mM	0.2 mM	0.50
F. primer	10 μ M	0.5 μ M	2.50
R. primer	10 μ M	0.5 μ M	2.50
Taq	1 u/ μ L	0.25 u	0.25
DNA template			5.00

The contents were mixed and subjected to the following cycling parameters in the same heating block used for the lysis.

Initial denaturation	94°C	2 min	} 30 cycles
Denaturation	94°C	30 sec	
Annealing	58°C	30 sec	
Extension	72°C	45 sec	
Final extension	72°C	7 min	
Soak	4°C	∞	

Gel electrophoresis:

The authenticity of the individual amplification was verified by resolving 10 μ L of the PCR on a 1.5% (w/v) agarose gel prepared in TBE buffer (45mM Tris borate, 1mM EDTA) and heated in the microwave until molten. 5 μ L of 10,000x Gel Red (Biotium; Cambridge, UK) was added to the molten agarose once it had cooled to \sim 50°C, and the gel was poured into the gel mount. Bands were visualised using an Alpha Imager UV transilluminator.

10 μ L of PCR sample + 2.5 μ L of 5X loading buffer (5% bromophenol blue, 30% glycerol in dH₂O) were loaded per well. 5 μ L of 1 kb DNA ladder (Promega, UK) was used.

Offspring of strains homozygote for *eat-4(ky5)* 614bp deletion were selected. The *eat-4(ky5)* homozygote YFP positive offspring were maintained and frozen down.

2.15 Molecular Biology

2.15.1 Generation of the construct *Peat-4::eat-4*

To confirm the *eat-4* gene involvement in the pumping behaviour with a rescue experiment (see **section 4.2.1**), a construct containing the *eat-4* cDNA under the control of the *eat-4* promoter region was made using the Gateway technology.

2.15.1.1 Construction of pENTRY_eat-4 gateway entry vector

2.15.1.1.1 PCR amplification

Primers were designed (Eurofins Genomics, Germany) to flank the *eat-4* cDNA and include the Start and Stop codon (in red in the sequences below).

Forward	eat-4_TS319_Fwd	5' AGCATGTCGTCATGGAACGAG 3'
Reverse	eat-4_TS319_Rev	5' ACCCTACCACTGCTGATAATGC 3'

The PCR reaction was performed with pfu polymerase and pfu buffer (Promega, UK) as followed

	Stock unit	Final unit	Volume (μL) 1 tube
Rnase free H ₂ O qsp			37.58
pfu buffer	10 X	1 X	5.00
dNTP mix	10 mM	0.2 mM	1.00
F. primer	10 μM	0.5 μM	2.50
R. primer	10 μM	0.5 μM	2.50
pfu	3 u/ μL	1.25 u	0.42
DNA template	325 ng/ μL	325 ng	1.00

Initial denaturation	95°C	2min	} 30 cycles
Denaturation	95°C	40sec	
Annealing	61°C	0.5min	
Extension	72°C	3.5min	
Final extension	74°C	10min	
Soak	4°C	∞	

The authenticity of amplification was verified on 1% agarose gel (data not shown). 8 μL of the total amplification volume + 2 μL of 5X loading buffer.

5 μL of Bioline Hyper Ladder 1

2.15.1.1.2 TOPO ligation

Ligation reaction was performed according manufacturer's protocol.

ddH ₂ O	0 μL
Salt solution	1 μL
PCR product	4 μL
pCR [®] 8/GW/TOPO [®] vector (Invitrogen).	1 μL
Final volume	6 μL

The reaction was incubated for 15min at room temperature and then placed immediately on ice.

2.15.1.1.3 Bacterial transformation

2 tubes of TOP-10 chemically competent bacteria were thawed on ice. 4 μ L of either the TOPO cloning reaction or the salt solution from the pCR[®]8/GW/TOPO[®] kit (negative control) were added to bacteria and incubated for 30 min on ice. Heat shock was performed by transferring the incubation to water (42°C) for 30 seconds before immediately placing it back on ice. 250 μ L of room temperature SOC medium were added and the bacteria were incubated at 37°C and shaken for 1 hour. The 50 μ L and 250 μ L volumes were spread over LB agar plates containing Spectinomycin at a final concentration of 100 μ g/mL.

Plates were left to dry for 10 min and incubated at 37°C overnight to allow successful transformants to grow. No colonies were observed on control plates (bacteria transformed with salt solution) while some were visible on plates containing bacteria transformed with the ligation product.

10 colonies were selected and cultured in 7.5mL of LB (see **section 2.3.6**) + Spectinomycin (100ng/ μ L) and incubated at 37°C overnight.

2.15.1.1.4 Restriction mapping of insert orientation

The *eat-4* cDNA is inserted through an un-orientated bias. To differentiate between the preferred orientation 5'-3' relative to 3'-5' orientation and empty vector, restriction enzyme digestion mapping was used (see **Figure 19**).

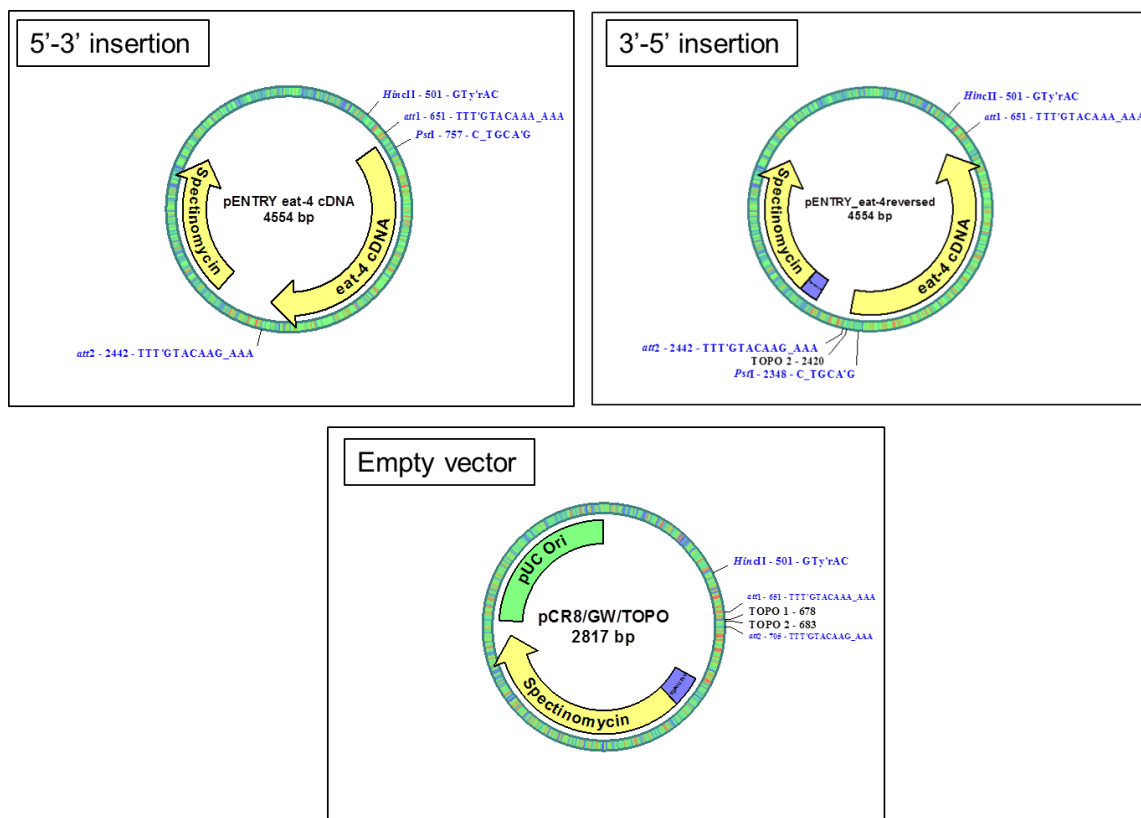


Figure 19: Restriction mapping of possible *eat-4* insert orientations.

The amplified *eat-4* cDNA can be inserted in two different orientations (5'-3' and 3'-5') or not at all (empty vector). *HincII* and *PstI* restriction sites are indicated.

Expected bands after *HincII*/*PstI* double digestion are: 256bp and 4298bp for the 5'-3' insertion, 1847bp and 2707bp for the 3'-5' insertion and 2817bp for the empty vector.

2.15.1.1.4.1 Crude mini-prep of DNA obtained by TOPO ligation:

1.5mL of the selected colonies (see **section 2.15.1.1.3**) was pelleted in a 1.5mL Eppendorf tube and the pellet re-suspended in 100 μ L of buffer P1 (from Qiagen kit). Membrane lysis was performed by adding 150 μ L of buffer P2. Tubes were inverted 5 times and incubated for 5min at room temperature. 150 μ L of Buffer P3 was immediately added and the tubes were gently mixed and spun at 13k rpm for 5 min in a bench tope centrifuge (Eppendorf 5417C).

Chapter 2

450µL of the supernatant was transferred into fresh tubes containing 900µL 100% EtOH, vortexed and spun for 5 min at 13k rpm again. After the supernatant was discarded, 100µL of 70% EtOH was added and the tube spun at 13K rpm at room temperature. The supernatant was discarded and the pellet air dried for 10 min before re-suspending in 20µL of ddH₂O.

2.15.1.1.4.2 Restriction digest

HincII and PstI were used to differentiate between empty vector or insertion in 5'-3' or 3'-5'.

Individual crude mini preps were incubated with restriction enzymes as indicated below.

Master mix

Volumes used for large volume are shown. The digest were incubated 2.5 hours at 37°C before being resolved on a 1% agarose gel. The 10µL digest volume was supplemented with 2.5µL of 5X loading buffer and total volume run on the gel. 5µL of Bionline Hyper Ladder 1 was used to orientate the fragments' size.

ddH ₂ O	3.4µL
NEB Buffer 3 10X	1µL
BSA 10X 1µg/µL	1µL
NEB HincII 10u/µL	0.3µL
NEB PstI 20u/µL	0.3µL
Crude-prep product	4µL
Final Volume	10µL

2.15.1.1.5 Minipreps and sequencing

Qiagen column kit was then used to perform mini preps on a colony exhibiting the digestion pattern of a 5'3' insertion.

The authenticity of the pfu generated clone *eat-4* cDNA was verified by sequencing (Eurofins Genomics, Germany) on both strands. The concentration of DNA was estimated by nanodrop at 78ng/µL.

2.15.1.2 Gateway recombination of pENTR_eat-4 with pDEST_eat-4:

Gateway cloning (Invitrogen) was used to directionally insert *eat-4* cDNA in the pENTR vector into a pDEST vector (made by Catriona Murray) containing 5.3Kb of the 5' end of the *eat-4* gene. This was done as indicated below in which the Clonase II was added last and the reaction vortexed twice briefly before incubation for 1 hour at 25°C. Finally 1 µL of proteinase K was added to terminate the reaction by incubation 10 min at 37°C.

pENTR_eat-4	1.92 µL (150ng final)
pDEST_eat-4	1.07 µL (150ng final)
TE Buffer	5.01 µL
Clonase II	2 µL
Final volume	10 µL

TOP-10 competent cells were mixed with 1 µL of the terminated reaction and transformed by heat shock as previously described. Antibiotic selection was made with Ampicillin at a final concentration of 100µg/mL.

2.15.1.2.1 Restriction digestion mapping of transformants

The confirmation of the recombination was made by following the digestion of crude mini preps (see **section 2.15.1.1.4.1**) using BamHI as indicated below.

ddH ₂ O	3.7µL
NEB Buffer 3 10X	1µL
BSA 10X 1µg/µL	1µL
NEB BamHI 20u/µL	0.3µL
Crude-prep product	4µL
Final Volume	10µL

The predicted restriction map for recombined and empty vector pDEST_peat-4 plasmid is represented in **Figure 20A**.

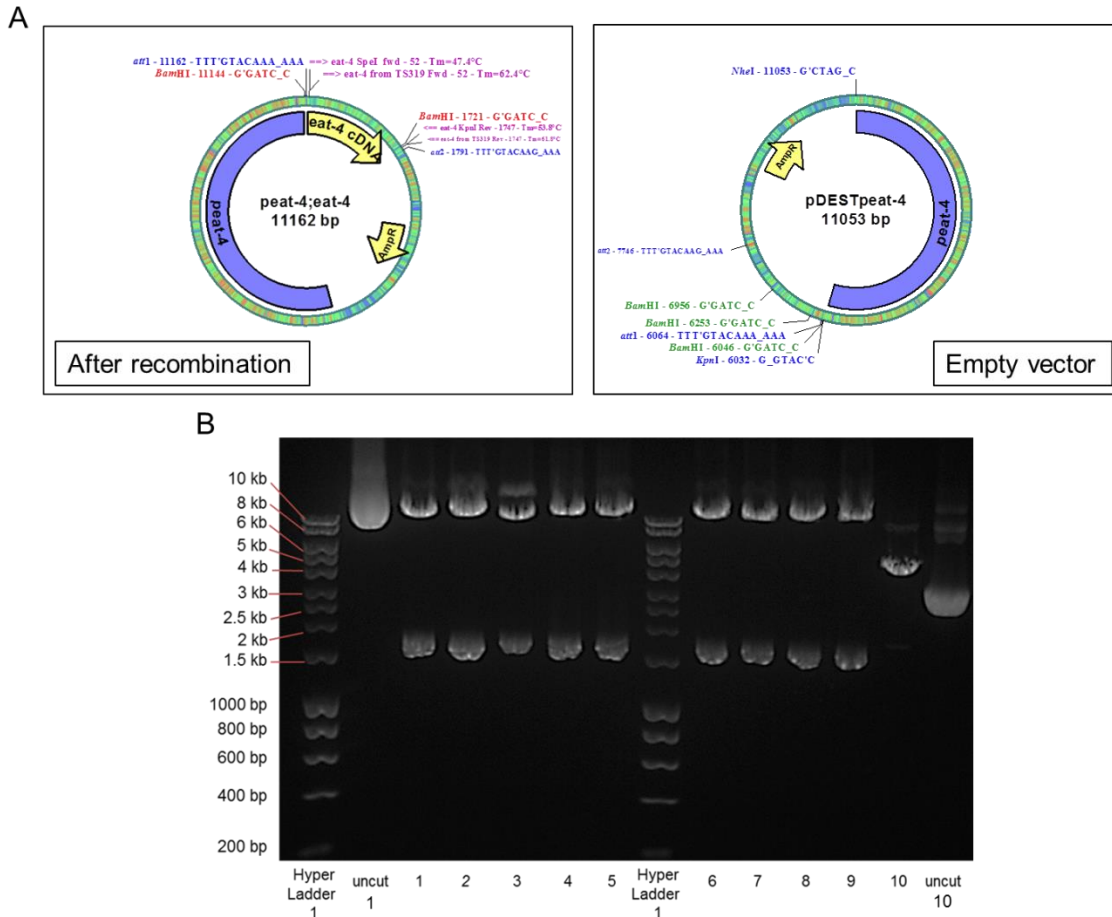


Figure 20: Restriction mapping of the *peat-4::eat-4* following recombination.

A. Representation of a pDEST-*peat-4* and the recombined *peat-4::eat-4* vectors. If the recombination worked, the expected bands after BamHI digestion are: 9423bp and 1739bp

In contrast, digestion of the pDEST_peat-4 without recombination should give the following bands: 10143bp, 703bp and 207bp.

B. 0.8% Agarose gel loaded with 10µL of digest + 2.5µL of 6X loading buffer. 5µL of Bioline Hyper Ladder 1 was used to orientate the fragments' size.

Of the ten colonies tested, nine generated the predicted restriction pattern (**Figure 20B**). Mini preps were performed (see **section 2.15.1.1.5**) on the colonies 2, 4, 6 and 7 and a Pst-1 digestion was performed on these mini

preps to independently show the plasmid contained the expected DNA (data not shown). All tested colonies appeared *peat-4;eat-4*.

The plasmid from colony 4 (**Figure 20B**) was sequenced (primers flanking the *eat-4* cDNA, sequencing on both strands) to authenticated the sequence.

2.15.2 Generation of the *Pmyo-2::npr-3* expression construct

2.15.2.1 *npr-3* cDNA amplification by PCR:

npr-3 cDNA was amplified from the C10C6.2 Gateway ENTRY plasmid. This plasmid lacks the first nucleotide 'A' from the ATG and the 'AA' from the stop codon 'TAA' (Reboul *et al.*, 2003) so the primers used for amplification contained 5' sequences containing the ATG and TAA to ensure the amplified cDNA contained a bona fide Start and Stop codon (indicated in red in the primer sequences below).

Primers:

Forward	Pnpr-3_atgFor	5' A TGGAGGGTGGTCGAAACTGTG 3'
Reverse	Pnpr-3_taaRev	5' T TATAAAAAGTTGATCTCCAGCT 3'

The PCR was performed with the designated template using the conditions indicated below.

	Stock unit	Final unit	Volume (μL)
Rnase free H2O			33.58
pfu buffer	10 X	1X	5.00
dNTP mix	2mM	0.2mM	5.00
For. primer	10μM	0.5μM	2.50
Rev. primer	10μM	0.5μM	2.50
pfu	3u/μL	1.25u	0.42
DNA template	60ng/μL	60ng	1.00

Fin: 50μL

Chapter 2

PCR conditions

Initial denaturation	95°C	2min
Denaturation	95°C	40sec
Annealing	52°C	0.5min
Extension	72°C	3min
Final extension	72°C	10min
Soak	4°C	∞

x30 cycles

2.15.2.2 Gel purification:

An analytical gel utilizing 5µl of the reaction was used to identify successful amplification (data not shown). The remaining reaction was resolved on a 1% agarose gel. A major band (**Figure 21**) was excised under UV light with a clean razor blade and placed into an Eppendorf tube. The DNA was eluted from the excised gel into 20µl of ddH₂O using Gel Purification Kit according to the manufacturer's instruction (Qiagen).

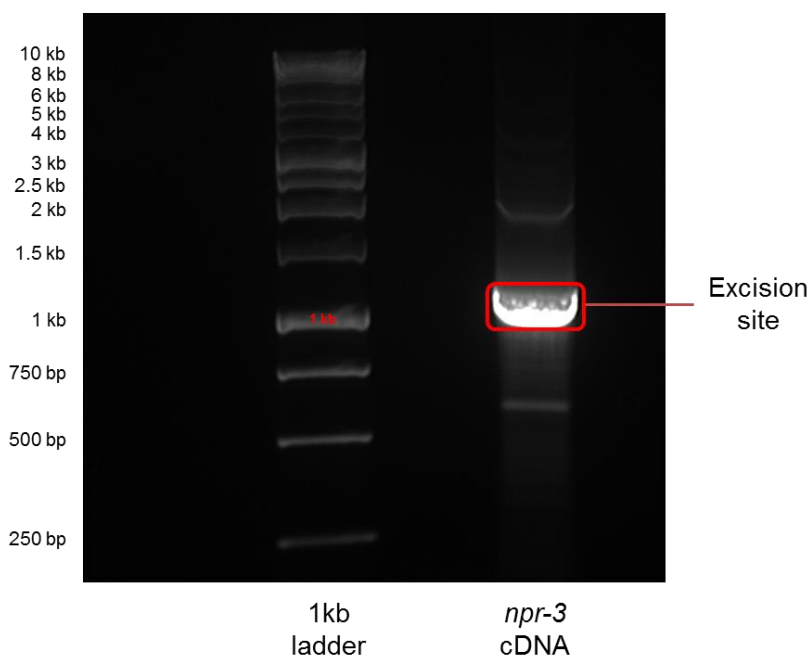


Figure 21: Gel electrophoresis of the amplified *npr-3* cDNA prior excision.

A 1% agarose gel was loaded with 45µL of PCR product + 5µL of 6X loading buffer. The expected band (circled in red) was excised under UV light.

2.15.2.3 Taq reaction:

A Taq polymerase reaction was performed on the gel-purified DNA to add a nucleotide 'A' overhang to the *npr-3* cDNA purified PCR product. The following were added directly to the purified PCR product:

Taq pol. Buffer 10X	3 μ L
dATPs 100mM	1.5 μ L
Taq polymerase	0.5 μ L

Incubation was conducted at 72 °C for 15 min.

2.15.2.4 TOPO ligation:

A TOPO ligation was conducted as described above (see **section 2.15.1.1.2**) and the ligated DNA was transformed into TOP-10 chemically competent bacteria (Invitrogen) (see **section 2.15.1.1.3**)

2.15.2.5 PCR screening for plasmid containing colonies

Colonies obtained from plating the transformed TOPO ligations (see **section 2.15.1.1.3**) were directly tested by PCR using bacteria stab as followed.

Ready Mix Go Taq 2X	12.5 μ L
Primer <i>npr-3</i> _ATG_For 10mM	1 μ L
Primer <i>npr-3</i> _TAA_Rev 10mM	1 μ L
ddH ₂ O	10.5 μ L
25 μ L	

Initial denaturation	95°C	10min	X25 cycles
Denaturation	95°C	30sec	
Annealing	52°C	30sec	
Extension	72°C	1.5min	
Final extension	72°C	10min	
Soak	4°C	∞	

Chapter 2

10µl of the amplified product was resolved on agarose gel. All tested colonies amplified a band of expected size relative to negative control (water blank).

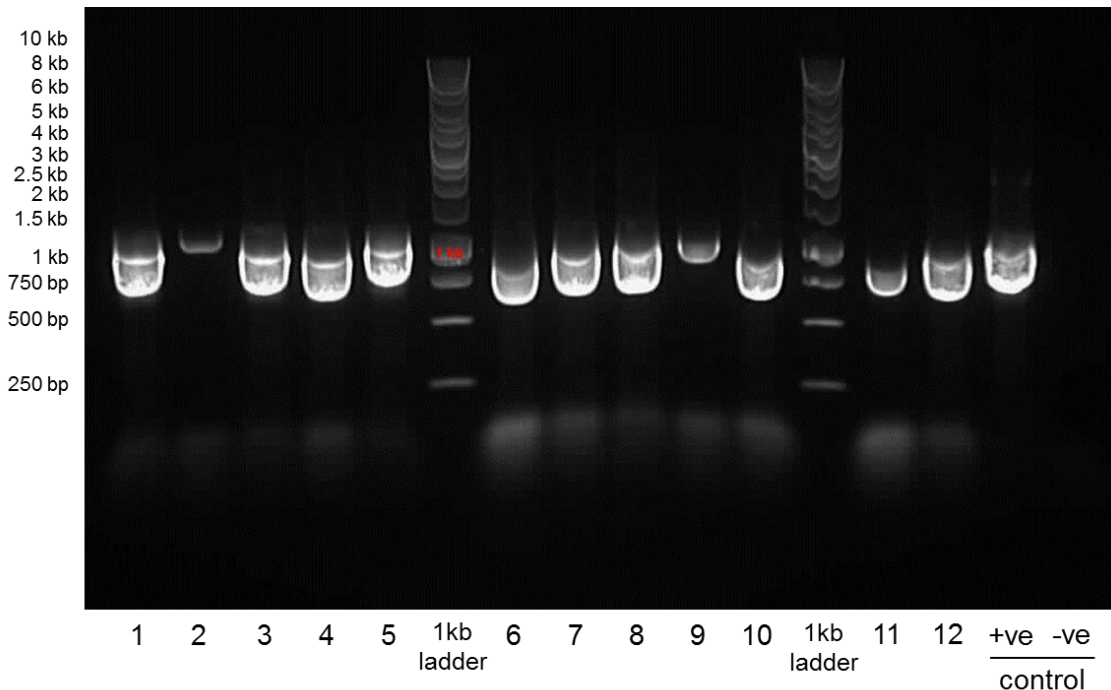


Figure 22: Verification of the *npr-3* cDNA insertion in the TOPO vector by gel electrophoresis:

10µL of DNA mixed with 2.5µL of 5X loading buffer was loaded on a 0.8% agarose gel. A similar band to the positive (+ve) control was expected in vectors inserted with *npr-3* cDNA.

'+ve control' used C10C6.2 plasmid as DNA template while '-ve control' used water.

2.15.2.6 Restriction digest mapping to authenticate pENTR_*npr-3* vector

Colonies 1 to 12 (**Figure 22**) were cultured overnight and plasmid DNA was extracted by crude mini preps (see **section 2.15.1.1.4.1**). 3µl of the crude mini preps were digested with EcoRI and Aval, as indicated below (**Table 1**), and

incubated at 37 °C for 2 hours before being mixed with 2.5 µL of 6X loading buffer and resolved on a 0.8% agarose gel (**Figure 24**). The expected bands for pENTR_npr-3 following *Ava*I (New England Biolabs, UK) and *Eco*RI (Promega, UK) digestion, depending on the insertion orientation, is summarised in **Figure 23**.

Buffer H 10X	1 µL
BSA 100X 10µg/µL	0.1 µL
DNA (TOPO ligation)	3 µL
ddH ₂ O	5.4 µL
<i>Eco</i> RI 12u/µL	0.5 µL
	10 µL

Buffer cutsmart 10X	1 µL
DNA (TOPO ligation)	3 µL
ddH ₂ O	5.8 µL
<i>Ava</i> I 50u/µL	0.2 µL
	10 µL

Table 1: Enzymatic digestion using *Eco*RI and *Ava*I.

Digestions were performed at 37 °C for 3 hours.

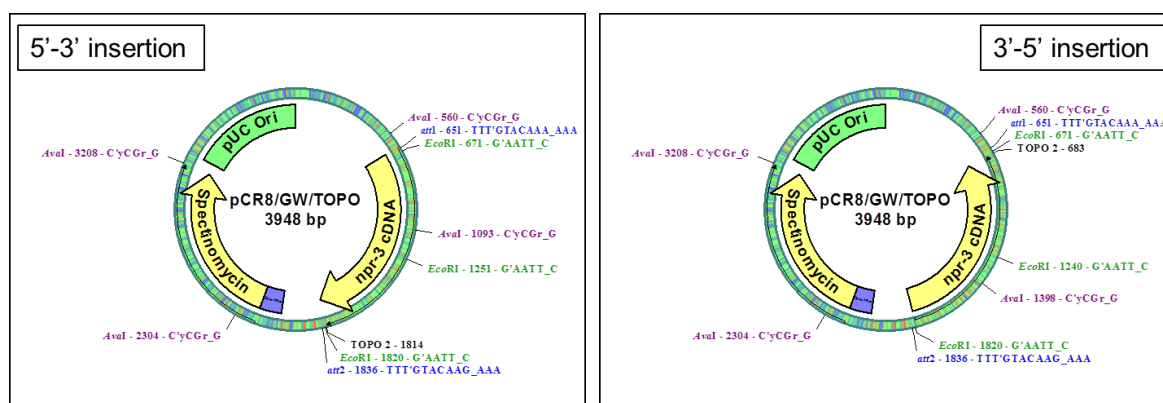


Figure 23: Restriction mapping of possible *npr-3* insert orientations

The amplified *npr-3* cDNA can be inserted in two different orientations (5'-3' and 3'-5'). *Ava*I (purple) and *Eco*RI (green) restriction sites are indicated.

If inserted in a 5'-3' configuration *Ava*I digestion is expected to give 4 bands (1300bp, 1211bp, 904bp and 533bp) and *Eco*RI digestion 3 bands (2799bp, 599bp and 589bp). If inserted in a 3'-5' configuration *Ava*I digestion is expected to give 4 bands (1300bp, 906bp, 904bp and 838bp) and *Eco*RI digestion 3 bands (2799bp, 580bp and 569bp).

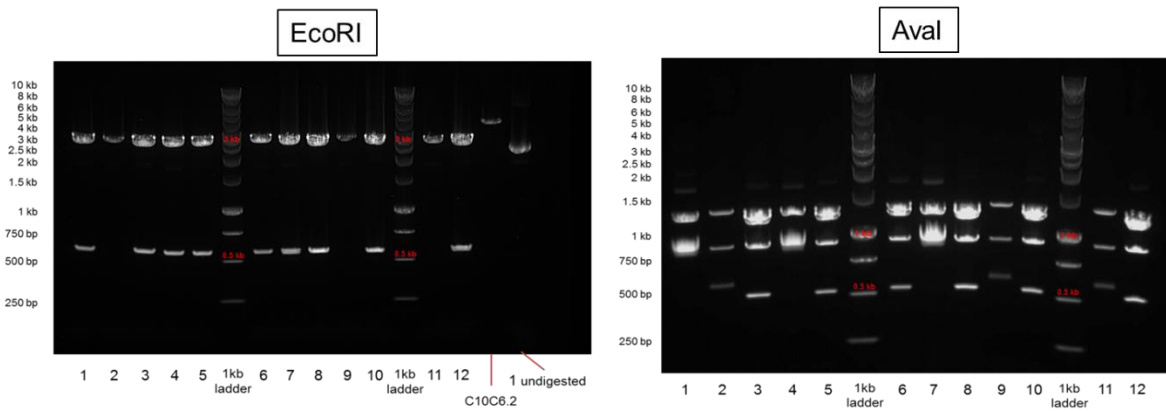


Figure 24: Restriction mapping of the pENTR_npr-3 following TOPO ligation.

Ligation products digested by EcoRI (left) and AvaI (right) were loaded, 10 μ L of DNA mixed with 2.5 μ L of 5X loading buffer, on a 0.8% agarose gel. 5 μ L of 1 kb ladder (Promega, UK) was loaded and the bands corresponding to 3 kb and 0.5 kb are indicated in red.

Plasmids from colonies 3, 5, 6, 8, 10 and 12 were identified as having *npr-3* cDNA integrated in 5'-3' orientation (**Figure 24**).

Mini preps (see **section 2.15.1.1.5**) were performed on colonies 3 and 5, and sequencing confirmed the presence of ATG and TAA codons authenticity of the intervening sequence.

2.15.2.7 Gateway recombination to generate *Pmyo-2::npr-3*

The recombination was as carried out (see **section 2.15.1.2**) using the following reagents

pENTR_npr-3	0.75 μ L (150ng final)
pDEST_pmyo-2	3.3 μ L (150ng final)
TE Buffer	3.95 μ L
Clonase II	2 μ L
Final volume	10 μ L

Crude mini preps (see **section 2.15.1.1.4.1**) were performed and 3 μ l subjected to Aval digestion as indicated below (**Table 2**) and resolved on an agarose gel (**Figure 25**) to verify recombination.

Buffer cutsmart 10X	1 μ L
DNA (TOPO ligation)	3 μ L
ddH ₂ O	5.8 μ L
AvaI 50u/ μ L	0.2 μ L
	10 μ L

Table 2: *Pmyo-2::npr-3* digestion with AvaI

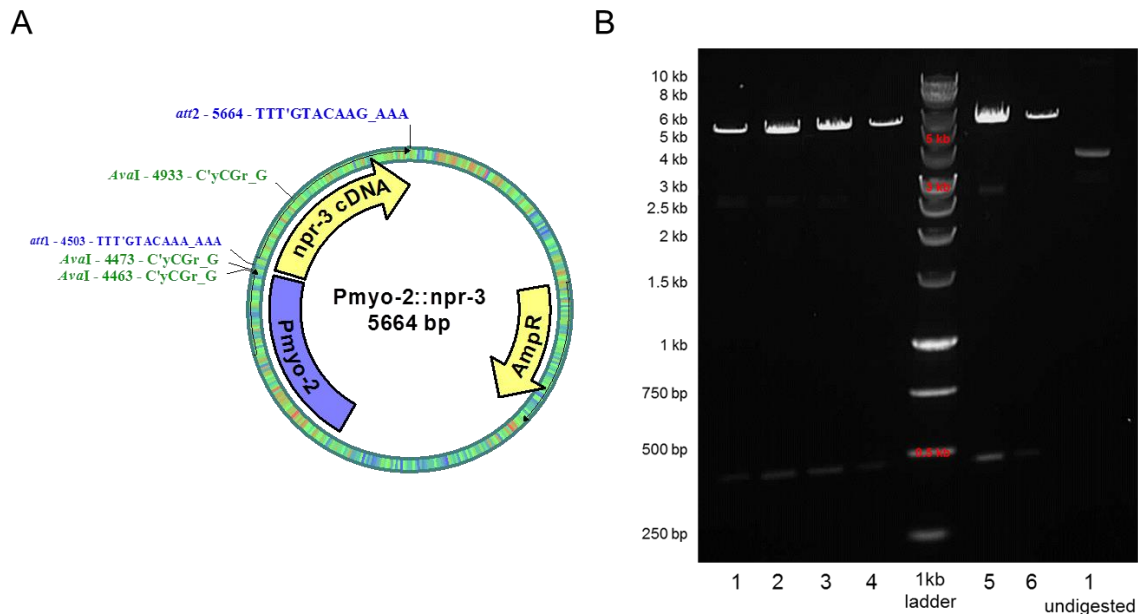


Figure 25: Restriction mapping of the *pmyo-2::npr-3* following recombination.

A. Representation of the expected *pmyo-2::npr-3* recombined vector. *Ava*I restriction sites are indicated in green. Expected bands following *Ava*I digestion: 5194bp, 460bp and 10bp.

B. Gel electrophoresis of recombinants digested with *Ava*I. 10 μ L of digested product + 2.5 μ L of 6X loading buffer were loaded in the 0.8% agarose gel. In red are indicated the 5kb, 3kb and 0.5kb bands of the 1kb ladder (Promega, UK).

Mini preps were performed on colonies 1 and 6 and DNA was sequenced (see section 2.15.1.1.5). Both were confirmed as correct *Pmyo-2::npr-3*. The construct was used to transform *npr-3(tm1583)* mutant by microinjection (see section 2.5).

Chapter 3: Development of “on” and “off” food paradigms to identify complex regulation of feeding behaviour in *C. elegans*

3.1 Introduction

The pharynx of the free living nematode *C. elegans* provides a powerful tool to investigate the mechanisms mediating feeding behaviours in response to food cues. The worm actively feeds on *E. coli* OP50 bacteria in laboratory conditions (See **section 1.1.1**). Observation of the pharyngeal rhythmic contraction relaxation cycle, pumps, revealed worms display a high-frequency pump rate (4-5 Hz) when in contact with food (Avery, 2003; Song and Avery, 2012; Song *et al.*, 2013).

The pharynx is modulated by its embedded pharyngeal nervous system, expressing a range of classical small molecule neurotransmitters, neuropeptides and receptors (Franks *et al.*, 2006) (See **section 1.2.2.2** and **Figure 13A**). Early studies, notably based on pharyngeal neurons laser ablation experiments, have assigned functional roles to specific neurons within the pharyngeal nervous system, in particular MC, which acts as a cholinergic pacemaker motor neuron (Raizen *et al.*, 1995) to drive the high rate of pumping in the presence of food. In order to reach such high frequency pumping rate, the duration of the pharyngeal pump is regulated by inhibitory glutamatergic transmission from the M3 neurons (Niacaris, 2003). In turn, MC, M3, M4 and the pharyngeal muscle itself are subject to regulation by 5-HT neurons to regulate the microcircuit to permit a sustained high frequency of pumping in the presence of bacteria (Raizen and Avery, 1994; Rogers *et al.*, 2001; Niacaris, 2003; Hobson *et al.*, 2006). The 5-HT responsible for these effects is believed to be released from the pharyngeal neuron NSM and/or the extra-pharyngeal neuron ADF (Cunningham *et al.*, 2012; Li *et al.*, 2012).

Chapter 3

The pharyngeal system is subject to regulation depending on the food context (Horvitz *et al.*, 1982). Early studies reported that *C. elegans* pumping, measured by feeding worms with iron particles, is reduced by at least half in the absence of food, although after more than four hours of food deprivation the worms started to pump again (Avery and Horvitz, 1990) even though there was no food in the vicinity. It has been suggested that this may be a result of the increasing need for food as starvation progresses (Avery and Horvitz, 1990). Furthermore it was observed that worms carrying mutations in the gene *unc-31*, which encodes CAPS, a calcium-binding protein required for exocytosis (Ann *et al.*, 1997), pumped constitutively in the absence of food (Avery *et al.*, 1993).

Since these early studies there have been a number of studies investigating *C. elegans* pharyngeal function in different behavioural contexts and during starvation. However, the distinct paradigms used in these studies made comparisons difficult. For instance, Keane *et al.* observed a marked reduction of the pumping rate in absence of food (< 1.5 Hz), however, worms used for these studies underwent various times of food deprivation (Keane and Avery, 2003). Similarly, some studies have been conducted at different time of food deprivation or even at different temperatures and using different methods to assess the pumping rate (Sze *et al.*, 2000; Greer *et al.*, 2008; You *et al.*, 2008; Lee *et al.*, 2011; Dwyer and Aamodt, 2013). Nonetheless, these results suggest a complex shifting behavioural response of the pharyngeal system which is dependent on the 'on' and 'off' food context. However, the temporal aspects of this behaviour and the role of discrete neural signals have not yet been defined.

In view of this under-investigated aspect of behaviour, and its broader interest with respect to understanding fundamental mechanisms of behavioural plasticity, the aim of this chapter was to study the pumping behaviour of *C. elegans* in the presence of food and following removal of food. For this purpose, an assay to investigate the temporal effects of food deprivation was developed. This was deployed to determine molecular modulators of the temporally regulated neuroadaptive response by investigating mutants that impact on specific neurotransmitter pathways. By

judicious investigation of a panel of mutants the aim was to advance our understanding of the on and off food states of the pumping behaviour.

3.2 Results

3.2.1 Food deprivation leads to reduction of the pharyngeal pumping rate in two distinct phases

When *C. elegans* were placed on a plate replete with *OP50 E. coli* bacteria, they dwelled and exhibited a pharyngeal pump rate of > 200 pumps per minute (ppm) (**Figure 26B**) (Raizen *et al.*, 1995; Walker *et al.*, 2002).

An experimental paradigm was designed to investigate the temporal aspects of food deprivation on the pumping behaviour (**Figure 26A**). This experiment utilized L4 worms which were grown overnight on food. A cleaning step was conducted first by transferring well-fed L4 +1 worms to an arena without bacterial food for 1 min before new transfer onto a 9 cm no food arena. As a control, the pumping rate of well-fed worms transferred to a new bacterial lawn was measured. This control showed that transferring worms induced mechanosensory-mediated inhibition of pumping that was followed by recovery to the normal pumping rate on food, as previously reported (Keane and Avery, 2003) (**Figure 26B**). On food, the recovery happens in less than 5 min following transfer.

In addition, transferred worms were observed on plates without food over a five hour period at indicated time points. Changes in the pumping rate were observed, and phases were defined arbitrarily on the basis of key changes in the behaviour (**Figure 26C**). The pumping rate was briefly observed immediately following transfer, and an initial pumping inhibition, as seen when worms were picked between food plates, was observed. Subsequently, the pumping rate remained low but slowly increased during the first 120 min of food deprivation, to about one quarter of the rate on food i.e. 50 ppm (**Figure 26C**). These first 120 min of food deprivation has been called "early phase" of the response to food removal. After the early phase there was a shift in the

behaviour in which the pumping rate became more erratic, with the rate of individual worms fluctuating between relatively low (0-20 ppm) and relatively high pump rates (100-200 ppm; **Figure 26D**). This was called the "late phase" of the response to food removal. Finally, in each experiment worms were placed back onto food and showed a rapid recovery of pumping. It is important to note that only freshly poured plates were used for this experiment (3 to 14 days old), as it has been observed the pumping behaviour off food may vary with older plates (data not shown).

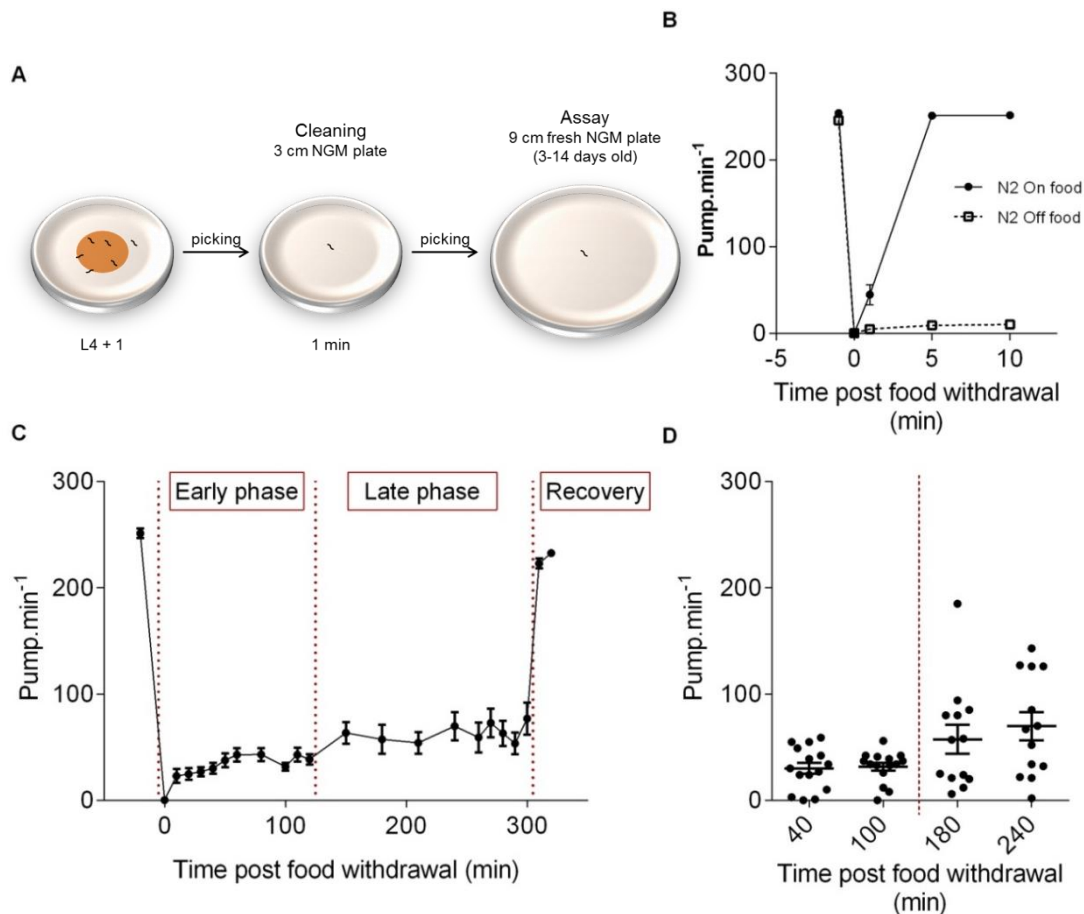


Figure 26: Modulation of pharyngeal pumping on and off an *E. coli* OP50 food source.

A. Schematic representation of the pumping off food assay.

B. Pumping rate of well-fed worms before and after pick mediated transfer to agar plates with or without an OP50 bacterial lawn. The on-food pumping is

stopped by the transfer and returns to pre-pick on food levels when returned to bacteria. There is a reduced but clearly measurable off food pumping rate after the initial pick mediated inhibition.

C. Extended time course in which worms handled as in **B** are monitored off food at indicated time points before being picked back onto a bacterial lawn. The adaptive response in pharyngeal pumping is segregated into 3 phases. These demarcations, defined by visual inspection, are indicated by broken lines highlighting an early phase (0 to 120 min), a late phase (120 min to 300 min) and a recovery (300-320 min) phase. These experiments represent mean of observations made on 15 individual worms.

D. Scatter plot of two time points of both the early (30 and 70 min) and erratic phase (180 and 240 min) to illustrate the increased variability during the erratic phase. Each datum point indicates a measurement made from a single worm.

3.2.2 ACh, glutamate and 5-HT food-dependent modulation of the pumping behaviour

Signalling through acetylcholine, glutamate and 5-hydroxytryptamine (5-HT or serotonin) neural pathways within the pharyngeal microcircuit have all been reported to be required to maintain a high pumping rate on food (Avery, 1993; Raizen *et al.*, 1995; Lee *et al.*, 1999; Niacaris, 2003; Song and Avery, 2012). In this study, strains deficient in these transmitters, harbouring mutations in the vesicular transporters for acetylcholine (*unc-17(e113)* and *unc-17(e245)*) (Alfonso *et al.*, 1993) or glutamate (*eat-4(ky5)*) (Lee *et al.*, 1999), or the rate-limiting 5-HT synthesis enzyme, tryptophan hydroxylase (*tph-1(mg280)*) (Sze *et al.*, 2000), have been used. The acetylcholine analysis uses hypomorphic strains as mutants completely lacking acetylcholine are non-viable (Alfonso *et al.*, 1993).

The deficiencies in these core regulators of pharyngeal function all showed a reduced pumping on food relative to wild type worms (**Figure 27A, B, C and D**) (Dent *et al.*, 1997; Sze *et al.*, 2000; McKay *et al.*, 2004). However none of these deficiencies completely prevented the pumping rate on their own, and with the exception of *unc-17(e245)*, the reduction was less than 50%.

The situation in the absence of food was strikingly different. The less severe of the hypomorphic mutant for acetylcholine, *unc-17(e113)* mutants, although not significant, showed a trend toward a reduced pumping rate, while *unc-17(e245)* mutant had a clear reduced pumping off food which supports an important cholinergic excitatory drive off food. In contrast to the stimulatory role of 5-HT and glutamate in the presence of food, as indicated by the reduced pumping in the respective mutants, the glutamate and 5-HT deficient mutants showed higher pumping rates compared to wild-type control in absence of food (**Figure 27C, D, E**). Furthermore, there is a temporal aspect to the 5-HT regulation, as this reduction was only apparently required following food deprivation of longer than four hours (**Figure 27C, D**).

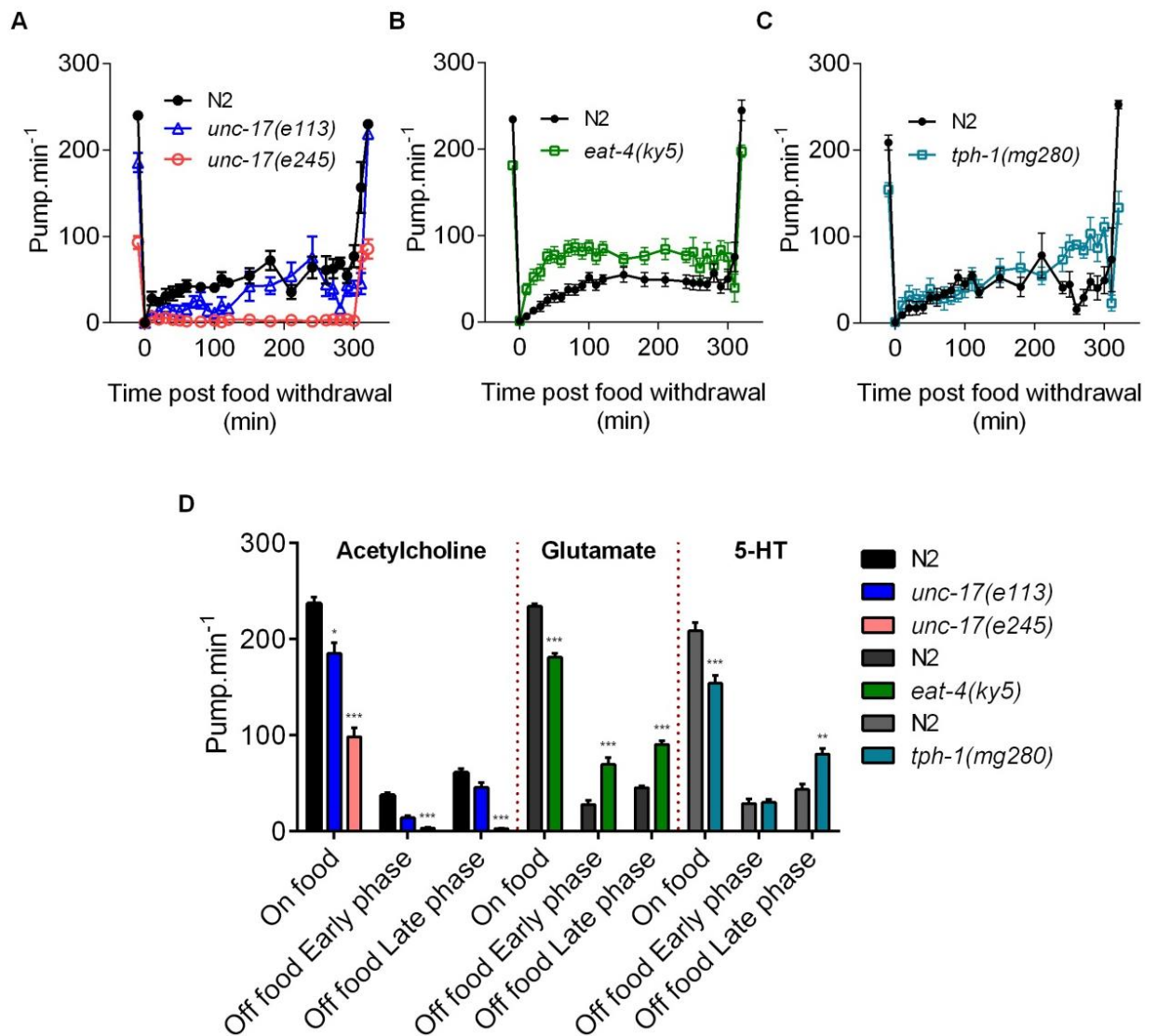


Figure 27: Comparison of the role played by major pharyngeal transmitters acetylcholine, glutamate and 5-HT to the pharyngeal pumping rate on and off food.

A. Acetylcholine: *unc-17(e113)* (-26 ± 11 ppm; $p = 0.029$ $n = 11$ N2, $n = 10$ *e113*) and *unc-17(e245)* (-158 ± 8 ppm; $p < 0.001$; $n = 20$ N2, $n = 20$ *e245*) mutants displays a lower pumping rate than N2 (wild-type) in the presence of food. *unc-17(e113)* showed no effect on the early phase ($p = 0.214$; $n = 9$) or erratic phase ($p = 0.902$; $n = 7$) relative to N2 ($n = 6$ and $n = 3$ for early and late phase respectively). However, *unc-17(e245)* displayed a reduced pumping rate off food during both early (-48 ± 8 ppm; $p < 0.001$; $n = 8$ N2 and *e245*) and late phase (-64 ± 12 ppm; $p < 0.001$; $n = 8$ N2 and *e245*) compared to N2.

B. Glutamate: *eat-4(ky5)* displays a lower pumping rate than N2 (-53 ± 5 ppm; $n = 19$ N2 and $n = 18$ *eat-4*) in the presence of food ($p < 0.001$). *eat-4(ky5)*

mutant pumps at a higher rate during the early ($p < 0.001$; $n = 16$) and late phase ($p < 0.001$; $n = 7$) of food deprivation. Both of these phases are elevated by 45 ppm indicating that *eat-4* mutants have a constitutive pumping phenotype. **C.** 5-HT: *tph-1(mg180)* displays a lower pump rate (-54 ± 12 ppm) than N2 in the presence of food ($p < 0.001$; $n = 8$ N2, $n = 10$ *tph-1*). No significant effect was observed in absence of food during the early phase ($p = 0.8521$; $n = 8$ N2, $n = 10$ *tph-1*) but a higher pumping rate (36 ppm) was observed during the late phase ($p = 0.0362$; $n = 5$ N2, $n = 5$ *tph-1*) for these mutants. **D.** Histogram representing the average pumping rate on food and off food during the early and late phases of figures B, C and D. * ($p < 0.05$), ** ($p < 0.01$) and *** ($p < 0.001$) compared to paired N2.

3.2.3 GABA and dopamine promote pumping during food deprivation

There is no evidence for pharyngeal synthesis of GABA and dopamine (Franks *et al.*, 2006) but there is potential for them to regulate pumping via input through the RIP interneurons circuits or humoral signals received by receptors expressed in the pharyngeal nervous system (Tsalik and Hobert, 2003; Sugiura *et al.*, 2005; Packham *et al.*, 2010).

These experiments used strains with mutations in the biosynthetic enzymes glutamic acid decarboxylase (*unc-25*), tyrosine hydroxylase (*cat-2*), dopamine beta hydroxylase (*tbh-1*) and tyrosine decarboxylase (*tdc-1*) deficient in GABA, dopamine, octopamine and tyramine respectively (McIntire *et al.*, 1993; Alkema *et al.*, 2005; Calvo *et al.*, 2011). A significant reduction in the pumping rate on food has been observed in mutants lacking the neurotransmitter GABA, suggesting it contributes to the stimulatory drive in the presence of food (**Figure 28A, C**). For the dopamine deficient mutant *cat-2* had no effect on food, however there was a small but significant reduction in pumping during the early phase of food deprivation, consistent with a net stimulation effect on pharyngeal function during this phase of the behaviour (**Figure 28B, C**). The effect was marginal compared to what was observed in the glutamate mutant *eat-4(ky5)*, and no difference was observed during the late phase between *cat-2(e1112)* and N2.

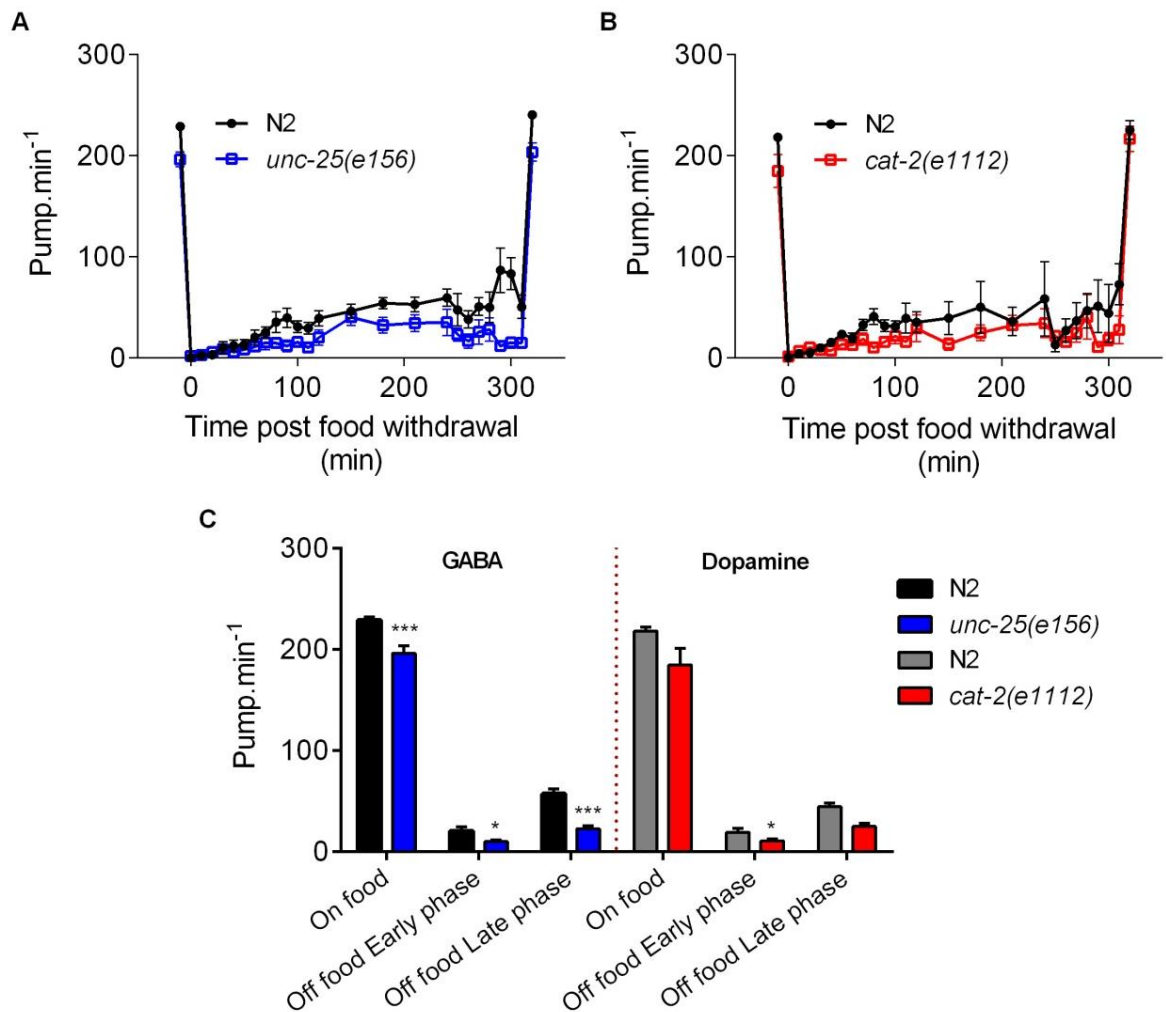


Figure 28: Modulation of pharyngeal pumping by major neurotransmitters that are synthesized extrinsically to the pharynx: GABA and dopamine.

A. GABA: *unc-25(e156)* pump less than wild-type N2 (-32 ± 7 ppm; $n = 12$ N2, $n = 10$ *unc-25*) in the presence of food ($p < 0.001$). A significant reduction of the pumping rate relative to N2 was observed during both early (-10 ± 8 ppm; $p = 0.0157$; $n = 11$ N2, $n = 9$ *unc-25*) and late (-44 ± 15 ppm; $p < 0.001$; $n = 7$ N2, $n = 7$ *unc-25*) phases of food deprivation.

B. Dopamine: *cat-2(e1112)* mutants display a similar pumping rate to N2 in the presence of food ($p = 0.0665$; $n = 12$ N2, $n = 13$ *cat-2*). The pump rate is slightly lower (9 ± 8 ppm; $n = 6$ N2, $n = 7$ *cat-2*) than N2 during the early phase ($p = 0.0452$), but not the late phase ($p = 0.2632$; $n = 3$ N2, $n = 6$ *cat-2*) of the food deprivation.

C. Histogram representing the average pumping rate on food and off food during the early and late phases of figures A, and B. * ($p < 0.05$), ** ($p < 0.01$) and *** ($p < 0.001$) compared to paired N2.

The behaviour of the mutants defective in tyramine and octopamine signalling were indistinguishable from wild-type controls, showing no role for these neurotransmitters in this feeding paradigm (Figure 29A, B, C).

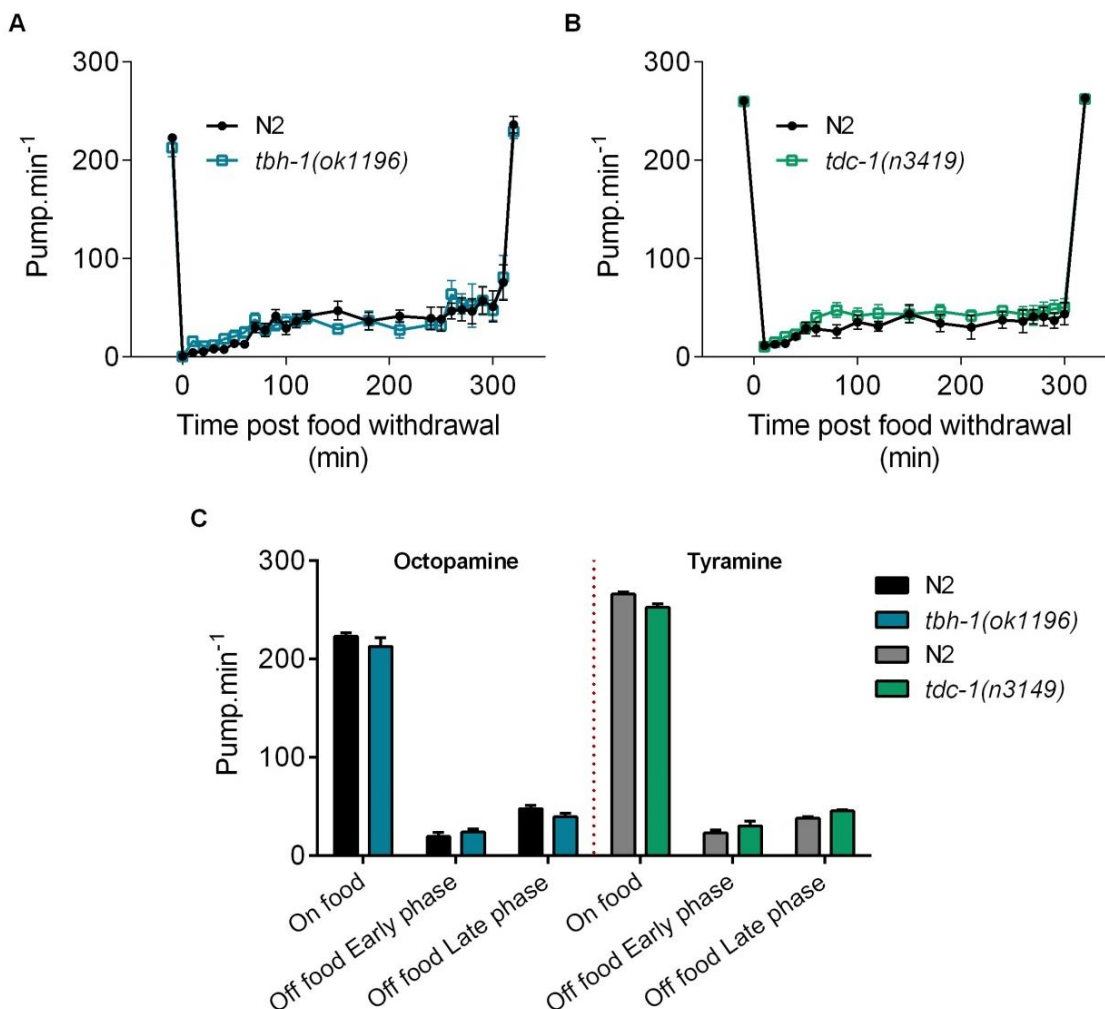


Figure 29: Modulation of pharyngeal pumping by major neurotransmitters that are synthesized extrinsically to the pharynx: octopamine and tyramine.

A. Octopamine: *tbh-1(ok1196)* pharyngeal pumping is similar to N2 in the presence ($p = 0.2805$; $n = 13$ N2, $n = 12$ *tbh-1*) and absence of food ($p = 0.1777$; $n = 12$ N2, $n = 11$ *cat-2* and $p = 0.4456$; $n = 5$ N2, $n = 6$ *cat-2* for the early and late phase respectively).

B. Tyramine: *tdc-1(n3419)* pumps at a similar rate compared to N2 both in the presence of food ($p = 0.3435$; $n = 17$ N2, $n = 17$ *tdc-1*) and in the absence of food ($p = 0.2577$; $n = 8$ N2, $n = 8$ *cat-2* and $p = 0.483$; $n = 8$ N2, $n = 8$ *cat-2* for the early and late phase respectively). Experiment performed by Jonathan Woolman under my supervision.

C. Histogram representing the average pumping rate on food and off food during the early and late phases of figures A and B. * ($p < 0.05$), ** ($p < 0.01$) and *** ($p < 0.001$) compared to paired N2.

3.2.4 *unc-31* pumps constitutively throughout food deprivation

Work previously conducted defined that *unc-31* mutants move more slowly in the presence of food (Charlie *et al.*, 2006) and show constitutive pumping in the absence of food (Avery *et al.*, 1993).

unc-31(e928) pumped at the same rate as wild-type in the presence of food. In the absence of food however, their pumping rate was markedly elevated (**Figure 30A, B**). These data reinforce the previous observations showing that *unc-31* alleles exhibit constitutive pharyngeal activity (Avery *et al.*, 1993), and suggest that *unc-31* mediates a net reduction on the pharyngeal pumping in response to food removal.

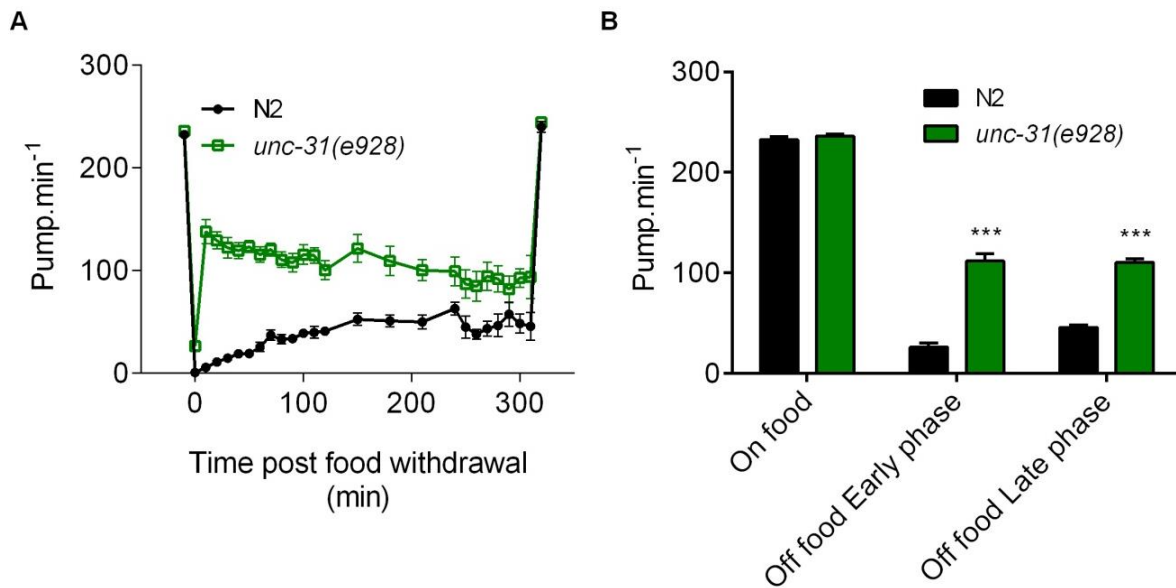


Figure 30: UNC-31 mediates the reduction of pumping rate observed in absence of food.

A. *unc-31(e928)* pumping rate on food was similar ($p = 0.3897$; $n = 11$ N2, $n = 9$ *unc-31(e928)*) to the paired N2 control. *unc-31(e928)* showed a marked increase in its pumping rate above 100 ppm during food deprivation which is significant during the early phase (86 ± 10 ppm; $p < 0.001$; $n = 15$ N2, $n = 15$ *unc-31(e928)*) and the late phase (65 ± 26 ppm; $p = 0.0072$; $n = 6$ N2, $n = 10$ *unc-31(e928)*).

B. Histogram representing the average pumping rate on food and off food during the early and late phases of figures A. * ($p < 0.05$), ** ($p < 0.01$) and *** ($p < 0.001$) compared to paired N2 control.

3.2.5 Neuropeptide signalling acts to maintain a slow pumping rate in the absence of food

UNC-31 is a regulator of neuropeptide transmission in *C. elegans* (Sieburth *et al.*, 2007) which suggests that neuropeptide transmitters underpin the *unc-31* phenotype. The worm expresses several important classes of neuropeptides including FMRFamide-like peptides (FLP) (Li and Kim, 2014; Peymen *et al.*, 2014) neuropeptide-like peptides (NLP) (Nathoo *et al.*, 2001) and insulin-like peptides (INS) (Lau and Chalasani, 2014) many of which have roles in

regulating feeding behaviour (Holden-Dye and Walker, 2013). These molecules are synthesised as single chain polypeptides that were proteolytically processed and packaged into secretory granules (see **section 1.1.2.4**). Mutants defective in the neuropeptide precursor processing enzymes EGL-3 (Kass *et al.*, 2001) and EGL-21 (Jacob and Kaplan, 2003) are depleted in neuropeptides (Husson *et al.*, 2006; Husson *et al.*, 2007) and provide a useful experimental tool for investigating the net effect of peptidergic signalling on behaviour (Mitchell *et al.*, 2010).

Three strains carrying mutations in *egl-3* were tested. The *ok979* allele is a predicted loss of function mutation (Husson *et al.*, 2006) and worms carrying this mutation showed significantly reduced pumping on food. Strikingly, during food deprivation, *egl-3(ok979)* mutants pumped rarely if at all (**Figure 31A, D**). When the *egl-3(ok979)* mutants were returned to food following prolonged starvation their pumping rate returned to the level observed prior to food deprivation. Two additional mutants of *egl-3*, *egl-3(n150)* and *egl-3(n588)*, showed a similar response to both the presence and absence of food as *egl-3(ok979)* (**Figure 4B**). The difference in the behavioural phenotype between *ok979* and the other alleles, *n150* and *n588*, may be explained by the latter two mutations resulting in a differential loss of the neuropeptide complement, as previously suggested from mass spectrometry analysis of these mutants (Husson *et al.*, 2006).

The *egl-21* mutants have a reduction in pumping both on and off food; however, the phenotype observed during food deprivation was not as severe as that observed for *egl-3(ok979)*. *egl-21* mutants do show some pumping motion in the absence of food (**Figure 31C**). The two mutants *egl-3* and *egl-21* have been investigated using mass spectrometry and they differ in the neuropeptides which are properly processed (Husson *et al.*, 2006; Husson *et al.*, 2007). Taken together, these data indicate that neuropeptide signalling is essential for pumping in the absence of food (**Figure 31A, B, C, D**).

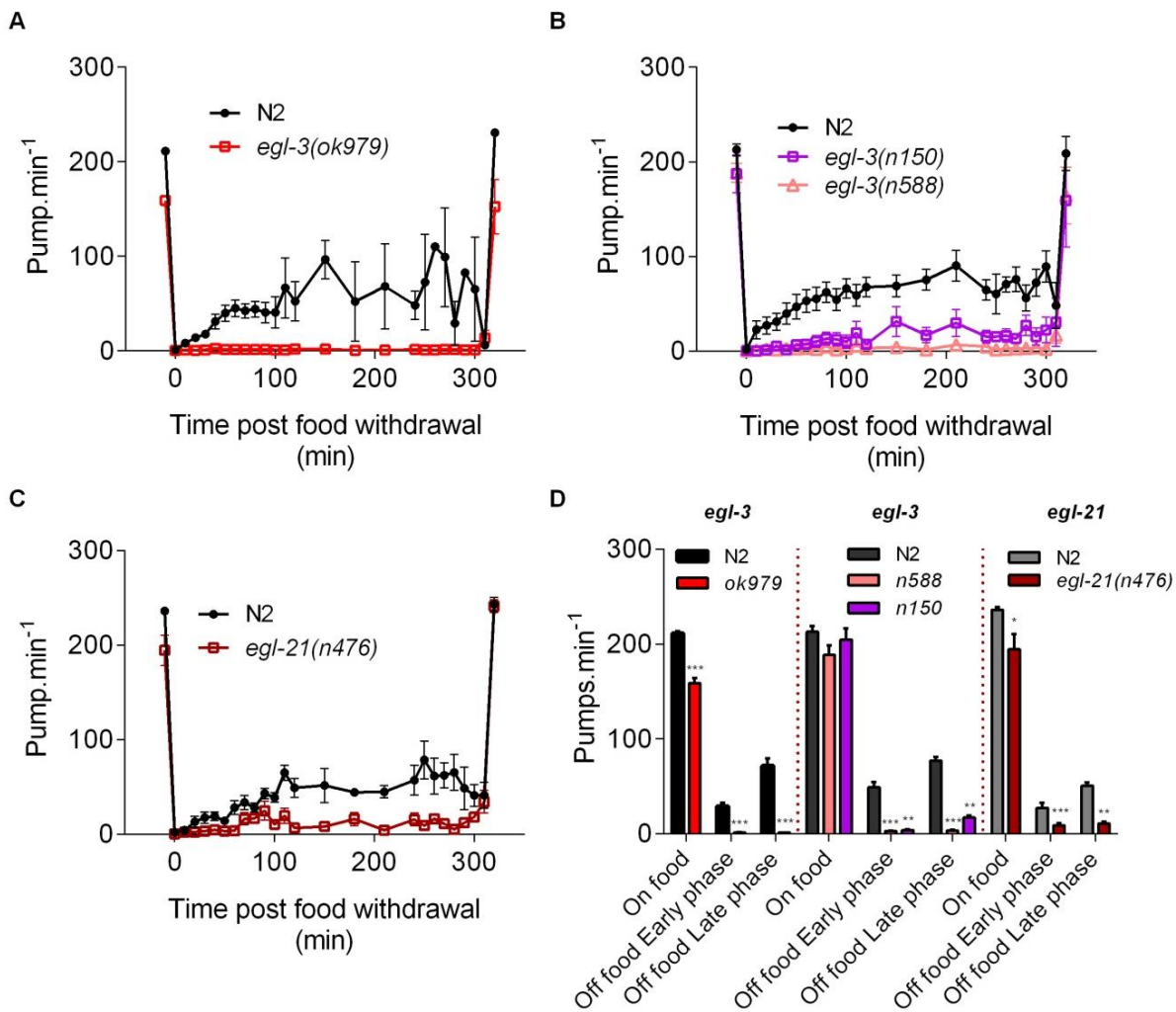


Figure 31: Mutants deficient in neuropeptide synthesis show a reduced pumping rate in absence of food.

A. *egl-3(ok979)* has a reduced pumping rate on food (-52 ± 6 ppm; $n = 10$ N2, $n = 10$ *egl-3(ok979)*) relative to wild-type N2 ($p < 0.001$). In the absence of food there was a significant reduction in the rate in both phases of food deprivation (early and late phase $p < 0.001$ with -22 ± 8 ppm; $n = 5$ N2, $n = 8$ *egl-3(ok979)*) and -70 ± 14 ppm; $n = 3$ N2, $n = 8$ *egl-3(ok979)*, respectively).

B. *egl-3(n588)* ($p = 0.0551$; $n = 12$ N2, $n = 12$ *egl-3(n588)*) and *egl-3(n150)* ($p = 0.5275$; $n = 12$ N2, $n = 10$ *egl-3(n150)*) have no reduction in pumping on food relative to N2. *egl-3(n588)* (early, -46 ± 12 ppm; $n = 11$ N2, $n = 10$ *egl-3(n588)*) and late phase -74 ± 14 ppm; $n = 6$ N2, $n = 8$ *egl-3(n588)* $p < 0.001$) and *egl-3(n150)* (early phase: -43 ± 15 ppm; $p = 0.0029$; $n = 12$ N2, $n = 7$ *egl-3(n150)*, late phase: -60 ± 18 ppm; $p = 0.0012$; $n = 6$ N2, $n = 6$ *egl-3(n150)*) exhibited a significant reduction in pumping in both phases of food deprivation.

C. *egl-21(n476)* displays a reduced pumping in presence of food (-41 ± 17 ppm; $n = 8$ N2, $n = 9$ *egl-21(n476)*) relative to N2 ($p = 0.0309$). In the absence

of food there is a significant reduction in both phases of the pharyngeal pumping (early phase: -19 ± 7 ppm; $p < 0.001$; $n = 8$ N2, $n = 8$ *egl-21(n476)* and late phase: -40 ± 13 ppm; $p = 0.0015$; $n = 5$ N2, $n = 9$ *egl-21(n476)*).

D. Histogram representing the average pumping rate on food and off food during the early and erratic phases of figures A, B, C and D. * ($p < 0.05$), ** ($p < 0.01$) and *** ($p < 0.001$) compared to paired N2 control.

3.2.6 Two parallel pathways fine-tune feeding behaviour in the absence of food

To investigate the relationship between the genotypes that gave the strongest phenotypes during food deprivation (*unc-31*, *egl-3* and *eat-4*) double mutants were generated. *unc-31* and *egl-3* mutants, as described above, are reported to be deficient in neuropeptide signalling. To determine the epistatic relationship between *unc-31* and *egl-3* mutants, the *unc-31(e928); egl-3(ok979)* double mutant was constructed and tested. In parallel experiments, in which the pumping rate of wild-type, *egl-3(ok979)*, *unc-31(e928)* and *unc-31(e928); egl-3(ok979)* were compared, the pumping rate of the double mutant was reduced relative to the wild-type's pumping rate both on and off food, similar to the *egl-3* single mutant (**Figure 32A**).

An *eat-4(n2472); egl-3(n150)* double mutant was investigated. In the absence of food, where glutamate drives a pumping reduction and in contrast EGL-3-processed neuropeptides have a net stimulatory effect, the pumping rate in the double mutant phenocopies wild-type (**Figure 32C**). This is in contrast to the *unc-31(e928); egl-3(ok979)* mutant in which the neuropeptide deficient mutant completely suppressed the constitutive pumping otherwise observed in *unc-31* (**Figure 32A**). These results suggest that the glutamatergic pathway is likely to function in parallel to *unc-31* and *egl-3*-dependent pathways (**Figure 32C**).

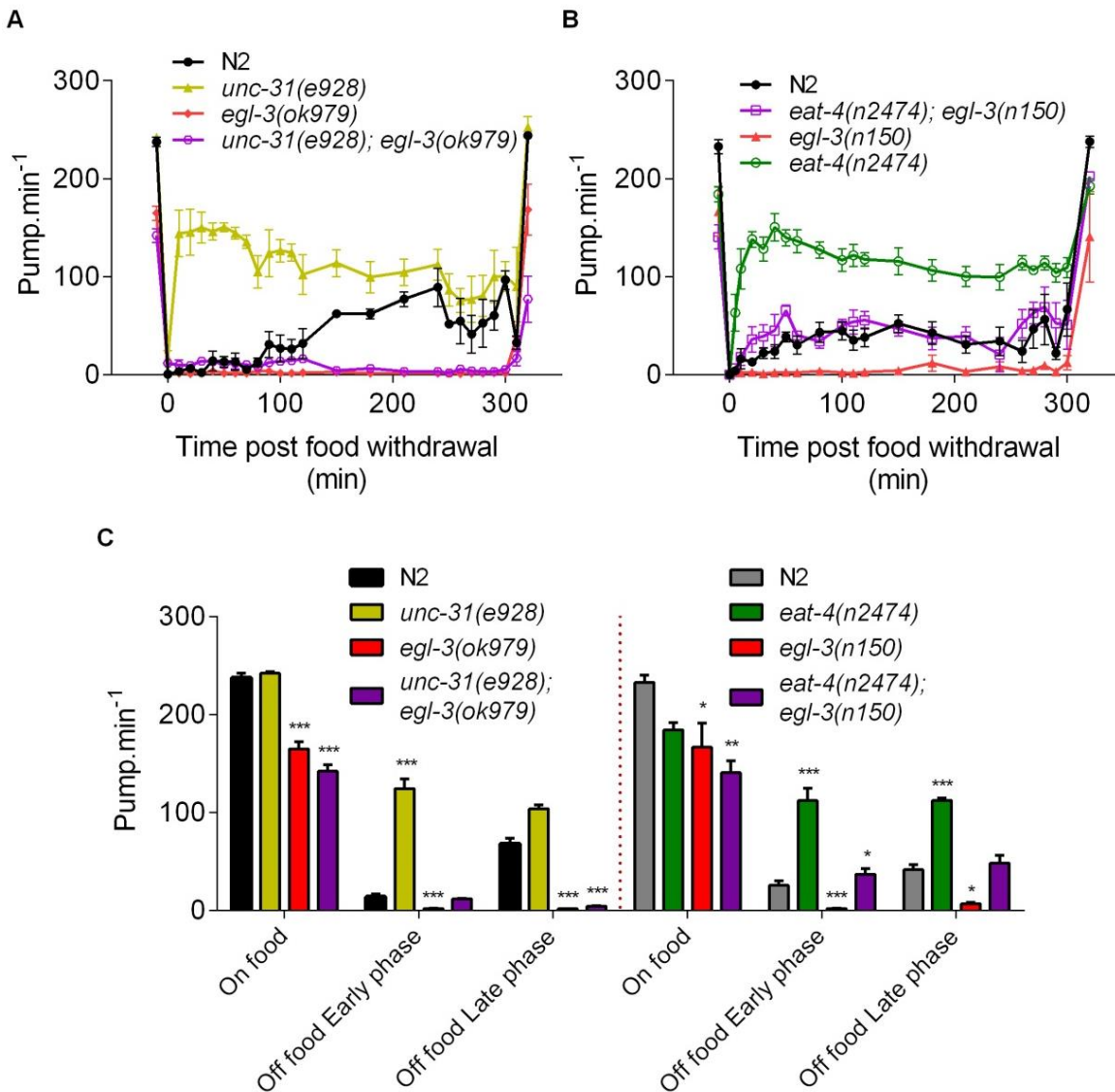


Figure 32: Epistatic analysis revealed *unc-31* and *egl-3* act in the same genetic pathway.

A. In the presence of food, the double mutants *unc-31(e928); egl-3(ok979)* displays a pumping rate similar to *egl-3(ok979)* single mutant (23 ± 8 ppm; $p = 0.0669$; $n = 8$ double mutant, $n = 8$ *egl-3(ok979)*) but lower than *unc-31(e928)* (-100 ± 5 ppm; $p < 0.001$; $n = 6$ *unc-31(e928)*). In response to food withdrawal the double mutant *unc-31(e928); egl-3(ok979)* displays a pumping rate similar to wild-type N2 during the early phase ($p = 0.5162$; $n = 5$ N2, $n = 8$ double mutant), but significantly lower during the late phase (-64 ± 8 ppm; $p < 0.001$; $n = 3$ N2, $n = 8$ double mutant).

B. No significant difference in the pumping rates on food of the double mutant *eat-4(n2474); egl-3(n150)* was observed compare to both *eat-4(n2474)* ($p = 0.2691$ $n = 7$ *eat-4(n2474)*, $n = 6$ double mutant) and *egl-3(n150)* ($p > 0.99$; $n = 7$ *egl-3(n150)*, $n = 6$ double mutant).

= 6 *egl-3(n150)*, n = 6 double mutant) single mutants. Double mutants *eat-4(n2474); egl-3(n150)* have an early phase significantly different to *eat-4(n2474)* (-75 ± 15 ppm; $p < 0.001$; n = 5 *eat-4(n2474)*, n = 6 double mutant) and *egl-3(n150)* (35 ± 9 ppm; $p < 0.001$; n = 6 *egl-3(n150)*, n = 6 double mutant). The late phase of *eat-4(n2474); egl-3(n150)* is also significantly different to *eat-4(n2474)* (-64 ± 18 ppm; $p < 0.001$; n = 4 *eat-4(n2474)*, n = 4 double mutant) and *egl-3(n150)* (41 ± 15 ppm; $p < 0.001$; n = 5 *egl-3(n150)*, n = 4 double mutant).

C. Histogram representing the average pumping rate on food and off food during the early and erratic phases of figures A and B. * ($p < 0.05$), ** ($p < 0.01$) and *** ($p < 0.001$) compared to N2 control.

Furthermore, the double mutant *eat-4(ky5); unc-31(e169)* exhibited an extreme off food pumping phenotype in that the constitutive pumping was additive. Indeed, the double mutants showed a pumping rate that was not discernibly different from the one displayed in the presence of food (**Figure 33**). This result confirms that the glutamatergic and *unc-31*-dependent inhibitory drive for pumping in the absence of food function in parallel pathways. Also of note is the observation that in the presence of food the *eat-4(ky5); unc-31(e169)* double mutant had a pumping rate significantly less than wild-type, similar to *eat-4*, again consistent with *unc-31* and *eat-4* lying in parallel pathways.

A simple model consistent with these data is shown in **Figure 33C**. *unc-31*- and *eat-4*-mediated reduction of pumping during food deprivation is via two distinct routes by which food removal imposes a cue-dependent reduction of pharyngeal pumping. The pathway(s) are predicted to be organised such that *unc-31* lies upstream of *egl-3*. This is surprising in the context of requirement for *unc-31* in neuropeptide signalling (Charlie *et al.*, 2006; Sieburth *et al.*, 2007; Speese *et al.*, 2007) and it suggests that the functional roles of *unc-31* and *egl-3* in peptide transmission do not completely overlap.

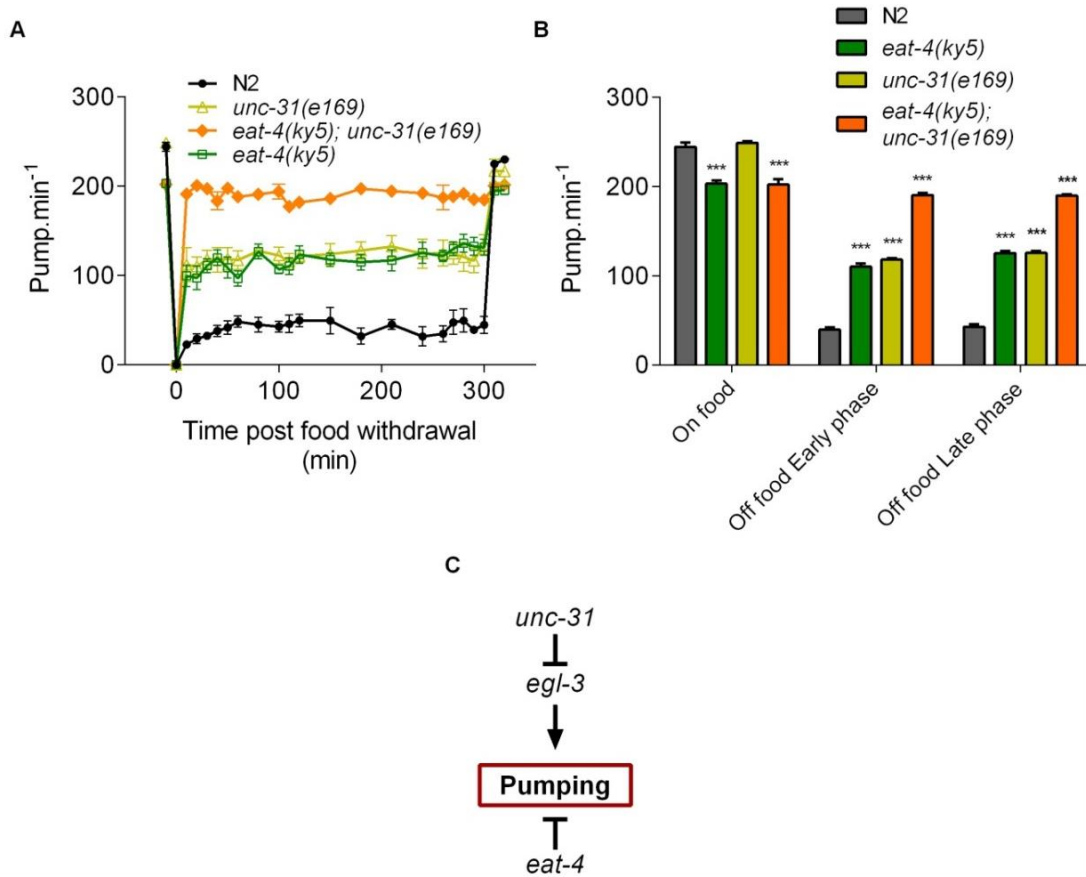


Figure 33: *eat-4(ky-5); unc-31(e169)* double mutant pumped at a similar rate in the presence or in the absence of food.

A. Double mutant *eat-4(ky5); unc-31(e169)* displays a reduced pumping rate in presence of food compared to wild-type N2 (-42 ± 6 ppm; $p < 0.001$; $n = 8$). In absence of food, both single mutant *eat-4(ky5)* and *unc-31(e928)* pumped constitutively higher than N2 during both early (71 ± 12 ppm; $p < 0.001$; $n = 8$ N2, $n = 8$ *eat-4(ky5)* and 79 ± 13 ppm; $p < 0.001$; $n = 8$ N2, $n = 8$ *unc-31(e928)* respectively) and late phase (83 ± 14 ppm; $p < 0.001$; $n = 7$ N2, $n = 8$ *eat-4(ky5)* and 83 ± 17 ppm; $p < 0.001$ $n = 7$ N2, $n = 8$ *unc-31(e928)* respectively). The double mutant *eat-4(ky5); unc-31(e169)* pumped at an even higher rate than the single mutants displaying, compare to N2, an increase of 151 ± 9 ppm ($p < 0.001$; $n = 8$ N2, $n = 8$ double mutant) for the early phase and 147 ± 12 ppm ($p < 0.001$; $n = 7$ N2, $n = 8$ double mutant) for the late phase, with a pumping rate reaching around 200 ppm. **B.** Histogram representing the average pumping rate on food and off food during the early and erratic phases of figures A and B. * ($p < 0.05$), ** ($p < 0.01$) and *** ($p < 0.001$) compared to N2 control. **C.** Schematic model representing the genetic interactions between *eat-4*, *egl-3* and *unc-31* in the control of the pharyngeal pumping rate in the

absence of food. A neuropeptide pathway and a glutamatergic pathway act in parallel to fine-tune the pumping rate off food. Epistasis analyses indicate *unc-31* acts downstream of *egl-3* in the neuropeptide pathway.

3.2.7 Laser ablation that disconnects the pharyngeal nervous system from the extrapharyngeal nervous system does not affect pharyngeal pumping

A pair of interneurons, designated RIP for "ring/pharynx interneurons", provides the sole anatomical connection between the pharyngeal nervous system and the main nervous system (Albertson and Thomson, 1976) (Figure 13). These neurons could provide a route for chemosensory and mechanosensory cues detected by extrapharyngeal sensory neurons to regulate pumping behaviour. It has previously been suggested that ablation of RIP has little effect on the pharyngeal function suggesting that extrapharyngeal chemosensory circuits either have no role in pumping regulation or function entirely through neurohormonal signals (Avery and Thomas, 1997). However, no assay has been conducted in the absence of food, and it is possible that RIP might be required for normal pumping behaviour in response to food removal. Indeed, the study described here hints that distinct pathways are modulating the pumping behaviour depending on the food context. Therefore, to test whether or not extrapharyngeal inputs might direct the pharyngeal response to food cues, we investigated pumping in animals in which RIP neurons were ablated with a laser.

To this purpose, the transgenic strain N2; *Ex[Pgpa-16::GFP]*, expressing GFP in 6 neurons including RIP (Jansen *et al.*, 1999), was used to help localise the RIP neurons for physical laser ablation. Ablation was conducted in L1-L2 larvae and the success of the ablation tested by observation of a sustained absence of GFP. Ablation of the RIP neurons had no effect on pumping rate either on or off food (**Figure 34A, B**). We assessed pumping for up to 120 min post-food withdrawal, and RIP ablation did not have a significant effect. Overall, it appears that extrapharyngeal inputs are not connected to the pharynx by this anatomically direct pathway to mediate the pumping behaviour.

Only 30% (6/20) of the RIP ablated worms assessed were still alive at the end of the test, i.e. ~70% of the tested worms died trying to escape the no food arena. In comparison, ~60% (7/12) of the control worms arrived to completion. Although not a direct measurement of locomotory behaviour, this could hint to an increased roaming behaviour when RIP is ablated.

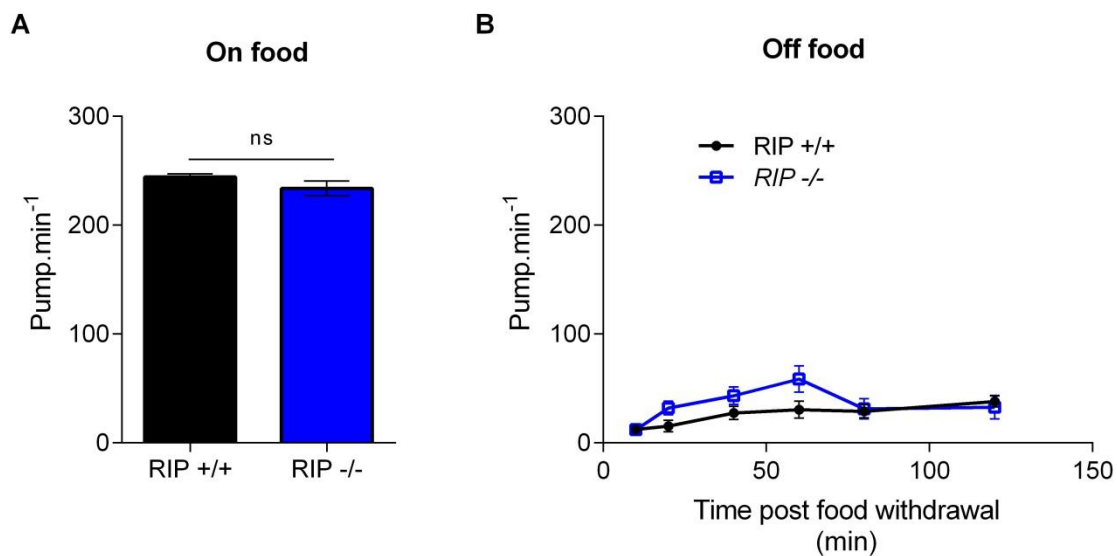


Figure 34: Pharyngeal pumping in the presence and absence of food in RIP ablated worms.

Worms expressing GFP under the *gpa-16* promoter were subjected to laser ablation to remove the cell bodies of the bilaterally localized RIP neurons that provide the only identified anatomical link between the extra pharyngeal and pharyngeal nervous system. Ablation was performed at L1 or L2 and confirmed 24 hours later. L4 ablated worms were picked the day before their pharyngeal pumping rate was measured in the presence (A) and at increasing times after the removal of food (B). There was no difference in the pumping on intact or laser ablated controls on food ($p = 0.189$; RIP +/+ $n = 14$; RIP -/- $n = 15$). There was a small difference in the pump rates in the absence of food this was not significant ($p = 0.496$; RIP +/+ $n = 7$; RIP -/- $n = 6$).

3.3 Discussion

3.3.1 An adaptive pumping behaviour in the absence of food

In this study a systematic analysis of *C. elegans* pharyngeal activity was carried out in the presence and absence of food. Two distinct phases of the *C. elegans* pharyngeal pumping response to food deprivation were observed: (1) an early phase (0-120 min) in which pumping is strongly reduced, and (2) a late phase (120-300 min) in which pumping remains reduced on average but varies over a wide range (0 – 150 ppm) (**Figure 26**). Food deprivation was initiated by manually removing the worm from food. This provides an environment that drives the worm to explore its environment after its food source has been depleted. What is the physiological significance of this residual pumping that occurs in the absence of food, given that this pumping does not lead to ingestion of bacteria? One interpretation is that the worm is enacting "fictive feeding", maintaining a basal pumping rate, which facilitates gustatory detection of food in the immediate vicinity (Avery and Horvitz, 1990). Alternatively, pumping in the absence of food might be required to permit fluid intake in the form of "drinking" however, in this case drinking would not be primordial for survival as *egl-3* mutants do not pump off food but survive prolonged periods of food-deprivation. The biological significance of this switch in behaviour in this late stage of food deprivation is intriguing: it might relate to a change in the worm's foraging strategy to conserve energy as its nutritional status starts to become compromised (Lee *et al.*, 2014).

Imaging sensory neuron activity has already established that presentation and removal of food cues can selectively activate and drive divergent downstream circuits modifying foraging behaviour (Chalasanani *et al.*, 2007). The temporal regulation of pumping behaviour following removal from food has interesting parallels to the worm's regulation of locomotory behaviour in which the worm initially exhibits a high frequency of reversals and turns called 'local area search' which transitions to periods of long forward runs i.e. 'dispersal' (Hills *et al.*, 2004; Gray *et al.*, 2005). The switch of the locomotory behaviour from local area search to dispersal occurs after 15 min, during the early phase, which is earlier in the food deprivation than the switch in the pharyngeal

behaviour from sustained to erratic pumping, suggesting differential regulation of these two food deprivation-dependent processes.

3.3.2 Inhibitory and excitatory pathways fine tune the pumping behaviour off food

In this chapter, the mechanism, or mechanisms, that leads to a marked reduction in pharyngeal pumping rate when the worm is moved to an environment without food has been investigated. At its simplest this suppression could be provided by the absence or reduction of an excitatory signal that normally drives feeding in the presence of food. Alternatively, there may be a mechanism to actively suppress pharyngeal activity in the absence of food, or, in a more complex model, pharyngeal pumping rate could be simultaneously modulated by signals stimulating and reducing the pumping rate. Interestingly, in the absence of food mutants that pumped at a higher rate (*eat-4* and *unc-31* mutants; see **Figure 27** and **Figure 30**), indicating a role in the reduction of the pumping rate, and also mutants that pumped at lower rate compared to wild-type (*unc-17*, *egl-3* and *egl-21* mutants; **Figure 27** and **Figure 31**) were observed. Therefore these data are consistent with the latter dual-process model in which food deprivation engages both excitatory and inhibitory tones to titrate pumping to a lower, off food, rate.

Evidence for such overarching inhibitory signals that suppress pharyngeal pumping in the absence of food comes from the mutant *unc-31* which pumps at a rate five times greater than wild-type off food. This can be explained by *unc-31*-dependent pathways being activated by food removal and imposing a pumping reduction and strongly suggests that removal of the food cue actively suppresses pharyngeal function. *unc-31* has previously been reported to pump constitutively when starved (Avery *et al.*, 1993) and as it plays a selective role in dense-core vesicle mediated exocytosis of neuropeptides (Sieburth *et al.*, 2007; Speese *et al.*, 2007; Hammarlund *et al.*, 2008) it might be predicted that mutants with defective peptidergic signalling would show a similar high level of pharyngeal activity in the absence of food. However, we found that during food deprivation the neuropeptide processing mutants *egl-3* and *egl-21* pump

at a very low frequency if at all, a result supported by a recent study showing a reduced pumping rate off food in *egl-3* mutants (Cheong *et al.*, 2015).

UNC-31 is widely expressed throughout the nervous system and is required for the post-docking fusion of the DCVs and therefore the release of neuropeptides. In this regard *unc-31* mutants were shown to display a reduced release of neuropeptides, although tagged NLP-21 neuropeptides (Sieburth *et al.*, 2007) or ectopically expressed ANF::GFP (Speese *et al.*, 2007) can still be detected in the coelomocytes, suggesting some neuropeptides can be released independently of *unc-31*. This indicates that not all the neuropeptides of a given type might be affected by *unc-31* mutation as a fraction of them might still be released, which is different to an *egl-3* mutation where a loss of processing affects all peptides of a given type.

It is therefore possible that the opposite behaviour of *unc-31* and *egl-3* in the absence of food is due to each mutant harbouring deficits in distinct neuropeptides, reducing or increasing the pumping rate respectively. *egl-3* mutants are deficient in FMRFamide-like and neuropeptide-like peptides, FLPs and NLPs (Husson *et al.*, 2006), but will likely still express neuropeptides belonging to other families e.g. the insulin-like peptides. *unc-31* on the other hand is involved more broadly in peptidergic signalling. There is indeed evidence for a role in both FLP and insulin-like peptide secretion (Charlie *et al.*, 2006; Sieburth *et al.*, 2007; Speese *et al.*, 2007; Leinwand and Chalasani, 2013). This different repertoire of residual neuropeptide function in *unc-31* and *egl-3* may provide an explanation for the differential impact of *unc-31* and *egl-3* mutations on pharyngeal pumping rate.

To test this, the double mutant *unc-31; egl-3* was made with the prediction that this would exhibit an intermediary phenotype and pump in a similar manner to wild-type in the absence of food if *unc-31* and *egl-3* each individually resulted in deficits in inhibitory and excitatory neuropeptides. However, the *unc-31; egl-3* double mutant pumped at a very low rate off food, similar to *egl-3*. This epistatic relationship suggests a genetic model in which a distinct inhibitory *unc-31* dependent signal functions upstream of an overriding excitatory *egl-3* dependent activation of pharyngeal pumping.

3.3.3 UNC-31 and EAT-4 are the main determinants of the reduction of the pumping rate observed in absence of food

The constitutive pumping of *unc-31* was phenocopied by the glutamate deficient mutant *eat-4* suggesting that the constitutive pumping in *unc-31* may be due to loss of glutamate signalling. This suggestion was initially attractive based on previous studies showing that the mammalian orthologue of *unc-31*, CAPS, has a critical role in the vesicle-mediated release of glutamate (Jockusch *et al.*, 2007). This suggests that the modulation of glutamate release was phylogenetically conserved. To test this, the double *unc-31; eat-4* mutant was made with the prediction that this would result in no further increase in pumping rate off food. This double mutant pumped at a lower rate than wild-type, similar to *eat-4* in the presence of food. However, in the absence of food the double mutant pumps at such a high rate as if the worm has not recognised the absence of food in the environment. Thus the high pumping rate phenotype of *unc-31* and *eat-4* mutants in the absence of food is additive. Therefore, it is clear that the constitutive pumping of *unc-31* cannot simply be explained by a deficit in glutamate signalling. Furthermore, the phenotype of the *unc-31* and *eat-4* double mutants, in which they appear to be unresponsive to food removal in terms of their pharyngeal pumping rate, indicate that together these signalling pathways are required in order to suppress pharyngeal pumping in the absence of food. Mammalian CAPS has also been related to vesicular uptake and storage of catecholamine (Speidel *et al.*, 2005). However, the relatively modest effect of these transmitters on the pharyngeal pumping off food suggests the *unc-31* mutant phenotype is not due to a defect in catecholamines.

To further test the relationship between *unc-31*, *egl-3* and *eat-4* in regulating pumping off food, the double mutant *eat-4; egl-3* was tested. The double mutant pumped in a similar manner to wild-type off food and this leads us to suggest that two distinct pathways, which have *unc-31/egl-3* and *eat-4* dependence, respectively drive the reduction of pumping when worms are off food.

3.3.4 Neuropeptide-dependent maintenance of a basal pumping rate in absence of food

The observation that the neuropeptide-deficient mutants *egl-3* and *egl-21* pump considerably less than wild-type, particularly during food deprivation, is important as it demonstrates a net stimulatory neuropeptidergic drive for pharyngeal pumping both in the presence and absence of food. *egl-3* mutants are deficient in over 65 neuropeptides (Husson *et al.*, 2006), and further work is required to determine which peptides promote feeding (see **Chapter 50**). In electrophysiological recordings from isolated pharynx a number of neuropeptides were shown to modulate pharyngeal pumping (Papaioannou *et al.*, 2005; Papaioannou *et al.*, 2008b). The neuropeptides leading to the most potent pumping stimulation are FLP-17A, FLP-17B and FLP-8. The encoding genes, *flp-17* and *flp-8* have a limited expression pattern; *flp-17* is expressed in the sensory BAG neuron and in the pharyngeal neuron M5 whilst *flp-8* is expressed in sensory neurons URXL/R, PVM (Li *et al.*, 1999a) and AUA (Kim and Li, 2004). The ablation of the RIP interneurons suggests that anatomically mediated point-to-point communication from outside the pharyngeal system is not needed for changes in state-dependent pharyngeal pumping. Taken together, these results suggest an important control from within the pharynx or from external neural pathways acting through volume transmission. Thus, FLP-17A and FLP-17B appear to be good candidates for the neuropeptides endogenous to the pharynx that could promote pumping and fictive pumping off food as only these peptides are present within the pharyngeal circuit. In addition, both FLP-17 and FLP-8 could act in a neurohormonal fashion to increase pumping rate in the presence and absence of food. There are also a number of inhibitory neuropeptides (Papaioannou *et al.*, 2005) and the scenario could be more complex with the net effect on pharyngeal pumping being determined by the summation of the effects of both peptides reducing and stimulating the pumping rate.

3.3.5 Role of the transmitters ACh, 5-HT, GABA and dopamine in the control of the pumping behaviour both on and off food

Acetylcholine appears to have a role in stimulating pumping both in the presence and the absence of food. Previously it has been shown that a muscarinic receptor signalling pathway in the pharyngeal muscle is activated

during starvation and this underpins an adaptive response to permit rapid re-feeding when food becomes available (You *et al.*, 2006), thus there may be a role for cholinergic signalling in the pumping behaviour off food. Interestingly, the fact that acetylcholine acts to increase the pumping rate off food and facilitates re-feeding reinforces the idea that the fictive feeding observed in absence of food would serve to sample the environment and facilitate the detection of gustatory cues.

The important role for these neurotransmitters, 5-HT, glutamate and acetylcholine in regulating the pharyngeal pump rate in this paradigm is consistent with their known role on the pharyngeal circuit with acetylcholine acting as the pacemaker neurotransmitter through cholinergic neuron MC (Avery and Horvitz, 1989), and glutamate and 5-HT signalling through M3 and NSM, respectively to fine tune the frequency of pumping (Avery, 1993; Franks *et al.*, 2006). GABA signalling provides a small net excitatory drive both in the presence and absence of food. In this case the effect derives from an extrapharyngeal circuit since neither GABA nor GABA receptors have been identified in the pharyngeal system (Franks *et al.*, 2006).

Nonetheless, and with respect to the context dependent regulation of pharyngeal pumping, the observations described in this chapter with 5-HT and glutamate mutants reinforces the view that the neuromodulation of pharyngeal pumping in the presence or absence of food involves different neural circuits.

The dopamine deficient mutant *cat-2* displayed a slight decrease in pharyngeal pumping compared to wild-type during the early phase of food deprivation, suggesting an excitatory role for dopamine in the pharyngeal system. Dopamine is expressed extrapharyngeally in a small subset of neurons (Sulston *et al.*, 1975), thus this regulation must be driven through a neurohormonal signal from outside the pharynx. It is interesting to note that there is a role for dopamine in initiating and sustaining the adaptive locomotory response to removal from food. Thus it has been demonstrated that a *cat-2* mutant does not exhibit local area search during the first five minutes of food deprivation (Hills *et al.*, 2004). These authors provided

evidence for a link between dopamine and glutamate signalling in local area search such that dopamine triggers the behaviour through a glutamate pathway during the early phase of removal from food. In this regard it is also noteworthy that the glutamate deficient mutant, *eat-4*, which showed a strong constitutive pumping during food deprivation is dysfunctional in local area search behaviour (Hills *et al.*, 2004), reinforcing the role of glutamate signalling in coordinating the behavioural repertoire to food removal (Chalasanani *et al.*, 2007). It is also known that dopaminergic signalling is important in modulating the locomotory behaviour of worms when they are re-introduced to food following a period of starvation (Sawin *et al.*, 2000), however, little is known of the impact of dopamine on pharyngeal function. We found that the fictive feeding phenotype of the *cat-2* mutants although significant is quite small. This is different from the regulation of the adaptive locomotory response in which dopamine is a significant determinant that acts through a glutamatergic pathway (Hills *et al.*, 2004).

3.3.6 Biogenic amine transmitters tyramine and octopamine do not regulate the pumping behaviour in this paradigm

The biogenic amine transmitter tyramine does not appear to have a role maintaining feeding on food or during food deprivation. This is despite the expression of receptors for this neurotransmitter within the pharyngeal nervous system. Thus, the receptors for tyramine, TYRA-2 (Rex *et al.*, 2005) and SER-2 (Tsalik and Hobert, 2003), are expressed in the pharyngeal muscle and in MC and NSM pharyngeal neurons, respectively. Exogenous addition of tyramine has been shown to decrease both the 5-HT stimulated pumping rate and pumping rate in the presence of food of wild type worms via the SER-2 receptor (Rex *et al.*, 2004). However, it has also been reported that a mutant, *ser-2(pk1357)*, displayed a similar feeding rate on food compared to wild-type worm (Li *et al.*, 2012). This is consistent with our observation that the pumping rate of the tyramine deficient mutant *tdc-1(n3419)* is similar to wild-type. Overall, it would seem that tyramine does not have a key role in modulating feeding behaviour in the context of the paradigm we deployed of feeding and food deprivation.

In this chapter, the biogenic amine octopamine deficient mutant *tbh-1(ok1196)* showed no significant effect on pharyngeal pumping rate either on or off food. Exogenous octopamine applied to intact worms and *in vitro* pharynx preparations is known to decrease the pumping rate on food (Horvitz *et al.*, 1982; Rogers *et al.*, 2001) via its action onto the extrapharyngeal receptor SER-3 (Suo *et al.*, 2006). In addition, it has reported that the *ser-3(ad1774)* mutant displayed a slightly reduced pharyngeal pumping rate compared to wild type in response to food deprivation both in the presence or absence of 5-HT (Carre-Pierrat *et al.*, 2006). Failure to see this in the current behavioural paradigm implies that additional contexts are required to trigger octopamine dependent regulation. In view of the role of octopamine in mediating reaction against aversive cues (Wragg *et al.*, 2007; Mills *et al.*, 2012), perhaps these represent routes that are not engaged in the current paradigm but which could represent additional octopamine dependent modulation of the pharynx.

3.4 Conclusion

In this chapter a paradigm was defined that highlights and provides a platform for deeper investigation of context-dependent modulation of the pumping behaviour. Through a systematic analysis of mutants defective in specific neurotransmitter signals, the roles of neurotransmitters was assigned to the regulation of the pumping behaviour in the presence of food, and to specific phases of the adaptive behavioural response observed when food is removed. These results reveal an interplay between several neurotransmitters and highlight stimulatory and inhibitory pathways that converge to regulate context-dependent feeding.

Analyses of switching context suggest the worm perceives the removal of food with two important consequences. The first is the activation of inhibitory pathways to reduce pumping. Importantly, genetic analyses argue for two pathways, *unc-31* and *eat-4*, acting independently of each other. Remarkably, in the absence of both *unc-31* and *eat-4* dependent suppression of pharyngeal pumping, worms pump at the same rate on and off food. In addition to this negative regulation, there is a stimulatory cholinergic and peptidergic drive. In

the absence of food the peptidergic component is more important in sustaining pumping than on food. This cue is independent of glutamate signalling but appears to lie downstream of *unc-31*.

In addition to providing insight into the complex regulation of pharyngeal activity in the absence of food, this analysis highlights distinct differences in the neural regulation of feeding behaviour on and off food (**Figure 35**). The modalities that are triggered have been poorly understood and coupling the sensory mutants with this cue-dependent assay will enable further investigation of this phenomenon. The genetic and cellular basis of the pumping behaviour will be investigated taking advantage of this assay as a benchmark, with the role of glutamate being the focus of **Chapter 4**. The peptides role will be detailed in **Chapter 5**.

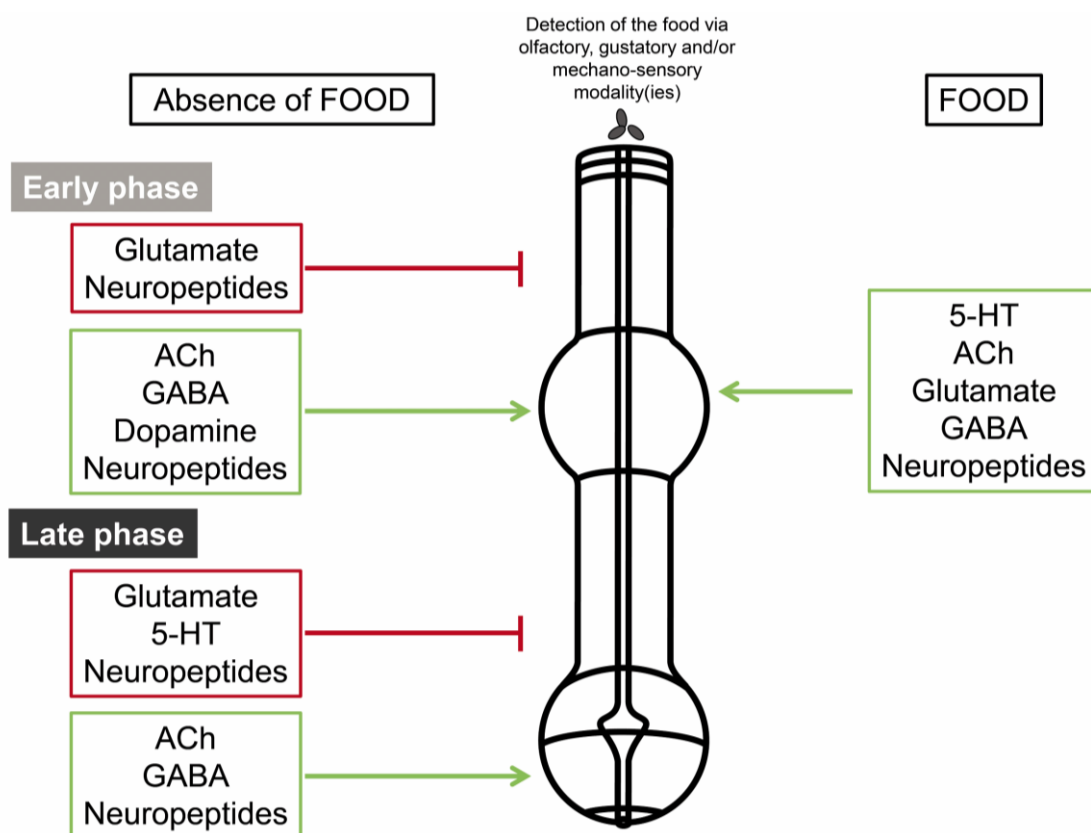


Figure 35: A summary of the multiple excitatory and inhibitory neural signals that regulate feeding behaviour in the presence of food and fictive feeding during food deprivation.

Presentation of food (right) facilitates pharyngeal pumping through several neurotransmitters that operate at the level of the pharynx (ACh, glutamate, 5-HT) or via neurohormonally mediated signalling (GABA, neuropeptides) directed to the pharynx. In contrast the removal of food generates at least two distinct routes in which glutamate (*eat-4*) and neuropeptides (*unc-31* dependent pathway) mediate inhibition that negatively regulates fictive feeding. This suggests at least two distinct circuits impose an inhibitory tone on the pharynx which is superimposed on a facilitatory regulation of pumping via a neuropeptide (*egl-3*) dependent pathway, GABA and ACh signalling and dopamine (early phase only) that promote pumping off food. The worm's food, bacteria, provide a complex environmental cue which is able to trigger chemosensory (olfaction, gustation) and mechanosensory modalities. Thus, physical detection of food presentation and removal may be mediated by previously described sensory pathways that utilize established extrapharyngeal sensors. Alternatively, more ill-defined intrapharyngeal detectors may mediate responses to gustatory and/or mechanosensation of bacteria.

This systematic characterisation of the signalling pathways implicated in a context dependent regulation of the pharynx provided the basis for more detailed investigation of key components in subsequent chapters, such as, glutamate, neuropeptides, sensory modalities and nutritional status

Chapter 4: Revealing and characterising the context-dependent regulation of pharyngeal pumping by the enteric glutamatergic neurons I2

4.1 Introduction

In the previous chapter, an assay was described to define the pharyngeal pumping between on and off food contexts. By providing new insights into the mechanisms modulating the pumping rate in the absence of food, this study highlighted that distinct neural pathways modulate pumping rate depending on the presence or absence of food. This is similar to the organisation of circuits observed in mammals (Aponte *et al.*, 2011).

The pumping behaviour in the absence of food is characterised by a markedly reduced pumping rate relative to the frequency in the presence of food (~ a fifth of its initial value). Chapter 3 revealed important classes of mutants, including the glutamate deficient mutant *eat-4* and the CAPS orthologue *unc-31*, a calcium-binding protein required for exocytosis, which exhibited an elevated rate in the absence of food, indicating a crucial role in the reduction of the pumping rate observed in response to food removal. The assay used to reveal the off food phenotype requires transfer of worms from an “on” food to an “off” food arena. A necessary intermediate in this assay is the pick mediated transfer from food via a cleaning plate onto a no food arena. The harsh touch associated with this pick-mediated transfer causes a complete inhibition of pumping. This pick-mediated inhibition of pumping is also apparent in the *eat-4* mutants but these mutants recover against this to generate an off food pumping rate that is much higher than that seen in N2. This indicates that glutamatergic transmission plays a potent and rather unexpected role and imparts a sustained inhibitory tone on the pharyngeal pumping in response to the removal of food.

There are two kinds of receptors glutamate can bind. The ionotropic receptors are ligand-gated ion channels, in other words, the binding of a ligand causes the opening of an ion channel and a flow of ions into or from the cell. The second type of receptors are metabotropic receptors, G-protein coupled receptors (GPCRs). The binding of GPCR triggers the activation of internal signalling pathways via the activation a second messenger (e.g. cAMP, cGMP or IP₃). Some of these second messengers may subsequently modulate ion channels (Lodish *et al.*, 2000). In *C. elegans*, as in mammals, the neurotransmitter glutamate can bind receptors from those two families. However, the nematode's genome encodes a sub-family of ionotropic receptors (iGluRs), the glutamate-gated chloride channels (GluCl), which aren't found in vertebrates (Nakanishi *et al.*, 1998; Brockie and Maricq, 2006; Dillon *et al.*, 2006). Therefore, glutamate receptors in *C. elegans* are usually divided in three categories, which are detailed below.

4.1.1 Ionotropic receptors (iGluR)

Most of the glutamate receptors in *C. elegans* are from the ionotropic type, a major class of heteromeric ligand-gated ion channels. At least 10 iGluRs subunits are found in the worm, the non-NMDA (N-methyl-D-aspartate) class that includes GLR-1 to GLR-8 (similar to AMPA and kainate subfamilies), and the 2 NMDA subunits NMR-1 and NMR-2 (Brockie *et al.*, 2001a; Brockie and Maricq, 2006).

The expression pattern of these iGluRs was extensively described using iGluRs GFP-fusion proteins (Brockie *et al.*, 2001a). GLR-1, GLR-2, GLR-4 and GLR-5 are expressed in numerous neurons including the command interneurons controlling the worm locomotion pattern (AVA, AVB, AVD, AVE and PVC, see session 2.2). NMR-1 and NMR-2 also appear to be found in the command interneurons. Conversely, both GLR-3 and GLR-6 are expressed in only one pair of neurons, namely RIA. Finally the two last subunits, GLR-7 and GLR-8 are mainly localised in the pharyngeal nervous system of the worm, although GLR-8 is also expressed outside of the pharynx.

GLR-1 function was the first identified and is the most extensively studied among the iGluRs. Different studies have shown a role for GLR-1 in the

regulation of the worm's locomotion, the backward movement induced by nose touch (Maricq *et al.*, 1995), the turning behaviour during local search for food (Chalasan *et al.*, 2007) and in the spontaneous switch from forward to backward movement (Brockie *et al.*, 2001b).

GLR-1 has also been linked to hyperosmotic condition avoidance (Mellem *et al.*, 2002), octanol avoidance (Chao *et al.*, 2004) or long-term memory (Rose *et al.*, 2003).

NMR-1 and GLR-2 have been implicated in the control of the avoidance behaviour in response to hyperosmotic conditions (Mellem *et al.*, 2002), and an *nmr-1* mutant displayed a reduced frequency of backward movement (Brockie *et al.*, 2001b).

4.1.2 Glutamate-gated chloride channels (GluCl)

Among the ionotropic receptors in *C. elegans*, a subfamily of glutamate-gated chloride channels (GluCl) has been identified. These anion channels (mainly inhibitors) appear to be unique to the invertebrate phyla. Orthologs for this family have been found in *Drosophila*, and the parasitic nematodes *Haemonchus contortus*, *Ascaris suum* and *Dirofilaria immitis* (Brockie and Maricq, 2006).

GluCls are not exclusively expressed in neurons but can also be found in different organs. Three of these subunits are indeed localised in the pharynx muscle, GLC-1 (GluCl α 1), GLC-2 (GluCl β) and AVR-15 (GluCl α 2) (Dent *et al.*, 1997; Laughton *et al.*, 1997; Ghosh *et al.*, 2012). GLC-1 can also be found in the intestine, the body wall muscles and in undefined head neurons, while GLC-2 expression is restricted to the pharyngeal muscle pm4 (metacorpus, see **Figure 12**) (Laughton *et al.*, 1997) where it forms a heteromeric channel with AVR-15 (Vassilatis *et al.*, 1997). GLC-1 and GLC-2 have also been shown to form functional heteromeric glutamate-gated chloride channels in *Xenopus* oocytes (Cully *et al.*, 1994). Finally, AVR-15 is localised in pm4 and pm5 (isthmus) pharyngeal muscle cells but also in extrapharyngeal neurons (RME, RMG, DA9 and VA12) (Dent *et al.*, 1997).

There are three other GluCl subunits known in *C. elegans*; AVR-14 (GluCl α 3), GLC-3 and GLC-4. GLC-3 is expressed in the interneuron AIY (Wenick and Hobert, 2004), GLC-4 in the intestine and in neurons localised in the head, tail and nerve ring (McKay *et al.*, 2003b), while AVR-14 is expressed in a subset of 40 neurons of the somatic nervous system among which are ALM, PDE, PHA, PHB, PHC, PLM, PVD (Dent *et al.*, 2000). *avr-14* can give two transcripts, interestingly, the alternative splicing process involved is known to be conserved in all the nematode species studied (Jagannathan *et al.*, 1999). In *H. contortus*, antibodies targeting specifically HcGluCl α 3A or HcGluCl α 3B, the two transcripts encoded by *Hcavr-14*, showed differential expressions. HcGluCl α 3A is expressed in chemosensory amphidal neurons while HcGluCl α 3B is expressed in pharyngeal neurons (Portillo *et al.*, 2003). However, *C. elegans avr-14* transcripts have not been shown to be expressed in the pharynx. Interestingly, when Dent *et al.* expressed RNA corresponding to the two *avr-14* transcript in *Xenopus* oocytes, only the oocytes expressing the *avr-14* transcript B responded to glutamate (Dent *et al.*, 2000).

As indicated in the introduction AVR-15 is known to drive the M3 repolarisation effect on the pharynx (Avery, 1993). AVR-15, AVR-14 and GLC-1 are known to be responsible for the sensitivity to the nematocide Ivermectin (Dent *et al.*, 2000). However, if the mutation in all 3 of these GluCl subunits is required for a full resistance in the laboratory N2 strains, it appears that the loss of function in only one subunit is sufficient for resistance in wild isolates such as CB4856 (Hawaii strain) (Ghosh *et al.*, 2012).

4.1.3 Metabotropic glutamate receptors (MGL)

Three G-protein coupled metabotropic glutamate receptors (MGL) have been identified in *C. elegans*; MGL-1, MGL-2 and MGL-3 (Dillon *et al.*, 2006). In mammals, there are 8 metabotropic glutamate receptors (mGluRs) divided in three subgroups; Group 1 (mGluRs 1 and 5), Group 2 (mGluRs 2 and 3) and Group 3 (mGluRs 4, 6, 7 and 8) that play distinct neuromodulatory roles in the mammalian brain (Ferraguti and Shigemoto, 2006; Niswender and Conn, 2010). Notably, in regard to feeding, among different roles mGluR5 appears to be involved in the regulation of appetite and energy balance in rodents as

mGluR5 knockout mice display the following specific feeding-related phenotypes: they weigh less relative to control mice, eat less when challenge with starvation and refeeding paradigm, and are resistant to effects induced by a high-fat diet such as weight gain and increases in plasma insulin and leptin levels (Bradbury *et al.*, 2005).

Comparison of *C. elegans* and mammals MGLs suggested that MGL-2, MGL-1 and MGL-3 were evolutionary precursors of the Group I, Group II and Group III respectively (Dillon *et al.*, 2006).

In worms, *mgl-1* is expressed in interneurons AIY, AIA, motorneuron RMD and pharyngeal neuron NSM (Wenick and Hobert, 2004; Greer *et al.*, 2008). *mgl-2* is neuronally expressed in unidentified neurons in the tail ganglia, the ventral cord and in the head (Reece-Hoyes *et al.*, 2007) and has been shown to be required for normal head movements and tap reversal reflexes. Finally, *mgl-3* is expressed in ADF, ASE and AWC sensory neurons, the RIB and RIC interneurons and the reporter construct appears occasionally in the BAG-ciliated neurons (Greer *et al.*, 2008). More recently, expression of the three MGL subunits have been observed in the pharyngeal neurons NSM (Dillon *et al.*, 2015).

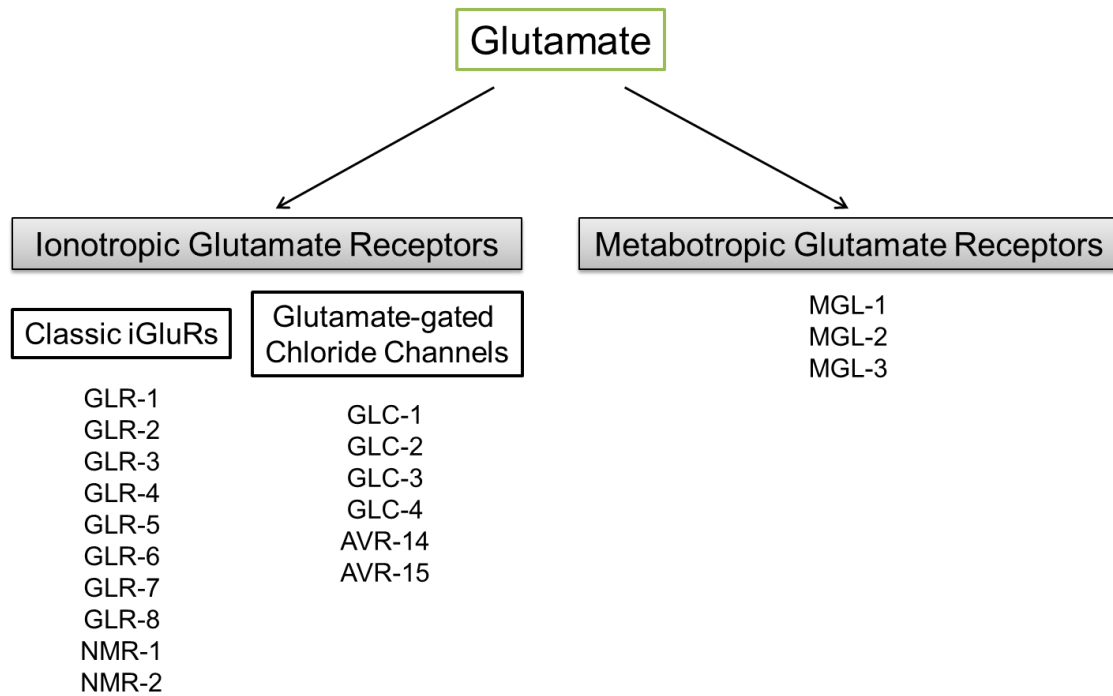


Figure 36: Glutamate receptors in *C. elegans*.

There are 19 known glutamate receptor subunits expressed in *C. elegans*' genome, divided in 2 main categories, ionotropic glutamate receptors and the metabotropic glutamate receptors. The ionotropic receptors have been subdivided into two groups, the classical ionotropic receptors sharing similarities with the mammalian equivalent, and the glutamate-gated chloride channels which are only found in invertebrates.

Worms which had their RIP interneurons ablated, the sole link between the somatic nervous system and the pharyngeal nervous system, showed no aberrant pharyngeal behaviour (see **Figure 34**), suggesting an important control from within the pharynx or from external neural pathways acting through volume transmission. Given the importance of glutamate signalling in the control of the pumping behaviour both on food, via the pharyngeal neuron M3 (Avery, 1993), and off food (see **Chapter 3**), coupled to the presence of other glutamatergic neurons in the pharyngeal nervous system, *viz*, I2, I5 and MI, (Serrano-Saiz *et al.*, 2013), the study in this chapter focuses on the investigation of glutamate-mediated microcircuits intrinsic to the pharynx involving controlling the pumping behaviour in a food-dependent context. Moreover, as the constitutive pumping off food of *eat-4* mutant happens early

upon food deprivation, only the early phase of the pumping off food phenotype has been investigated here.

4.2 Results

4.2.1 Pharyngeal response to food removal is dependent on glutamate signalling

To better detail how glutamatergic signalling modulates the pumping rate, a new experimental paradigm was designed. As described above and in chapter 3, the harsh touch on the worm during transfer off food induces a cessation of pumping in wild type worms (Keane and Avery, 2003). One could therefore hypothesise that the elevated pumping rate displayed by *eat-4* mutants in absence of food could be due to the non-detection, and reaction, to the harsh touch and therefore a less severe, if any, reduction of pumping. However, *eat-4* mutants appeared to undertake a reduction of pumping upon transfer onto the assay plate as no pump were observed at the moment of picking (**Figure 37B**). After 5 min, the *eat-4* mutants were pumping at a lower rate than their usual constitutive rate off food (~65 ppm compared to a pumping rate above 100 ppm usually observed off food). The pumping rate of *eat-4* mutants only reached 100 ppm 10 min following the transfer off food, indicating that a 10 min period is sufficient for *eat-4* mutants to fully recover from the harsh touch effect induced by picking.

As a consequence, the established pumping off food assay was modified to investigate the key temporal window in which the early phase of the pumping off food behaviour has recovered from the potentially confounding pick-mediated inhibition. The details of this assay have been designed as illustrated in **Figure 37A**. Briefly, the pumping rate on food of L4+1 worms was assessed prior to transfer onto a 'cleaning' plate then onto the 9 cm plate used for the off food assay. Individual worms were followed for 45 min and their pumping rate assessed at 3 time points; 15, 30 and 45 min following removal of food. The first time point set up at 15 min allows to record pump activity post pick-mediated inhibition while the last time point at 45 min ensure that the *eat-4* mutant will display a constitutive pumping rate. Having three time points also

allow to decrease the variability that can occur during an off food pumping assay.

As previously reported, *eat-4(ky5)* mutant displayed a marked reduction in its pumping rate in presence of food (~185 ppm) compared to its paired N2 (~250 ppm). Furthermore, in this modified assay, there was a sustained increase in the *eat-4* pump rate off food relative to N2 with an average pumping rate above 100ppm (**Figure 37C, D and E**). This highlights the distinct contribution of glutamatergic transmission to the different food contexts. To validate the glutamate involvement in both on food and off food pumping behaviours, *eat-4* function was restored by expressing wild-type *eat-4* cDNA under the control of the endogenous *eat-4* promoter. Six lines for the strain *eat-4(ky5); Ex[Peat-4::eat-4]* were generated and tested. As the construct injected has not been integrated, some transgenic strains might only have an incomplete restoration due to mosaic expression of the transgene. In the presence of food, the six tested strains showed a rescued phenotype as their pumping rates were significantly different from *eat-4(ky5)* mutants (**Figure 37C**). However, only half of them showed a complete rescue, *i.e.* no significant difference with the paired N2; 7.1, 8.6 and 7.4 strains. In the absence of food, the strains 7.1, 8.6 and 7.4 displayed a complete rescue with less than a 10 ppm difference with N2 (**Figure 37D**). Surprisingly, the *eat-4(ky5); Ex[Peat-4::eat-4]* strains 8.3 and 8.4 appeared not significantly different from N2 despite their average pumping rate being ~ 35 ppm higher than N2. Finally, 8.1 displayed a partially rescued phenotype with a pumping rate significantly different from both *eat-4(ky5)* (- ~40 ppm) and N2 (+ ~60 ppm) (**Figure 37E**).

Overall, these results confirm that the deficit in pumping displayed by *eat-4(ky5)* mutants both on and off food was indeed caused by the absence of a wild-type copy of *eat-4*.

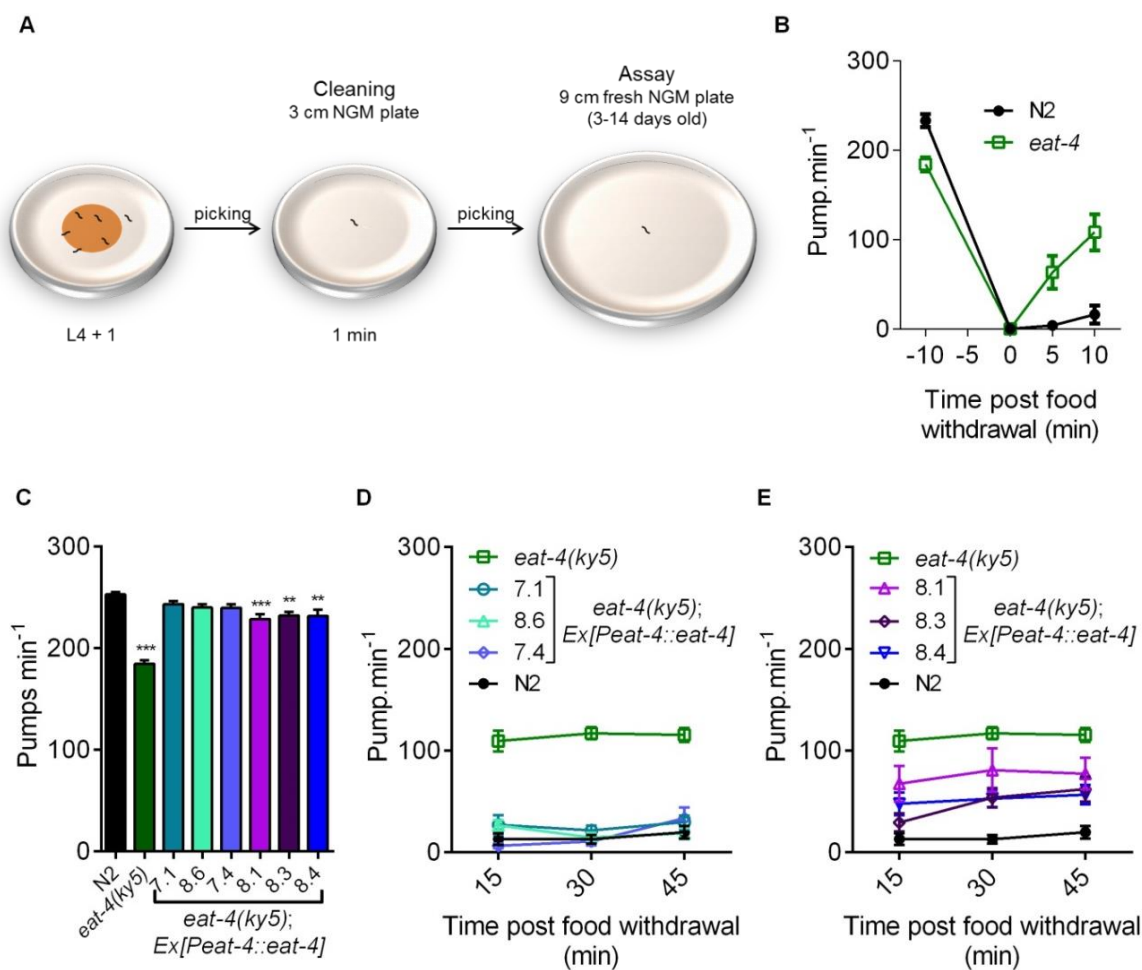


Figure 37: *eat-4*-dependence of on and off food pharyngeal pumping behaviours reveals distinct context dependent regulation by glutamatergic transmission.

A. Synchronised L4+1 worms are investigated for their pumping rate on food before a short cleaning step on a unseeded plate and being picked onto a 90 mm non-seeded plate. After a 15 min recovery period, the pumping rate off food is recorded for 1 min at the indicated time intervals. **B.** Following transfer off food, *eat-4* mutants reached a pumping rate above 100 ppm in 10 min. **C.** *eat-4(ky5)* pumping rate in presence of food is significantly lower than the paired control N2 (-68 ± 4 ppm; $p < 0.001$). In contrast, *eat-4(ky5); Ex[Peat-4::eat-4]* transgenic strains 8.6, 7.1 and 7,4 were pumping at a similar rate than N2 (8.6 $p = 0.609$; 7.1 $p = 0.99$; 7.4 $p = 0.559$). The strains 8.1, 8.3 and 8.4 pumped significantly different from *eat-4(ky5)* ($p < 0.001$ for all) and from N2 ($p < 0.001$, $p = 0.008$ and $p = 0.006$ respectively) indicating a partial rescue. 14 to 16 worms have been assessed per strain. **D. E.** In absence of food, *eat-4(ky5)* mutant displayed a higher pumping rate than N2 paired control (100

± 6 ppm $p < 0.001$, $n = 10$ N2 $n = 8$ *eat-4(ky5)*). The transgenic strains *eat-4(ky5)*; *Ex[Peat-4::eat-4]* 8.6 ($p = 0.99$), 7.1 ($p = 0.66$), 7.4 ($p = 0.99$), 8.3 ($p = 0.170$) and 8.4 ($p = 0.065$) showed no significant differences with N2. 8.1 pumped significantly higher than N2 (60 ± 12 ppm; $p < 0.001$) but lower than *eat-4(ky5)* mutant (-39 ± 12 ppm; $p = 0.043$).

4.2.2 Light induced glutamatergic neurons activity decrease the pumping rate in the presence but not in the absence of food

The investigation of context dependent regulation of the pharynx suggests distinct regulation “on” and “off” food. The pivotal role of M3 in enabling the pharynx to drive the fast rates associated with pumping on food is an important determinant of the on food pump rate, in contrast with the significance of the distinct inhibitory regulation in absence of food. Our observation of the off food pumping response in which active reduction of pumping arises in response to food removal indicates that shifting context is key to the expression of the phenotype. Accordingly, in order to assess the inhibitory potential of the glutamatergic tone upon food withdrawal, an optogenetics approach was employed that utilized an integrated transgenic strain that expressed ChR2 selectively in the glutamatergic neurons (Hu *et al.*, 2013). Upon blue UV-light, ChR2 undergoes a conformational change triggering an influx of ions leading to the artificial activation/depolarisation of the neurons in which it is expressed (Fenno *et al.*, 2011). This effect is dependent on the presence of retinal in the food source, and worms that were not fed with retinal can be used as control.

First, the consequence of light-activating glutamatergic neurons in a N2 background was investigated. This deployed N2; *Is[Peat-4::ChR2;mRFP]* transgenic worms and these worms appeared to pump at a similar rate compared to N2 both in an “on” food arena and in the absence of food without light activation, regardless of the presence or absence of retinal, indicating that the presence of the transgene itself did not impact on pharyngeal behaviour. In contrast, when these worms were on food, but illuminated by

light to activate their glutamate neurons, they showed a pronounced reduction of pumping (**Figure 38A**). This effect was dependent on light illumination and absent in worms subjected to the same treatment but cultivated on retinal free plates. This implies that light activation is generating an off food pump rate despite the presence of food. The illumination reduced the pumping rate of wild-type worm in the presence of food to ~65ppm (**Figure 38A**) thus confirming the potent ability of glutamate dependent circuits to reduce pharyngeal pumping. In the absence of light activation, but after the removal of food, the ChR2-expressing worms exhibited the expected reduced pumping rate described for N2 after 30 min of food deprivation (**Figure 38 and Chapter 3**). However, this reduced pumping rate was not further decreased when these worms were illuminated, and there was no change in the pharyngeal pumping (**Figure 38B**). Thus, the *eat-4* dependent imposition of reduced pharyngeal pumping triggered when worms are removed from food can be artificially imposed on the worm in the presence of food by light-activating a glutamate dependent circuit. This circuit exhibits some context dependence as the pump rate measured in the absence of food is refractory to this glutamate dependent inhibition. One explanation for this striking observation is that the glutamatergic neurons are already activated in a no food context thus occluding the superimposed light dependent reduction in pumping.

These results are consistent with the previous observation that transition from an on food to and off food context executes a shift in the glutamate tone on the pharyngeal pumping from a stimulatory to an inhibitory one. This overriding inhibitory tone that actively responds to the removal of food can also be artificially activated to reduce the pharyngeal pumping rate.

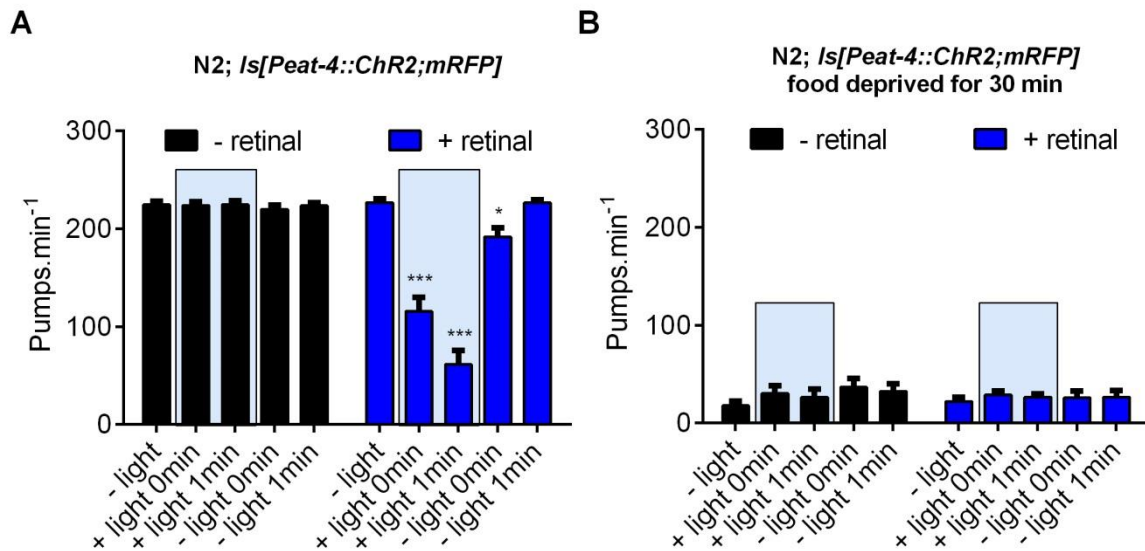


Figure 38: Artificial activation of a glutamatergic inhibitory tone by optogenetics.

A. In the presence of food, *N2; Is[Peat-4::ChR2;mRFP]* pumped at 225 ppm in absence of light. Illuminating *N2; Is[Peat-4::ChR2;mRFP]* worms led to a decrease of the pumping rate during the 1st minute (-111 ± 9 ppm; $p < 0.001$) and a marked reduction during the 2nd minute (-166 ± 9 ppm; $p < 0.001$). No effects were observed without retinal ($p = 0.99$ after 2min of light). 10 worms were used per condition. **B.** Food deprived worms for 30 min pumped between 18 and 36 ppm. The presence of light did not affect the pumping of *N2; Is[Peat-4::ChR2;mRFP]* worms ($p = 0.763$ and $p = 0.935$ for the 1st and 2nd min of light respectively; $n = 9$). No effects were observed without retinal ($p = 0.752$ after 2min of light; $n = 6$).

Excitation wavelength used was 480/40nm.

The optogenetics investigation was extended by investigating how on and off food pumping are modulated in the strain *eat-4(ky5); Is[Peat-4::ChR2;mRFP]*. This strain will have light activated glutamate neurons unable to release glutamate because they lack vesicular glutamate. This will not preclude other co-stored transmitters or neuromodulators that function in these glutamate circuits. As expected these strains showed the reduced pumping on food associated with *eat-4* deficiency (~190 ppm) and showed

constitutive pumping off food (~115 pps). Interestingly the stimulation of this strain on food retains a semblance of the reduction seen when that experiment is performed in a N2 background (**Figure 39A**). However, this artificially enforced inhibition in an on food context is much reduced. This difference suggests that glutamate is an important determinant of this activity dependent release in pharyngeal pumping. However the residual inhibition that follows light activation of glutamate neurons suggests that there are additional routes that can actively exert a reduction in pharyngeal pumping. Routes that nonetheless require glutamatergic neurons activity.

Extending this approach to the off food context showed that the *eat-4* deficient strain has a pronounced pumping off food due to the loss of the glutamate-dependent reduction in pumping. Interesting this genetically modulated elevation of pumping in absence of food is markedly reduced by the light activation of glutamatergic neurons that are not releasing glutamate (**Figure 39B**). This observation reinforces the conclusion made on food, the key role of glutamate-mediated reduction of pumping, and highlights additional non glutamate-dependent determinants that are revealed when the nervous system is devoid of glutamate transmission.

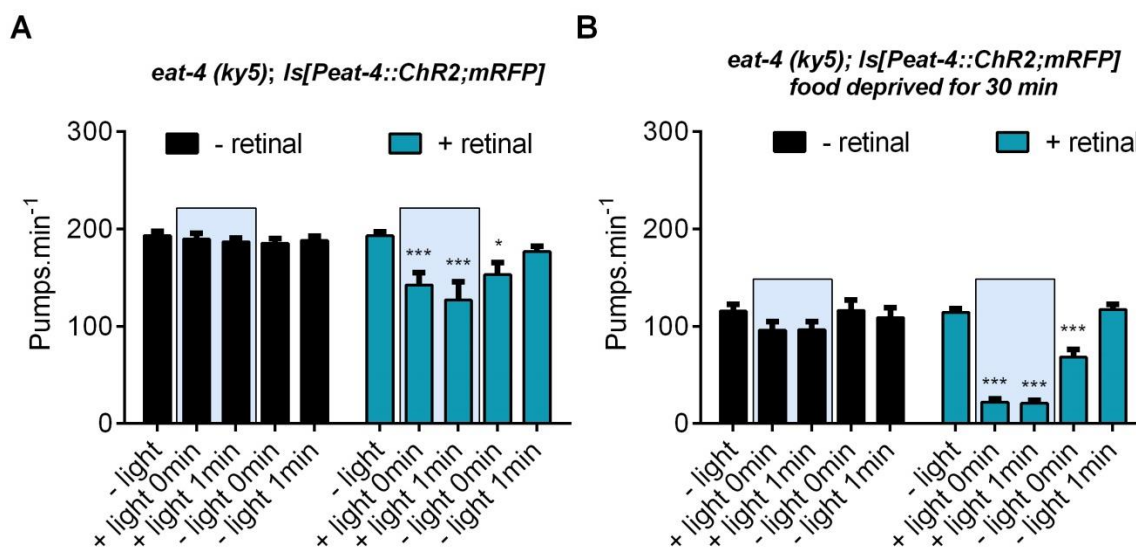


Figure 39: Artificial light-activation of glutamatergic neurons can reduce the pumping rate in a glutamate-independent fashion.

A. *eat-4(ky5); Is[Peat-4::ChR2;mRFP]* worms pumped at ~190 ppm in the presence of food but with no light. 2 min of UV light triggered a significant decrease in *eat-4(ky5); Is[Peat-4::ChR2;mRFP]* pumping rate on food (-51 ± 10 ppm; $p < 0.001$ and -66 ± 10 ppm; $p < 0.001$ for the 1st and 2nd min respectively, $n = 11$). No significant effect was observed without retinal ($p = 0.984$; $n = 8$). **B.** Food deprived *eat-4(ky5); Is[Peat-4::ChR2;mRFP]* worms for 30 min showed a pumping rate of ~115 ppm without light. When illuminated, *eat-4(ky5); Is[Peat-4::ChR2;mRFP]*, a reduction of the pumping rate was observed (-92 ± 8 ppm; $p < 0.001$ and -93 ± 8 ppm; $p < 0.001$ for the 1st and 2nd min respectively, $n = 11$), reducing the *eat-4(ky5)* pump rate to a level similar to N2 off food ($p = 0.99$). No significant effect was observed without retinal ($p = 0.984$ $n = 8$ on food and $p = 0.99$; $n = 5$ off food after 2min of light). Excitation wavelength used was 480/40nm.

4.2.3 Glutamate released upon food removal does not act directly onto the pharynx muscles

In the previous chapter (**Chapter 3**) it was shown that the rates of pumping on and off food were unaffected when the RIP neurons, forming the single connectome mediated interaction between the sensory and integrating levels of the extrapharyngeal and pharyngeal nervous systems, were ablated. This raised the possibility that the glutamate response is mediated by volume transmission or components that are intrinsic to the pharynx. As receptor signalling is likely to mediate the consequence of the off food glutamate signalling, a screen of candidate glutamate receptors was designed to help define the molecular and cellular intermediates of the *eat-4* dependence of pumping. Investigation of the core cycle has identified that the pharyngeal muscle is sensitive to release of glutamate from the pharyngeal motoneuron M3 that imposes an important inhibitory response via the glutamate gated chloride channel AVR-15 that speeds up repolarization of the muscle during the pump, decreasing the pump duration. Indeed the loss of this activity is the major determinant of the *eat-4* dependence of the pumping behaviour on food

(Dent *et al.*, 1997). As sustained activation of these receptors from additional sources of glutamate could feasibly inhibit the muscle, whether the pharyngeal muscle expressed glutamate receptors mediating the pumping response was first investigated.

The role of the glutamate receptors expressed in the pharynx muscle was assessed to test this hypothesis. Three glutamate receptor subunits are known to be expressed in the pharynx muscle; *avr-15*, *glc-1* and *glc-2* (Dent *et al.*, 1997; Laughton *et al.*, 1997; Ghosh *et al.*, 2012). *avr-15(ad1051)* mutant showed a reduced pumping rate in the presence of food (**Figure 40C**), as expected given the extended pump duration displayed by this mutant compared to wild-type worms (Dent *et al.*, 1997). *glc-2(ok1047)* also pumped slower than the wild-type paired control while *glc-1(pk54::Tc1)* behaved similarly to N2. In contrast, despite reinforcing the significance of muscle glutamate signalling to sustaining pumping on food, none of the same glutamate receptor mutants displayed a different behaviour in the absence of food relative to N2 (**Figure 40D, E and F**).

Overall these results showed the involvement of *avr-15* and *glc-2* receptors in the pumping behaviour on food, but reveal that the glutamate released in response to the removal of food does not act directly onto the pharynx muscle.

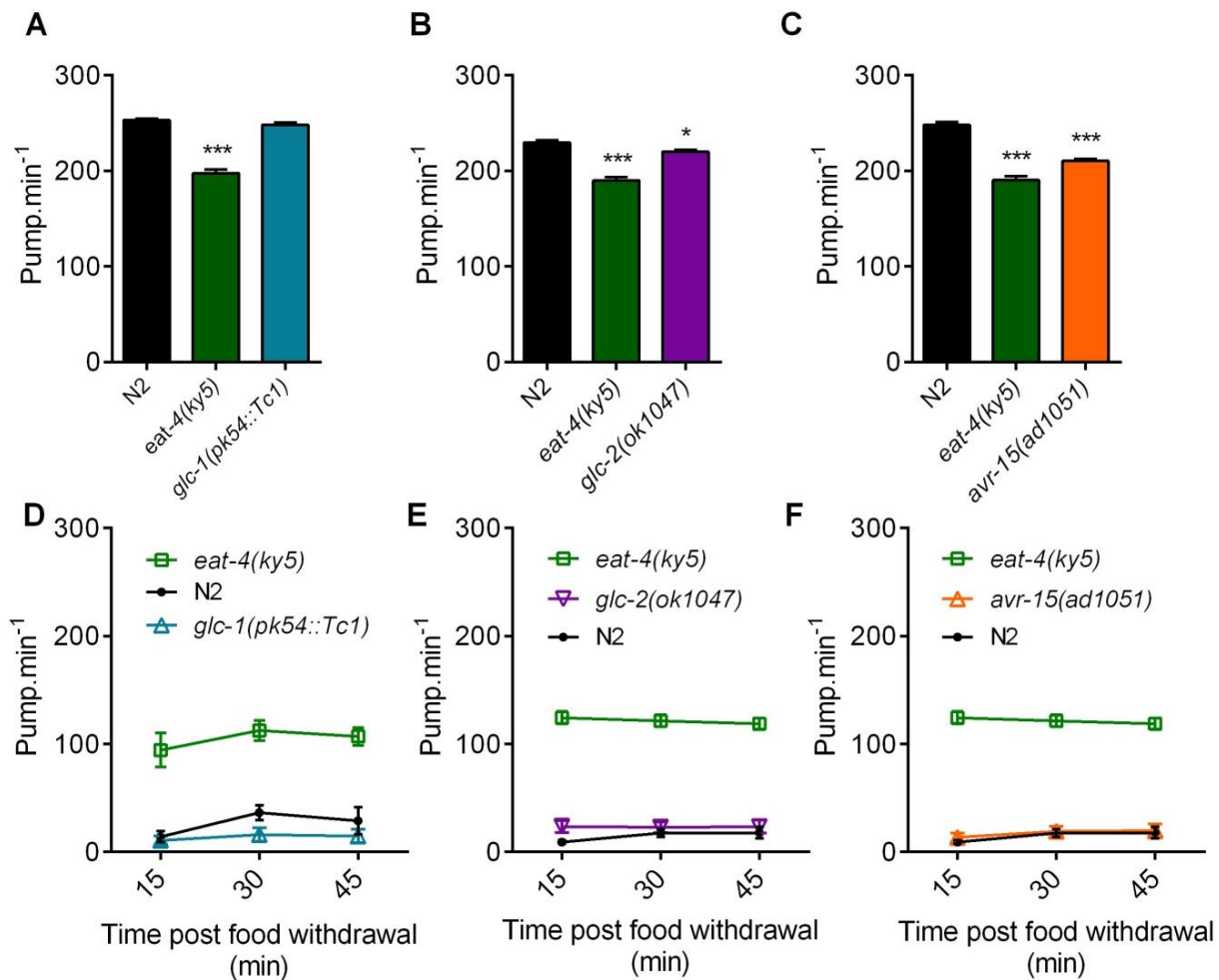


Figure 40: A comparison of pumping behaviours on and off food in N2 and mutants deficient in pharyngeal muscle glutamate receptors.

A-C. On food pumping rate of *glc-1(pk54::Tc1)*, *glc-2(ok1047)* and *avr-15(ad1051)* relative to paired N2 and *eat-4* mutants, (A.) *glc-1(pk54::Tc1)* (n = 12) pumped at the same rate than N2 (n = 13) (p = 0.64) while (B.) *glc-2(ok1047)* (n = 15) and (C.) *avr-15(ad1051)* (n = 16) pumped significantly slower than their paired N2 (-10ppm; p = 0.045 and -38ppm; p < 0.001 respectively). *glc-1(pk54::Tc1)* (50ppm; p < 0.001), *glc-2(ok1047)* (30ppm; p < 0.001) and *avr-15(ad1051)* (20ppm; p < 0.001) pumped higher than their paired *eat-4(ky5)*.

In the absence of food (D.) *glc-1(pk54::Tc1)* (p = 0.672; n = 6 N2 and *glc-1*), (E.) *glc-2(ok1047)* (p = 0.524; n = 11 N2 and n = 7 *glc-2*) and (F.) *avr-15(ad1051)* (p = 0.99; n = 8 N2 and n = 11 *avr-15*) displayed a similar pumping rate to their paired N2.

4.2.4 Ionotropic glutamate-gated receptors (iGluRs) do not modulate the pumping behaviour

To resolve candidates for the site of action of the released glutamate in response to food cues, 10 additional glutamate receptor mutants were screened for the pumping behaviour on and off food. This experimental approach enabled us to define candidate receptors and further resolve how they contribute to the distinct role that glutamate plays in these distinct contexts. There are three subtypes of glutamate receptors in *C. elegans*, ionotropic receptors (iGluRs), metabotropic receptors (MGL) and glutamate-gated chloride-channels (GluCl) that extends beyond those identified as being expressed in the pharynx (Brockie *et al.*, 2001a; Brockie and Maricq, 2006; Dillon *et al.*, 2006; Dillon *et al.*, 2015).

Four iGluRs mutants were available for this assay; *glr-1*, *glr-2*, *glr-7* and *nmr-1*. Based on a comparison of N2 pumping rates, none of these iGluRs mutants showed any deficit in their pumping on food phenotype (**Figure 41A**). Conversely, no involvement in the control of the pumping rate off food was observed as all the iGluRs mutants behaved similarly to N2 (**Figure 41B, C**).

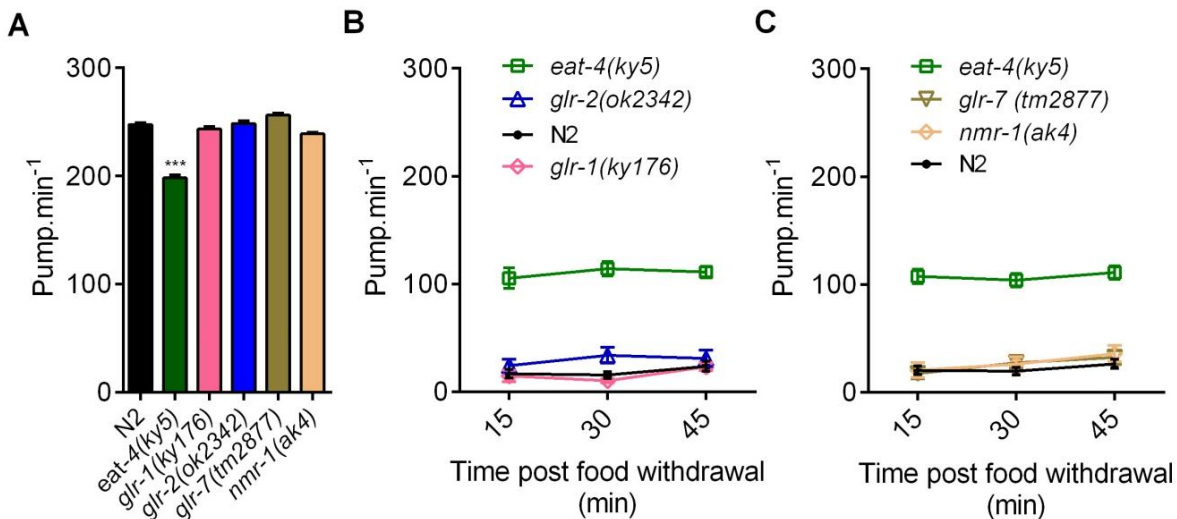


Figure 41: Ionotropic glutamate receptors do not act in the modulation of the pumping behaviour.

A. In the presence of food, *eat-4(ky5)* mutant pumped slower (-49 ± 3 ppm; $p < 0.001$; $n = 57$) while *glr-1(ky176)* ($p = 0.99$; $n = 16$), *glr-2(ok2342)* ($p = 0.99$; $n = 19$), *glr-7(tm2877)* ($p = 0.418$; $n = 20$) and *nmr-1(ak4)* ($p = 0.414$; $n = 20$) pumped at a similar rate to the N2 paired control ($n = 59$).

B. C. In absence of food, *eat-4(ky5)* pumped at a higher rate (98 ± 6 ppm; $p < 0.001$; $n = 12$) than N2 ($n = 20$) while *glr-1(ky176)* ($p = 0.99$; $n = 5$), *glr-2(ok2342)* ($p = 0.99$; $n = 13$), *glr-7(tm2877)* ($p = 0.99$; $n = 12$) and *nmr-1(ak4)* ($p = 0.99$; $n = 8$) pumped at a similar rate to N2.

4.2.5 Investigation of metabotropic glutamate receptors (MGLs) revealed a role for MGL-2 in the control of the pumping rate on food

Next, the role of metabotropic receptors (MGL) on the control of the pumping behaviour was investigated. Among the MGL mutants tested, only *mgl-2(tm355)* displayed a reduced pumping rate on food relative to the paired N2. However the phenotype was not as profound as the one observed in *eat-4(ky5)* mutant (**Figure 42A**). None of the MGL receptors appeared to play a role

in the pumping behaviour in absence of food when assayed under the experimental conditions used here (**Figure 42B**), indicating no involvement in the control of the pumping behaviour in absence of food.

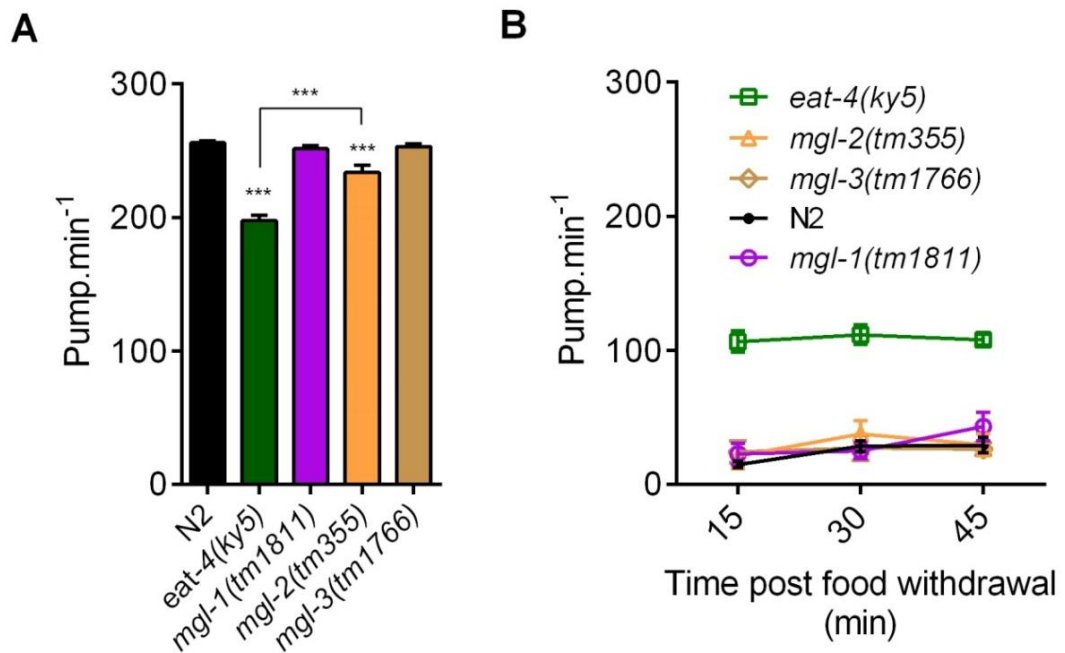


Figure 42: Metabotropic glutamate receptor MGL-2 modulates the high pumping rate observed on food.

A. On food, *eat-4(ky5)* (-58 ± 4 ppm; $p < 0.001$; $n = 39$) and *mgl-2(tm355)* (-22 ± 4 ppm; $p < 0.001$; $n = 17$) displayed a reduced pumping rate than N2 ($n = 33$). *mgl-1(tm1811)* ($p = 0.99$; $n = 19$) and *mgl-3(tm1766)* ($p = 0.99$; $n = 19$) pumped similarly to N2.

B. In response to food removal, *eat-4(ky5)* (84 ± 8 ppm; $p < 0.001$; $n = 14$) displayed a higher pumping rate than wild-type ($n = 14$). *mgl-1(tm1811)* ($p = 0.99$; $n = 7$), *mgl-2(tm355)* ($p = 0.99$; $n = 15$) and *mgl-3(tm1766)* ($p = 0.99$; $n = 7$) display a similar pumping rate to N2.

4.2.6 Glutamate-gated chloride-channel *avr-14* acts to reduce the pumping rate in response to food removal

Last, the glutamate-gated chloride-channels (GluCl) were screened for a role in the pumping behaviour. Unlike the previously tested *glc-2(ok1047)* and *avr-15(ad1051)* mutants (**Figure 40B, C**), neither *glc-3(ok321)*, *glc-4(ok212)* nor *avr-14(ad1302)* mutants displayed any significant differences compared to their paired N2 (**Figure 43A, C**). In absence of food, *glc-3(ok321)* and *glc-4(ok212)* behaved similarly to N2. However, the strong and sustained elevation of *avr-14(ad1302)* pumping off food relative to N2 control showed the power of this approach. There was a significantly increased pumping rate in these mutants off food relative to N2 (57 ± 7 ppm). This robust response, although marked, was smaller than the elevated *eat-4(ky5)* rate as *avr-14(ad1302)* pumped significantly slower than *eat-4* off food (-50 ± 6 ppm) (**Figure 43D**).

The observation that *avr-14* was a key determinant of the modulation of the pumping rate in absence of food was reinforced by measuring the pumping of *avr-14* mutants expressing a wild-type *avr-14* under the control of its endogenous promoter. This was sufficient to fully rescue the *avr-14(ad1302)* high pumping rate off food as *avr-14(ad1302); Ex[P_{avr-14}::*avr-14* gDNA]* pumping rate displayed no significant differences with the paired N2 control (**Figure 43E**).

Taken together these results highlight a selective contribution of distinct glutamate receptors. They highlight the important role of pharyngeal *avr-15* and *glc-2* receptor subunits in defining the *eat-4* dependence of pumping on food. Interestingly, however, they highlight the unexpected and relatively selective role of *avr-14* in mediating the distinct *eat-4* dependence of pumping off food.

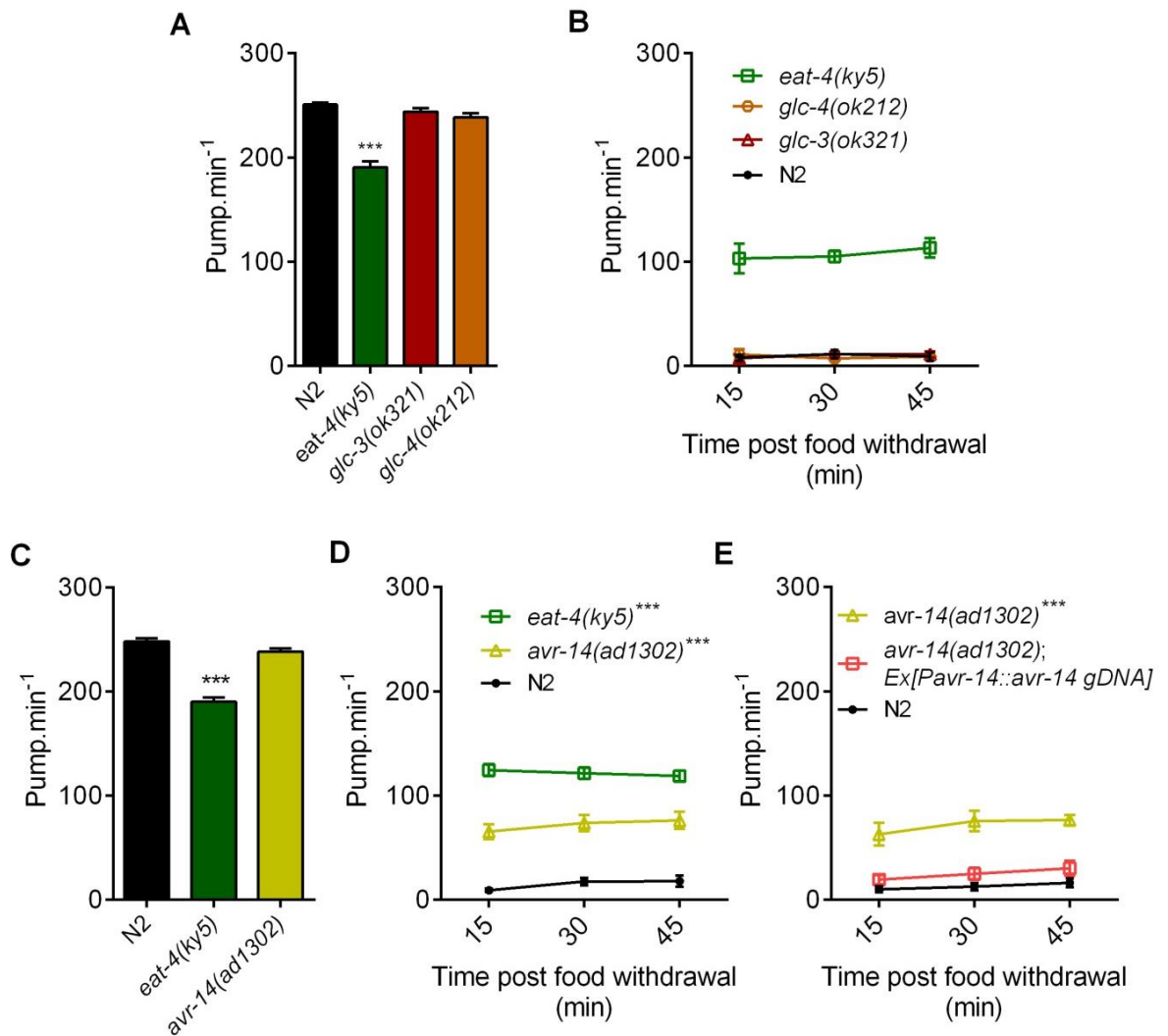


Figure 43: Glutamate-gated chloride channels *avr-14* mediates the reduction of the pumping rate in absence of food.

A. *eat-4(ky5)* pumped slower on food (-60 ± 5 ppm; $p < 0.001$; $n = 17$) while *glc-3(ok321)* and *glc-4(ok212)* behaved the same than N2 ($n = 17$) ($p = 0.99$ for both with $n = 13$ *glc-3(ok321)* and $n = 12$ *glc-4(212)*). **B.** In absence of food, *eat-4(ky5)* displayed a higher pump rate (98 ± 6 ppm; $p < 0.001$; $n = 8$) compare than N2 ($n = 8$). *glc-3(ok321)* ($p = 0.99$; $n = 8$) and *glc-4(ok212)* ($p = 0.99$; $n = 9$) pumped at a similar level than their paired N2. **C.** *avr-14(ad1302)* ($p = 0.207$; $n = 15$), but not *eat-4(ky5)* (-58 ± 5 ppm; $p < 0.001$; $n = 14$), displayed a similar rate on food to N2 ($n = 14$). **D.** In absence of food, *avr-14(ad1302)* ($n = 11$) pumped higher than N2 ($n = 8$) (57 ± 7 ppm; $p < 0.001$) but lower than *eat-4(ky5)* ($n = 11$) (-50 ± 6 ppm; $p < 0.001$). **E.** *avr-14(ad1302); Ex[Pavr-14::avr-14 gDNA]* ($n = 8$) pumped similarly to N2 ($n = 5$) ($p = 0.99$)

and significantly slower than *avr-14(ad1302)* ($n = 8$) (-47 ± 8 ppm; $p < 0.001$) in the absence of food.

4.2.7 *avr-14* expression pattern investigation reveals expression in the pharyngeal nervous system

The functional data presented in this study indicated that this important determinant would be intrinsic to the pharynx. However, *avr-14*, unlike other GluCl, has not been implicated in pharyngeal function nor reported to be expressed in this circuit. *avr-14* is known to be expressed in the somatic nervous system and abundantly in the nerve ring as reported using a transcript reporter *Ex[P_{avr-14}::GFP]* (Dent *et al.*, 2000). The abundant expression clearly excludes pharyngeal muscle (**Figure 44A-C**) but the pattern in the nerve ring confounds ready assignment of potential expression in the underlying pharyngeal nervous system. To overcome this, micro-dissection on worms expressing GFP under *avr-14* promoter was performed to isolate pharynxes (**Figure 44D**). Observation of dissected pharynxes under confocal or epifluorescence microscope ensures the removal of confounding nerve ring staining (**Figure 44E**). Using this technique, expression of *avr-14* in the pharyngeal nervous system was revealed (**Figure 44E-J**). As the transgenic line used is not integrated, expression may vary however, GFP was clearly visible in at least eight pharyngeal neurons, with four soma in the terminal bulb and four in the proximal bulb. Based on their position (Fang-Yen *et al.*, 2012a) and shape (Albertson and Thomson, 1976), soma located in the terminal bulb were identified as M1 (**Figure 44H, I**), M2 (**Figure 44E, G-I**) and I5 (**Figure 44E, G-I, L-N**). Indeed, M1's soma is located subdorsally and possesses a single process running anteriorly through the pharynx and reaching the lips where it splits in two. M2L/R are a pair of neurons with a cell body localised on the dorsal side in an anteriorly position relative to I5 with a single process ending in the anterior bulb. I5 has a very large cell body which is located on the ventral side of the terminal bulb. Furthermore, to confirm the expression of *avr-14* in the glutamatergic I5 neuron, the N2; *Ex[P_{avr-14}::GFP]* strain has been crossed with the transgenic wild-type strain expressing mRFP in glutamatergic neuron. The strain used for crossing was the strain used in the optogenetics experiments described above which also expressed ChR2 (**Figure 38**). The pharynx of the transgenic strain has been dissected, isolated and observed under a

fluorescent microscope for co-localisation. A colocation between a soma expressing *avr-14::GFP* and a glutamatergic soma believed to be the I5 neuron was observed (**Figure 44H-K**).

Similarly, soma from three neurons were identified in the anterior bulb, NSM, M4 and I2. NSM cell bodies are located subventrally in the anterior bulb, just anterior to the nerve ring, and have two processes running posteriorly through the isthmus (Axang *et al.*, 2008) (**Figure 44E-J**). The M4 cell body is localised dorsally near the nerve ring and has two ventral processes running posteriorly through the isthmus reaching the terminal bulb before eventually running dorsally back in the isthmus (**Figure 44H-I**). Finally, I2 cell bodies are localised on the ventral side anteriorly to NSM, and have processes running anteriorly with proprioceptive-like free subcuticular endings near the lips (**Figure 44E-J**).

Overall, these results indicate the previously reported expression of the glutamate-gated chloride channel *avr-14* extends to at least 6 neurons in the pharyngeal nervous system. This expression includes both glutamate releasing neurons I5 and I2 and non-glutamatergic neurons NSM, M1, M2 and M4 which would allow *avr-14* to modulate pharyngeal function. This is not a function currently described to *avr-14* but both our genetic and expression analysis reinforce an important role in the dynamic *eat-4* dependence of pumping in response to food removal. Importantly, these observations add further weight to a role from within the pharynx and its embedded microcircuit.

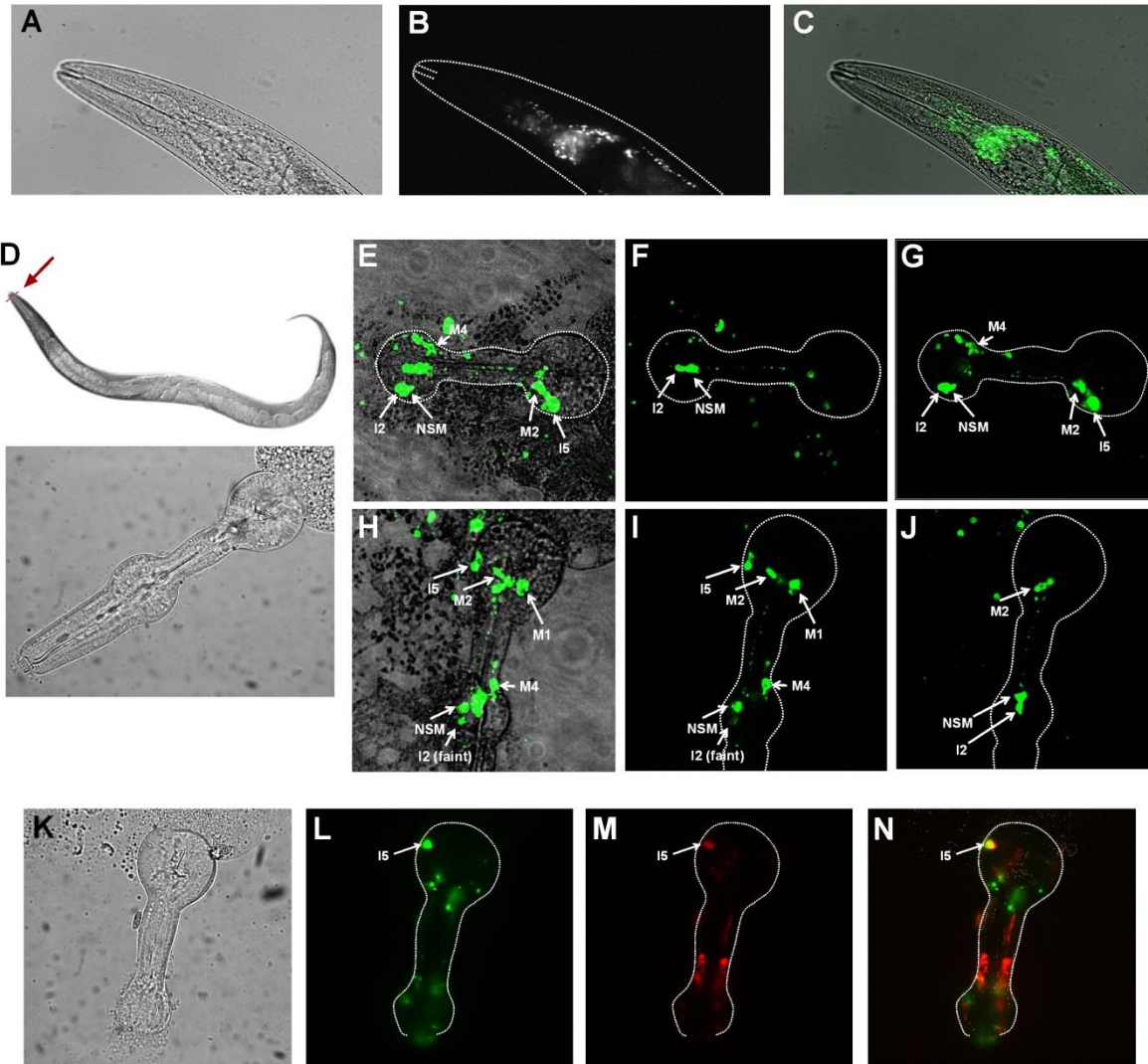


Figure 44: *avr-14* is widely expressed in *C. elegans* nervous system but revealed as being integral to the pharyngeal microcircuit in the isolated pharynx.

A-C. *avr-14::GFP* expression in the whole intact worm.

D. Dissected pharynx. A razor blade was used to cut the tip of the worm nose in M9 + BSA solution at the point indicated by red line (red arrow). The pharynxes isolated from the cuticle were then separated from the body and put on a 2% agarose pad.

E-J. Confocal images of N2; *Ex[P_{avr-14}::GFP]* isolated pharynxes. (E) and (H) are superimposed stacks. (F), (G), (I) and (J) represent the GFP expression of 1 z stack. Expression is observed in 6 neurons identified as I2, I5, M1, M2, M4 and NSM.

K-N. DIC (K), GFP (L), mRFP (M) and merged (N) images of N2; *Ex[Pavr-14::GFP]; Is[Peat-4::ChR2::mRFP]* isolated pharynxes. Yellow represents co-localisation.

4.2.8 M3 motoneurons modulate the pumping rate in presence of food but not in its absence

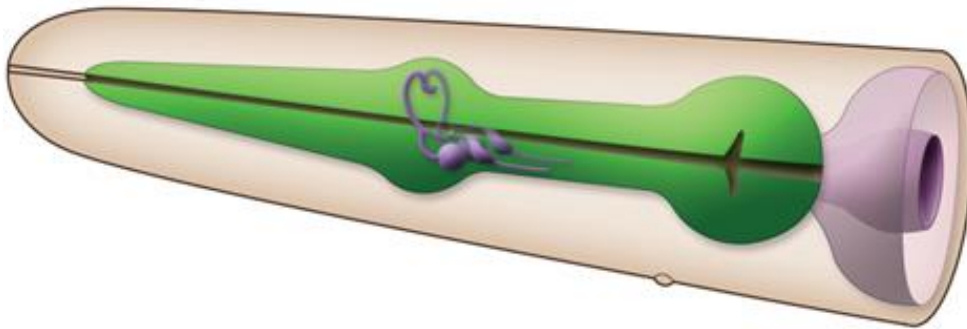
Guided by the evidence indicating important regulation through mechanisms intrinsic to the pharynx we used cell specific approaches to resolve the circuit basis for the *eat-4* dependence of the pumping rate, i.e. to determine which pharyngeal neuron(s) was/were releasing glutamate in response to food cues. *eat-4* has been shown to be expressed in 4 or 5 pharyngeal neurons; M3, I2, I5, MI (Serrano-Saiz *et al.*, 2013) and NSM (Lee *et al.*, 1999) depending on the reporter construct used to probe this.

As detailed above, the glutamatergic motoneuron M3 has been shown to be an important regulator of the pumping rate in the presence of food, triggering repolarisation that leads to muscle relaxation thereby shortening the pump duration (Avery, 1993) and thus permitting a fast frequency. In this regard, M3 ablation has previously been shown to decrease the pumping rate in the presence of food (Avery, 1993). Although the investigation of the pharyngeal GluCl reinforced the important role of the M3 mediated acceleration of repolarization in sustaining the high pumping rate on food, it remains possible that M3 could act as an important source of the *eat-4* dependence of pumping in absence of food. To formally test this, the pumping rate in both on and off food contexts of M3 deficient worms was investigated. For this purpose the mutant strain *ceh-2(ch4)*, in which M3 is non-functional, was used (Aspöck, 2003).

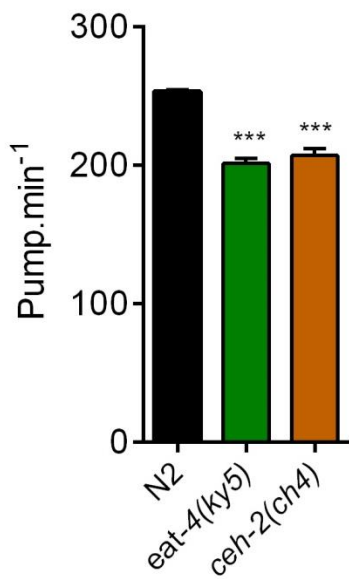
When compared to N2, *ceh-2(ch4)* displayed a reduced pumping rate on food as would be predicted from observations made in worms in which M3 is laser ablated (Avery, 1993; Raizen *et al.*, 1995). This effect is again very similar to the pumping reduction on food observed in *eat-4(ky5)* mutants (**Figure 45B**), reinforcing the pivotal role of M3-mediated glutamate release in the defining reduced pumping on food. Conversely, *ceh-2(ch4)* showed no difference to the N2 worms' pumping rate off food (**Figure 45C**), indicating

that M3 is not involved in the modulation of the pumping behaviour in absence of food. This reinforces our previous finding showing that the pumping behaviours on food and off food were controlled by distinct circuits/pathways that we can now extend to individual cells.

A



B



C

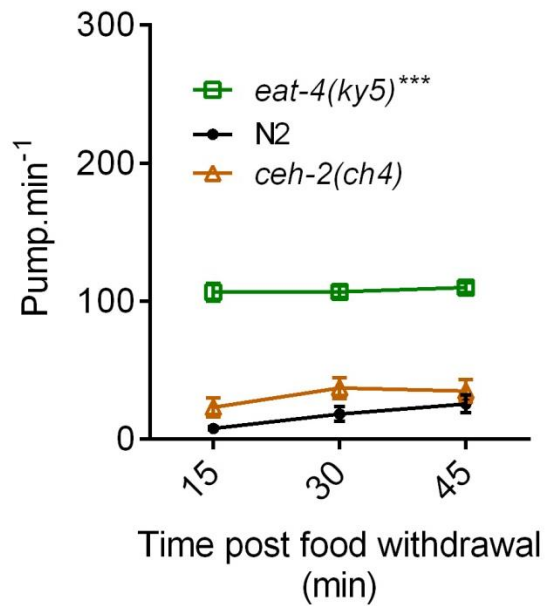


Figure 45: Genetic disruption of pharyngeal glutamatergic neuron M3 reveals that M3 modulates the pumping rate in presence but not in absence of food.

A. Cartoon representation of the pharyngeal neuron M3. Taken from *WormAtlas*

B. M3 non-functional mutant *ceh-2(ch4)* pumped slower in the presence of food (-46 ± 5 ppm; $p < 0.001$; $n = 20$) relative to the paired N2 ($n = 20$).

C. In the absence of food *ceh-2(ch4)* displayed a similar pumping rate ($p = 0.089$; $n = 8$) to N2 ($n = 11$).

4.2.9 Pharyngeal glutamatergic neuron I2 is a major determinant of the pumping behaviour off food but is not involved in the pumping regulation on food

I2s are a bilateral pair of glutamate releasing pharyngeal neurons with a poorly described function but with proposed blue light mediated inhibition of pharyngeal function on food (Serrano-Saiz *et al.*, 2013; Bhatla and Horvitz, 2015). To investigate if pharyngeal release of glutamate executed by I2 leads to an increased inhibitory tone, the neuron was genetically ablated by expressing the Caspase activator *Csp-1b* (Denning *et al.*, 2013) in I2 via the promoter for the I2 expressed neuropeptide *flp-15* (Bhatla and Horvitz, 2015).

On food, N2; *Is[Pflp-15::Csp-1b]* displayed a similar pumping rate to its paired N2 control (**Figure 46B**). Conversely, N2; *Is[Pflp-15::Csp-1b]* pumped like the *eat-4(ky5)* mutant off food (**Figure 46C**). This indicates that the glutamate releasing neuron I2 mediates the pumping behaviour in absence of food. Furthermore, based on the penetrance of the phenotype relative to *eat-4(ky5)*, it suggests that I2 is a singular cellular determinant of the *eat-4* deficient pumping off food phenotype.

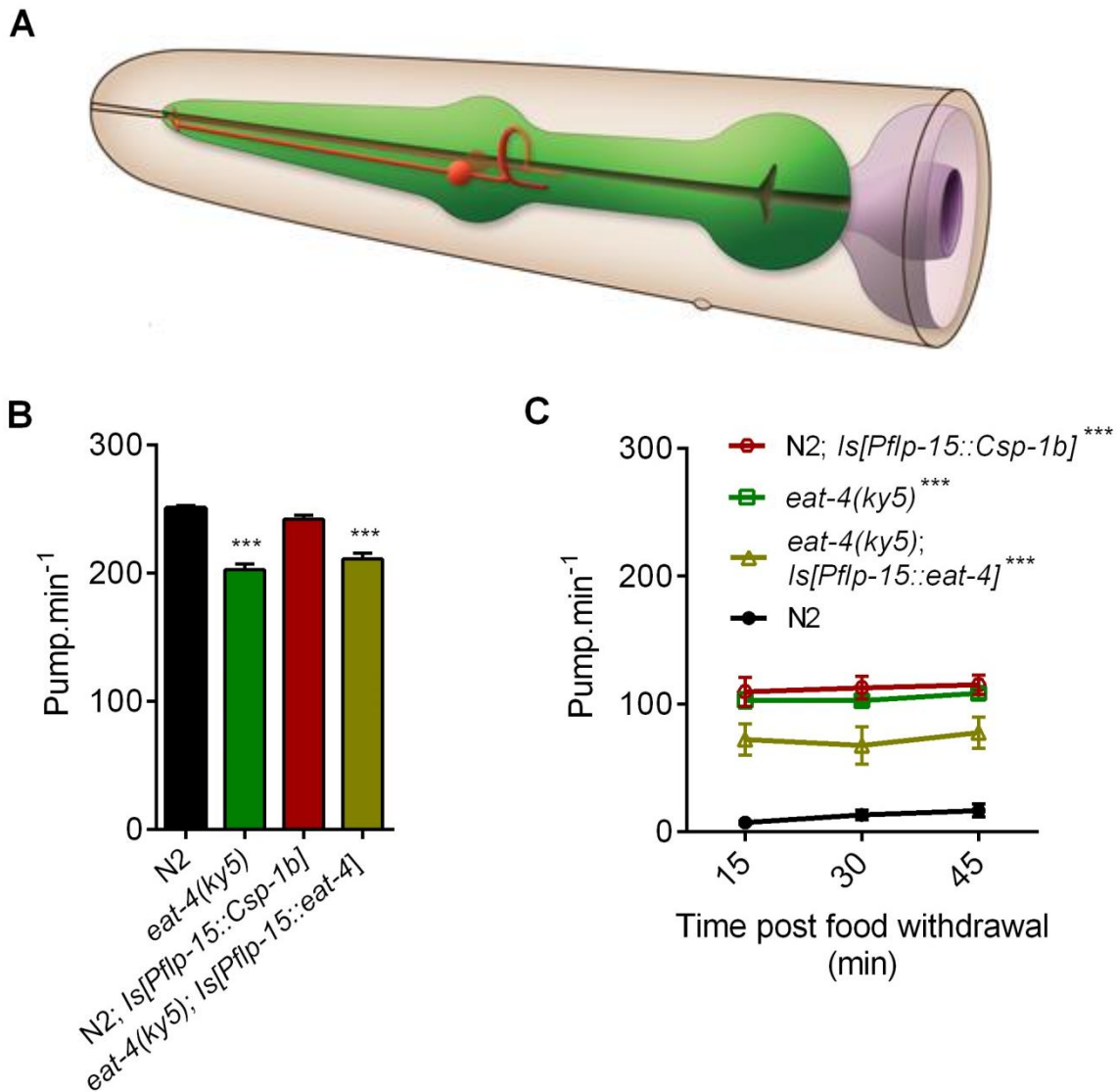


Figure 46: I2 pharyngeal neurons modulate the off food pumping behaviour via glutamate release.

A. Cartoon representation of the pharyngeal neurons I2. Taken from *WormAtlas*

B. In the presence of food, N2; *Is[Pflp-15::Csp-1b]* (I2 genetically ablated; n = 20) pumped at a similar rate to the wild-type (n = 20) paired control (p = 0.213). *eat-4(ky5); Is[Pflp-15::eat-4]* (n = 16) pumped slower than N2 (-40ppm; p < 0.001) at a similar rate than *eat-4(ky5)* (n = 12) mutants (p = 0.57).

C. In absence of food, N2; *Is[Pflp-15::Csp-1b]* (n = 10) displayed a higher pumping rate to N2 (n = 8) (101 ± 9 ppm; p < 0.001) at a similar level than *eat-4(ky5)* (n = 10) mutant (p = 0.99).

eat-4(ky5); Is[Pflp-15::eat-4] (n = 6) mutant pumped off food at a higher rate than N2 (60 ± 11 ppm; $p < 0.001$) but slower than *eat-4(ky5)* (-32 ± 10 ppm; $p = 0.023$).

To test this hypothesis, worms expressing ChR2 under the *flp-15* promoter control were investigated and the pumping rate on and off food, with and without illumination to activate ChR2, were compared. On food, the transgenic strain N2; *Ex[Pflp-15::ChR2;YFP]* pumped at a similar rate to N2 control. Light activation of I2 in wild-type worms led to a reduction of this on food rate (**Figure 47A**). This imposition of an I2 mediated inhibitory tone was not seen in worms on plates without retinal, indicating it is selective. This robust inhibition was less marked than that observed in N2; *Ex[Peat-4::ChR2;mRFP]*, expressing ChR2 in glutamatergic neurons. In addition, while I2 expressing ChR2 worms pumped like N2 off food in the absence of light, subsequent illumination did not significantly decrease the low off food pump rate (**Figure 47B**). These results are similar in pattern to what was observed in the worms expressing ChR2 in glutamatergic neurons (**Figure 38**) and reinforce that much of the glutamate that imposes an off food inhibition of pumping is triggered by local release within the pharynx, and I2 is an important determinant of this activity.

Interestingly, the similarity to the results obtained extends to those in which the glutamate release is executed in a genetic background that precludes glutamate release. In the context of an I2 selective activation, the worm retains a light induced reduction of pumping (**Figure 47C**). This suggests that I2 contain additional determinants that act with the released glutamate to execute an off food reduction in pharyngeal function.

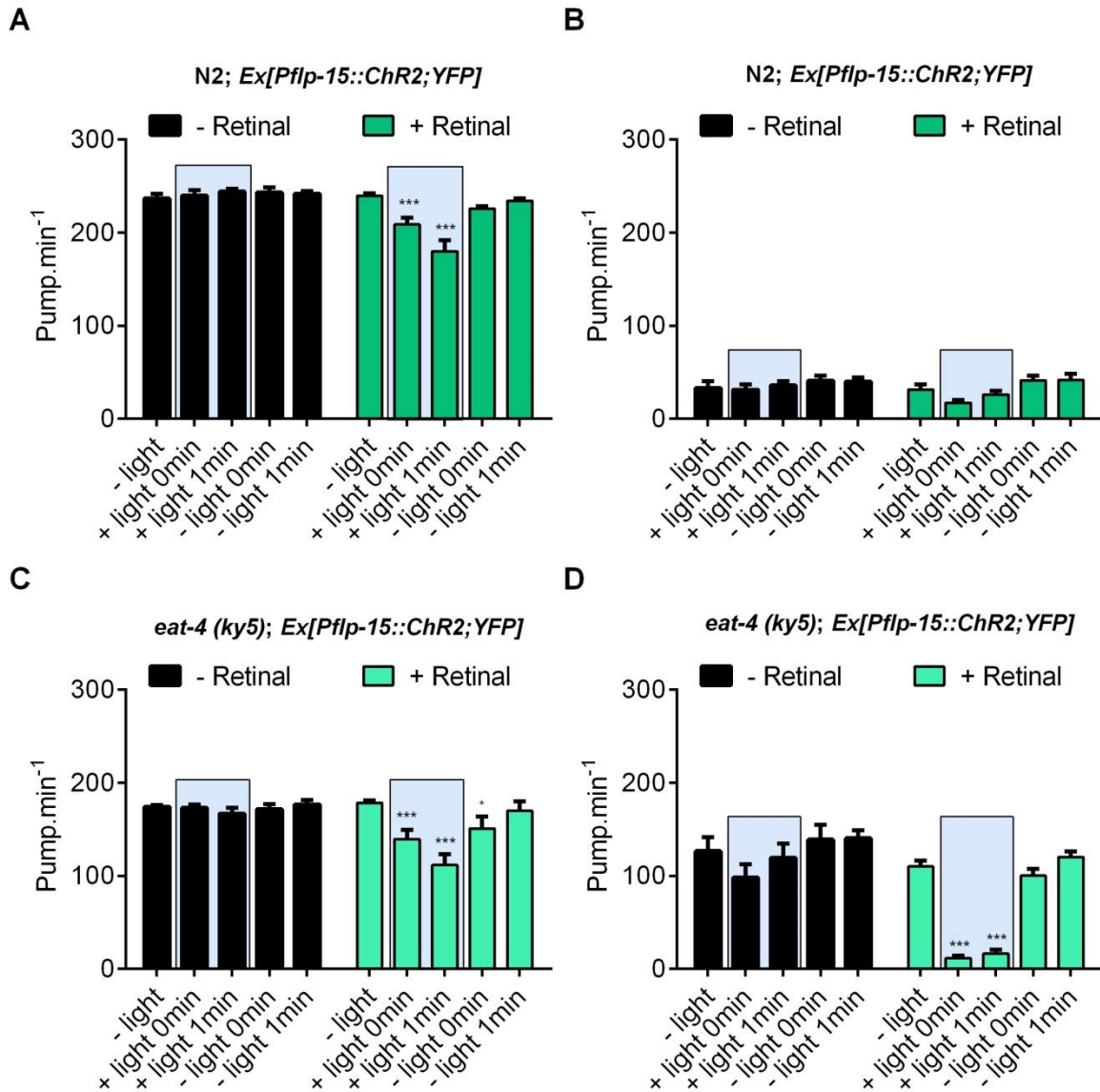


Figure 47: Light activation of pharyngeal neurons I2 reduces the pumping rate.

A. UV-light activation of I2 neurons led to the reduction of N2 pumping rate in presence of food (-59 ± 11 ppm; $p < 0.001$; $n = 14$). **B.** Illumination of N2; *Ex[Pflp-15::ChR2;YFP]* worms did not change the pumping behaviour in the absence of food ($p = 0.84$; $n = 10$). **C.** In an *eat-4(ky5)* mutant background, UV-light activation of I2 also triggered the reduction of the pumping rate in the presence of food (-67 ± 14 ppm; $p < 0.001$; $n = 9$). **D.** In absence of food, the presence of light reduced the high pumping rate displayed by *eat-4(ky5)* (-93 ± 7 ppm; $p < 0.001$; $n = 8$) to a similar level than N2 off food ($p = 0.18$). Excitation wavelength used was 480/40nm.

Furthermore, the level of activity in I2 neurons in function of the food context was investigated using a calcium imaging approach. N2; *Is[Pflp-15::GCaMP3]* transgenic strain expressing the genetically encoded calcium indicators (GECIs) GCaMP3 (Tian *et al.*, 2009) specifically in I2 neurons was used (Bhatla and Horvitz, 2015). Calcium activity in I2 was reported to increase with light, therefore a lower power (2 mW/mm²) and reduced exposure time (100–200 ms, 1 fps) was used in this assay. Only the first frame of the recorded videos was analysed to avoid the effect of light. Well-fed or 30 min food-deprived L4+1 transgenic worms were placed on a 10% agarose pad and immobilised using polystyrene beads (Kim *et al.*, 2013). Soma of I2 neurons in worms food-deprived for 30 min showed an increase of ~49% in calcium activity relative to that observed in well-fed worms (**Figure 48**), suggesting an elevated activity of I2 in absence of food.

Overall, these results indicate I2 neurons play a major role in the inhibition of the pumping rate in response to food removal.

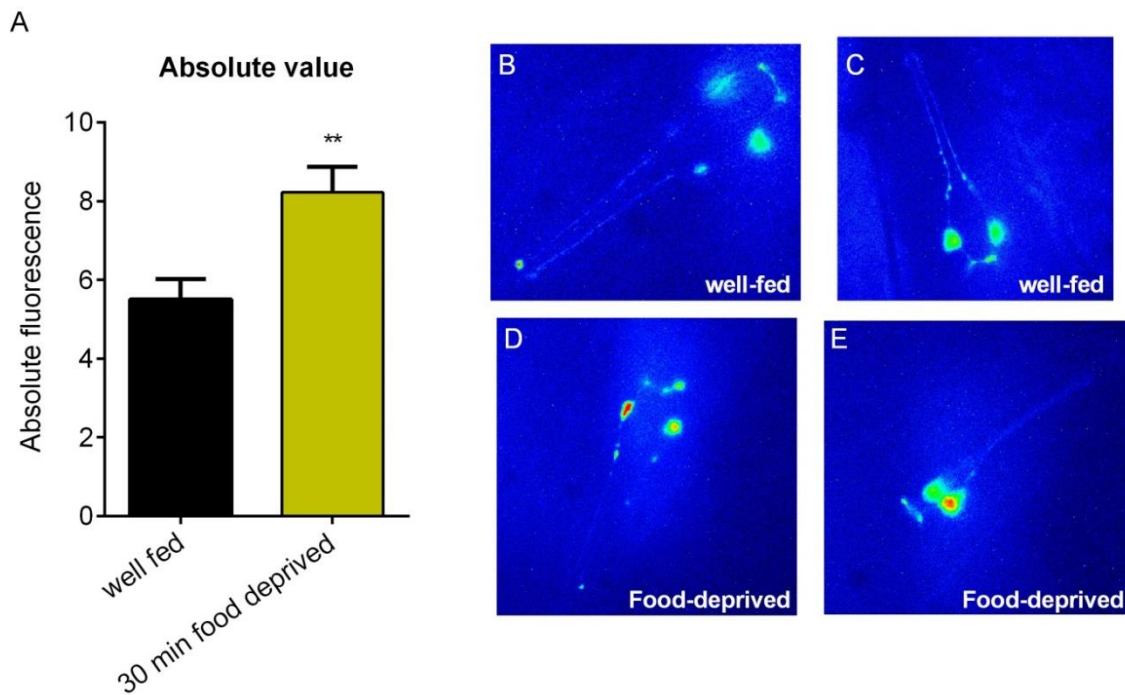


Figure 48: Increase calcium activity observed in I2 neurons in absence of food.

A. N2; *Is[Pflp-15::GCaMP3]* worms food-deprived for 30 min displayed an increased I2 neurons' calcium activity ($p = 0.0019$; $n = 24$) relative to I2 in well fed worms ($n = 25$).

B-C. Calcium images of N2; *Is[Pflp-15::CaMP5]* well-fed worms.

D-E. Calcium images of N2; *Is[Pflp-15::CaMP5]* Food-deprived for 30 min

4.2.10 I2 acts to reduce the pumping rate in an off food context via both glutamate- dependent and independent pathways

The observations made are consistent with the pivotal role of I2-mediated glutamate release in imposing the key inhibitory tone that reduces pumping. However, the supporting evidence from receptor studies and optogenetic activation in *eat-4* deficient backgrounds suggest that I2's glutamate is not the sole source of this off food reduction in pumping.

To investigate this further, *eat-4* wild-type cDNA was expressed under the *flp-15* promoter in an *eat-4(ky5)* background. As expected, *eat-4(ky5); Is[Pflp-15::eat-4]* transgenic strain showed a similar pumping rate on food compared

to *eat-4(ky5)* mutant (**Figure 47C**), consistent with the non-involvement of I2 in sustaining the high pump rate on food. In contrast, restoring *eat-4* release glutamate in I2 led to a reduction of the elevated pumping rate of *eat-4(ky5)* (-32 ± 10 ppm) off food (**Figure 46D**), consistent with the important role of I2-mediated glutamate release in sustaining a reduced pumping rate in an off food context. However, *eat-4(ky5); Is[Pflp-15::eat-4]* pumped at a higher rate than N2 (60 ± 11 ppm) indicating that glutamate released from I2 is not the sole determinant of the I2-dependent pumping reduction in absence of food. Furthermore, this result also indicates that I2 do not account for the entire glutamatergic inhibitory tone, suggesting that glutamate is also released from at least one another neuron.

Overall, these results showed that in response to food removal, I2 is an important determinant of the sustained reduction in pumping rate via both a glutamate-dependent and independent circuit.

4.2.11 Gap junction communication between neurons appears to play a role in the regulation of the pumping rate in the absence of food

From the results described above, it appears that glutamatergic neurons I2 can reduce the pumping rate in response to food withdrawal in a glutamate-independent fashion. The possibilities would involve neurohormonal transmission driven by neuropeptides (see **chapter 5**) or point to point communication via gap junctions.

Two innexins (main component of gap junction in the nematode) mutants have been assessed to investigate the role of gap junction in the pumping behaviour; *unc-7(e5)* and *unc-9(e101)*. The choice of these two mutants was guided by their abundance in the worm's nervous system so they could serve as proof of concept.

In the presence of food, both mutants exhibited a wild-type pumping rate, indicating gap junctions employing these innexins do not mediate the high sustained pumping rate observed on food (**Figure 49A**). Conversely, in absence of food, both *unc-7(e5)* and to a lesser extent *unc-9(e101)* pumped at a

significantly higher rate than the N2 paired control. However, both pumping rates were lower than the one displayed by the *eat-4(ky5)* mutant (**Figure 49B**).

Overall, these results reveal a role for gap junctions in the regulation of the pumping behaviour off food, but not on food.

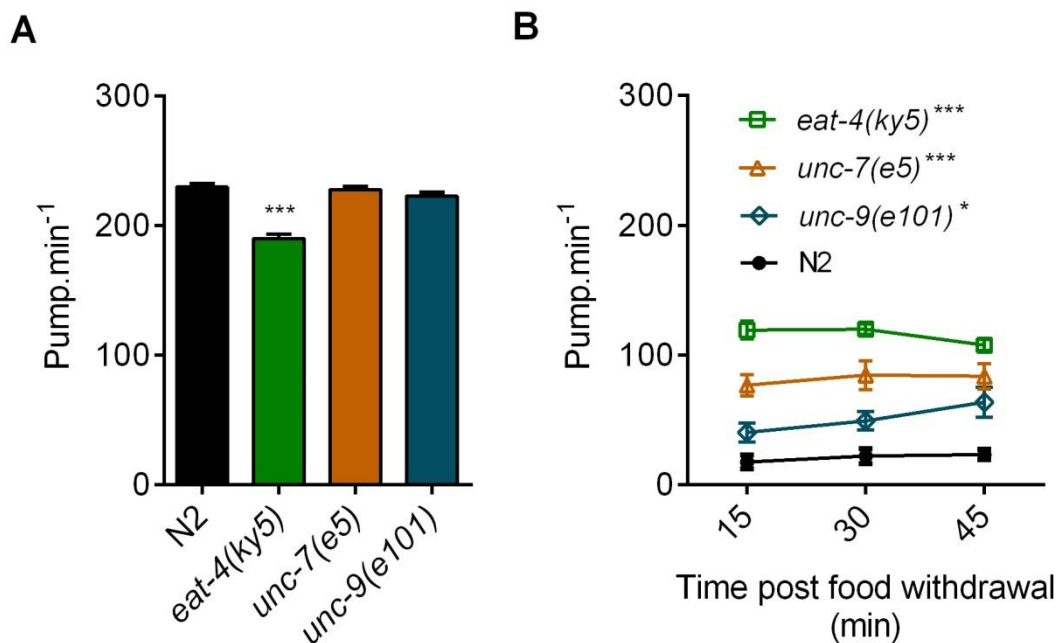


Figure 49: UNC-7 and UNC-9 innexins mediate the reduction of the pumping rate in absence of food.

A. Both *unc-7(e5)* ($p = 0.99$) and *unc-9(e101)* ($p = 0.79$) mutants pumped at a similar rate to N2 in the presence of food. *eat-4(ky5)* ($p < 0.001$) displayed a lower pumping rate to N2 ($P < 0.001$).

B. In absence of food, both *unc-7(e5)* (61 ± 10 ppm; $p < 0.001$, $n = 12$) and *unc-9(e101)* (30 ± 10 ppm; $p = 0.038$; $n = 10$) pumped faster than the N2 paired control ($n = 7$), but not as fast as *eat-4(ky5)* ($n = 10$) mutants ($p = 0.004$ and $p < 0.001$ for *unc-7(e5)* and *unc-9(e101)* respectively). *unc-7(e5)* pumped at a higher rate than *unc-9(e101)* ($p = 0.0101$).

At least 10 worms per mutant strains have been used, 8 worms for the N2 paired control.

4.3 Discussion

Chapter 3 presented the glutamate dependence of the pumping behaviour. Interestingly, glutamate signalling acts differentially depending on the food context, stimulating the pumping rate in the presence of food while reducing it when food is removed. The presence of two distinct circuits controlling feeding is conceptually very similar to that observed in mammals (Aponte *et al.*, 2011). The results obtained in this chapter reinforced these initial findings and shed light on distinct microcircuits modulating the two aspects of the worm's pumping behaviour. The opposite effect of glutamate on pumping depending on the presence or absence of food hinted on distinct glutamate releasing cellular determinants selectively activated to control the pumping behaviour.

4.3.1 M3 and I2 neurons are selectively recruited depending on the food context

The glutamatergic motorneuron M3 is known for its crucial role in sustaining the high frequency pump rate observed on food (Avery, 1993). Using a mutant in which the pharyngeal neuron M3 is non-functional, *ceh-2(ch4)*, a marked decrease of the pumping rate was observed, similar to that observed in glutamate deficient worms and consistent with previously published results on laser-ablated M3 worms (Avery, 1993; Raizen *et al.*, 1995; Aspöck, 2003). Interestingly however, no aberrant behaviour was observed in absence of food, indicating M3 released glutamate does not modulate the pumping rate when food is removed, reinforcing the notion that the two opposing behaviours actively engage distinct circuits.

Similarly, a mutant for the glutamate-gated chloride channel *avr-15* showed the same deficit in pumping on food compared to M3 and glutamate deficient worms, but showed a wild type pumping rate in absence of food. Thus, when food is present, M3 releases glutamate directly onto the receptor AVR-15 on the pharyngeal muscles pm4 and pm5 (including the proximal bulb, the isthmus and a small part of the terminal bulb) (Dent *et al.*, 1997). This has

the effect of terminating an individual pump by repolarizing the muscle, therefore shortening the pump duration and increasing the capability for sustaining a high pumping rate as observed in presence of food (Dent *et al.*, 1997). This microcircuit however, has no role in modulating the pumping rate when food is lacking, and M3 appeared to be selectively recruited in response to food cues. Interestingly, release of 5-HT by the pharyngeal neuron NSM has been shown by Li and colleagues to sustain the high pump rate in response to food (Li *et al.*, 2012). However, Ashrafi's group found that 5-HT released from NSM was not required for the pumping behaviour on food (Cunningham *et al.*, 2012), therefore NSM involvement in the pumping behaviour on food remains to be clarified.

In contrast, the pharyngeal glutamatergic neuron I2, recently implicated in the timing of a pumping inhibition in response to a light and hydrogen peroxide (Bhatla and Horvitz, 2015), showed an opposite pattern to M3. Worms with genetically ablated I2 neurons behaved normally on food. However, they displayed a marked elevation of their pumping rate in response to food deprivation, an elevation similar to that observed in *eat-4(ky5)* mutants. Thus, I2 appeared to be recruited selectively in absence of food to reduce the pumping rate.

4.3.2 Glutamate receptors drive the food context dependent pumping behaviours

Glutamate receptors were screened for their role in the modulation of the pumping behaviour. In addition to AVR-15, the GluCl receptor GLC-2 and the metabotropic receptor MGL-2 act to increase the pumping rate in response to food. However, their effect appeared less relative to AVR-15 as mutant for these receptors only showed a slight reduction in the pumping rate. *glc-2* is localised in the proximal bulb (pm4 muscle) at a localisation overlapping with M3 (Laughton *et al.*, 1997). It is therefore possible that M3 also acts on the pumping on food behaviour by releasing glutamate onto GLC-2. In the absence of food, neither GLC-2 nor MGL-2 are involved in the modulation of pumping. Furthermore, none of the receptors expressed in the pharyngeal muscle, AVR-15, GLC-1 and GLC-2 are involved in the pumping behaviour off food,

indicating that unlike in the “on” food context, glutamate is not directly acting onto the pharynx in absence of food. This is a surprising result as AVR-15 was shown to drive the inhibitory effect of the glutamate released by I2 neurons in response to light and hydrogen peroxide (Bhatla and Horvitz, 2015). However, the non-involvement of these receptors is reinforced by the ability of artificially activated glutamatergic neurons using optogenetics to reduce the pumping rate even in absence of glutamate transmission.

Interestingly, the mutant for the metabotropic receptor *mgl-1* has recently been shown to display an elevated pumping rate (~30 ppm relative to the 10 ppm displayed by N2) after 5 min of food deprivation but not after 95 min (Dillon *et al.*, 2015). In this chapter, *mgl-1* mutant had no effect after 15 to 45 min of food deprivation. One possible explanation could be that MGL-1 is only required at a very early phase of the off food pumping behaviour, i.e. the first 5 min or so. However, it is also possible that worms have not completely recovered from the inhibitory effect of the harsh touch, induced by the transfer of worms off food, after only 5 min. One explanation could be that MGL-1 plays a role in the inhibitory effects induced by harsh touch, or the recovery from it, and does not play a direct role in the reduction of the pumping rate in response to the absence of food.

The GluCl receptor AVR-14 was the only receptor found to act to reduce the pump rate off food. Mutation in *avr-14* indeed only affects the pumping rate in absence of food, *avr-14(ad1302)* exhibiting an elevated pumping rate when placed on a no food arena. One could therefore hypothesize that I2 released glutamate was acting through AVR-14 to reduce the pumping rate in absence of food. Interestingly, this study indicates previously undescribed *avr-14* expression on 6 pharyngeal neurons identified as I2, I5, M1, M2, M4 and NSM. A non-integrated line was used and therefore, this list is not exhaustive. Because of the technique itself, which involves dissecting the pharynx from the body of the worm, processes running anteriorly toward the lips were often cut and therefore it makes the identification of neurons with projections in this part of the pharynx more complex. Nonetheless, these findings reinforce the idea of I2 releasing glutamate onto an *avr-14*-expressing neuron to reduce the pumping rate. Rescue experiments would be required to determine which *avr-*

14-expressing neuron is responsible for driving the reduction of pumping off food. Since I2 only possesses synaptic connections with M1 and NSM (White *et al.*, 1986), it would be interesting to observe the effect of restoring *avr-14* activity specifically in these two neurons.

Importantly, AVR-14 activity in the absence of food appeared to only account for part of the glutamate dependent role on the pumping rate as *avr-14(ad1302)* mutant pumping rate, while elevated relative to wild-type, was lower than the constitutive pumping rate of *eat-4* mutants. This indicates that at least one other receptor is mediating the glutamate dependent effect on the pumping rate in the absence of food. Only 13 of the 19 known glutamate receptors have mutants available and were thus assessed here. It is therefore possible that one of the remaining receptors is mediating this effect. The iGluR GLR-8 would be a good candidate to assess given its expression in 11 pharyngeal neuron types (Brockie *et al.*, 2001a), however *glr-8* function remains unknown. Furthermore, although no *nmr-2* expression has been shown in the pharynx, *nmr-2* has been shown to play a role in the memory associated with NaCl avoidance following starvation conditioning (Kano *et al.*, 2008) and would therefore be an interesting candidate to investigate.

4.3.3 Wider roles of I2 and downstream mediators

As AVR-14 can only account for part of the glutamate dependent role on the pumping rate off food, it also cannot account for the whole effect mediated by I2. There are two possible explanations, firstly, I2 is releasing glutamate acting on at least two distinct glutamate receptors to mediate its effect on the pump rate off food, or secondly, I2 also acts on the pharynx through a glutamate-independent system. Interestingly, the results depicted in this study using optogenetics showed I2 was able to reduce the pumping rate even in absence of glutamate transmission. Furthermore, restoration of glutamate transmission from I2 only in a glutamate deficient mutant failed to completely rescue the aberrant pumping behaviour displayed by the *eat-4* mutant. Together, these two results suggest I2, in response to food removal, reduces

the pumping rate via two parallel pathways, one involving release of glutamate potentially acting through AVR-14, and one being glutamate-independent.

The glutamate-independent pathway could be driven by neurohormonal transmission via release of neuropeptides. This hypothesis is further investigated in Chapter 5. Alternatively, the glutamate-independent pathway could be mediated by direct communication through gap junctions. Interestingly, two innexins, the main structural component of the nematode's gap junction (Phelan *et al.*, 1998), were shown to have a role in the reduction of the pumping rate off food, but not on food. This indicates that gap junction communication plays a part in the reduction of the pumping rate off food. However, it remains to be determined if this gap junction-mediated effect acts in parallel or is part of the glutamate pumping dependence off food. *unc-7* is widely expressed within the somatic nervous system but can also be found in one pharyngeal neuron, I1, where UNC-7 allows the gap junction between RIP and I1 (Starich *et al.*, 2009). It is, however, unlikely that this specific gap junction accounts for the role of UNC-7 on the pumping off food behaviour as RIP ablation has no effect on this behaviour (see **Chapter 3**). Interestingly, UNC-7 is known to regulate the tail tap reduction in pumping behaviour (Lee *et al.*, 1999). *unc-9* is also mainly expressed outside the pharynx but can be found in the pharyngeal neurons I1, I6, M5 and NSM (Altun *et al.*, 2009) and could therefore act in the intrinsic microcircuit described here. There is no known gap junction involving NSM, however, the expression of at least one innexin in these neurons indicates otherwise. NSM thus expresses both *avr-14* and *unc-9*, therefore suggesting a hypothetical model in which I2 releases glutamate onto NSM which activates the AVR-14 receptor which in turn leads to the reduction of pumping rate via the action of an UNC-9-based gap junction.

4.4 Conclusion

This chapter describes investigation of the glutamate-dependence of pumping and defines distinct circuits regulating the pumping behaviour on and off food. Pharyngeal cellular and molecular determinants, selectively recruited depending on the food context, have been determined for both glutamate-dependent regulation of pumping as summarised by the model

illustrated in **Figure 50**. Although significant they also make clear that other modulators may contribute to the glutamate-dependence or extend regulation to parallel pathways that act against constitutive pumping off food or impart inhibitory tone.

In the presence of food, M3 activity allows sustained high pumping rate by releasing glutamate directly onto the pharynx muscle via the glutamate receptor AVR-15, and potentially via GLC-2. The metabotropic receptor MGL-2 also has a small part in this modulation of pumping.

I2 is a key component of the pharyngeal microcircuit controlling the pumping behaviour in absence of food. Interestingly, I2 is acting to reduce the pumping rate via two pathways, one involving the release of glutamate, and in parallel a glutamate-independent pathway through gap junction and/or neurohormonal signalling. Findings displayed in this chapter highlight that unlike what happens on food, released glutamate in response to food removal does not act directly on the pharyngeal muscle. The glutamate-gated chloride channel AVR-14 was shown here to mediate part of the glutamate-dependent reduction of pumping off food and its expression in the pharyngeal nervous system was determined for the first time. As I2 and AVR-14 cannot account for the entire pumping reduction mediated by glutamate off food, it is likely that another glutamatergic neuron together with another glutamate receptor, acts to reduce the pumping rate but remain to be revealed.

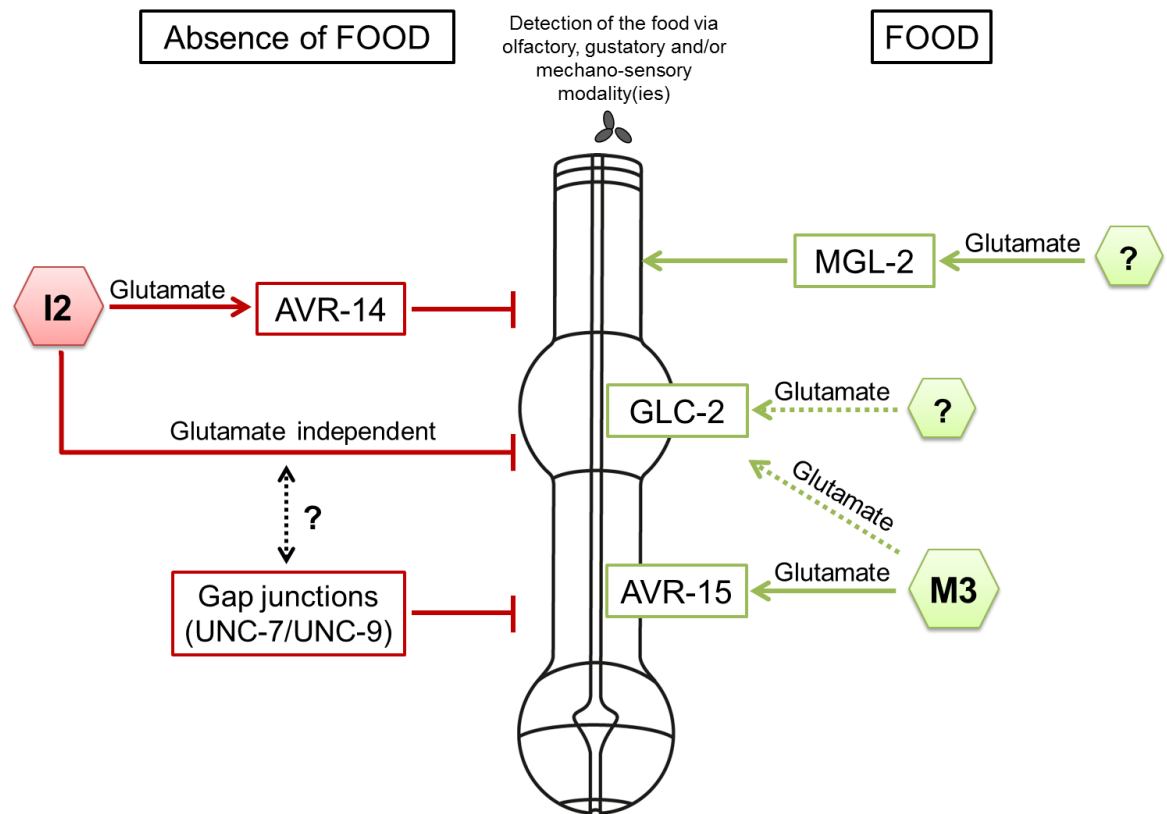


Figure 50: Schematic representation of the context dependent glutamate dependence of the pumping behaviour.

In response to food, M3 release glutamate directly onto the pharynx to increase the pumping rate through the AVR-15 receptor. To a lesser extent, the glutamate-gated chloride channel GLC-2, expressed onto the pharyngeal muscle, mediates the high pumping rate on food, although it is not clear whether it is in response to glutamate released from M3 or another neuron. Finally, glutamate signalling acts via MGL-2 in the control of the pumping behaviour on food, but the effects appear marginal relative to the role of AVR-15.

In absence of food, I2 neurons act as a major determinant of the reduction of the pumping rate. I2 impose this inhibitory tone both via glutamate release acting on a downstream neuron through AVR-14 receptor, and a glutamate-independent pathway. Gap junctions mediate the reduction of pumping off food, although it is not clear whether it is part of the glutamate-independent pathway from I2 or acting in parallel of I2 signalling.

Red lines indicate signalling reducing the pumping rate while conversely, green lines indicate stimulation of the pump rate. Dotted line represents putative connection

Chapter 5: Neuropeptide modulation of context-dependent pharyngeal behaviour

5.1 Introduction

egl-3 and *unc-31* mutants analysis from chapter 3 indicates a crucial role for neuropeptides in the modulation of the pumping rate. The opposing pumping phenotypes displayed by these mutants showed the ability for neuropeptides not only to reduce the pumping rate in absence of food, but also to exert a stimulatory effect onto the pharynx to maintain a basal pumping rate. Whether it is possible that each of these phenotypes account for the defect of a single neuropeptide, the complete opposite pumping phenotypes displayed by *egl-3* and *unc-31* mutants are likely to represent the sum effect of affected neuropeptides, and the identification of individual peptides playing a role in the regulation of the pumping rate off food has been conducted in this chapter. There are 250 neuropeptides encoded by around 115 genes in *C. elegans* (Li, 2005; Holden-Dye and Walker, 2013), hence the necessity to develop different strategies to narrow down the number of candidates. Three main approaches have been chosen in this purpose.

Husson and colleagues published the peptide profiles of mutants for all the *kpc* members (see **section 1.1.2.4**), however, these profiles were limited by the technique itself as among the aforementioned ~250 peptides present in the worm, only 78, encoded by 35 peptide genes, were detectable, and this completely excludes the insulin-like peptides (INS) (Husson *et al.*, 2006). The less potent *egl-3/kpc-2* mutations, *n588*, only contained 13 detectable neuropeptides (none in *gk328* and only 1 in *ok979*), leaving 65 peptides that potentially could account for *egl-3* pumping phenotype, and this without taking into account neuropeptides which were not detected by this method. The first approach used here to reduce the number of peptide candidates that modulate the worm's pumping rate was to take advantage of these published neuropeptide profiles, firstly by assessing the *kpc* mutants' phenotypes and then by correlating it to their neuropeptide profile. The logic behind this approach was that mutants displaying a reduced pumping rate were lacking

stimulatory neuropeptides, while these peptides should be present in mutants with a wild-type phenotype. In practice, if one of the *kpc* mutants would phenocopy *egl-3/kpc-2* pumping phenotype, then the peptides responsible for this should be missing in both strains while conversely be found in *kpc* mutants displaying a wild-type pumping behaviour. Interestingly, *kpc* mutants, other than *egl-3/kpc-2*, showed a less severe deficit in normally processed neuropeptides and their analysis as described should allow to refine the number of potential candidates in the control of the pumping phenotype.

The second approach consisted in screening mutants for deorphanized neuropeptide receptors, meaning receptors for which one or several ligands are known. The idea here was that if a receptor is involved in the control of the worm's pumping behaviour, then at least one of its ligand is too. There are many categories of peptides GPCR receptors (see **section 1.3.3.1**), but the most studied is the neuropeptide Y (NPY)/RFamide-like receptor (NPR) family, a subdivision of the Rhodopsin family. For this reason and also because of the known role of neuropeptide Y in the regulation of feeding in mammals (Gehlert, 1999; Kaga *et al.*, 2001), available mutants for 12 of these NPR receptors were chosen for this approach.

Finally, the last approach used in this chapter was based on two previously published studies of the effects of individual NLP and FLP neuropeptides added exogenously to cut head preparations (Papaioannou *et al.*, 2005; Papaioannou *et al.*, 2008a). The aim of this last approach was to complement the pool of candidates extracted from the two previous approaches by selecting genes for which encoded peptides induced stimulation of the pumping rate when added to isolated pharynx preparations.

Overall these 3 approaches (**Figure 51**) should considerably narrow down the numbers of neuropeptide genes potentially implicated in the control of the worm's pumping behaviour and allow further investigation of this more limited pool of candidates.

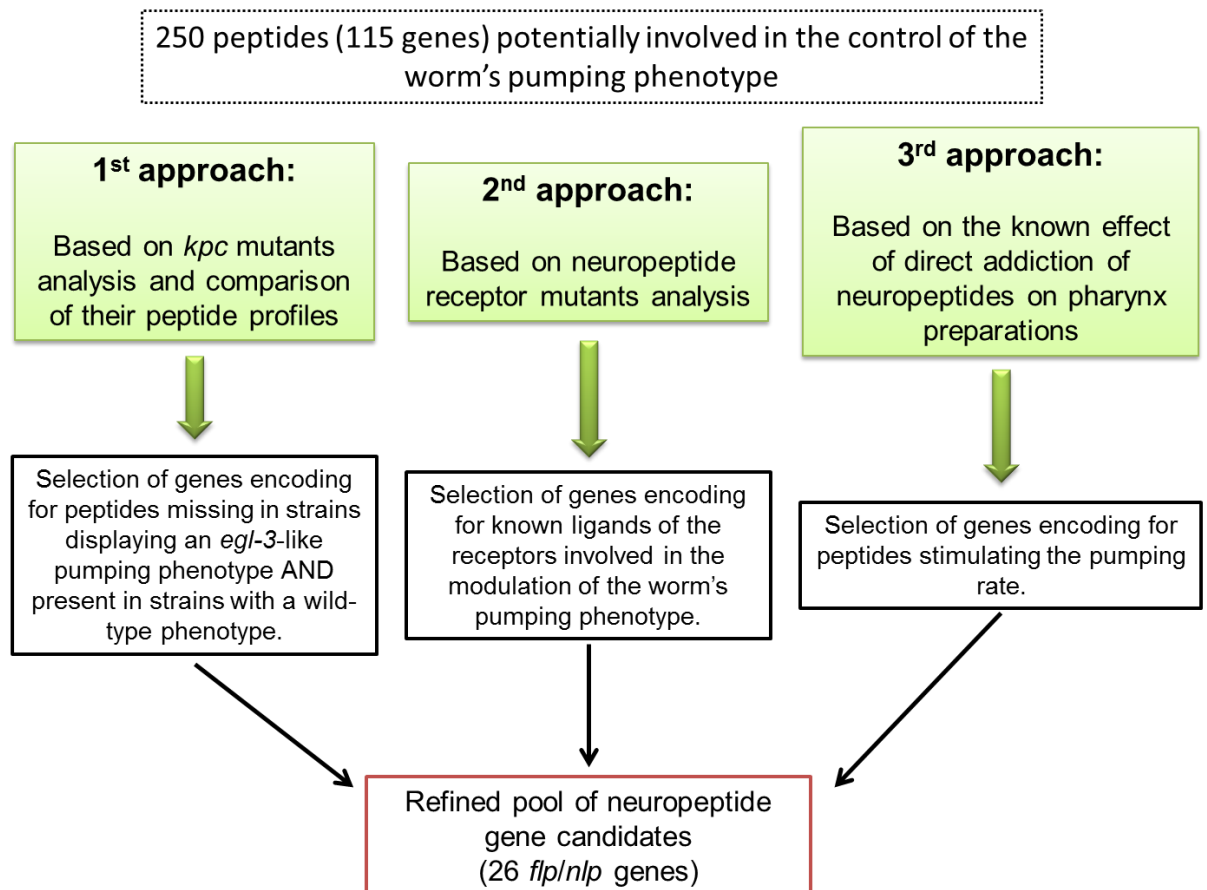


Figure 51: Schematic representation of the strategy used to narrow down the neuropeptide candidates that can modulate the worm's pumping phenotype.

5.2 Results

5.2.1 Approach 1: the proprotein (*kpc*) convertase family

The first approach performed to narrow down neuropeptide candidates in the control of the worm's pumping behaviour was based on the published

neuropeptide profiles, obtained with a mass spectrometry based technique, of the *kex2*/subtilisin-like proprotein convertases (*kpc*) family (Husson *et al.*, 2006). As described above, the *kpc* family possesses four genes: *kpc-1*; *egl-3/kpc-2*; *aex-5/kpc-3* and *bli-4/kpc-4*. Protracted pumping assays in absence of food have been performed and the mutants' pumping phenotypes were then compared with their peptide profiles to extrapolate neuropeptide with a potential role in the modulation of pumping rate.

While *egl-3/kpc-2* acts to increase the pumping rate in the presence of food, none of the other *kpc* appeared to be involved in the control of the pumping phenotype in the presence of food, as the mutants pumped similarly to N2 (**Figure 52**). In absence of food, *aex-5(sa23)/kpc-3* was the only *kpc* mutant displaying an *egl-3*-like phenotype i.e. a pumping rate significantly lower than wild type ($p < 0.001$) during both early and late phase, and this despite the relatively low pumping rate of paired N2 during this experiment.

Conversely, *bli-4(e937)/kpc-4* mutant pumping in absence of food showed a slightly higher rate than N2 during the early phase ($p < 0.001$) but a similar rate in the late phase ($p = 0.09$) (**Figure 52**). Finally, the observation of *kpc-1(gk-8)* pumping phenotype did not reveal any significant difference compare to N2 ($p = 0.243$ and $p = 0.822$ for the early and late phase respectively) (**Figure 52**). However, it is important to notice that *kpc-1(gk-8)* mutant displayed an uncoordinated phenotype in the head region making the counting of pharyngeal pumps prone to imprecision. This caveat led me to ignore *kpc-1(gk-8)* peptide profile in the selection of individual peptide candidates.

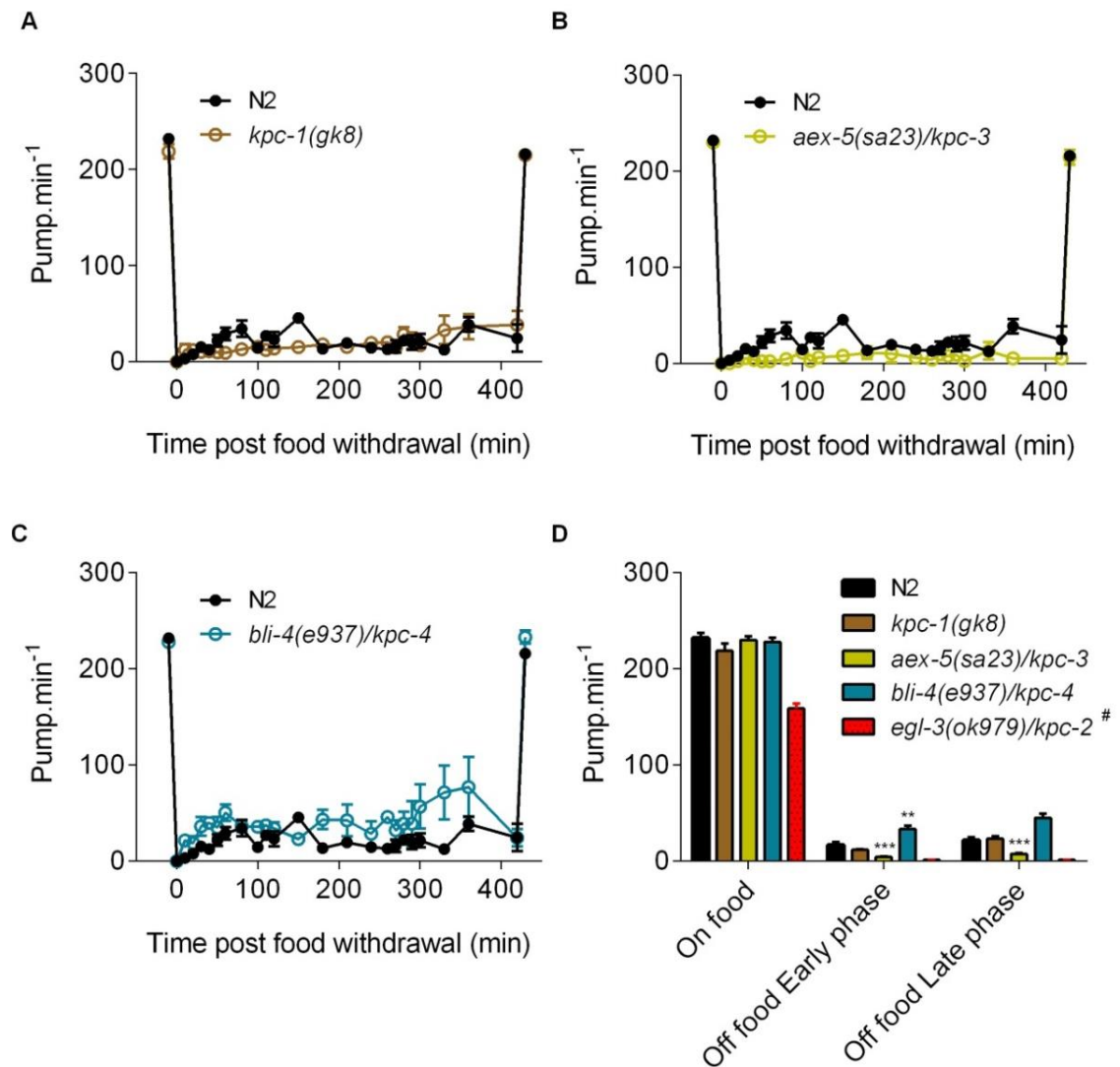


Figure 52: Pumping off food phenotype of the *kpc* family members.

A. *kpc-1(gk8)* possessed similar early ($p = 0.243$; $n = 6$ N2 and 8 *kpc-1(gk8)*) and late phases ($p = 0.822$; $n = 6$ N2 and 7 *kpc-1(gk8)*) to N2. **B.** *kpc-3(Sa23)* possessed a significantly reduced pumping rate during both early phase (-13 ± 5 ppm; $p = 0.001$; $n = 6$ N2 and 7 *aex-5(sa23)*) and erratic phase (-14 ± 9 ppm; $p = 0.006$; $n = 6$ N2 and 5 *aex-5(sa23)*). **C.** *kpc-4(e937)* possessed a significantly increased pumping rate during the early phase (17 ± 9 ppm; $p = 0.006$; $n = 6$ N2 and 6 *bli-4(e937)*) but not the late phase ($p = 0.09$; $n = 6$ N2 and 4 *bli-4(e937)*).

D. *kpc-1(gk8)* ($p = 0.669$; $n = 8$), *aex-5/kpc-3(sa23)* ($p = 0.99$; $n = 8$) and *bli-4/kpc-4(e937)* ($p = 0.99$; $n = 7$) mutants showed a similar pumping rate in the presence of food compared to N2 ($n = 7$).

Histogram representing the average pumping rate on food and off food during the early and late phases of figures A, B and C.

Chapter 5

#*egl-3(ok979)* results (data from **Figure 31**) were added for visual comparison.

* ($p < 0.05$), ** ($p < 0.01$) and *** ($p < 0.001$) compared to paired N2.

To summarise, this *kpc*-family mutant analysis has shown that at least one *aex-5/kpc-3* processed peptide, similarly to *egl-3*-dependent peptides, acts to stimulate the pumping rate in absence of food (but not when food is present). Conversely, *bli-4/kpc-4*-dependent peptides only induce a weak pumping reduction off food during the early phase but not during the late phase nor in the presence of food.

According to these results, mutations in *egl-3* and *aex-5/kpc-3* lead to similar consequences on the pumping phenotype off food, and more precisely to the active maintenance of the basal pumping rate. If we assume that the shared phenotype derives from shared determinants, one would define candidates based on their common absence from both backgrounds. Conversely, and to provide additional iterative power to this approach, these neuropeptides should be found in *bli-4(e937)/kpc-4*'s peptide profile as this strain maintains a basal pumping rate off food. Using this method of selection, peptides encoded by *nlp-8*, *nlp-16*, *flp-3*, *flp-14*, *flp-18* and *flp-27* appeared to be the most interesting candidates (Husson *et al.*, 2006). The example of *flp-18* encoded peptides is shown in **Figure 53**. It will therefore be interesting to assess the role of those neuropeptides genes in the regulation of the worm pumping behaviour.

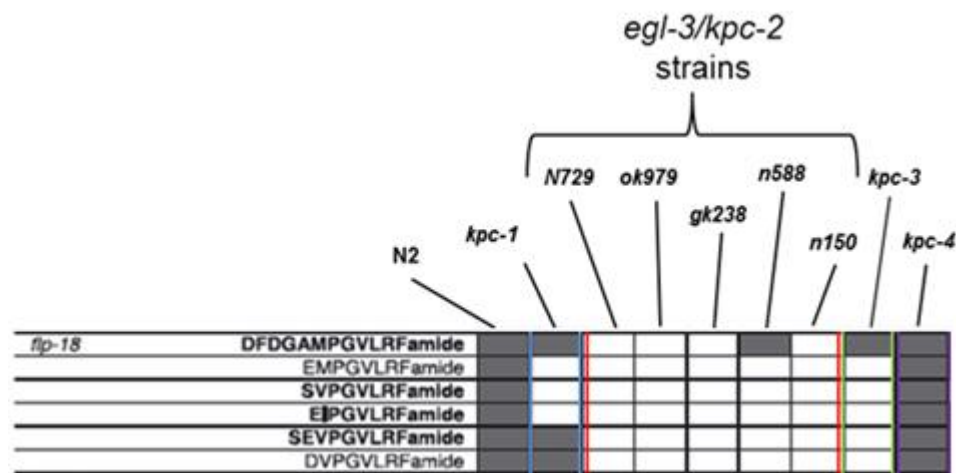


Figure 53: *flp-18* encoded peptides profile of the *kpc*-family mutants.

Modified from Husson et al. 2006

Most of the detected *flp-18* encoded peptides are found missing in the different *egl-3* strains and in the *kpc-3* mutant which displayed an *egl-3*-like PoffF phenotype.

In the contrary, *kpc-4* mutant, which is able to pump in absence of food, expresses all of these peptides.

5.2.2 Approach 2: neuropeptide receptor mutants screen

The second approach set to identify individual neuropeptides modulating the worm's pumping behaviour was undertaken by screening twelve neuropeptide-Y-like receptor (*npr*) mutants for *egl-3*- and *unc-31*-like on and off food feeding behaviours to subsequently select their known ligands as candidates for a role in the modulation of the worm's feeding rate.

The pumping rate on food of L4+1 worms was assessed first directly from the plates they have been grown on (Figure 54). Two *egl-3* strains were used as positive paired control during the assay, *egl-3(ok979)* and *egl-3(n150)*, and pumped at a significantly lower rate on food than N2 with *egl-3(ok979)* null mutant showing the strongest reduction (as previously noted in Chapter 3). Among the receptor mutants, four out of twelve displayed a significantly

reduced pumping rate on food, namely *npr-3(tm1583)*, *npr-4(tm1782)*, *npr-1(ky13)* and *npr-5(ok1583)*. However, only *npr-5(ok1583)* pumped at a similar level to *egl-3(ok979)* ($p = 0.99$).

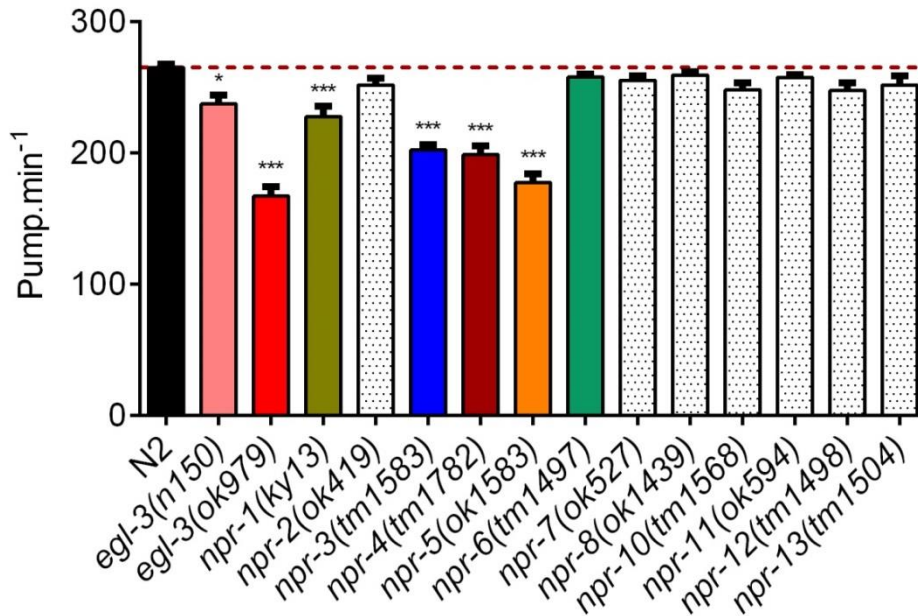


Figure 54: Screen of neuropeptide receptor mutants for their pumping on food phenotype.

L4+1 staged worms were assessed directly on the plate they were cultured on. Both *egl-3* mutant strains, *n150* (-28 ± 7 ppm; $p = 0.018$, $n = 15$) and *ok979* (-98 ± 8 ppm; $p < 0.001$, $n = 10$) displayed a significantly reduced pumping rate on food compared to N2 ($n = 15$).

npr-1(ky13) (-37 ± 7 ppm; $p < 0.001$, $n = 15$), *npr-3(tm1583)* (-63 ± 7 ppm; $p < 0.001$, $n = 15$), *npr-4(tm1782)* (-66 ± 7 ppm; $p < 0.001$, $n = 15$) and *npr-5(ok1583)* (-88 ± 8 ppm; $p < 0.001$, $n = 10$) also showed a reduced pumping rate on food relative to N2. Of these mutants, the reduced pumping was elevated relative to *egl-3(ok979)* except for *npr-5(ok1583)* which showed no significant difference to *egl-3(ok979)* ($p = 0.99$).

npr-2(ok419), *npr-6(tm1497)*, *npr-7(ok527)*, *npr-8(ok1439)*, *npr-10(tm1568)*, *npr-11(ok594)*, *npr-12(tm1498)* and *npr-13(tm1504)* pumped at a similar rate to N2 ($p > 0.99$; $n = 15$ for all).

* indicates a significant difference with N2 with $p < 0.05$

*** corresponds to $p < 0.001$.

The pumping off food phenotype was then assessed. The aim of this specific assay was to test as many worms in the shortest amount of time possible, then to confirm any potential pumping behaviour by conducting further assays. In this purpose, 5 worms per mutant strains were picked onto 90 mm non-seeded plates and the worms pumping rate on each plate was assessed between 90 and 150 min after food removal when the difference between N2 and *egl-3* mutants is clearly visible and in order to avoid as much as possible any erratic pumping behaviour (see **chapter 3**). Four assays have been performed in total (**Figure 55**). Once again, *egl-3(ok979)* and *egl-3(n150)* were used as paired positive controls and showed as expected a significantly lower pumping rate compare to N2. Only one mutant, *i.e. npr-6(1497)*, showed a significant difference to N2 with a slightly more elevated pumping rate (~60 ppm), but the increase was marginal compared to what is observed in an *unc-31* mutant. No mutants were observed to significantly pump at a lower rate than N2, however, 4 *npr* mutants were found to display no significant difference with *egl-3(ok979)* mutant's pumping rate, *viz, npr-1(ky13), npr-3(tm1583), npr-4(tm1782)* and *npr-5(ok1583)*, suggesting a potential role for those receptors in the control of the maintenance of a basal pumping rate in absence of food.

It is likely that the non-synchronisation of the period of food deprivation between the different assays has led to an increased variability in pumping rate, as the pump rate increases over time during the early phase, and this might explain why none of those 4 mutants appeared significantly different to N2. Further investigation was therefore required to confirm the phenotype of these 4 aforementioned mutants.

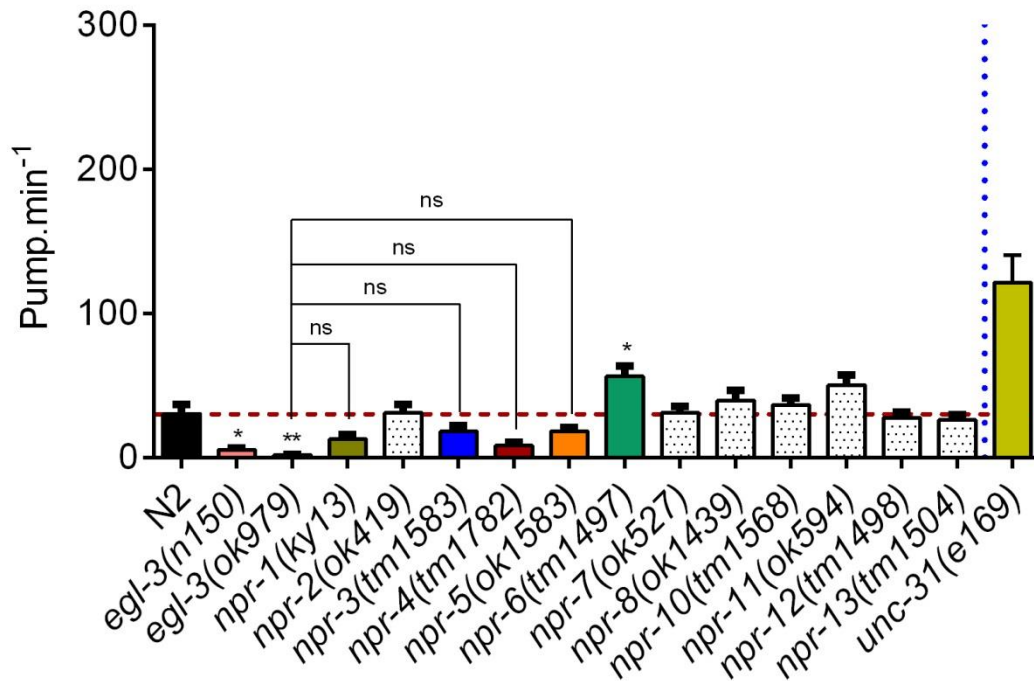


Figure 55: Screen of neuropeptide receptors mutants for their pumping off food phenotype.

Each histogram represents the average of 4 distinct assays. 5 L4+1 worms were transferred per 9cm non seeded plate and the pumping rate has been assessed between 90 and 150 min following removal of food. *unc-31(e169)* was not assessed in parallel (data were taken from **Figure 33** after 120min off food) but was added to the figure for better visual comparison.

Both *egl-3* strains displayed a marked reduction of their pumping rate in absence of food (-25 ± 6 ppm; $p = 0.011$; $n = 29$ and -27 ± 7 ppm; $p = 0.004$; $n = 22$ for *n150* and *ok979* respectively) compared to the paired N2 control ($n = 25$). *npr-6(tm1497)* showed a faster pumping rate than N2 (26 ± 7 ppm; $p = 0.019$; $N = 22$).

None of the other receptor mutants assessed showed a significantly different pumping rate off food compared to N2 ($p > 0.99$ for all except for *npr-4(tm1782)* $p = 0.098$ and *npr-11(ok594)* $p = 0.309$).

npr-1(ky13) ($p = 0.99$; $n = 20$), *npr-3(tm1583)* ($p = 0.99$; $n = 19$), *npr-4(tm1782)* ($p = 0.99$; $n = 25$) and *npr-5(ok1583)* ($p = 0.99$; $n = 17$) were not significantly different to *egl-3(ok979)*.

*: indicates a significant difference with N2 ($p < 0.05$).

** $p < 0.01$. ns: indicates no significant difference with *egl-3(ok979)*.

Protracted assays were then performed to confirm the *egl-3*-like phenotype observed in *npr-3(tm1583)*, *npr-4(tm1782)* and *npr-5(ok1583)* mutants (**Figure 56**). As predicted from the preliminary screen, the three neuropeptide receptor mutants displayed a significantly lower pumping rate in absence of food in both early and erratic phases. *npr-4(tm1782)* showed the most striking phenotype with almost no pumping motion observed, while *npr-5(ok1583)* mutant showed a less-marked, but significant, pumping off food during the early phase. As reported above (**Figure 54**) the three *npr* mutants pumped markedly lower than N2 in the presence of food, displaying a pumping rate of around 165 ppm (**Figure 56**), similarly to what is observed in an *egl-3(ok979)* mutant.

Overall, these results indicate that neuropeptide receptors NPR-3, NPR-4 and NPR-5 play a role in the control of the worm feeding behaviour by promoting stimulation of the pumping rate independently of the food context, and this confirms a neurohormonal regulation of the maintenance of a basal pumping rate in absence of food.

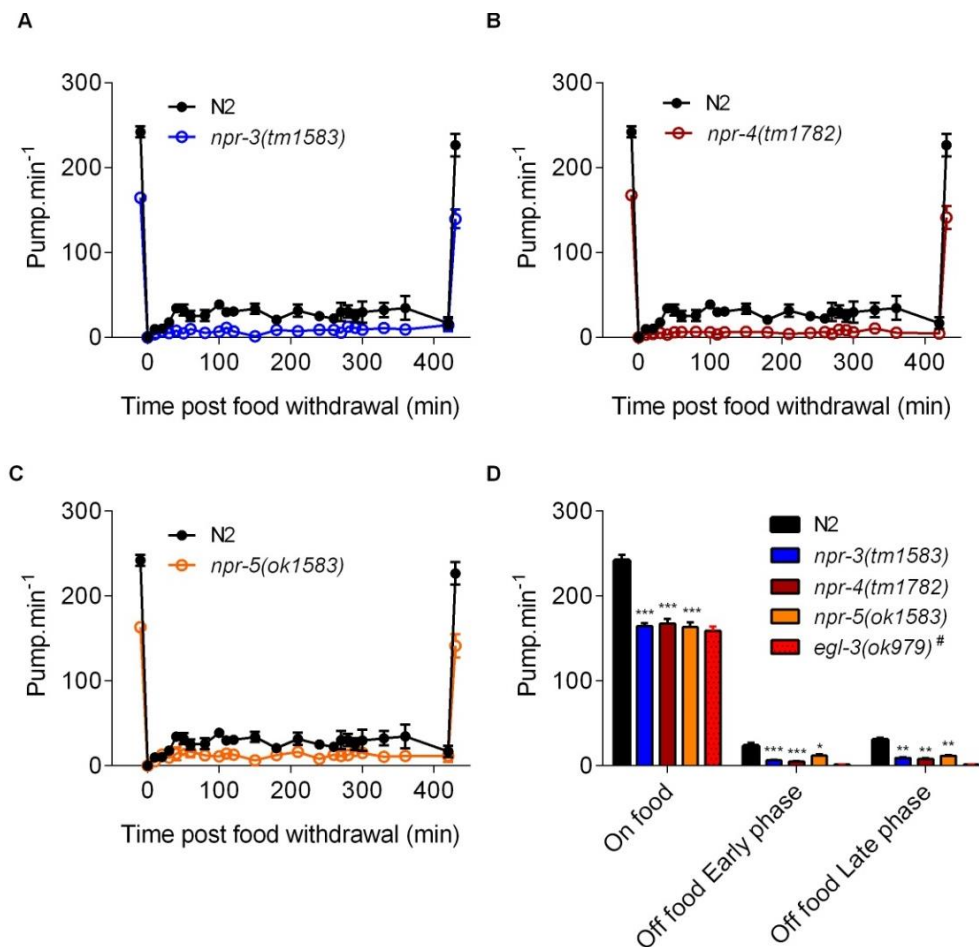


Figure 56: Pumping off food phenotype of *npr-3*, *npr-4* and *npr-5* mutants.

A. *npr-3(tm1583)* mutant displayed a reduced pumping rate on food (-77 ± 8 ppm; $p < 0.001$; $n = 7$ *npr-3(tm1583)* and N2) and in absence of food during both early (-17 ± 5 ppm; $p < 0.001$; $n = 7$ *npr-3(tm1583)* and $n = 6$ N2) and late phase (-22 ± 9 ppm; $p = 0.002$; $n = 7$ *npr-3(tm1583)* and $n = 5$ N2). **B.** *npr-4(tm1782)* on food pumped at a slower rate (-74 ± 8 ppm; $p < 0.001$; $n = 7$) than N2 ($n = 7$). When *npr-4(tm1782)* mutants were removed from food, they displayed a significantly reduced pumping rate both during early (-19 ± 5 ppm; $p < 0.001$ $n = 6$ N2 and $n = 7$ *npr-4*) and late phase (-23 ± 11 ppm; $p = 0.011$; $n = 5$ N2 and $n = 4$ *npr-4*) compare to N2.

C. In the presence of food, *npr-5(ok1583)* pumped at a lower rate than N2 (-79 ± 8 ppm; $p < 0.001$; $n = 7$ *npr-4* and N2). *npr-5(ok1583)* showed a reduced pumping rate both during the early (-12 ± 7 ppm; $p = 0.021$; $n = 6$ N2 and $n = 7$ *npr-5*) and late phase (-19 ± 10 ppm; $p = 0.006$; $n = 5$ N2 and $n = 6$ *npr-5*) compare to its paired N2. **D.** Histogram representing the average pumping rate on food and off food during the early and late phases of figures A, B and C.

#*egl-3(ok979)* results (data from **Figure 31**) were added for visual comparison.

* ($p < 0.05$) ** ($p < 0.01$) and *** ($p < 0.001$) compared to paired N2.

npr-1(ky13) mutant and the not previously screened *npr-9(tm1652)* were assessed for the shorter time course of 90 min post food removal, however, unlike the preliminary screen described in **Figure 55**, the food deprivation periods have been strictly timed. Conversely to what was observed for *npr-3(tm1583)*, *npr-4(tm1782)* and *npr-5(ok1583)* mutants, *npr-1(ky13)* did not show a different pumping phenotype to N2 as could have been expected from the initial screen (**Figure 57**). Similarly, the mutant strain *npr-9(tm1652)* showed no significant differences of pumping rate in absence of food with the paired control N2 and with *npr-1(ky13)*. These results indicate that these two neuropeptide receptors do not play a role in the regulation of the pumping rate in the absence of food.

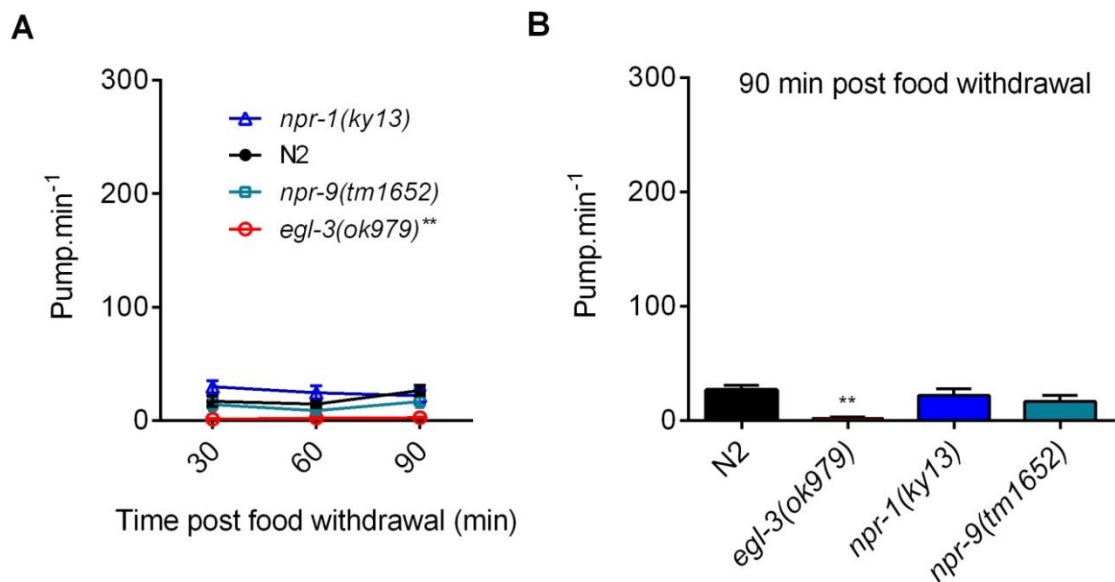


Figure 57: *npr-1(ky13)* and *npr-9(1562)* mutation did not affect the PoffF phenotype.

A. Pumping rate has been assessed 30 min, 60 min and 90 min following the removal of food as previously described. *egl-3(ok979)* displayed a marked

reduction of its pumping rate in absence of food (17 ± 5 ppm; $p = 0.005$; $n = 7$) compared to the N2 paired control ($n = 9$). Conversely, neither *npr-1(ky13)* ($p = 0.99$; $n = 8$) nor *npr-9(1562)* ($p = 0.99$; $n = 7$) showed any significant differences with N2.

B. Histogram representation of the 90 min time point from **A.**

Overall, this receptor screen revealed that NPR-3, NPR-4 and NPR-5 play a role in the EGL-3-dependent modulation of the basal slow pumping behaviour observed in absence of food. Therefore, known ligands for these receptors potentially play a role in this same phenotype and have been selected as candidates for further investigation. Briefly, *flp-15* encoded peptides are the only ones known to bind NPR-3 (Kubiak *et al.*, 2003) while *flp-18*-encoded peptides share high affinity binding with NPR-4 and NPR-5 (Lowery *et al.*, 2003; Cohen *et al.*, 2009). NPR-4 also possesses a high affinity for *flp-4*-encoded peptides and NPR-5 for *flp-21s*. Interestingly, *flp-3*, *flp-14* and *flp-18* peptides, encoding for known ligands to NPR-4 and NPR-5, have also been selected as candidates during the first approach making use of the *kpc* family mutants' peptide profiles showing consistency between the two strategies.

Conversely, NPR-6 appeared to modulate part of the pumping reduction observed when food is removed and therefore known ligands for this receptor could also be involved in part of the pumping off food modulation. However, *npr-6(tm1497)* pumping phenotype appeared quite marginal in the initial screen and furthermore, its phenotype has not been confirmed by further investigation. Nonetheless, it is interesting to note that NPR-6 known ligands, *flp-18* and *flp-21* encoded neuropeptides, are also ligands of NPR-4 and NPR-5 (but also of NPR-1).

A summary of these receptors, their known ligands, expression patterns and known roles can be found in **Table 3**.

	Ligands (gene encoding peptide)		Expression pattern	Known role	References	Role on the pumping rate:	
	EC50 < 1.5µM	EC50 > 1.5µM				On food	Off food
NPR-1	<i>flp-18</i> <i>flp-21</i>		AQR, ASE, ASG, ASH, URX, IL2L/R, OLQ, AUA, SAAD, RMG, SMBD, M3 , VD, DD, PQR, PHA, PHB, RIV, RIG, SDQ muscle in the terminal bulb of the pharynx , excretory duct cell and excretory canal	Feeding behavior; aerotaxis; thermal avoidance; ethanol tolerance; innate immunity	de Bono and Bargmann, 1998 Rogers <i>et al.</i> 2003 Gray <i>et al.</i> 2004 Milward <i>et al.</i> 2011	Stimulation	none
NPR-3	<i>flp-15</i>		ventral nerve cord both excitatory and inhibitory motoneurons	Locomotion	Keating <i>et al.</i> 2003 Kubiak <i>et al.</i> 2003	Stimulation	Stimulation
NPR-4	<i>flp-4</i> <i>flp-18</i>	<i>flp-1</i> <i>flp-3</i> (> 10µM) <i>flp-11</i> (> 10µM) <i>flp-15</i> (> 10µM) <i>flp-14</i> (> 10µM)	PQR, BQG, AVA, RIG, BDU coelomocytes, part of the intestine and rectal gland cells	Fat storage; olfaction; foraging; reproduction	Lowery <i>et al.</i> 2003 Cohen <i>et al.</i> 2009 Peymen <i>et al.</i> 2014	Stimulation	Stimulation
NPR-5	<i>flp-18</i> <i>flp-21</i>	<i>flp-1</i> <i>flp-3</i>	ADF, ASE, ASG, ASI, ASJ, ASK, AWA, AWB AIA, AUA, IL2 PHA, PHB head, neck and body muscles	Fat storage; dauer formation	Lowery <i>et al.</i> 2003 Cohen <i>et al.</i> 2009 Kubiak <i>et al.</i> 2008	Stimulation	Stimulation
NPR-6	<i>flp-18</i> <i>flp-21</i>		Head and tail unidentified neurons	Reproduction	Keating <i>et al.</i> 2003 Lowery <i>et al.</i> 2003	none	Reduction

Table 3: Expression pattern and known ligands of neuropeptides Y-like receptors involved in the regulation of the pumping phenotype.

5.2.3 Approach 3: selection of peptides inducing stimulation when exogenously added

The last approach used to refine the number of potential peptide candidates involved in the modulation of the pumping behaviour was to make direct use of two previously published studies investigating the effect of exogenously added neuropeptides on the pumping rate of cut head preparations (Papaioannou *et al.*, 2005; Papaioannou *et al.*, 2008a). A table summarising their findings can be found in **Table 4**. Briefly, the peptides inducing the most potent pumping stimulation were FLP-8, FLP-17A and FLP-17B when added at a concentration of 100nM. To a lesser extent, NLP-10A, FLP-2A, FLP4A, FLP-5A, FLP-6, FLP-14A and FLP-22, when added at 1µM,

Chapter 5

induced a stimulation of pumping while only a weak stimulation was observed with the addition of NLP-1A, NLP-2A and NLP-3. The genes encoding for these peptides were then added to the pool of candidates for further investigation.

Gene	Expression in the pharynx	Peptide tested (1)	Presence in <i>egl-3</i> mutants (2-3)	Action on isolated pharynx (2-3)	Concentration
<i>nlp-1</i>	None	NLP-1A	No	Weak stimulation	1 μM
<i>nlp-2</i>	None	NLP-2A	?	Variable stimulation	1 μM
		NLP-2B	?	No effect	1 μM
<i>nlp-3</i>	I1, I2, I3, I4, M1, M3, NSM, I6, M2	NLP-3	?	Weak stimulation	1 μM
<i>nlp-8</i>	I2, processes in pharynx	NLP-8	No	Weak reduction	1 μM
<i>nlp-10</i>	pharyngeal neurons	NLP-10A	?	Stimulation	1 μM
<i>flp-1</i>	M5	FLP-1A1 (PF1)	In <i>n588</i>	Reduction	1 μM
		FLP-1A2 (PF2)	In <i>n588</i>	Reduction	1 μM
<i>flp-2</i>	I5, MC, M4	FLP-2A	No	Stimulation	1 μM
<i>flp-3</i>	None	FLP-3A	No	Reduction	1 μM
<i>flp-4</i>	I5, I6, NSM	FLP-4A	?	Stimulation	1 μM
<i>flp-5</i>	(I2), I4, M4, pm	FLP-5A	?	Stimulation	1 μM
<i>flp-6</i>	I1, I4	FLP-6 (AF8)	?	Stimulation	1 μM
<i>flp-7</i>	None	FLP-7A	No	No effect	1 μM
<i>flp-8</i>	None	FLP-8 (AF1)	?	Potent stimulation	100nM
<i>flp-9</i>	Not determined	FLP-9A	No	Reduction	1 μM
<i>flp-10</i>	None	FLP-10A	?	No effect	1 μM
<i>flp-11</i>	None	FLP-11A	No	Potent reduction	100nM
<i>flp-12</i>	None	FLP-12A	?	No effect	1 μM
<i>flp-13</i>	I5, M3, M5	FLP-13A	In <i>n588</i>	Potent reduction	100nM
<i>flp-14</i>	Not determined	FLP-14A	?	Stimulation	1 μM
		FLP-14B [†]	?	Reduction	1 μM
		FLP-14C	?	No effect	1 μM
<i>flp-15</i>	I2, pm	FLP-15A [†]	No	Reduction	1 μM
<i>flp-16</i>	Not determined	FLP-16A (AF15) [†]	?	Reduction	1 μM
<i>flp-17</i>	M5	FLP-17A	?	Potent stimulation	100nM
		FLP-17B	?	Potent stimulation	100nM
<i>flp-18</i>	M2, M3	FLP-18A [†]	No	Reduction	1 μM
<i>flp-19</i>	None	FLP-19A	No	Reduction	1 μM
<i>flp-20</i>	None	FLP-20	?	No effect	1 μM
<i>flp-21</i>	MC, M4, M2	FLP-21 (AF9) [†]	?	Reduction	1 μM
<i>flp-22</i>	None	FLP-22	No	Stimulation	1 μM
<i>flp-23</i>	Not determined	FLP-23	?	No effect	1 μM

Table 4: Summary of the effects of exogenously added neuropeptides on the pumping rate of isolated pharynxes.

Sources: (1) Husson et al. 2006; (2) Papaioannou et al. 2005 ; (3) Papaioannou et al. 2008.

'Stimulation' indicates mutants displayed a lower pumping rate than wild-type. Conversely, 'reduction' indicates mutants pumped faster than wild-type worms. Stimulatory effects were recorded in absence of 5-HT, while reduction was observed in presence of 5-HT, except for FLP-14B, FLP-15A, FLP-16A, FLP-18A, and FLP-21 where a rate reduction has only been observed without 5-HT, when pumping frequency was low (marked with on the '†' table).

5.2.4 Individual candidate neuropeptides appear to have opposite roles on the pumping behaviour

To further investigate the role in the worm's pumping behaviour of the selected candidate neuropeptide genes isolated from the three strategies described above, available mutants for these genes have been obtained and their pumping phenotypes assessed. The Venn diagram represented in **Figure 58** shows the different candidates selected using each approach and the overlap between these approaches. From the 115 neuropeptide genes, 26 were selected in total. Four of them were commonly isolated by two approaches; *nlp-1*, *flp-3*, *flp-4* and *flp-18*, while only one was isolated from the three approaches together; *flp-14*. The selection of candidates to further assess was based on their interest, i.e. overlap in different approaches, but mainly by the availability of mutants for these neuropeptide genes, there is for instance no mutant available for *flp-4* and *flp-14*. With this caveat, a first batch of mutants, containing *flp-1*, *flp-3*, *flp-15*, *flp-18* and *flp-21*, has been tested.

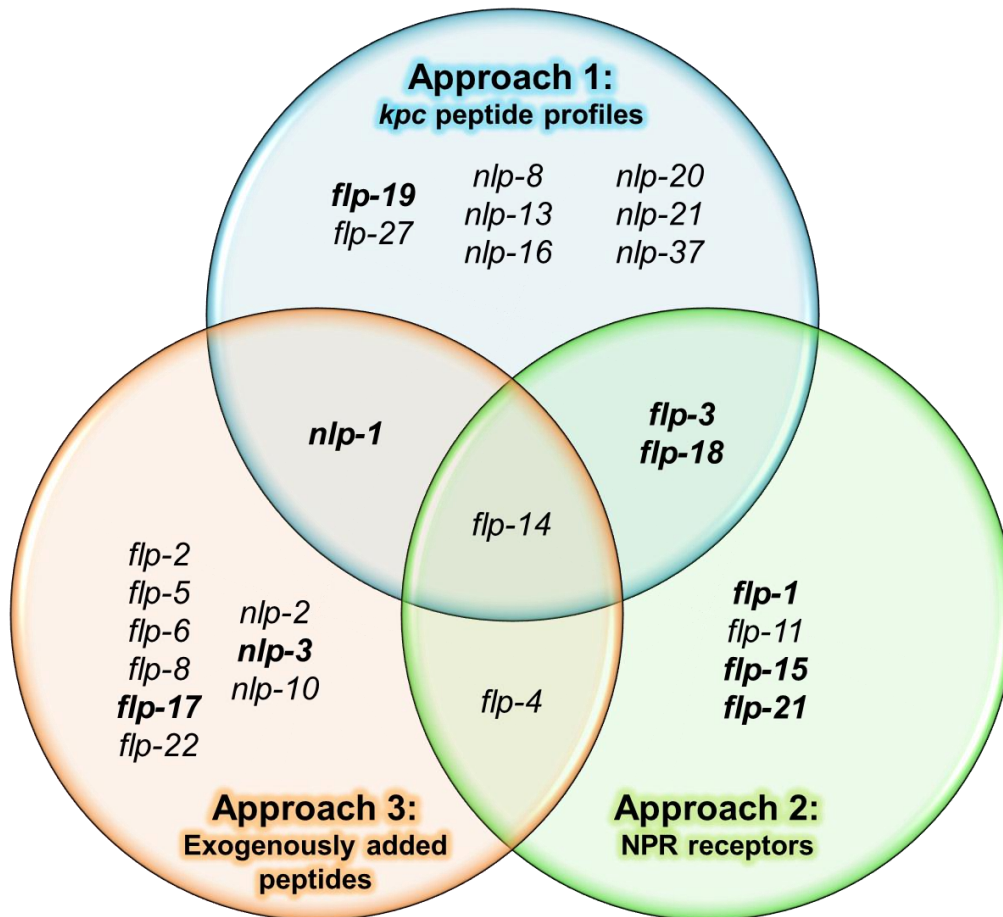


Figure 58: Venn diagram representing the neuropeptide genes selected for further investigation for their role in the control of the worm's pumping behaviour.

Only one gene was selected in all three approaches; i.e. *flp-14*, however in the 1st approach selecting known ligands to neuropeptide-Y receptors, FLP-14 peptides only bind to NPR-4 at really high doses (> 10 μ M). Genes written in bold represents genes for which mutant has been tested.

In the presence of food, while *flp-15(gk1186)* and *flp-21(ok889)* mutants behaved similarly to N2, *flp-1(yn2)*, *flp-3(ok3265)* and *flp-18(gk3063)* displayed a lower pumping rate compared to the paired control N2. *flp-1(yn2)* displayed the most marked behaviour with a reduced pumping rate (~ -50 ppm) at a level

close to *egl-3(ok979)* (**Figure 59A**) compared to the smaller reduction showed by *flp-3(ok3265)* and *flp-18(gk3063)* (~ -20 ppm).

In the absence of food, *flp-15(gk1186)* and *flp-21(ok889)* appeared to phenocopy the *egl-3(ok979)* PoffF phenotype, namely a strongly reduced pumping rate close to 0 ppm. *flp-18(gk3063)* mutant strain also pumped at a lower rate than N2, however, significantly higher than *egl-3(ok979)* ($p = 0.045$) (**Figure 59C**). Conversely, *flp-1(yn2)*, and to a lesser extent *flp-3(ok3265)*, displayed a higher pumping rate than the N2 paired control with an average rate around 60 ppm for *flp-3(ok3265)* and 115 ppm for *flp-1(yn2)*. These two last results were unexpected as these neuropeptide gene mutants were selected as candidates for their ability to mimic *egl-3* mutants pumping phenotype, however, both *flp-1* and *flp-3* mutants displayed an *unc-31/eat-4*-like off food behaviour instead. Therefore, both *flp-1* and *flp-3* could account, at least in part, for the *unc-31* phenotype. The expression pattern of the *flp* genes mentioned in this study is summarized in **Table 6**.

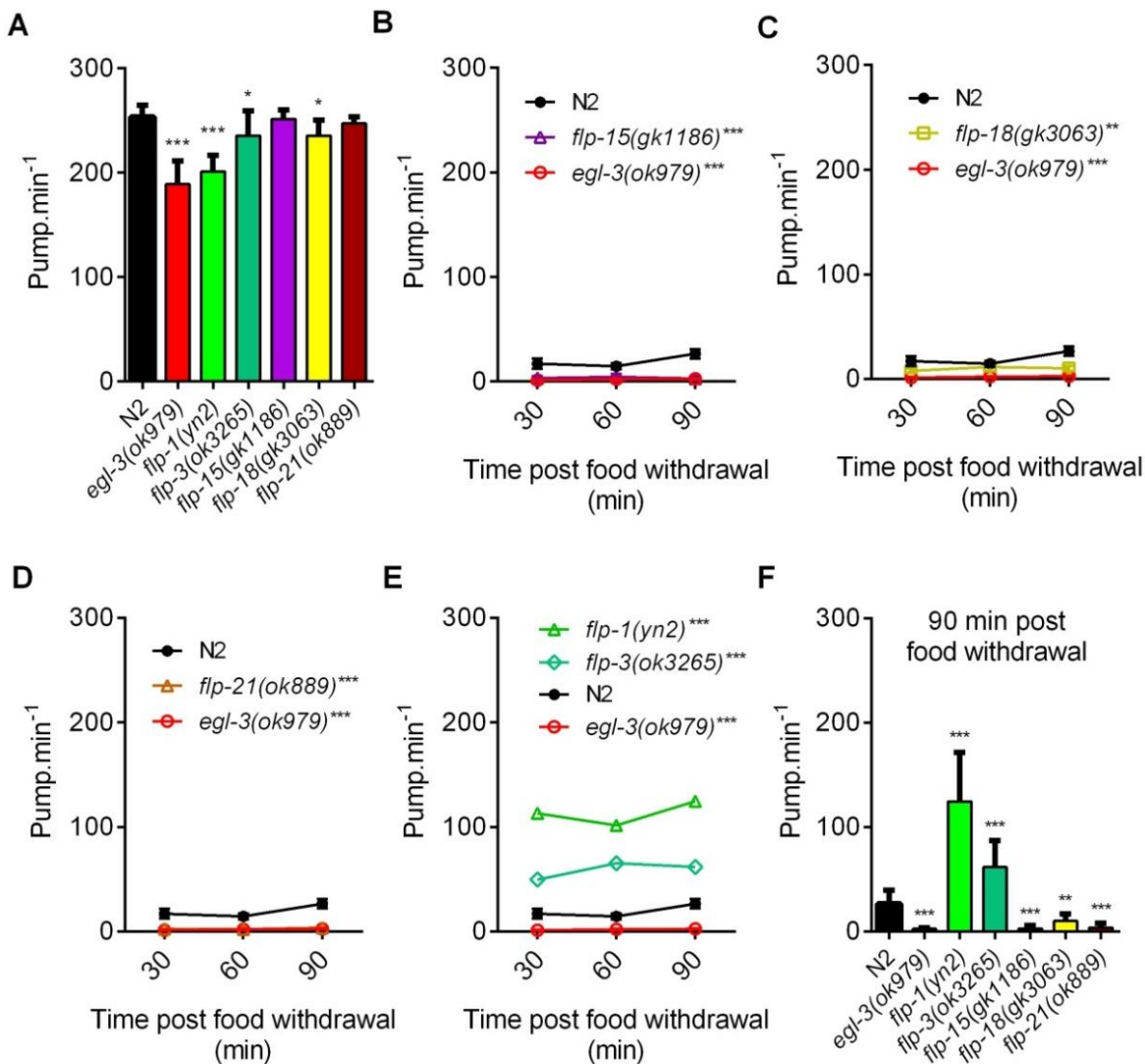


Figure 59: Neuropeptide mutant strains candidate analysis of on and off food pumping phenotype.

A. In the presence of food, *egl-3(ok979)* (-64 ± 5 ppm; $p < 0.001$; $n = 15$), *flp-1(yn2)* (-52 ± 5 ppm; $p < 0.001$; $n = 17$), *flp-3(ok3265)* (-18 ± 5 ; $p = 0.0105$; $n = 19$) and *flp-18(gk3063)* (-18 ± 5 ppm; $p = 0.011$; $n = 19$) pumped at a lower rate compared to N2 ($n = 20$). *flp-15(gk1186)* ($p = 0.99$; $n = 18$) and *flp-21(ok889)* ($p = 0.99$; $n = 17$) pumped at a similar rate to N2.

flp-1(yn2) was the only mutant displaying a similar pumping rate compare to *egl-3(ok979)* ($p = 0.631$). **B - E.** Neuropeptide mutants pumping in absence of food. All strains were tested in parallel, but results have been plotted onto 4 graphs for greater clarity. *egl-3(ok979)* (-17 ± 5 ppm; $p = 0.005$; $n = 7$), *flp-15(gk1186)* (-16 ± 2 ppm; $p < 0.001$; $n = 7$), *flp-18(gk3063)* (-10 ± 2 ppm; $p = 0.003$; $n = 8$) and *flp-21(ok889)* (-17 ± 2 ppm; $p < 0.001$; $n = 10$) pumped at a lower rate than N2 ($n = 9$). *flp-15(gk1186)* and *flp-21(ok889)* displayed no

significant differences with *egl-3(ok979)* ($p = 0.387$ and $p = 0.302$ respectively) unlike *flp-18(gk3265)* ($p = 0.045$). Both *flp-1(yn2)* (94 ± 8 ppm; $p < 0.001$; $n = 7$) and *flp-3(ok3265)* (40 ± 7 ppm; $p < 0.001$; $n = 8$) pumped at a higher rate than N2. F. Histogram representation of the 90 min time point from B-E.

Other individual neuropeptides, not selected by the previous strategies, were selected for their ability to modulate pumping when added exogenously to cut head preparations, and for which mutants were available, have been assessed.

FLP-17 shows potent excitatory activity on pharyngeal pumping and is expressed in BAG and the pharyngeal neuron M5 (Papaioannou *et al.*, 2005; Papaioannou *et al.*, 2008b) and was therefore a good candidate to act in the *egl-3*-dependent fictive feeding behaviour. In the presence of food, *flp-17(ok3587)* mutant displayed an *egl-3(ok979)*-like phenotype with a reduced pumping rate (**Figure 60A**), a result confirming the excitatory potential of FLP-17. However, no effect was observed in absence of food (**Figure 60B, C**).

Similarly, NLP-1 and NLP-3 triggered a weak excitation on the isolated pharynx preparation. *nlp-3* is known to be expressed in many pharyngeal neurons including I2 (Nathoo *et al.*, 2001; Papaioannou *et al.*, 2008a) while *nlp-1*, although not reported in the pharynx but in the intestine, regulates acetylcholine-induced muscle contraction (Li *et al.*, 1999b). Neither *nlp-1(ok1168)* nor *nlp-3(ok2688)* showed significant differences on or off food (**Figure 60**).

FLP-19, unlike FLP-17 caused inhibition on isolated pharynxes preparations (Papaioannou *et al.*, 2005) and was therefore selected as a candidate to play a role in the *unc-31*-dependent inhibition of the pumping rate in response to food deprivation. However, *flp-19(ok2460)* mutant behaved similarly to N2 both on and off food (**Figure 60D-F**).

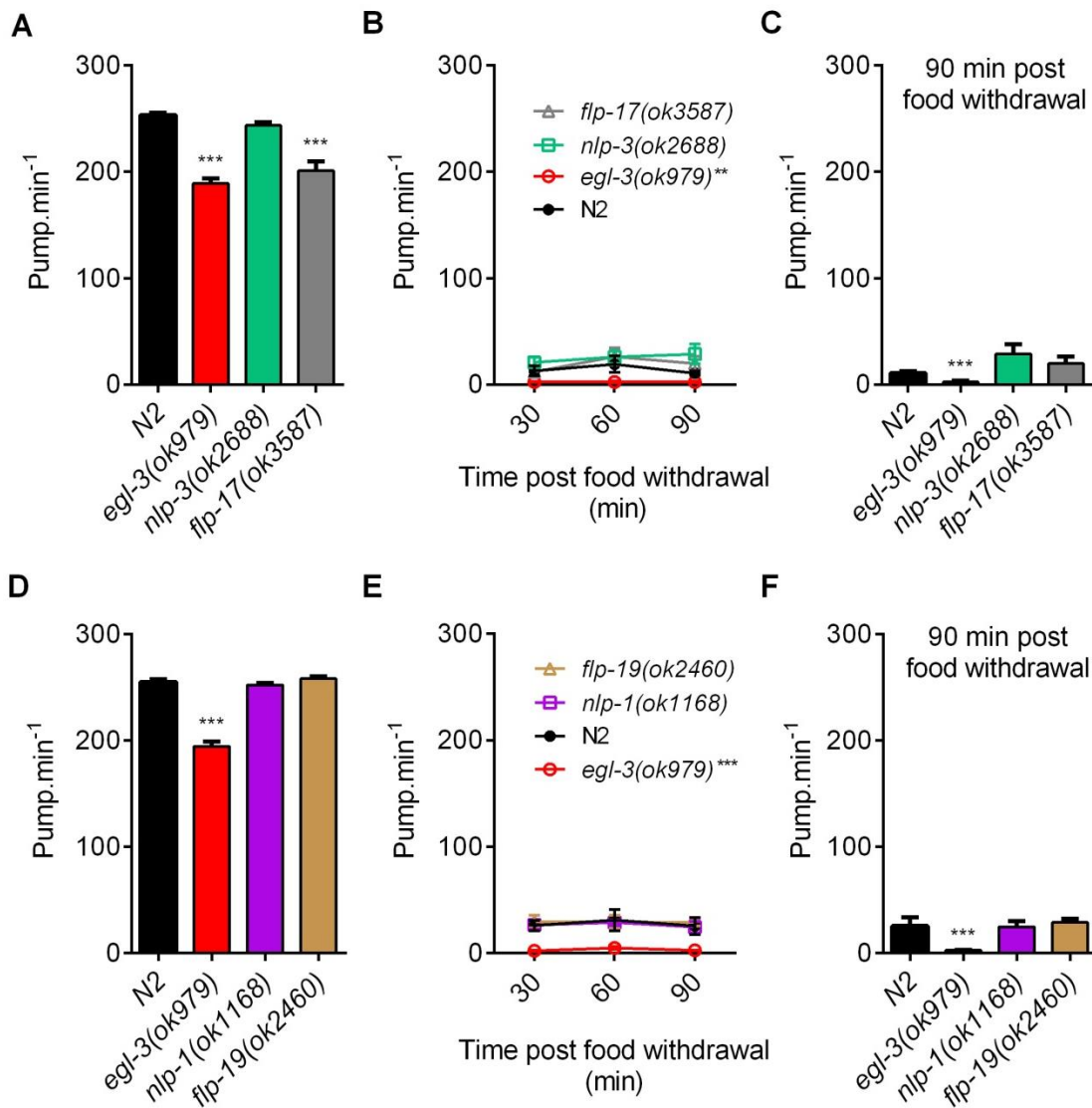


Figure 60: Screen of individual neuropeptides

A. *egl-3(ok979)* (-64 ± 7 ppm; $p < 0.001$; $n = 20$) and *flp-17(ok3587)* (-52 ± 7 ppm; $p < 0.001$; $n = 21$) displayed a significantly reduced pumping rate to the paired N2 ($n = 20$), unlike *nlp-3(ok2688)* ($p = 0.99$; $n = 20$).

B. In the absence of food, *egl-3(ok979)* (-12 ± 5 ppm; $p = 0.009$; $n = 8$), but not *nlp-3(ok2688)* ($p = 0.103$; $n = 8$) and *flp-17(ok3587)* ($p = 0.442$; $n = 17$) pumped slower than N2 ($n = 7$).

D. When food is present, *egl-3(ok979)* (-61 ± 4 ppm; $p < 0.001$; $n = 17$) pumped lower than N2 ($n = 20$). *nlp-1(ok1168)* ($p = 0.99$; $n = 20$) and *flp-19(ok2460)* ($p = 0.99$; $n = 20$) displayed a similar pumping rate to N2.

E. Neither *nlp-1(ok1168)* ($p = 0.896$; $n = 8$) nor *flp-19(ok2460)* ($p = 0.816$; $n = 9$) showed any significant difference with N2 ($n = 6$) while *egl-3(ok979)* (-24 ± 6 ppm; $p < 0.001$; $n = 6$) displayed a reduced pumping rate off food.

C.F. Histogram representations of the 90 min time point from **B** and **E**.

5.2.5 *npr-3* rescue in pharyngeal muscle

flp-15 mutant displayed a reduced pumping rate in absence of food, similar to the mutant for its receptor *npr-3* (Figure 59B and Figure 56). However, *flp-15* is mainly expressed in the I2 neurons (*flp-15* promoter being used for I2 specific expression), and the ablation data indicate I2 acts to reduce the pumping rate in response to food withdrawal. Therefore, the fact that the neuropeptides encoding gene *flp-15* act to stimulate the pumping rate was a surprising result. This would indicate that I2 is not only able to act negatively on the pharynx pumping frequency, but also, in parallel, to actively stimulate the pumping rate to maintain a basal rate in absence of food. In a simple model, one would therefore hypothesize that *flp-15* neuropeptides released from I2 would act directly onto the pharynx muscle via the NPR-3 receptor.

To test this hypothesis, a construct expressing *npr-3* wild-type cDNA in the pharynx muscle only (*myo-2* promoter) was generated and injected to transform the *npr-3(tm1583)* mutant. The transgenic line generated was then tested for its pumping off food phenotype during the first 90 min of food deprivation (Figure 61). As previously observed, the *npr-3(tm1583)* mutant displayed almost no pumping motion in absence of food. *npr-3(tm1583); Ex[Pmyo-2::*npr-3*]* transgenic strain pumped slower than the paired N2 controls but showed no significant difference with *npr-3(tm1583)*. However, *npr-3(tm1583); Ex[Pmyo-2::*npr-3*]*, unlike in *npr-3(tm1587)*, showed an increase of pumping motions after 90 min of food deprivation suggesting a trend toward a partial rescue. As this is a non-integrated line, mosaic expression of the transgene may affect the results; it would be better to test different transgenic lines with a higher n number.

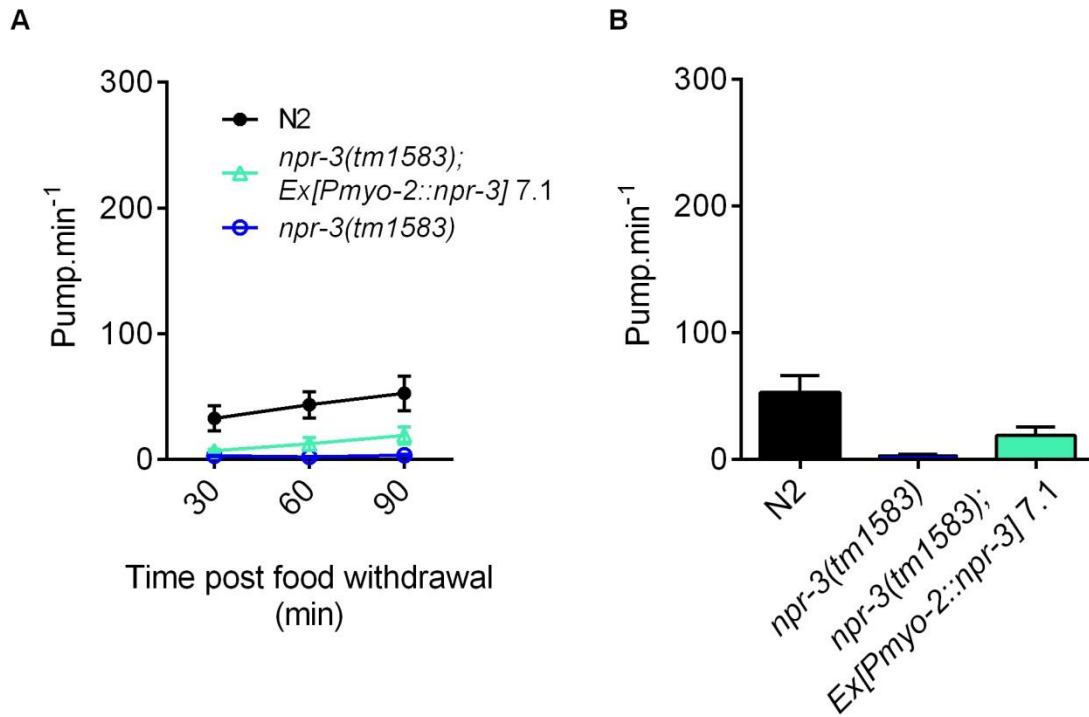


Figure 61: *npr-3(tm1583)* pharyngeal pumping rate off food following specific expression of *npr-3* cDNA in the pharynx muscle.

In absence of food *npr-3(tm1583)* pumped lower (-40 ± 9 ppm; $p < 0.001$; $n = 6$) than the paired N2 control ($n = 5$). *npr-3(tm1583); Ex[Pmyo-2::npr-3]* showed a slightly higher, but not significant (10 ± 8 ppm; $p = 0.719$; $n = 8$), pump rate compared to *npr-3(tm1583)*, and a significantly reduced rate (-30 ± 9 ppm; $p = 0.719$) than N2.

5.3 Discussion

Neurohormonal signalling is crucial in the regulation of the worm's pumping behaviour. We have seen in the previous chapters that *egl-3* and *unc-31*, respectively involved in the processing and release of neuropeptides, were major determinants. *egl-3*-processed neuropeptides act to stimulate the pumping rate both in the presence and the absence of food. *unc-31*, likely through the action of neuropeptides, has no role in the presence of food but acts to reduce the pumping rate when food is lacking. To refine our

understanding of the neurohormonal control of the pumping rate, the investigation of individual neuropeptides was undertaken. However, there are around 250 neuropeptides encoded by 115 genes in the *C. elegans* genome and there is therefore the necessity to narrow down potential candidates.

The mutant analysis of *kpc*-family members has shown that *aex-5(sa23)/kpc-3* displayed an *egl-3*-like off food phenotype while *bli-4(e937)/kpc-4* pump in absence of food with a slight but significant increased rate during the early phase (**Figure 52**). Interestingly, Husson *et al.* in 2006 have published the neuropeptide profile of the four *kpc*-family members including *egl-3/kpc-2* (Husson *et al.*, 2006). Therefore, according to the aforementioned results, neuropeptides which are important for the maintenance of the basal pumping rate in absence of food should be missing in both *egl-3* mutant strains and *aex-5(sa23)/kpc-3*, but present in *bli-4(e937)/kpc-4*. Using this method of selection, peptides encoded by *nlp-8*, *nlp-16*, *flp-3*, *flp-14*, *flp-18* and *flp-27* appeared to be the most interesting candidates. It is important to note that this *kpc* family screen is highly dependent on the known peptide profiles for those mutants, where only a small portion of all the neuropeptides found in *C. elegans* are detected, and notably with the absence of insulin-like peptides, hence the importance to combine it with other approaches.

The genetic screen for neuropeptide receptor mutants has pinpointed three NPY-like receptors involved in the *egl-3*-dependent adaptive feeding behaviour in absence of food; NPR-3, NPR-4 and NPR-5 (**Figure 56**). Expression patterns and known ligands for these receptors have been summarised in **Table 3**.

NPR-3 is widely expressed in the ventral nerve cord in both excitatory and inhibitory motoneurons (Keating *et al.*, 2003). Two ligands encoded by the same gene are currently known to bind NPR-3: FLP-15A and FLP-15B (Kubiak *et al.*, 2003). *flp-15* is expressed in the phasmid neurons PHA and PHB, known to modulate chemorepulsion behaviour (Hilliard *et al.*, 2002), in the pharyngeal interneuron I2 (Li and Kim, 2008), and in non-neuronal cells, viz, in the pharyngeal muscles, socket and/or sheath cells (**Table 6**) (Kim and Li, 2004). The role of these peptides is not clearly known yet, however, exogenous addition of one *flp-15* peptide, FLP-15A, in an isolated pharynx preparation

induces an inhibition of pumping (Papaioannou *et al.*, 2005). As for NPR-4, it is expressed in PQR (O₂ sensing) and BAG (CO₂ sensing) sensory neurons, in AVA, RIV and BDU interneurons but also outside the nervous system (Cohen *et al.*, 2009). Peptides encoded by at least 7 *flp* genes are believed to be NPR-4 ligands (*flp-1*, 3, 4, 11, 14, 15, 18 encoded peptides). NPR-5 is expressed in a subset of sensory neurons (ADF, ASE, ASG, ASI, ASJ, ASK, AWA, AWB, IL2, PHA, PHB), in AIA and AUA interneurons and outside the nervous system (Cohen *et al.*, 2009). Two FLP peptides are known to be NPR-5 ligands: FLP-18 and FLP-21.

From the preliminary receptor screen, only one receptor appeared to be acting in the reduction of the pumping rate in absence of food; NPR-6. *npr-6(tm1497)* showed a slightly increased rate off food compared to N2. However, this mutant strain hasn't been further analysed and it is therefore possible that the phenotype observed is due to the variability inherent in the assay used for the initial screen, as has been observed with *npr-1(ky13)* (see **Figure 56** and **Figure 57**). Moreover, *npr-6(tm1497)* phenotype was pretty marginal compared to the high pump rate displayed by *unc-31* mutants off food and further investigation was therefore not conducted. It is nonetheless interesting to see that NPR-6 known ligands, *flp-18* and *flp-21* encoded peptides, are also shared by NPR-4 and NPR-5. If *npr-6(tm1497)* phenotype is confirmed, the dichotomy between this receptor and NPR-3 and NPR-4 which have opposite roles could be explained by a difference in activity of the ligand neuropeptides encoded by the same genes. One remarkable example of this is the effects of *flp-14* encoded peptides on the pumping rate of isolated pharynx preparations previously published (**Table 5**) (Papaioannou *et al.*, 2005) where FLP-14A has a stimulatory effect while FLP-14B triggers a reduction and FLP-14C shows no effect.

The biggest limitation of the neuropeptide-receptor mutants' screen, however, comes from the limited knowledge about these receptors and their known ligands. As this database is far from being exhaustive, with a lot of orphan GPCRs, it is possible that neuropeptides acting through specific receptors are not detected using this method since their ability to bind thereof has not been demonstrated yet. A summary of the role, expression pattern and known ligands of the neuropeptide receptors mentioned in this discussion can be found in **Table 3**.

The third approach, based on the previously described effect of exogenous individual peptides on pharynx preparation (Papaioannou *et al.*, 2005; Papaioannou *et al.*, 2008a), shed light on 12 genes encoding for neuropeptides stimulating the pump rate. These include *nlp-2*, *nlp-3*, *nlp-10*, *flp-2*, *flp-5*, *flp-6* and *flp-22*, uniquely selected by this approach, but also *nlp-1* which was conjointly selected by the *kpc* mutants peptide profile approach, *flp-4* which was also found in the neuropeptide receptors approach, and *flp-14*, selected by all approaches.

From the three approaches detailed in this study, the number of potential neuropeptide genes controlling the pumping rate was decreased to 26 (**Figure 51**). 9 genes were investigated, based on two main criteria; prioritising genes identified from multiple approaches, then on the availability of mutants for these genes. Interestingly, only a few genes were selected by multiple approaches (see **Figure 58** for summary). *flp-14* was the only one shared by all approaches, but unfortunately, no mutant was available for it. Similarly, *flp-4* was pulled down from both approaches 2 and 3 but no mutant was available. The three other genes selected by multiple approaches, viz, *nlp-1*, *flp-3* and *flp-18*, were further investigated for their role in the modulation of the pumping rate. Subsequently, *flp-17* was chosen for the ability of its encoded peptides to induce a potent stimulation of the pumping rate, while *nlp-3* and *flp-15* were further tested because of their expression in I2 neurons. Finally, *flp-1*, *flp-19* and *flp-21* peptides led to a reduction of pump rate when exogenously added, a surprisingly opposite result to what would be expected from approach 1 or 2 which aimed to select candidates which stimulated pumping rate. It was therefore of interest to investigate mutants for these genes.

Chapter 5

Gene	Expression in the pharynx	Peptide tested (1)	Presence in <i>egl-3</i> mutants (2-3)	Action on isolated pharynx (2-3)	Concentration	Context dependent effect observed on pumping rate:	
						On food (a)	Off food (a)
<i>nlp-1</i>	None	NLP-1A	No	Weak stimulation	1µM	No effect	No effect
<i>nlp-2</i>	None	NLP-2A	?	Variable stimulation	1µM		
		NLP-2B	?	No effect	1µM		
<i>nlp-3</i>	l1, l2, l3, l4, M1, M3, NSM, l6, M2	NLP-3	?	Weak stimulation	1µM	No effect	No effect
<i>nlp-8</i>	l2, processes in pharynx	NLP-8	No	Weak reduction	1µM		
<i>nlp-10</i>	pharyngeal neurons	NLP-10A	?	Stimulation	1µM		
<i>flp-1</i>	M5	FLP-1A1 (PF1)	In <i>n588</i>	Reduction	1µM	Stimulation	Reduction
		FLP-1A2 (PF2)	In <i>n588</i>	Reduction	1µM		
<i>flp-2</i>	l5, MC, M4	FLP-2A	No	Stimulation	1µM		
<i>flp-3</i>	None	FLP-3A	No	Reduction	1µM	Stimulation	Reduction
<i>flp-4</i>	l5, l6, NSM	FLP-4A	?	Stimulation	1µM		
<i>flp-5</i>	(l2), l4, M4, pm	FLP-5A	?	Stimulation	1µM		
<i>flp-6</i>	l1, l4	FLP-6 (AF8)	?	Stimulation	1µM		
<i>flp-7</i>	None	FLP-7A	No	No effect	1µM		
<i>flp-8</i>	None	FLP-8 (AF1)	?	Potent stimulation	100nM		
<i>flp-9</i>	Not determined	FLP-9A	No	Reduction	1µM		
<i>flp-10</i>	None	FLP-10A	?	No effect	1µM		
<i>flp-11</i>	None	FLP-11A	No	Potent reduction	100nM		
<i>flp-12</i>	None	FLP-12A	?	No effect	1µM		
<i>flp-13</i>	l5, M3, M5	FLP-13A	In <i>n588</i>	Potent reduction	100nM		
<i>flp-14</i>	Not determined	FLP-14A	?	Stimulation	1µM		
		FLP-14B [†]	?	Reduction	1µM		
		FLP-14C	?	No effect	1µM		
<i>flp-15</i>	l2, pm	FLP-15A [†]	No	Reduction	1µM	No effect	Stimulation
<i>flp-16</i>	Not determined	FLP-16A (AF15) [†]	?	Reduction	1µM		
<i>flp-17</i>	M5	FLP-17A	?	Potent stimulation	100nM	Stimulation	No effect
		FLP-17B	?	Potent stimulation	100nM		
<i>flp-18</i>	M2, M3	FLP-18A [†]	No	Reduction	1µM	Stimulation	Stimulation
<i>flp-19</i>	None	FLP-19A	No	Reduction	1µM	No effect	No effect
<i>flp-20</i>	None	FLP-20	?	No effect	1µM		
<i>flp-21</i>	MC, M4, M2	FLP-21 (AF9) [†]	?	Reduction	1µM	No effect	Stimulation
<i>flp-22</i>	None	FLP-22	No	Stimulation	1µM		
<i>flp-23</i>	Not determined	FLP-23	?	No effect	1µM		

Table 5: Comparison of the effects of neuropeptides on the pharyngeal pumping activity of isolated pharynxes and their role on pumping behaviours.

Sources: (1) Husson *et al.* 2006; (2) Papaioannou *et al.* 2005 ; (3) Papaioannou *et al.* 2008.

(a) Results described in this chapter.

‘Stimulation’ indicates mutants displayed a lower pumping rate than wild-type. Conversely, ‘reduction’ indicates mutants pumped faster than wild-type worms.

Stimulatory effects were recorded in absence of 5-HT, while reduction was observed in presence of 5-HT, except for FLP-14B, FLP-15A, FLP-16A, FLP-18A, and FLP-21 where a rate reduction has only been observed without 5-HT, when pumping frequency was low (marked with on the 'T' table).

5.3.1 Neuropeptides exhibiting a stimulatory effect on the pumping rate off food

Of all the 9 selected candidates tested in absence of food, three of them, *flp-15(gk1186)*, *flp-18(gk3063)* and *flp-21(ok889)* mutants showed a significantly reduced pumping rate (**Figure 59**). *flp-15(gk1186)* and *flp-21(ok889)* completely phenocopied *egl-3(ok979)*, displaying almost no pump motion during food deprivation, while *flp-18(gk3063)* showed a less severe reduction (**Figure 59B-E**). These results indicate a stimulatory role for the neuropeptides encoded by these genes. Interestingly, whether this role is in accordance with the role for their receptors NPR-4 and NPR-5 when food is absent, these results are in contradiction with the effect observed by exogenous addition of peptides encoded by these genes on cut head preparations (Papaioannou *et al.*, 2005). FLP-15A, FLP-18A and FLP-21(AF9) indeed led to a reduction of the basal pump rate. This discrepancy could be explain for *flp-15* and *flp-18* by the fact that only one peptide has been assessed per gene (as explained above) but not for *flp-21* which only encodes for one neuropeptide. Another explanation could be the difference of context between an intact animal and a severed head, or the concentration of peptides used which might not represent the physiological reality, i.e. low concentrations of peptide might have one effect while higher concentrations have the opposite effect.

Nonetheless, expression patterns of those neuropeptide encoding genes have been summarised in **Table 6**. Surprisingly, while most of those genes are expressed in the pharyngeal nervous system, there is no known expression of their related receptors outside of the central nervous system (**Table 3** and **Table 6**) (Kim and Li, 2004). This could indicate a communication from the

Chapter 5

pharynx to the central nervous system, or reflect the fact that these FLP peptides are ligands to other receptors which have not been determined yet or might simply indicate that pharyngeal expression of these receptors have not been investigated in enough details (for example by dissecting the pharynx).

Gene	Exp. in the somatic NS	Exp. in the pharyngeal NS	Exp. outside the NS	Known Receptor(s)	Pumping on food behaviour	Pumping off food behaviour
<i>flp-1</i>	AIA, AIY, AVA, AVE, AVK, RIG, RMG	M5		NPR-4 NPR-5 NPR-11 NPR-22 CKR-2a	Reduced (<i>egl-3</i> -like)	Increased (<i>unc-31</i> -like)
<i>flp-3</i>	IL1, PQR, OLL, URB			NPR-4 (> 10 μ M) NPR-5 (> 1.5 μ M) NPR-10	Reduced	Increased (halfway <i>unc-31/N2</i>)
<i>flp-15</i>	PHA	I2	socket/sheath cells/pharyngeal muscle	NPR-3 NPR-4 (> 10 μ M)	Wild-type	Reduced (<i>egl-3</i> -like)
<i>flp-18</i>	AIY, AVA, RIG, RIM	M2, M3		NPR-1 NPR-4 NPR-5 NPR-6 NPR-10 NPR-11	Reduced	Reduced
<i>flp-21</i>	ADF, ADL, ASE, ASG, ASH, ASI, ASJ, ASK, FLP, RMG, URA, URX	M2, M4, MC	Intestine	NPR-1 NPR-5 NPR-6 NPR-11	Wild-type	Reduced (<i>egl-3</i> -like)

Table 6: Expression pattern and pumping phenotypes of the candidate *flp* mutants assessed.

Sources: Lowery *et al.* 2003; Keating *et al.* 2003 ; Cohen *et al.* 2009; Fröoninckx *et al.* 2012; Peymen *et al.* 2014.

To date, *flp-15*'s role is relatively ill-defined. However, its expression in the pharyngeal neurons I2, a major determinant in the modulation of the pumping

rate in absence of food, is particularly interesting (Kim and Li, 2004). As described in the previous chapter, I2 act to reduce the pumping rate in response to food removal via a glutamate-dependent and independent pathway, the latter being thought to involve neurohormonal or gap junction signalling. Peptides expressed in I2 could therefore modulate this effect; yet *flp-15* encoded peptides appeared to have a net stimulatory effect in absence of food as the mutant pumped less than N2 off food (**Figure 59**). This would suggest that in response to food removal, I2 is not only able to reduce the pumping rate but also to actively maintain the pumping motion at a basal rate by releasing FLP-15 peptides, allowing continuous sampling of the environment, and therefore acting as a hub in the control of the pumping phenotype off food. A simple model would be that the FLP-15 peptides released from I2 would bind the NPR-3 receptors directly onto the pharynx muscle to stimulate the pumping rate (**Figure 62**). Whether FLP-15 peptides act via NPR-3 directly onto the pharynx remains unclear, however, the first experiment conducted attempting to restore *npr-3* expression in the pharynx only showed a trend toward an elevation of *npr-3(tm1583)* mutant's pumping rate (**Figure 61**). Further investigations need to be performed in order to confirm this hypothesis. Moreover, the possibility also exists that FLP-15 is released from PHA phasmid sensory neuron.

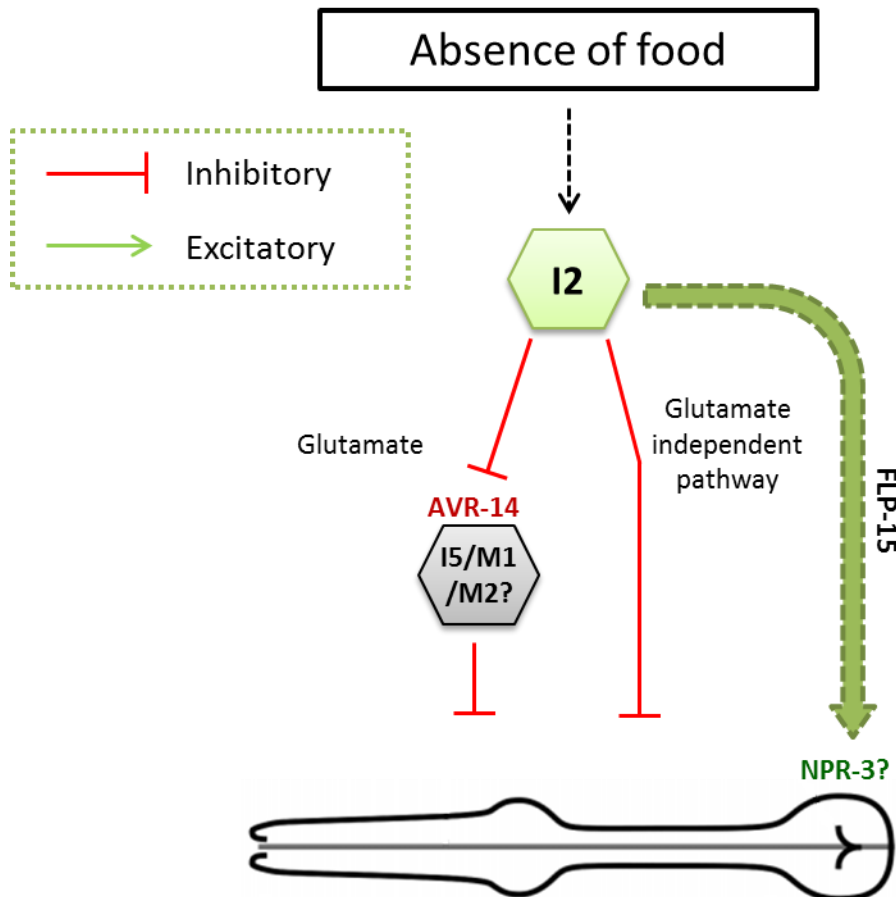


Figure 62: Hypothetical model of I2 modulating both the reduction of the pumping rate and the maintenance of the basal pumping rate in absence of food.

In this model, removal of food activates I2 neurons which in turn fine tune the pumping behaviour by reducing the pumping rate through 2 distinct pathways and maintaining a slow basal pumping rate. The first inhibitory pathway is glutamate-dependent where glutamate is not released directly onto the pharynx but acts on a pharyngeal neuron expressing the glutamate-gated chloride channel AVR-14. In contrast, the second pathway is glutamate independent, and may involve neuropeptide transmission or gap junction communication.

In parallel, I2 also release the *flp-15* encoded peptides inducing a stimulatory tone which maintains a slow pumping rate in absence of food.

There are three other neuropeptide genes known to be expressed in I2; *nlp-3*, *nlp-8* and *flp-5* (Nathoo *et al.*, 2001; Kim and Li, 2004). *flp-5* and *nlp-3* are part of the pool of candidate genes from the third approach (exogenously added neuropeptides), while *nlp-8* was found in approach 1 (*kpc* mutants) (Figure 58). It is interesting to note that all known peptides expressed in I2 were selected as candidates in this study. *nlp-3*, was not found involved in the modulation of the worm's pumping behaviour as *nlp-3(ok2688)* mutant showed no aberrant behaviour in the presence or absence of food. *flp-5* single mutant was not available while *nlp-8* mutant was found sick and is believed to carry other mutations.

flp-18 is expressed in two pharyngeal neurons, the cholinergic M2 and glutamatergic M3 neurons, three interneurons AIY, AVA, RIG and the motorneuron RIM (Table 6). *flp-18* plays a role in olfactory behaviour and locomotion adaptation to food deprivation (via NPR-4), *flp-18(db99)* mutant failing to enter the dispersal phase following the local search area; but also in the regulation of fat storage, with *flp-18(db99)* mutant showing an excess in lipid storage. *flp-18* also plays a role in the regulation of dauer formation (Cohen *et al.*, 2009). FLP-18 peptides modulate these phenotypes through release from the same neuron, AIY, then acting through NPR-4 and NPR-5 receptors (Cohen *et al.*, 2009). Interestingly, Cohen and colleagues did not observe any pumping defect in the presence of food in their *flp-18(db99)* mutant, which is contrary to what is described here, i.e. a slight decrease of ~20 ppm, with a different allele (*gk3063*).

flp-21 is expressed in the central nervous system, notably in a range of amphid sensory neurons, and the pharyngeal nervous system in M2, M4 and MC (Table 6). In the literature, FLP-21 is mainly known as an NPR-1 ligand acting to inhibit social feeding behaviour (Rogers *et al.*, 2003; Boender *et al.*, 2011). However, *npr-1(ky13)* mutant displayed no defect in the pumping phenotype and therefore FLP-21 must act through another receptor. Aside from NPR-1, FLP-21 can bind to NPR-5, NPR-6 and NPR-11 (Lowery *et al.*, 2003; Cohen *et al.*, 2009; Peymen *et al.*, 2014). Since NPR-6 might act to reduce the pumping rate while NPR-11 has no role in the pumping phenotype in absence of food (Figure 55), it is likely that FLP-21 acts through NPR-5 to maintain the

basal pumping phenotype in absence of food. However, no pharyngeal expression of *npr-5* is known to date. It is therefore possible that FLP-21 might act through another receptor which remains to be determined.

Surprisingly, mutants for candidates selected solely based on their stimulatory effect when externally added to isolated pharynx, viz, *nlp-1*, *nlp-3* and *flp-17*, did not show any role in the modulation of the worm's pumping behaviour in response to food deprivation.

5.3.2 Neuropeptides mediating the reduction of the pumping rate in absence of food

Surprisingly, two of peptide gene candidates tested, *flp-1(yn2)* and *flp-3(ok3265)* pumped significantly higher than N2 off food, indicating a role in the reduction of the pumping rate off food. Given that both peptide mutants have been isolated in a screen designed to discover neuropeptides genes involved in the *egl-3*-dependent maintenance of the basal pumping rate off food, those two mutants were expected to display a reduced pump rate. While *flp-1* and *flp-3* cannot explain the *egl-3* phenotype off food, it is then possible they are both part of the *unc-31*-dependent reduction of the pumping rate in absence of food (see **chapter 3**).

FLP-1 has been shown to be important in the regulation of various phenotypes such as well-coordinated or sinusoidal movement and egg-laying. FLP-1 exogenous application on isolated pharynx preparations has been previously shown to reduce the pharyngeal pumping (**Table 5**) (Papaioannou *et al.*, 2005), in accordance with the mutant analysis performed in this study (**Figure 59**). Off food, the *flp-1(yn2)* mutant showed a striking increased pumping, phenocopying *eat-4* and *unc-31* mutants or and I2 ablated worm. One could therefore hypothesized that FLP-1 could act downstream of I2 to regulate the pumping rate in response to food withdrawal. Interestingly, *flp-1* is expressed in M5 (**Table 6**), a cholinergic pharyngeal motorneuron, and if I2s do not possess direct connections with M5, a microcircuit between the two can be drawn with either I6 or M1 between them. Notably I2 communicates with

M1 via both chemical synapses and gap junctions, therefore either or both glutamate-dependent and glutamate-independent inhibition of the pumping rate by I2 could be involved here. Besides, M1 is a putative site for the glutamate receptor AVR-14 (see **Figure 44**) shown to account for part of the glutamate role in absence of food in the previous chapter. *flp-1* is also expressed in the central nervous system, notably in sensory neurons (**Table 6**). It is therefore possible that FLP-1 acts as a neurohormonal signal from the central nervous system to the pharyngeal nervous system and muscle bypassing the RIP-11 bridge to modulate the pumping rate. Interestingly, *flp-1(yn2)* mutant displayed an *egl-3*-like phenotype on food, indicating once again the discrepancy between the circuits controlling the pumping phenotypes on and off food. However, it has been recently demonstrated that the deletion in the *flp-1(yn2)* mutant was also affecting a neighbour gene, *daf-10*, and therefore it is important to keep in mind these phenotypes observed in this mutant strain could account either to *flp-1* or *daf-10* (Chris Li unpublished data). *daf-10* encodes for a component of the *C. elegans* intraflagellar transport (IFT) complex A and its activity is required for the proper development of the ciliated amphid and phasmid sensory neurons (Starich *et al.*, 1995). As will be described in the next chapter, mutations affecting the cilia formation or function lead to an elevated pumping rate in absence of food but not in presence of food, therefore suggesting that the *flp-1(yn2)* pumping phenotype off food, but not on food, could be explained by the mutation in *daf-10*. Further investigation of a clean *flp-1* mutant and a *daf-10* mutant would thus be crucial to confirm these results.

As with *flp-1*, although to a lesser extent, *flp-3* appeared to reduce the pumping rate in absence of food, in line with exogenous application on pharynx preparations reducing the pumping rate (**Table 5**). There is no known other function for FLP-3 to date. However, since FLP-3 has only been shown to be expressed outside of the pharynx, it is possible the FLP-3 might serve to carry information that has been centrally integrated to the pharynx.

5.3.3 Neuropeptides modulating the high pumping rate in response to food

Four of the neuropeptide genes tested appeared to be important in the high frequency pump rate observed in response to the presence of food.

FLP-17 appears to be important on food as *flp-17(ok3587)* mutant showed a reduced pumping rate similar to *egl-3(ok979)*, a result that resonates with the potent stimulatory effect of FLP-17A and FLP-17B exogenously added to pharynx preparation (**Table 5**) (Papaioannou *et al.*, 2005). *flp-17* is expressed in the sensory BAG neuron and in the pharyngeal neuron M5 (Kim and Li, 2004; Ringstad and Horvitz, 2008) and therefore could act intrinsically to the pharynx or as a humoral signal. However, when M5 ablation reduces the pumping rate on food (Raizen *et al.*, 1995), it does so only by a slight amount of around 20 ppm and could therefore not entirely explain the *flp-17(ok3587)* defective phenotype. Thus one could hypothesize FLP-17 is released from the O₂/CO₂ sensing BAG neuron to increase the pumping rate in response to food cues. FLP-17's only known receptor, EGL-6, hasn't been tested in this study (Ringstad and Horvitz, 2008).

FLP-1, FLP-3 and FLP-18 also play a stimulatory role in the control of the pumping on food. *flp-1(yn2)* mutant showed the most severe phenotype, similar to *egl-3(ok979)*, while *flp-3(ok3265)* and *flp-18(gk3063)* displayed a more marginal but significant decrease in pumping rate (**Figure 59**). It would therefore be interesting to investigate the synergy between these neuropeptides to identify whether they are working in single or parallel pathways.

Once again, these results put more weight on the idea that on and off food phenotypes are controlled by distinct circuits. *flp-1* and *flp-3* have indeed opposite roles depending on the food context, while *flp-17* has no role off food. Only *flp-18* is stimulatory in both cases, however, the effects observed are always marginal compared to other mutants.

5.4 Conclusion

Neuropeptidergic signalling plays a major and complex role in the control of the worm's pumping behaviour (**Figure 63**). Identification of individual neuropeptide genes showed the complexity of this system where stimulatory peptides act together with peptides inducing a pumping reduction to fine tune the worm's pumping rate, depending on the food context. As with the classical neurotransmitters, some neuropeptides show an opposite role depending on the presence or absence of food.

The complexity of this system and the difficulty in identifying neurohormonal circuits controlling the feeding behaviour arises from the complex relationship between peptides and receptors. Indeed, one given neuropeptide can bind, with variable affinities, multiple receptors while one given receptor can be activated by a range of distinct neuropeptides, resulting in an astonishing number of potential combinations and responses. Furthermore, neuropeptides encoded by the same gene can have opposite effects on the same phenotype and therefore mutant analyses for neuropeptide genes are likely to reflect a sum effect of all the peptides it encodes for.

Overall however, the study depicted in this chapter reinforces the model of a pumping behaviour differentially regulated by distinct signalling pathways depending on the food availability, and has shed light on the role in the modulation of the pumping on food phenotype of 4 neuropeptide genes, *flp-1*, *flp-3*, *flp-17* and *flp-18*, for 4 GPCR receptors, NPR-1, NPR-3, NPR-4 and NPR-5. Since FLP-15 peptides, which are the only known ligands to NPR-3, are not involved in the control of the pumping phenotype in the presence of food, then the ligand(s) acting through NPR-3 and accounting for the pumping stimulation effect observed in the presence of food are still unknown.

In absence of food, 5 neuropeptide genes have been found to fine tune the pumping rate, *flp-3* and potentially *flp-1* act to reduce the pumping rate while *flp-15*, *flp-18* and *flp-21* act to maintain the basal pumping rate observed in absence of food. At least 3 GPCR receptors account for these effects; NPR-3, NPR-4 and NPR-5.

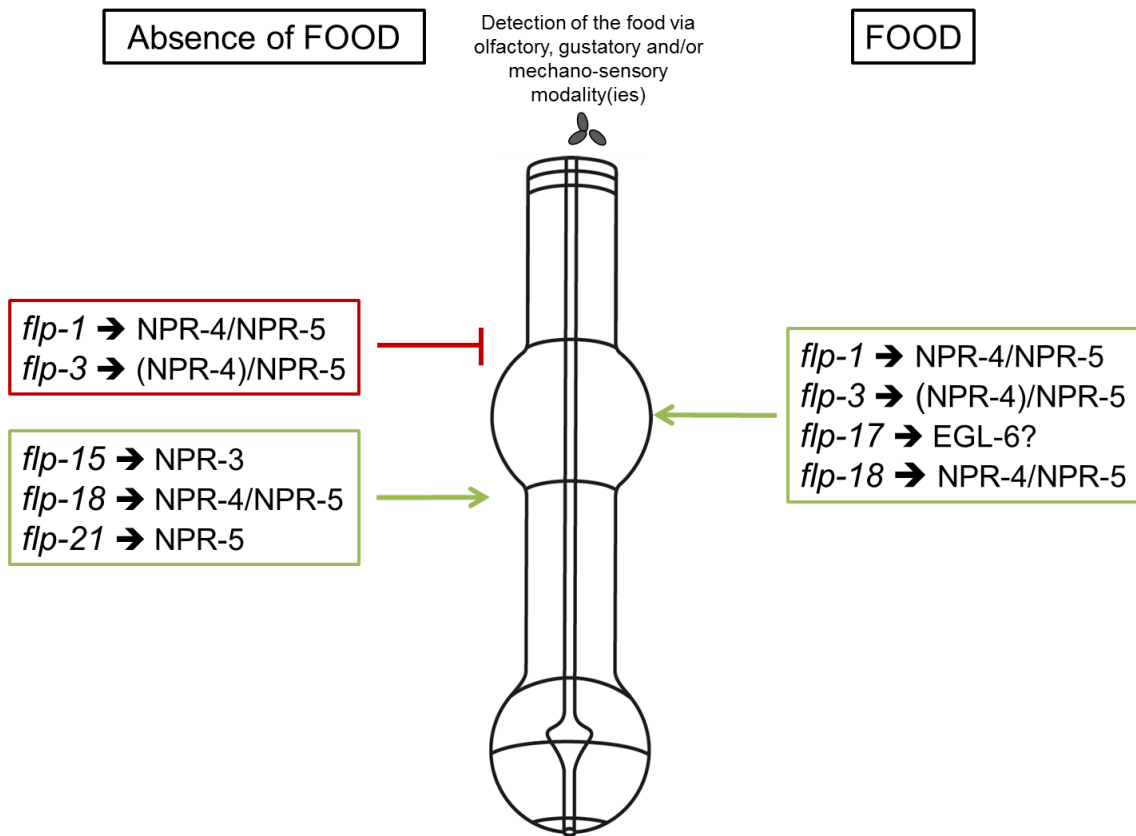


Figure 63: Model of the modulation of the pumping phenotype on and off food by individual neuropeptides.

In green boxes are represented genes encoding for neuropeptides acting to increase the pumping rate. In red, genes encoding for neuropeptides acting to reduce the pumping rate.

GPCRs indicated are based on known binding activity (Lowery *et al.*, 2003; Cohen *et al.*, 2009; Peymen *et al.*, 2014) with neuropeptides and role in the modulation of pumping rate described in this study. Between brackets, receptors with a low binding affinity for the neuropeptide (> 10 μ M). EGL-6 is the only known receptor binding *flp-17* peptides, but hasn't been tested in this study.

Chapter 6: Investigation of the sensory modalities that modulate the food-dependence of pumping behaviour

6.1 Introduction

The *eat-4* or *unc-31* mutant pumping phenotypes in the absence of food suggest these genes engage pathways that determine the worms' ability to selectively perceive food removal. The experiments using the double mutant suggest more than one pathway. In the previous chapters the possibility was raised that the cues explicitly sensed by the removal of food could be detected directly by the pharyngeal nervous system. Notably, the pharyngeal neurons I2 were described as a major determinant of the circuit controlling the "off" food behaviour. Indeed, I2s have proprioceptive-like free subcuticular endings at the tip of the pharynx and calcium imaging showed an increased activity in response to food removal. This hypothesis is also supported by the non-involvement of RIP in the control of the pumping behaviour (see **Chapters 3 and 4**). However, the RIP ablation results do not necessarily imply that the pumping behaviour off food is exclusively regulated by a neuronal circuit intrinsic to the pharynx. Part of the cues from the environment could indeed be sensed and centrally integrated to impart a control on the pharynx, by-passing the RIP-I1 neural connection, possibly via neurohormonal transmission (**Chapter 3**). In support of this idea, **Chapter 5** showed that neurohormonal signalling plays a determinant role in the control of pumping behaviour. In the absence of food, it modulates both inhibition of the high frequency rate displayed on food (*flp-1* and *flp-3*) and the maintenance of the slow basal pumping rate (*flp-15*, *flp-18* and *flp-21*).

The sensory modalities detecting the food cues, and subsequently leading to the appropriate pumping response associated with the presence or absence of food remain to be determined. Different cues from food, or its absence, can be detected by the worm. Chemical cues, soluble (gustatory) (Hukema *et al.*, 2008) or volatile (olfaction) (Bargmann *et al.*, 1993), mechanosensory cues via

the physical presence of bacteria (Hills *et al.*, 2004), or even metabolic cues, such as a change in the nutritional status of the worm all impact on feeding (Srinivasan *et al.*, 2008). Alternatively, temperature sensing could also play a role as worms can retain a memory of the temperature at which they found sufficient food and thermotax towards this specific temperature on a thermal gradient (Hedgecock and Russell, 1975). Finally, worms can sense gaseous concentrations, such as, O₂ and CO₂ which are thought to be directly linked to the presence of respiring bacteria with a large amount of food correlated with lower O₂ and higher CO₂ (Gray *et al.*, 2004; Bretscher *et al.*, 2008).

One hypothesis is that the presence of food could be detected by sensory neurons localised in the central nervous system. *C. elegans* have ciliated sensory neurons stacked within sensory organs localised in the head (amphids) (Ward *et al.*, 1975) and the tail (phasmids and deirids) (Hall and Russell, 1991). Sensory amphid neurons can sense a range of cues. For example, ASE gustatory neurons can sense salt and water-soluble attractants, including Na⁺, Cl⁻, cAMP, biotin, lysine, and serotonin (Bargmann and Horvitz, 1991). Amphid wing olfactory neurons, AWA, AWB and AWC sense volatile odours (Bargmann *et al.*, 1993; Chalasani *et al.*, 2007). Oxygen can be sensed by URX, AQR, and PQR neurons to avoid extremes of concentration (Gray *et al.*, 2004). Finally, physical stimuli can be sensed by mechanosensory neurons CEP, ADE and PDE (Hills *et al.*, 2004).

Studies have shown that bacteria can be detected by a chemosensory system to direct the worm towards food (Ward, 1973; Grewal and Wright, 1992; Pierce-Shimomura *et al.*, 1999; Gray *et al.*, 2005; Werner *et al.*, 2014). Similarly, worms can physically detect the presence of food by mechanosensation to adapt their locomotory behaviour in order to stay on the food patch (Sawin *et al.*, 2000; Flavell *et al.*, 2013). Furthermore, the chemosensory neuron AWC has been shown to selectively respond to the removal of food cues (Chalasani *et al.*, 2007) and in turn affect the locomotion. However, little is known about the nature, or site of detection, of the sensory modalities modulating the pumping behaviour in response to the shifting gustatory, olfactory, mechanosensory and nutritional cues in response to food or its absence.

In this chapter, the roles of chemosensory and mechanosensory modalities in the control of the worm's pumping behaviour on and off food have been further investigated. For this purpose, cilia mutants deficient in chemosensation were assessed for their "on" and "off" food pumping behaviours. Finally, mechanosensation was assessed using polystyrene microspheres to mimic the physical presence of bacteria.

6.2 Results

6.2.1 The role of ciliated sensory neurons in the regulation of pumping off food suggests central integration of the response to the absence of food

C. elegans nematodes direct their locomotion toward bacteria (chemotax) by detecting and following volatiles gradients and water soluble cues (Grewal and Wright, 1992). Most chemosensory neurons in *C. elegans*, localised in the amphid and phasmid organs, are ciliated, and their sensory functions are tightly linked to these cilia (Perkins *et al.*, 1986). Cilia defective mutants have thus been used to investigate the global role of sensory neurons from the central nervous system in the modulation of the pumping behaviour. Five different mutants have been used. *osm-3* encodes a kinesin-2 family member (Snow *et al.*, 2004), *osm-6* a component of the intraflagellar transport (IFT) particle (Collet *et al.*, 1998), *che-3* a dynein heavy chain (DHC) 1b isoform (Wicks *et al.*, 2000), *che-12* a protein involved in the formation of distal ciliary segments (Perkins *et al.*, 1986), and *che-13* encodes a component of the intraflagellar transport (IFT) complex B (Haycraft *et al.*, 2003). Overall, all these genes play a part in cilia formation and/or cilia maintenance and therefore in the sensory function of neurons (Kaplan and Horvitz, 1993). Each of these genes has a different pattern of expression, with the *osm-6(p811)* mutant expressed in most ciliated sensory neurons.

The pumping behaviour in the presence of food was first assessed, using the paradigm described in **Chapter 4 (Figure 37)**. Surprisingly, none of the

Chapter 6

cilia mutations appeared to affect the high pumping rate on food (**Figure 64A, B**), indicating that the sensory function of these neurons of the central nervous system is not required to regulate the pumping rate in the presence of food, suggesting that the chemosensory cues from the food are not sufficient to increase the pumping rate.

In contrast, all the cilia deficient mutants tested showed an aberrant pumping behaviour in absence of food. Indeed, both *che-3(e1124)* and *che-12(p1812)* mutants displayed a pumping rate similar to the paired *eat-4(ky5)* mutants (**Figure 64C**), while *che-13(e1805)* also pumped at a higher rate than N2 but not as high as *eat-4(ky5)* (**Figure 64D**). *oms-3(p802)* appeared to only have a limited effect, although significant, on the pumping behaviour off food with a maximum pumping rate of 44 ppm (**Figure 64C**). Interestingly, the mutant *osm-6(p811)* showed a markedly elevated pumping rate, reaching an even higher rate than *eat-4(ky5)* mutant (up to ~180 ppm) (**Figure 64C**).

Overall, these results indicate that ciliated sensory neurons specifically act in response to the removal of food to reduce the pumping rate.

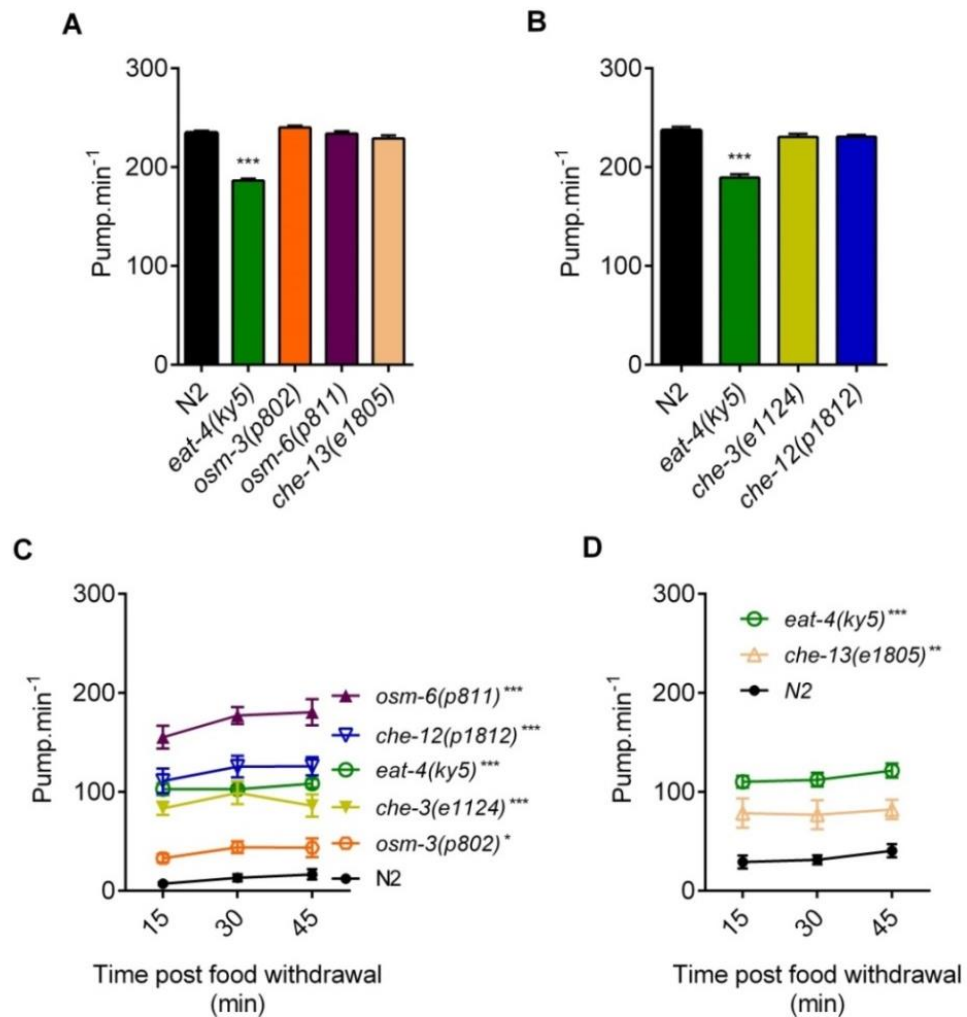


Figure 64: Mutations affecting cilia of sensory neurons selectively affect the pumping behaviour in absence of food.

A.B. In presence of food, none of the cilia deficient mutants displayed a significantly different behaviour relative to the paired N2 controls ($p = 0.99$ for each strain). In both experiments, *eat-4(ky5)* mutant strain displayed a slower pumping rate (-49 ± 3 ppm and -48 ± 5 ppm for **A** and **B** respectively; $p < 0.001$). **C.** In absence of food, cilia defective mutants pumped faster than the N2 paired control ($n = 9$); *osm-3(p802)* (27 ± 8 ppm; $3 p = 0.036$; $n = 7$), *osm-6(p811)* (162 ± 8 ppm; $p < 0.001$; $n = 7$), *che-3(e1124)* (79 ± 8 ppm; $p < 0.001$; $n = 7$) and *che-12(p1812)* (112 ± 8 ppm; $p < 0.001$; $n = 8$). Similarly to *eat-4(ky5)* (92 ± 8 ppm; $p < 0.001$; $n = 10$). *che-3(e1124)* ($p = 0.99$) and *che-12(p1812)* ($p = 0.188$) pumped at a similar rate to *eat-4(ky5)*, *osm-6(p811)* pumped faster (70 ± 8 ppm; $p < 0.001$) and *osm-3(p802)* displayed a lower pumping rate (-65 ± 8 ppm; $p < 0.001$) relative to *eat-4(ky5)*. **D.** *eat-4(ky5)* (79 ± 13 ppm; $p < 0.001$; $n = 8$) and *che-13(e1805)* (43 ± 12 ppm; $p = 0.005$; n

=11) pumped higher than the N2 paired control (n = 7). *che-13(e1805)* (-35 ± 12 ppm; p = 0.019) pumped lower than *eat-4(ky5)*.

Mutants assessed in parallel were plotted in the same graph.

6.2.2 No ciliated neurons are observed in the pharyngeal nervous system

Ciliated sensory neurons are only known in the central nervous system of the worm. Therefore, the results presented above would indicate that there is centrally integrated information modulating the pharyngeal pumping behaviour in the absence of food. However, analysis of the *eat-4* mutants phenotype off food showed pharyngeal nervous system is a major determinant in this behaviour (see **Chapter 4**). One could therefore hypothesise that the cilia mutations described above could affect pharyngeal neurons which haven't been previously reported to be ciliated, although some pharyngeal neurons such as NSM or I2 are thought to have sensory functions, but this is poorly defined (Albertson and Thomson, 1976; Axang *et al.*, 2008). In order to test this hypothesis, N2 worms were incubated with Dil, a dye known to fill neurons possessing cilia in contact with the environment; 6 amphid (ASI, ADL, ASK, AWB, ASH and ASJ) and the two phasmid (PHA and PHB) neurons (Herman, 1984).

Worms were then imaged with an epifluorescence microscope. To ensure fluorescence from pharyngeal neurons was not obscured by a stronger marking in somatic neurons, both intact worms and surgically isolated pharynxes (see **Chapter 4**) were observed. Pharynxes were isolated following 3 hours Dil incubation (10 µg/mL in M9) and 3 washing steps (M9) to ensure neurons were stained *in vivo*. In intact worms, head and tail neurons were marked in red (**Figure 65A-E**) as previously reported (Herman, 1984). However, no fluorescence was observed in pharyngeal neurons of isolated pharynxes. Fluorescence was only observed in the grinder, likely representing swallowed dye (**Figure 65E-G**).

These observations indicate there are no ciliated neurons in the pharyngeal nervous system, and suggest that the results observed with the cilia deficient

mutants are likely to be due to the disrupted function of sensory neurons from the central nervous system.

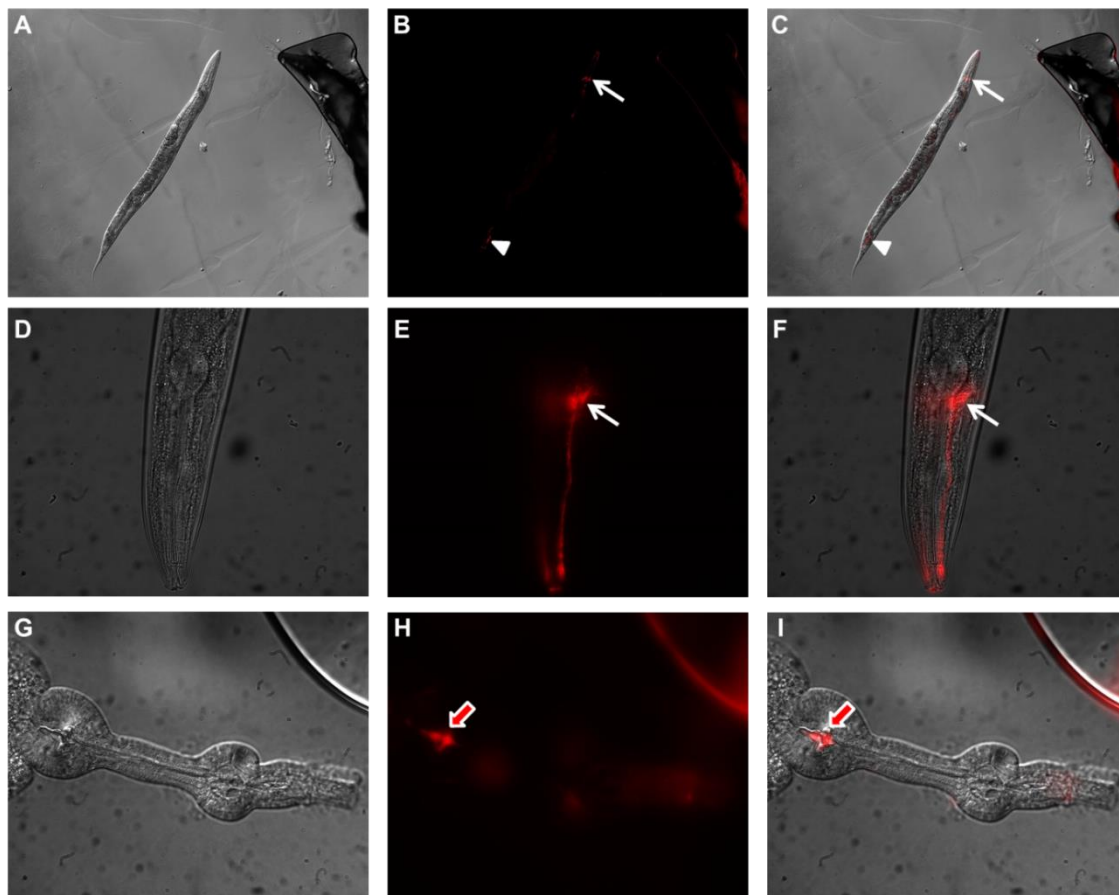


Figure 65: DiI staining does not stain pharyngeal neurons.

A-F. DiI staining of intact worms. DiI dye is taken up by neurons with functional cilia. Head and tails neurons are filled with dye. Michael Koelle's protocol (http://www.ihcworld.com/_protocols/lab_protocols/koelle-lab-protocols.htm) was used to stain amphid neurons ADL, ASH, ASI, ASJ, ASK, AWB (arrows) and phasmid PHA and PHB neurons (arrow heads).

G-I. Isolated pharynxes of worms incubated with DiI. Surgery took place after the staining process. No neuronal staining is observed. DiI is observed in the pharynx lumen in the grinder region (red arrows).

Two worms for each condition (intact and isolated pharynxes) were tested.

6.2.3 Cell specific restoration of glutamate transmission in the AWC sensory neurons is not sufficient to rescue the *eat-4* mutant aberrant pumping behaviour off food

The aberrant pumping rates off food displayed by the cilia deficient mutants suggest that the worm can perceive the removal of food cues, via the ciliated sensory neurons, to trigger an appropriate reduction of the pumping rate when food is lacking. Therefore, the inability of the glutamate deficient *eat-4* mutants to execute a reduction in pumping in the absence of food might relate to the recently identified glutamatergic dependence of an OFF signalling modality mediated by the AWC sensory neuron (Chalasani *et al.*, 2007). As the reduction of the pumping rate in the absence of food is an active process (i.e. not due to a lack of excitatory cues, see **Chapter 3**) one can hypothesise that the removal of cues from the food would act as an upstream cue that communicates into the pharynx to reduce pharyngeal function. To test if the critical determinant of the pumping behaviour off food lies at the level of the extrapharyngeal sensory systems that detect food removal, the consequence of selectively rescuing *eat-4* in the key odour off neuron AWC was investigated. Indeed, if AWC amphid chemosensory neurons have a basal activity in presence of odours, their removal would trigger a transient activity in AWC that is penetrant enough to regulate downstream circuits and robustly regulating local search area behaviour (Chalasani *et al.*, 2007). The consequence of AWC activation upon odour removal for pharyngeal function has not been investigated but represents an important route to mediate the kind of inverted signalling that underpins processes that allow OFF cues to trigger modulation of function. With respect to local area search, restoring *eat-4* expression in AWC in an *eat-4* mutant background is enough to at least partially rescue the locomotion behaviour of *eat-4* mutants (Chalasani *et al.*, 2007). Based on these results, whether the restoration of *eat-4* wild-type cDNA in AWC neurons under conditions that rescue the disrupted local area could similarly rescue the *eat-4* dependent disruption of the pumping behaviour off food was tested.

eat-4 mutants were first compared to the transgenic line and measured for their local search area phenotype (reversals followed by Omega turns). This experiment was conducted as a positive control to validate the construct efficiency to restore *eat-4* expression in AWC. Indeed, *eat-4(n2474); Ex[PAWC::*eat-4*]* strain also displayed a partially rescued locomotion phenotype

(reversals followed by Omega turns) compared to *eat-4(n2474)* during the first 6 min post food removal (**Figure 66A**). The phenotype was rescued for the 5 following minutes (**Figure 66B**).

The pumping behaviour was next investigated against this background of a AWC dependent rescue of *eat-4* locomotion deficiency. Restoring *eat-4* expression in AWC had no effect on the pumping deficiency on food as indicated by the low pumping rate displayed by *eat-4(n2474); Ex[PAWC::*eat-4*]*, similarly to *eat-4(n2474)* (**Figure 66C**). In a similar way, and unlike locomotion, restoring *eat-4* expression in AWC did not rescue the off food phenotype (**Figure 66D**) thus indicating the glutamate transmission from AWC, an important off food signalling neuron, does not provide a significant determinant of the active modulation that produces a reduced pumping rate in response to food withdrawal.

These results suggest that an important glutamatergic regulator of OFF signalling does not underpin the active suppression of pumping that follows removal of the food cue.

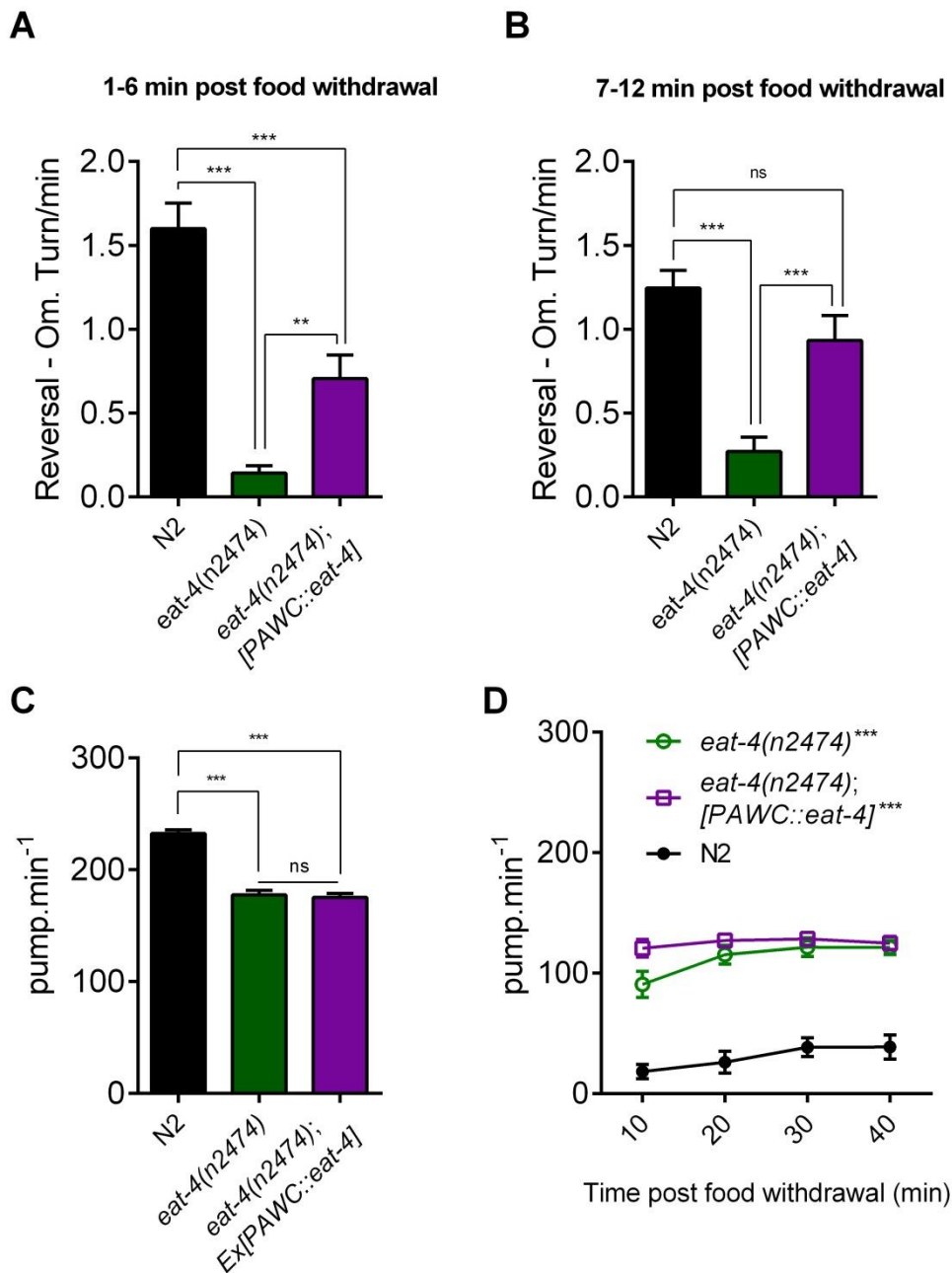


Figure 66: Rescue of *eat-4* in AWC sensory neurons does not restore glutamatergic dependent regulation of pharyngeal pumping ‘on’ and ‘off’ food.

The number of omega turns preceded by a reversal (rev-Om) was assessed for 2 periods of 5min following food withdrawal as detailed in Chalasani *et. al* 2007.

A.B. *eat-4(n2474)* displayed a significant defect in the locomotion pattern with a reduced number of rev-Om during both the first ($p < 0.001$) and second period of time ($p < 0.001$).

Rev-Om in *eat-4(n2474); [PAWC::eat-4]* was also significantly reduced compared to N2 in the first 5min period ($p < 0.001$) but not during the second period ($p = 0.209$). Moreover, the number of rev-Om in the transgenic line was significantly higher than in *eat-4(n2474)* during both periods of time ($p = 0.008$ and $p < 0.001$ respectively) measured. Between 14 and 15 worms were used per strain.

C. In the presence of food, both *eat-4(n2474)* and *eat-4(n2474); [PAWC::eat-4]* pumping rates were significantly lower than the N2 paired control ($p < 0.001$) and no difference was observed between the two strains ($p = 0.999$). 9 to 10 worms tested per strain.

D. In absence of food, *eat-4 (n2474)* and *eat-4(n2474); [PAWC::eat-4]* ($p < 0.001$) displayed a significantly higher pumping rate ($p < 0.001$) relative to paired N2 control. *eat-4(n2474)* and *eat-4(n2474); [PAWC::eat-4]* pumping rate off food were similar ($p = 0.218$). 8 to 10 worms tested by strain.

6.2.4 Glutamatergic thermo/CO₂ sensory neuron AFD modulates the pumping behaviour off food

The second neuron tested for a role in the reduction of the pumping rate in response to food removal was the AFD pair of glutamatergic neurons. AFD is a thermo/CO₂ sensory neuron expressing the genes *osm-6* and *che-3*, involved in the formation and/or function of the cilia (Collet *et al.*, 1998; Wicks *et al.*, 2000). Mutants for both genes are characterised by a markedly elevated pumping rate in absence of food (**Figure 64C**). However, *osm-3* is not expressed in AFD neurons (Tabish *et al.*, 1995). This is interesting as *osm-3(p802)* mutants only showed a weak increased pumping rate off food, suggesting that neurons affected by the *osm-3* mutation are not major determinants for the regulation of the pumping behaviour off food. Although this specific pattern of expression is not exclusive to AFD, the existence of the *ttx-1(p767)* mutant makes the investigation of AFD's role rapidly assessable. Indeed, *ttx-1* encodes for a homeodomain protein, a member of the OTD/OTX subclass of homeodomain transcription factors, which has a significant role in

Chapter 6

the specification of AFD and associated thermosensory function. Its transcription regulation underpins normal expression of genes such as *gcy-8*, *nhr-38*, *ceh-14*, *tax-2*, and *dac-1* (Satterlee *et al.*, 2001).

When food is available, *ttx-1(p767)* mutants displayed a significantly lower pumping rate relative to N2 paired controls but the deficit in phenotype was not as profound as *eat-4(ky5)* mutants (**Figure 67B**). This result indicates that AFD contributes to the stimulatory pathways that sustain the high pumping rate on food. In contrast, in absence of food, *ttx-1(p767)* displayed an elevated pumping compared to N2 worms, indicating a role in the reduction of the pumping rate in response to the removal of food (**Figure 67C**). However, this enhanced pumping was more modest than *eat-4(ky5)* (**Figure 67C**). Together, these results indicate that the glutamatergic sensory neurons AFD have opposite roles depending on the food context, acting to reduce the pharyngeal pumping rate in the absence of food, and stimulating pumping in response to food.

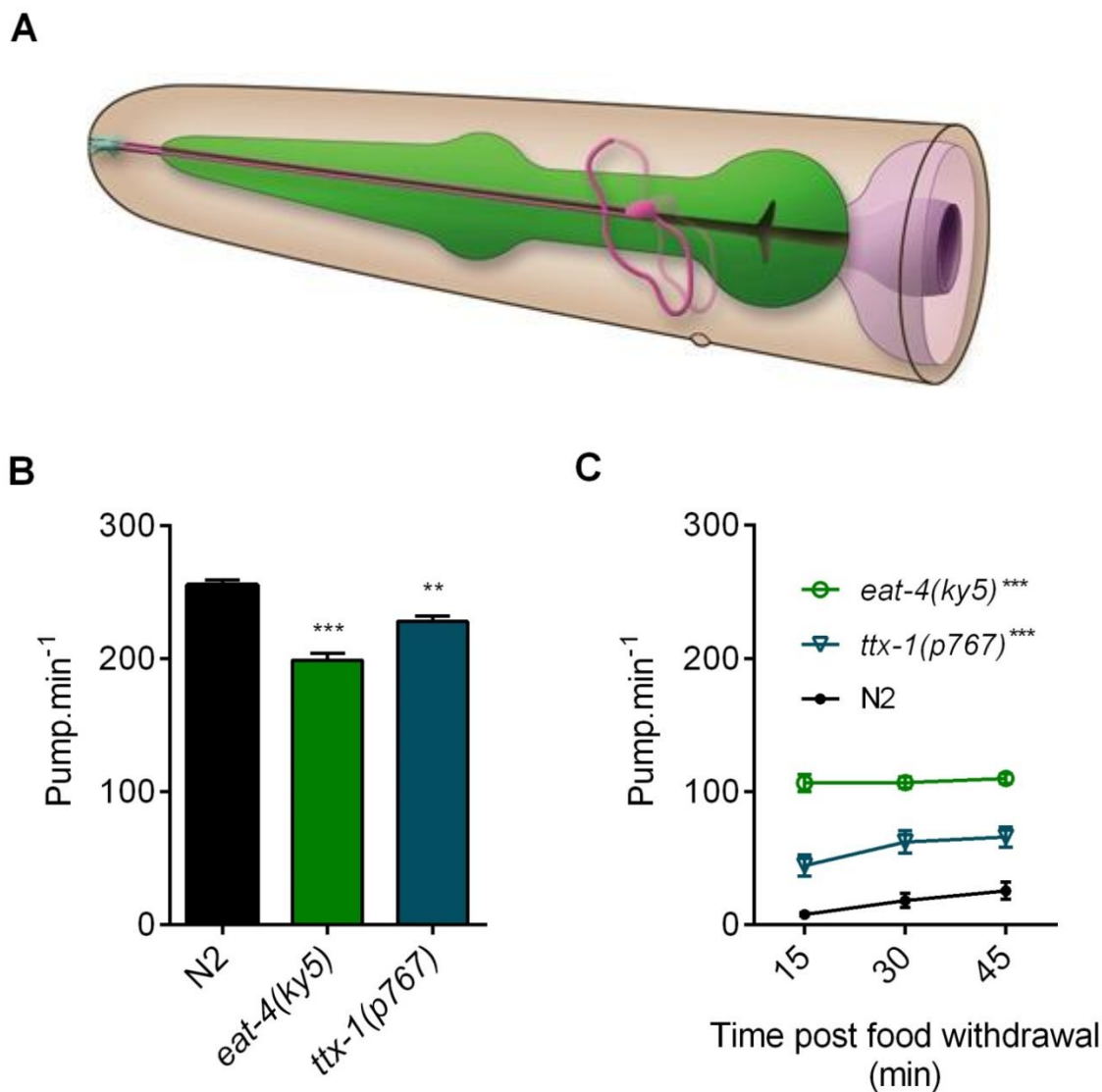


Figure 67: Glutamatergic neuron AFD has an opposite effect on the pumping rate in presence and in absence of food.

A. Cartoon representation of the pharyngeal neuron AFD. Taken from *WormAtlas*

B. In the presence of food, *ttx-1(p767)* ($n = 7$) pumped at a lower rate than the N2 ($n = 8$) paired control (-27 ± 6 ppm; $p = 0.001$) but faster than *eat-4(ky5)* (29 ± 6 ppm; $p < 0.001$; $n = 11$). *eat-4(ky5)* displayed a lower pumping than N2 (-56 ± 6 ppm; $p < 0.001$).

C. In the absence of food, *ttx-1(p767)* ($n = 12$) pumped at a higher rate than N2 ($n = 11$) (40 ± 6 ppm; $p < 0.001$) but lower than *eat-4(ky5)* ($n = 13$) (90 ± 6 ppm; $p < 0.001$). *eat-4(ky5)* displayed a significantly faster pumping rate than N2 ($p < 0.001$).

6.2.5 Physical contact with food is required to increase the pumping rate

According to the results described in this chapter, the absence of chemosensory cues is crucial for a normal pumping behaviour off food. However, in the presence of food, chemosensory modality appears not to be required for normal pumping. One could hypothesize that gustatory or mechanosensory modalities may be involved, and therefore that contact with food must be required to induce a high pumping rate. In order to test this hypothesis, a re-entry on food experiment was designed. Briefly, three synchronised L4+1 worms were transferred onto a no food arena for cleaning for 1 min. The worms were then transferred to the edge of a food-containing plate, i.e. outside the patch of bacteria (**Figure 68A**). An individual worm was observed (one going towards the food) and the pump frequency recorded as soon as the nose of the worm was in contact with the food. Importantly, the worms were not reaching the bacteria before at least 5 min post transfer onto the plate, which ensured that no mechanosensory effects of the harsh touch were observed. While moving towards the food, N2 worms displayed a normal slow pumping rate off food (data not shown) as can be observed by an average pump frequency during the first second post contact with food of around 1.3 Hz (**Figure 68B**). Interestingly, the pump frequency rapidly increased to 4 Hz within around 10 seconds of entering the food lawn.

These results confirmed that 'smelling' odours from food is not sufficient for the worm to trigger a high pumping rate, but that direct contact with the food is required. As suggested by the sudden increase in the first 2 seconds (pumping rate starts being recorded when worm's tip touches the food) and direct visual observation, the pump frequency starts increasing as soon as the worm's lips touch the food, suggesting that ingestion of bacteria is required to increase the pumping rate.

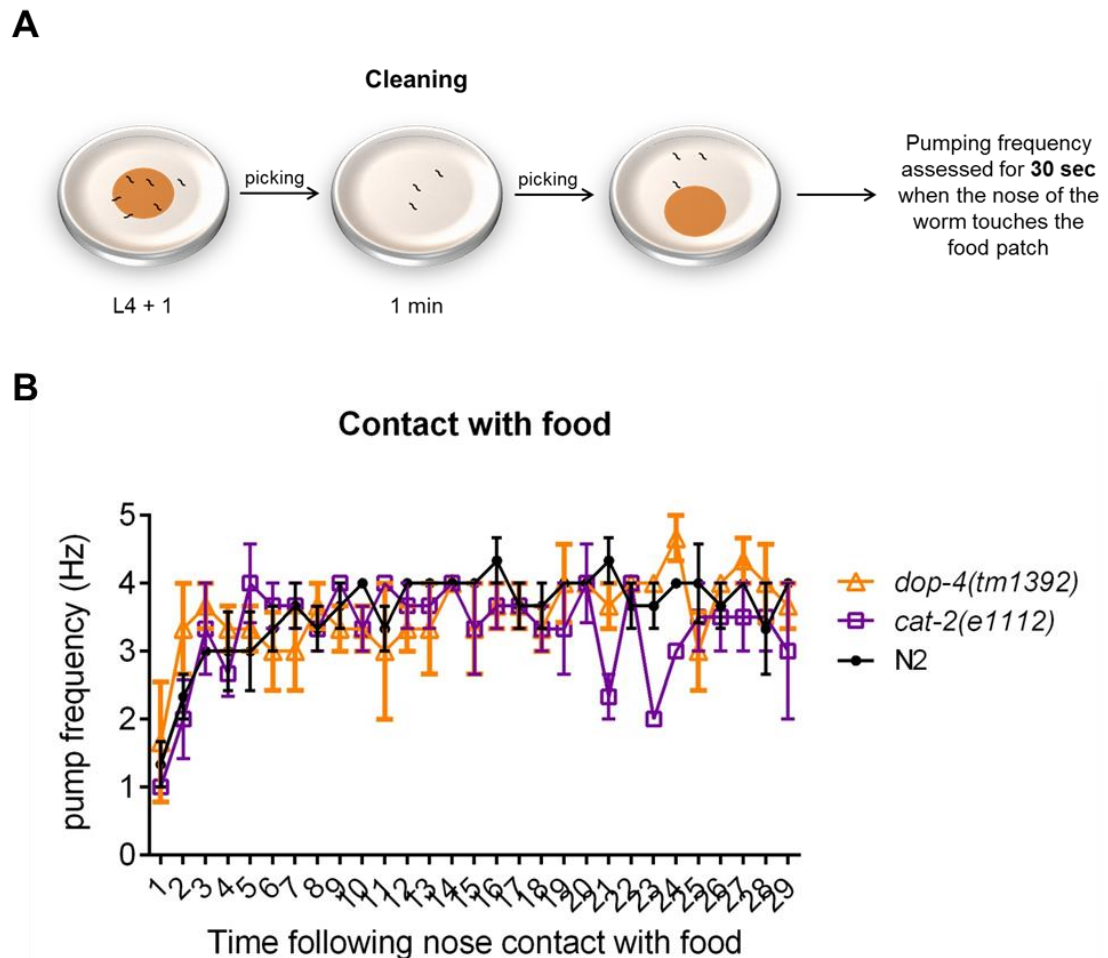


Figure 68: Pumping increase following contact with food appears not to require dopamine signalling.

A. 3 L4-1 synchronised worms were transferred onto a ‘cleaning’ plate for 1 min before being picked onto a non-seeded edge of a bacteria lawn containing plate. Pump frequency was assessed as soon as the top of the nose of one worm touched the bacteria lawn using an online counter

(<http://wormweb.org/countdown>).

B. Worms did not initiate an increase of pumping rate prior to contact with the bacteria lawn, displaying a pump frequency of around 1 Hz. A fast increase was observed immediately prior to contact with food, with a pump frequency reaching a normal on food value (> 4 Hz) 7-10 seconds after nose contact. Both *cat-2(e1112)* ($p = 0.842$) and *dop-4(tm1392)* ($p = 0.99$) showed no significant differences with N2. 3 worms were tested.

6.2.6 Dopaminergic signalling is not required for the high pumping rate observed upon contact with food

The worm's locomotory behaviour is food-dependent (see **section 1.2.1.2**). Notably, when in contact with food, worms display an Area-Restricted Search (ARS) behaviour characterised by an increase in turning events permitting a longer stay in the same area. Interestingly, this ARS behaviour has been shown to be dependent of dopaminergic signalling. The presence of food is proposed to be physically perceived by dopaminergic mechanosensory neurons (ADE, PDE and CEP), triggering release of dopamine which in turn promotes the ARS behaviour by increasing frequency of high-angled turns (Hills *et al.*, 2004). Furthermore, ablation of dopaminergic neurons reduces the slowing response to food (Sawin *et al.*, 2000). Therefore, mechanosensation of food by dopaminergic neurons appears to play an important role in the detection of food and thus in the modulation of food related behaviour.

To test whether dopaminergic signalling was also required for the re-entry on food pumping behaviour, two mutants strains *cat-2(e1112)*, encoding a tyrosine hydroxylase affecting the dopamine levels, and *dop-4(tm1392)*, encoding a pharyngeal dopamine receptor, were tested for their re-entry on food behaviour. Neither *cat-2(e1112)* nor *dop-4(tm1392)* showed any difference in the rate at which they shifted and sustained the high pump rate with the paired N2 controls, suggesting that dopaminergic signalling is not modulating the increase of pumping rate in response to contact with food (**Figure 68B**).

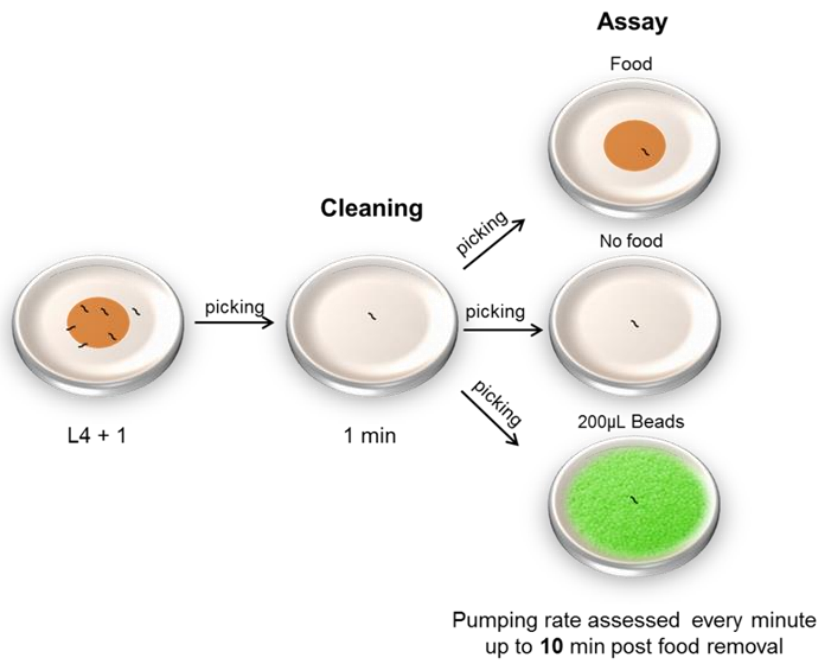
6.2.7 Mechanosensory cues trigger a burst in pumping rate

The physical presence of food increases the pumping rate. However, how food is being perceived remains unclear. In a simple model, food can be physically perceived by two sensory modalities; gustatory or mechanosensory. To test the latter, fluorescent polystyrene beads (microspheres) were used to mimic the physical presence of food. To stay as close as possible to the size of OP50 bacteria (Fang-Yen *et al.*, 2009), 0.50µm diameter Fluoresbrite® YG

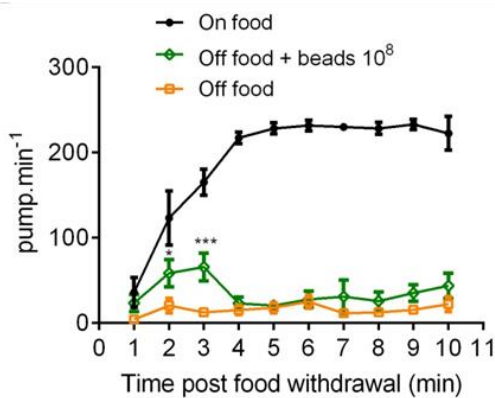
Carboxylate Microspheres (Polysciences, Inc.) were used. Furthermore, two previous studies have shown the worm's ability to swallow and accumulate these beads in the intestine (Fang-Yen *et al.*, 2009; Kiyama *et al.*, 2012). A preliminary experiment was designed to compare the effect of contact with beads on the pumping behaviour with contact of OP50 (**Figure 69A**). Briefly, L4 + 1 synchronised worms underwent a 1 min cleaning step before transfer onto an OP50 containing plate, a no food arena or a plate coated with beads. The pumping rate of an individual worm was assessed every minute for 10 min.

As previously described (see **Figure 26B**), when placed back on food, worms recovered a normal pumping rate in less than 5 min in the presence of food (**Figure 69B, C**). In the absence of food, worms displayed a typical pumping rate (~15 ppm). When placed in the presence of beads, worms displayed a short but significant increase of their pumping rate after 2 and 3 min (~65 ppm after 3min). However, this elevation of pumping was not sustained and the pumping rate was then similar to the no food condition. Interestingly, almost each of the 9 worms tested on beads showed a transient burst in pumping during the 10 min of this assay, with some individual pumping rates reaching well above 100 ppm, a phenomenon never observed in absence of food. This effect of the beads is represented by the scatter point representation (**Figure 69C**).

A



B



C

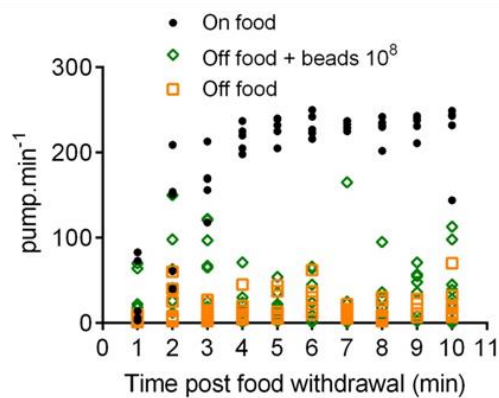


Figure 69: Physical contact with beads triggers a transient increase of the pumping rate.

A. Schematic representation of the assay. Synchronised L4 + 1 worms were transferred for 1 min onto a cleaning plate then picked onto either a seeded plate, a non-seeded plate or a plate seeded with 10^8 beads spread in total.

B. In the presence of food, worms recovered a normal pumping rate (> 200 ppm) 4 min after they were placed onto the assay plate. The presence of beads did not significantly change the average pumping rate of N2 worms off food ($p = 0.1108$; $n = 7$ off food and $n = 9$ on beads). Transient increase of pumping were observed in the presence of beads, with a significantly higher pumping rate observed after 2 min ($p = 0.039$) and 3 min ($p < 0.001$) in the presence of beads. Burst of increased pumping rate with beads can be observed in figure **C.**, a scatter point representation of **B.**

To try to determine why the elevation of the pumping rate was not sustained, fluorescent images of the worms were taken after 10 min of contact with beads. Interestingly, beads were mainly localised in the pharynx lumen in the isthmus region (**Figure 70**). Beads were only rarely observed in the intestine and in small quantities as observed on **Figure 70E**.

Overall, these observations suggest the accumulation of beads in the isthmus clog the pharynx and could therefore explain why the worms only show bursts of pumping in the presence of beads.

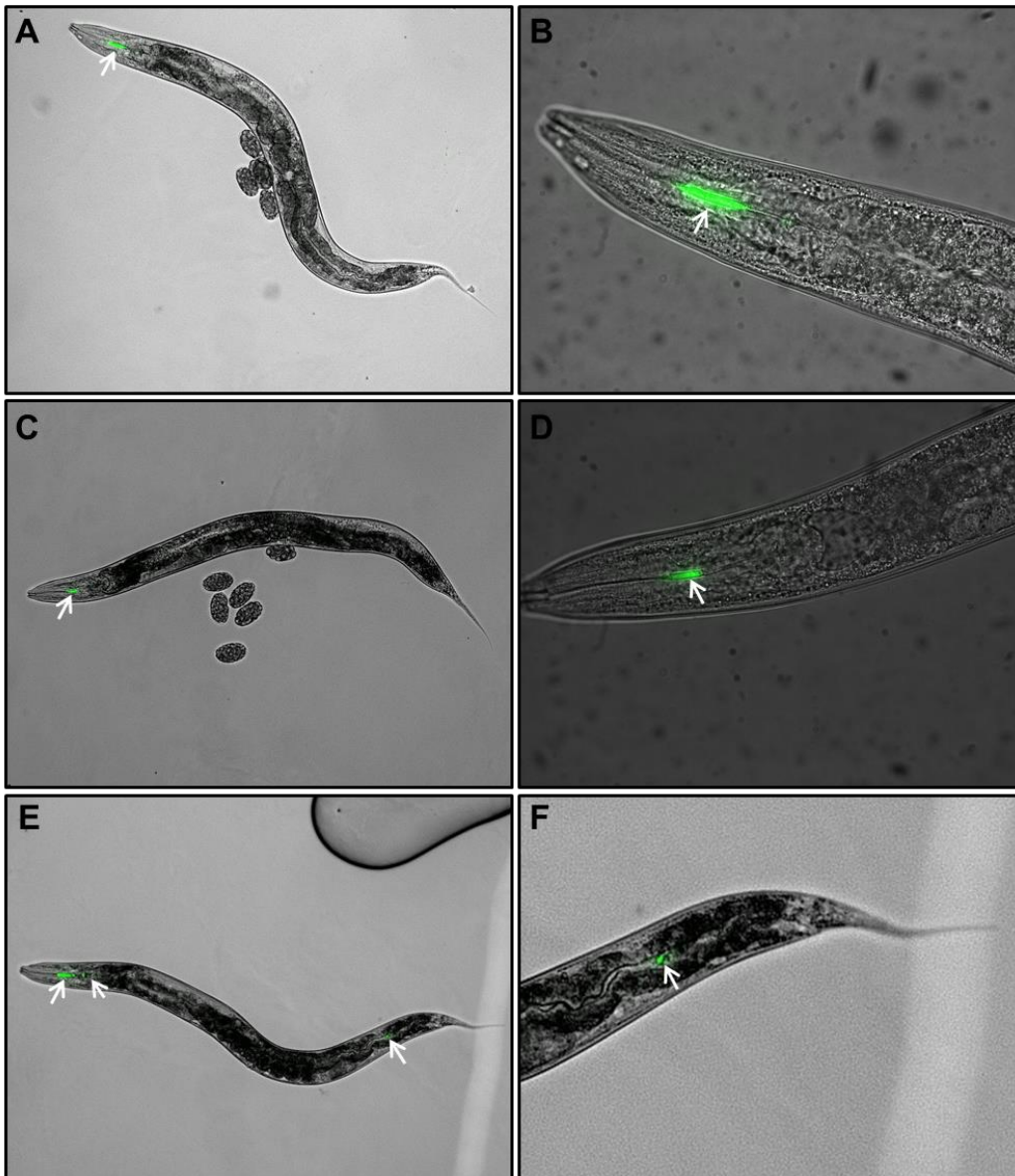


Figure 70: Epi-florescence microscopy images of worm fed with 0.5 μm beads for 10 min.

A.-F. Representative epifluorescence microscope images of worms exposed to Fluoresbrite® YG Carboxylate Microspheres for 10 min.

After 10 min of incubation with beads, accumulation was observed in the isthmus in all worms. Only one worm was observed with a few beads in the intestine (E. F.).

Arrows indicate the location of the beads in the gut.

6.2.8 Prolonged exposure to beads increases the pumping rate

The protocol described above failed to see bead accumulation past the pharynx. However, a previous study using these polystyrene microspheres had shown accumulation in the intestine (Kiyama *et al.*, 2012). To investigate if longer bead incubation time would permit the worms to ingest the beads and if the enteric accumulation was important in pumping, a new experiment was designed. Following the initial 1 min cleaning step, worms were either transferred onto a control plate which has been previously spread with 300 μ L of S-basal (the solution used to dilute the beads) or onto a plate containing 300 μ L of beads (**Figure 71A**). The pumping rate was assessed for 1 min after 30 and 60 min post removal of food.

After 30 min, N2 worms on beads pumped at an elevated rate (\sim 60 ppm) relative to the no beads condition (\sim 15 ppm) (**Figure 71B**). Interestingly, after 60 min, the pumping rate of worms placed on beads was further increased reaching around 150 ppm. Furthermore, the pumping rate displayed by the worms on the plates spread with S-basal displayed a pumping rate similar to that expected off food, indicating that the increase observed in the presence of beads is not due to the S-basal. Together, these results indicate that the prolonged presence of a mechanical stimulus is able to stimulate the pumping rate.

Finally, worms which have been in contact with beads for 30 min were imaged. Accumulation of beads was still observed in the isthmus, however, unlike that previously observed after 10 min of contact with beads, the presence of microspheres was detected in the worm's intestine (**Figure 71C**), suggesting a correlation between the ingestion of beads and a sustained increase in the pumping rate.

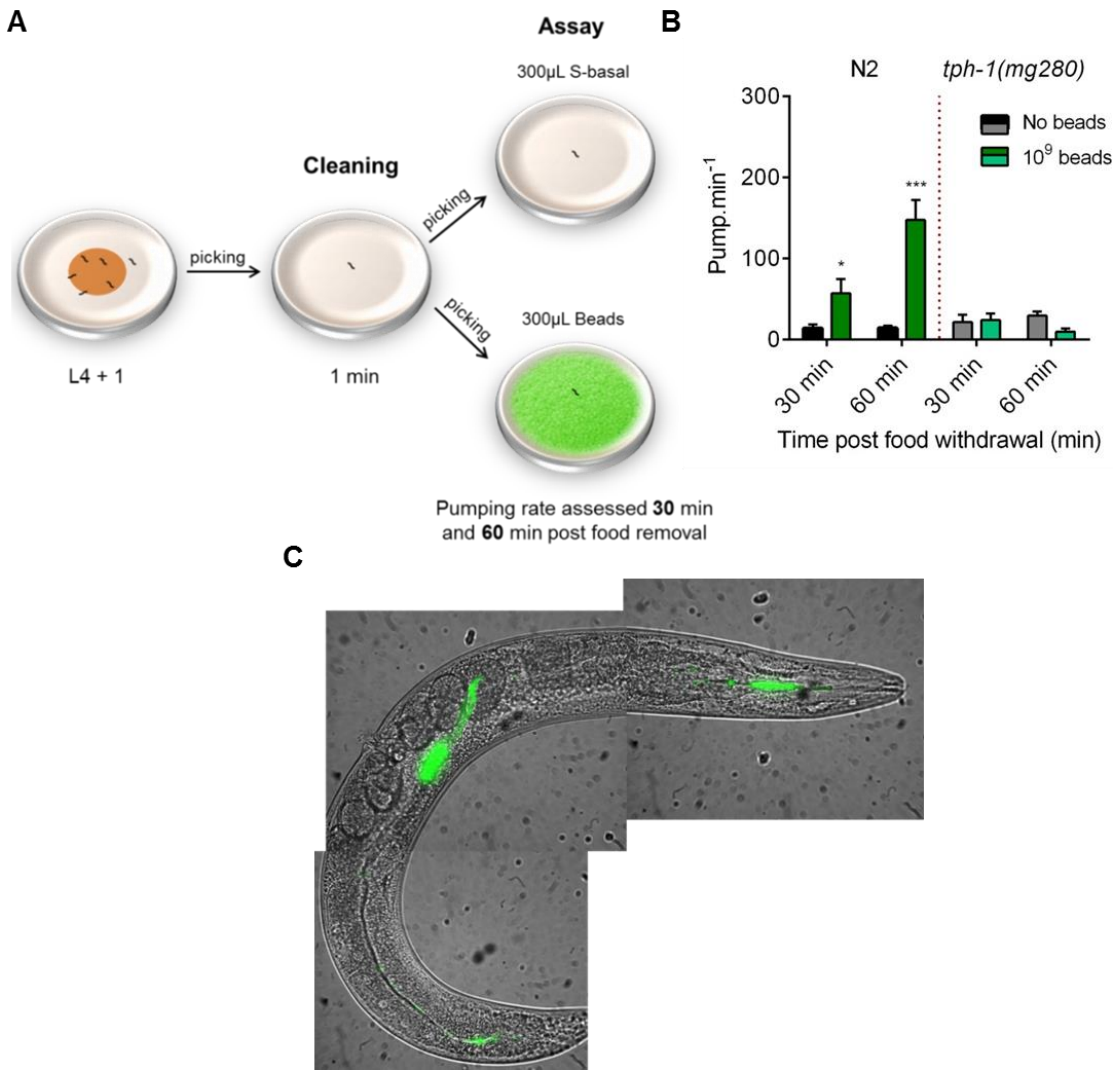


Figure 71: High pumping rate observed after an hour in the presence of bead is 5-HT-dependent

A. Schematic description of the experiment. After transfer onto a cleaning plate, synchronised L4 + 1 worms were either picked onto a control plate spread with 300µL of S Basal or 300µL of 10⁹ beads/mL (3.10⁸ beads per plate).

B. N2 worms displayed an increased pumping rate after 30min (43 ± 16 ppm; p = 0.026 n = 6) and 60 min (133 ± 15; p < 0.001 n = 4 and 5) in presence of beads. In contrast, *tph-1(mg280)* mutants did not increase their pumping rate neither after 30min (p = 0.99 n = 7) nor 60 min (p = 0.346 n = 5 and 6) in the presence of beads.

C. Collage of 100X images of a representative N2 worm 'fed' with beads for 30 min. 2 worms were observed.

6.2.9 Increase of pumping rate in response to prolonged exposure to beads is dependent on 5-HT signalling

To better determine the mechanism controlling this pumping response to prolonged exposure to beads, a mutant analysis was conducted. A recent study showed that the pharyngeal neuron NSM released 5-HT in response to food to modulate the worm's locomotory behaviour (Flavell *et al.*, 2013). The released 5-HT from NSM is believed to act outside of the pharynx suggesting the possibility that food is being detected from inside the pharynx (Flavell *et al.*, 2013). 5-HT signalling was therefore a good candidate to modulate the increase of pumping in response to the mechanical stimulus from the beads. In this regard, the *tph-1(mg280)* mutant, deficient in 5-HT biosynthesis was assessed for its pumping rate in response to beads. Interestingly, no increase of pumping rate was observed both after 30 and 60 min of contact with beads, worms were pumping at a similar rate relative to the *tph-1(tm280)* on S-basal (Figure 71B).

These results indicate that 5-HT is a major determinant in the elevation of the pumping rate observed in response to prolonged exposition to beads.

6.3 Discussion

6.3.1 Pharyngeal pumping rate is reduced in response to the absence of bacterially derived chemosensory stimulation

In this chapter the role of sensory modalities in the perception of food and the subsequent modulation of the pumping behaviour were investigated. A chemosensory role was assessed using cilia deficient mutants, in which ciliated sensory neurons are not functional. Ciliated neurons as defined by the expression and dependence on the presence of a cilium, only appear to be present in the central nervous system, as reinforced by the Dil staining analysis (Figure 65). The published expression pattern of *che-3* indicates expression in the pharyngeal neuron tentatively identified as I4, however, only a weak expression was observed, and only in a subset of animals (Wicks *et al.*, 2000).

Chapter 6

Furthermore, I4 morphology does not suggest potential sensory functions (Albertson and Thomson, 1976). Behavioural analysis of these cilia mutants surprisingly revealed no role for their function in the control of the high pumping rate observed in the presence of food, indicating that the detection of odours from the food is not sufficient to trigger a pharyngeal response. In contrast, all the cilia mutants assessed in this chapter displayed an elevated pumping rate in absence of food, indicating ciliated sensory mutants play a role in the reduction of the pumping rate observed in response to food removal and indicate that the removal of food itself is being perceived by these neurons.

A previous study investigated the effects of three other cilia deficient mutants, *che-2*, *che-11* and *osm-5* on the pumping rate (Lee *et al.*, 2011). All of them displayed a similar pumping rate to N2 in the presence of food, similarly to the mutants tested here. The authors did not observe any effect of these mutations on the pumping rate off food. However, they used a different paradigm to the one used here, and the pumping rate displayed by the N2 worms was higher than reported here (*i.e.* 80% of the well-fed pumping rate), which could explain why no effect in these mutants is apparent. Furthermore, the time for which the worms have been food deprived in this experiment is not known, and the pumping rate has only been assessed for 10 sec.

Interestingly, from the cilia mutants assessed, *osm-6*, which is expressed in most ciliated neurons (Collet *et al.*, 1998), displayed the most severe phenotype off food, with a pumping rate higher than *eat-4* mutants, indicating that ciliated mutants account for most of the reduction effect in response to food removal. However, this result does not exclude the possibility of having the removal of food sensed by the pharyngeal nervous system as a reduction of around 80 ppm is still observed when *osm-6(p811)* mutants are transferred from a food to a no food arena (**Figure 64C**), indicating a circuit reducing the pumping rate is still active in this mutant. Since the *osm-6* mutation affects most sensory neurons of the central nervous system (Collet *et al.*, 1998), this is consistent with the suggestion of a role for a circuit intrinsic to the pharynx. Analysis of double mutants for cilia genes, encompassing all ciliated neurons, or I2 ablation in an *osm-6* mutant background would add weight to this hypothesis.

6.3.2 The rate of pumping as the worm enters a bacterial lawn

In the earlier experiments designed in **Chapter 3** worms were transferred from food to a food free arena by picking. To investigate the converse of this, and to avoid the confound of pick-mediated inhibition of pumping an assay was designed around the transition from no food to food by visual observation of a worm as it spontaneously entered a food lawn. Interestingly, no elevation of pumping rate was observed in an off food worm while moving towards food from a bacteria-free part of a plate (**Figure 68B**). This would indicate that while the removal of odours from food is crucial to actively trigger a reduction of pumping, the reintroduction of bacteria-associated odours does not reverse this reduction. Therefore, it is possible that once activated, the reduction of pumping is sustained further down in the circuit, and that activation of another circuit in response to food is required to actively act against the inhibitory tone instigated by original removal from food.

6.3.3 Glutamate transmission from AWC neurons is not sufficient to modulate the pumping rate

Nonetheless, taken together, these results not only suggest that it is the removal of food itself which is sensed to trigger an active reduction of pumping, but also indicate that the increase of the pumping rate in the presence of food is not initiated by the sensing of the food cues by the ciliated sensory neurons outside the pharynx. In this regard, glutamate transmission in AWC sensory neurons is known to mediate olfactory perception and locomotory response to odour withdrawal (Chalasanani *et al.*, 2007; Chalasanani *et al.*, 2010). However, the restoring of *eat-4* expression specifically in AWC did not rescue the *eat-4* mutant pumping behaviours (**Figure 66C, D**). This result could suggest AWC is not involved in the control of the pumping behaviour off food, however, it is not implausible that AWC affects this behaviour in a glutamate independent manner. Alternatively, it is possible that the putative effects of AWC on the pumping rate act through another glutamatergic neuron downstream of AWC. Indeed, supposing that AWC is sensing the removal of

food, AWC output would eventually have to impinge on the pharyngeal nervous system and/or the pharynx to act on the pumping frequency.

6.3.4 Glutamate signalling in the central nervous system from AFD sensory neurons modulates pumping behaviour on and off food

The investigation was extended to consider the role of the glutamatergic ciliated thermo/CO₂ sensory neuron AFD. AFD which expresses *osm-6* and *che-3* was directly investigated using a mutant for *ttx-1*. This transcription factor is required for the specification of AFD. *ttx-1(p767)* mutants showed a context-dependent pumping behaviour indicating a stimulatory role in the pumping rate on food and a role in the reduction of pumping in absence of food. Since AFD are glutamatergic neurons, and although the glutamate dependence of AFD remains to be proven, AFD could account for part of the glutamate-dependence of the pumping behaviour off food. Part only, since the elevated pumping rate displayed by *ttx-1* mutants is lower relative to *eat-4* mutants, quite similar to the pumping rate displayed by the glutamate-gated chloride channel *avr-14* mutants (see **Figure 43D**). This is interesting as the pharyngeal neurons I2 have been shown to account for around half of the glutamate dependence of pumping (see **Figure 46C**), and therefore, it is possible that AFD accounts for the remaining half. This would lead to a model in which in response to food removal, glutamate is released both from the central and the pharyngeal nervous system to reduce the pumping rate. However, it is also possible that AFD and I2 act in the same circuit and the analysis of the effect of I2 ablation in a *ttx-1(p767)* mutant background would help clarify this.

The fact that *ttx-1* has a role in the pumping rate on food appears to conflict with the lack of effect of *osm-6* and *che-3* and either suggests that the role of AFD in the presence of food is not sensory (AFD could act as an interneuron) or that AFD neurons have sensory functions which do not utilize functional cilia. However, in absence of food, AFD likely acts as a sensory neuron. AFD can perceive changes in CO₂ concentration or in temperature (Mori and Ohshima, 1995; Bretscher *et al.*, 2011). Therefore, one could imagine that the change in CO₂ concentration between the presence and the absence of respiring bacteria might be sensed by AFDs which in turn trigger an

appropriate pharyngeal response. Together, these results not only show a role for AFD in the regulation of the pumping behaviour but also confirm that the pumping rate off food is regulated in part from outside of the pharynx. Furthermore, the opposite effect displayed by *ttx-1(p767)* mutants, depending on the food context, once again reinforces the idea that the pumping rate on and off food are modulated by distinct pathways.

6.3.5 Physical contact with food increases the pharyngeal pumping rate in a dopamine-independent fashion

Ciliated sensory neurons do not modulate the pumping rate in response to food cue, indicating that chemosensory cues from food do not trigger an increase of pumping rate. Therefore, the presence of food must be perceived by another sensory modality, involving proximal or direct contact with food, such as gustatory or mechanosensory modalities. A food assay was conducted to test this theory (**Figure 68A**), showing worms start increasing their pumping rate almost immediately after the worms' lips contact with the food. Interestingly, this result reinforces the idea that the 'fictive feeding' observed off food, a slow basal pumping rate (see **Chapter 3**), is important to sample the environment, bringing the food cues into the pharynx where they can be perceived. Alternatively it is possible that gustatory cues are being perceived by receptors localised on the sensory neurons of the central nervous system.

Dopamine is known to be an important determinant in the regulation of the worm's locomotory behaviour when it is in contact with food (Sawin *et al.*, 2000). Indeed, when in contact with food, dopaminergic mechanosensory neurons release dopamine which acts with glutamate to mediate the Area-Restricted Search behaviour, characterised by an increase of high-angled turns in order to restrict the search around the area where food was last found (Hills *et al.*, 2004). However, preliminary experiments performed in this chapter suggest dopaminergic signalling is not required for the change of pumping behaviour when entering food, as the dopamine deficient *cat-2* and the pharyngeal dopamine receptor *dop-4* mutants displayed a similar re-entry

phenotype to N2 (**Figure 68B**). These results reinforce the non-involvement of dopamine in the pumping behaviour on food observed in **Chapter 3**.

6.3.6 Mechanosensory cues in the pharynx increase the pumping rate in a 5-HT-dependent fashion

The high rate characterising the pumping behaviour on food requires physical contact with food. This confirms the involvement of either or both mechanosensory and gustatory modalities. The role of the former was investigated in this chapter using polystyrene microspheres, mentioned as beads here, to mimic the physical presence of bacterial food. Given that the main mechanosensory neurons localised in the worm central nervous system are dopaminergic, the non-involvement of dopamine signalling in this specific behaviour hinted toward a mechano-detection from within the pharynx. In this regard, beads small enough for the worm to swallow were chosen. Previous studies showed that worms could pump and ingest beads with a diameter less than 4.5 μm (Fang-Yen *et al.*, 2009). However, to stay closer to the size of their usual source of food, the *E. coli* OP50, beads with a diameter of 0.5 μm were chosen. Indeed, 0.5 μm corresponds to the bacterium's short axis (Fang-Yen *et al.*, 2009) and a previous study showed worms were able to swallow and ingest these specific beads (Kiyama *et al.*, 2012).

To first investigate the immediate effect of contact with beads, worms were transferred onto a plate spread with beads following a cleaning step. The pumping rate was then immediately assessed every minute for 10 min (**Figure 69A**). When placed in contact with beads, worms displayed a burst of pumping rate during the first 10 min. However, this elevation was not sustained, and microscope observation after 10 min in contact with beads showed beads were clogged in the isthmus region of the pharynx. This could explain why elevation of the pumping rate was not sustained. One reason for the beads to jam the worm's pharynx could come from the difference between beads and the bacterial lawn. Indeed, in the bacterial lawn on the agar plate, the bacteria are

bathed in liquid, which might facilitate ingestion. This is not the case with the beads, as their solvent, S-basal, is absorbed by the agar. However, Kiyama and colleagues showed that beads were present in the worm's intestine after 15 min (Kiyama *et al.*, 2012).

Effects of prolonged contact with beads were then investigated. This time, worms were placed in bead-containing arena and the pumping rate assessed after 30 min and 60 min. Interestingly, the pumping rate of N2 worms in contact with beads was significantly increased, reaching 150 ppm after 60 min of exposure, relative to S-basal control (**Figure 71B**). Observation of microscope images revealed that beads were indeed ingested after 30min of exposure. This reinforced the idea that beads clogging the pharynx cause the cessation of the initial increase of pumping following contact with beads. These results suggest that mechanical stimuli perceived in the pharynx trigger an elevation in the pumping rate. However, the possibility that the physical presence of the beads is being perceived outside of the pharynx cannot be ruled out, and further experiments, using beads worms cannot swallow, are required to test this hypothesis.

Nonetheless, mechanical stimuli are sufficient to increase the pumping rate, however, not to a similar level to that observed in presence of food. It is possible that the clogging effect of the beads is responsible for this constraint. Alternatively, it is likely that mechanosensation itself is not sufficient and that a full, fast pumping response also requires the presence of gustatory cues. One possible model could be that the detection of a physical presence in the pharynx triggers an initial increase of pumping rate in order to accumulate cues reaching the sensory receptors in the pharynx. Then detection of gustatory cues would further increase, and sustain, the elevated pumping rate. Furthermore, the presence of beads in the intestine is correlated with the sustained increase of the pumping rate following prolonged exposure to beads. Therefore it is possible that physical contact in the pharynx triggers an initial increase in pumping rate but the presence of a mechanical stimulus in the intestine may be required to sustain an elevated pumping rate.

Finally, a mutant analysis study of this pumping revealed that the elevation following prolonged exposition to beads is dependent on 5-HT signalling. This

is not surprising, given the well-known role of 5-HT in the pumping response to food. The role of 5-HT in the pumping behaviour in the presence of food was described in Chapter 3. Furthermore, previous studies have shown that exogenous application of 5-HT on food deprived worms led to a dramatic increase of pumping rate, leading to elevated pumping similar to that observed on food (Hobson *et al.*, 2006). The only serotonergic neurons in the pharyngeal nervous system are NSMs. Interestingly, the NSMs have a long thin process going along the isthmus which may function as proprioceptive and could sense bacteria in the pharynx lumen (Axang *et al.*, 2008) (**Figure 72**). Furthermore, 5-HT released from NSMs was shown to promote dwelling behaviour in response to food (Flavell *et al.*, 2013). As the 5-HT released acts on neurons in the central nervous system, one could hypothesise that NSMs sense the presence of food in the pharynx to modulate the locomotory behaviour. Indeed, it is unlikely that food is being detected outside of the pharynx to trigger a neuronal circuit that would signal to the pharyngeal nervous system to signal back to the command neurons of the central nervous system.

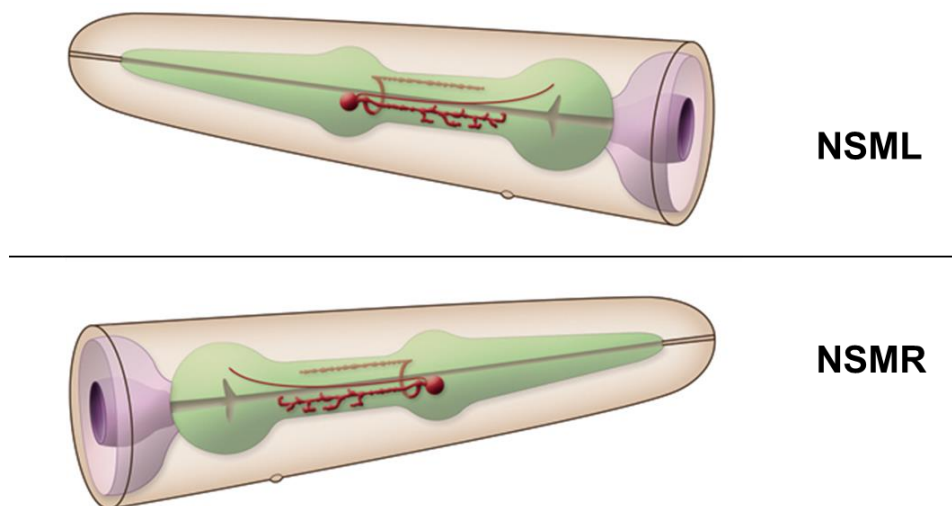


Figure 72: Cartoon representation of the pharyngeal neuron NSM.

NSM cell bodies are localised in the proximal bulb of the pharynx. The major process of each neuron bifurcates near the cell body to form two thick processes. Another long, thin process originates from the cell body and

extends toward the terminal bulb crossing the isthmus. This process is proposed to have proprioceptive functions. *Taken from WormAtlas.*

6.4 Conclusion

In this chapter, the sensory modalities involved in the modulation of pumping behaviours have been investigated. Surprisingly, olfaction is not required for a normal pumping behaviour in presence of food. In contrast, worms deficient in olfaction displayed aberrant pumping behaviours in absence of food, indicating this modality plays a crucial role in the reduction of the pumping rate in response to food removal, and thus while ‘smelling’ food-associated cues is not sufficient to stimulate the pumping rate, the removal of ‘odours’ from food leads to a dramatic reduction. The glutamatergic thermos/CO₂ sensory AFD neurons have been discovered as a determinant of this off food circuit.

Additional experiments conducted in this chapter showed that physical contact between the tip of the worm’s head and the bacterial lawn is required for an increase of the pumping rate. Furthermore, using polystyrene microspheres small enough for the worms to swallow as a mechanical stimulus showed that mechanosensation, likely in the pharynx lumen, was sufficient to trigger an increase of pumping rate. This pharyngeal response to mechanical stimulus was shown to be driven by 5-HT that could be released from NSM pharyngeal neurons. However, the involvement of NSM remains to be determined.

Overall, these findings coupled with the known role of chemosensation in locomotion suggest the following model (**Figure 73**) in which worms placed off food utilise chemosensation to perceive and direct themselves toward a source of food. While moving towards food, worms displayed a normal pumping off food behaviour, *i.e.* a slow basal pumping rate, likely to sample the environment. Once reaching food, bacteria are being pumped in as a result of the basal pumping rate, permitting physical detection of bacteria inside the pharynx through mechanosensory and potentially gustatory modalities. This has the effect to both stop the reduction of the pumping rate, triggered in response to food removal, and in parallel to increase the pumping rate back to the high pump frequency observed on food.

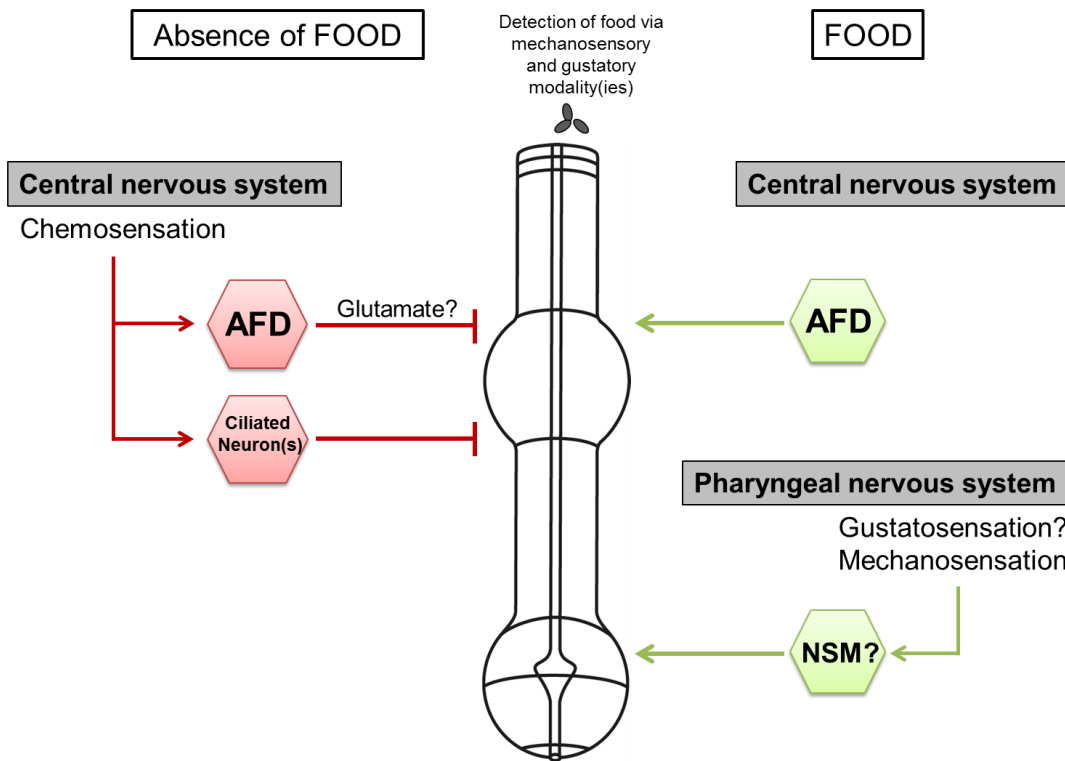


Figure 73: Schematic representation of the context-dependent involvement of sensory modalities in the control of the pumping behaviour.

In presence of food, AFD neurons from the central nervous system stimulate the pumping rate. In parallel, the presence of food in the pharynx is detected via mechanosensory and potentially gustatory modalities leading to a 5-HT dependent increase of the pumping. 5-HT is likely to be released from NSMs, the only serotonergic neurons in the pharynx.

In absence of food, the removal of odours from food is detected by ciliated chemosensory neurons including AFD leading to the reduction of the pumping rate.

Chapter 7: Nutritional status and pumping behaviour in response to food-deprivation

7.1 Introduction

Cellular and molecular mechanisms controlling the worm's pumping behaviour both in the presence or absence of food were investigated and described in the previous chapters. The pumping response to food removal showed complex modulation involving distinct central and pharyngeal microcircuits were acting to reduce the pump rate. In parallel an active stimulation of pumping was occurring to maintain a slow basal rate (see **Figure 26**). The focus of these studies was on the early stage of this pumping response to the absence of food. Interestingly, however, chapter 3 described a temporal aspect of the pumping off food with increasing time. Indeed, protracted assays showed a behavioural adaptation of pumping with an increased time of food deprivation. The pumping behaviour off food was therefore divided into two main phases: (1) the early phase with a slow increase of pumping following the initial cessation due to the harsh touch effect up to ~30 ppm, (2) a late phase, after 2 hours of deprivation, characterised by an important fluctuation of the pump rate from very low to very high values (**Figure 26**). How is this adaptation mediated and why remains to be addressed.

Studies using other pumping off food paradigms, with different periods of food deprivation, have also shown an increase over time (Avery and Horvitz, 1990; Dwyer and Aamodt, 2013). One reason for the overall increase of the pumping rate could come from an increased urgency to feed. If the basal pumping rate off food is indeed required to sample the environment, and bring the food cues to the enteric system where they can be sensed, then an overall increase of pumping would increase the probability of bringing food and associated cues into the pharynx and gut. This could facilitate detection of small amount of food that could be crucial for survival. One could thus

Chapter 7

hypothesise this increased urge for food could come from a hunger signal, and could therefore be directly linked to the worm's nutritional status.

Prior studies have shown the nutritional status of worms can modify feeding behaviours, with both homeostatic and possibly hedonic-like systems (reward-based feeding) appearing to mediate the worm's feeding behaviour (see **section 1.4.3**) (Lutter and Nestler, 2009). Supporting this concept, worms which have undertaken a period of food deprivation will show an enhanced food intake (Avery and Horvitz, 1990) and displayed an enhanced slowing response when reintroduced to food (Sawin et al., 2000), both directly proportional to the length of food deprivation. Similarly, the hedonic-like system is represented by the worms' innate preference for high quality food, *i.e.* food that will best promote growth (Avery, 2003). Indeed, worms which had been exposed to high-quality food will prefer a similar source of food when given the choice in binary choice assays (Shtonda and Avery, 2006). Similarly *C. elegans* quiescence behaviour, defined by a cessation of feeding and movement thought to be equivalent to satiety in mammals, is dependent to the quality of food, but also to the worms' feeding history, with food deprived worms more likely to enter quiescence after re-feeding (You et al., 2008). Overall, these findings hint at a strong link between metabolism, nutritional status, and feeding behaviours.

When food environment is lacking, animals cannot acquire energy for basal functions (growth, reproduction, foraging). Therefore, resistance to starvation is tightly linked to the ability to internally store and release pre-stored energy when required (Robin *et al.*, 1988; Thouzeau *et al.*, 1999; Bertile *et al.*, 2003; Wang *et al.*, 2006). *C. elegans*' fat stores are held in lipid droplets mainly found in the intestine, but also in the skin-like epidermal/hypodermal cells (Mullaney and Ashrafi, 2009). These essential lipid stores are found in two types of organelles (see **section 1.4.2.1**), the neutral lipid droplets (Zhang *et al.*, 2010b) encapsulated by a phospholipid monolayer and represent the majority of intestinal fat (Zhang *et al.*, 2010a), and the lysosome-related organelles (LROs), also called gut granules (Schroeder *et al.*, 2007), which store a smaller proportion of intestinal fat (O'Rourke *et al.*, 2009), and are cell type-

specific subcellular structures which have common features with endosomes and lysosomes (Marks *et al.*, 2013).

Fat stores were first imaged using electron microscopy (Mullaney and Ashrafi, 2009). Other techniques have since been used to visualise fatty acids, notably based on biochemical staining of lipids, including Sudan Black (McKay *et al.*, 2003a), Nile Red (Ashrafi *et al.*, 2003) and fluorescent lipids that accumulate in the key stores (e.g. BODIPY-labeled fatty-acids) (O'Rourke *et al.*, 2009; Wahlby *et al.*, 2014) (see **section 1.4.2.1**).

However, label-free techniques were more recently developed to overcome these limitations, such as Stimulated Raman-Scattering (SRS) and Coherent Anti-Stokes Raman Scattering (CARS) (Yen *et al.*, 2010) or, although not specific to lipids, nuclear magnetic resonance (NMR)-based metabolomics method (Blaise *et al.*, 2007; Pontoizeau *et al.*, 2014). Finally, the recent discovery of protein associated to lipid storage organelles permitted to fluorescently tag specifically these subcellular compartments to visualise changes in stability or mobilisation (Xu *et al.*, 2012; Zhang *et al.*, 2012).

In order to investigate the nutritional status of a worm during food deprivation, and determine whether this nutritional status may correlate with the adaptive changes observed in the pumping behaviour in absence of food (**Figure 26**), and notably account for the switch from the early to the late phase observed after two hours of food deprivation, different methods aiming to observe the main sources of energy storage, such as lipids or carbohydrates, at key time points of food deprivation have been undertaken.

7.2 Results

7.2.1 Lipids consumption during food deprivation

The first approach used in this study was an established lipid stain method for biochemical measurement. Two fat soluble dyes have been used to observe lipid stores in *C. elegans*: Sudan black (Kimura *et al.*, 1997) or Nile Red (Ashrafi

Chapter 7

et al., 2003). Sudan black was preferred here as fat droplets in the hypodermis are not stained by Nile Red (Mullaney and Ashrafi, 2009).

In a preliminary experiment the synchronized wild type worms (L4 +1) used for this experiment have been either kept well-fed or food deprived for different amount of time: 2, 5, 10 and 24 hours. Every population of food deprived worms was coupled with well-fed worms of the same age as control. As can be seen in **Figure 74**, the fat storage was very consistent between the control groups. No diminution in the fat stores has been observed during the first five hours of food deprivation. The first significant decrease appeared in worms that have been food deprived for 10 hours, and a further reduced amount of fat droplet is then observed after 24 hours of food deprivation.

These results suggest that the lipid stores begin to reduce between 5 and 10 hours of food deprivation. As indicated (**Chapter 3**), the distinct stages of the pharyngeal pumping are all documented within 5 hours. The depletion of fat is assumed to indicate switch in metabolism. Therefore, the switch in energy stores consumption from carbohydrates to lipids as well as the changes in the internal amount of fat available could not account for the adaptive change observed in the pumping behaviour 2 hours after food removal.

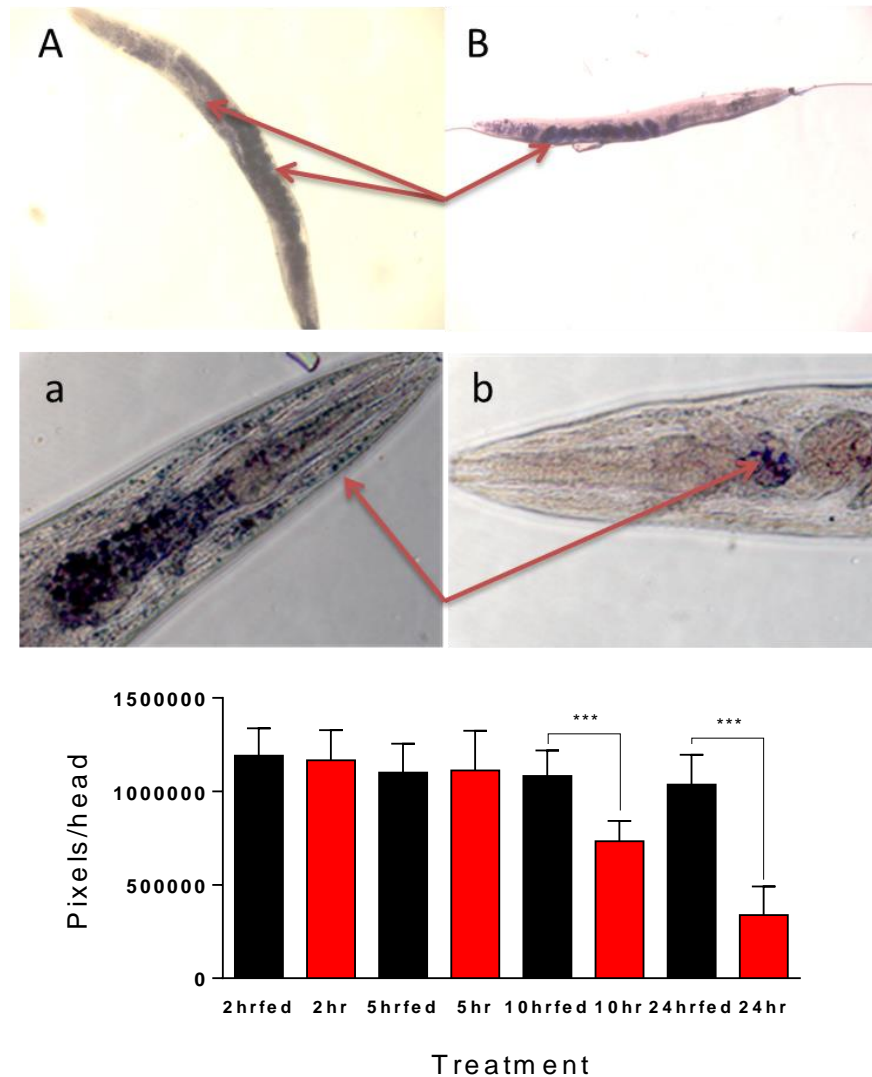


Figure 74: Sudan black staining of wild type well-fed or starved worms' lipid stores.

Top: Pictures of well-fed (A,a) and food-deprived worms for 24 hours (B,b). Red arrows are pointing out the stained fat droplets.

Bottom: Fat storage in *C. elegans* at different stages of food deprivation. Fat was visualised using Sudan Black staining. The intensity was measured by highlighting the stains and disregarding the rest of the animal. Pixels in a specified area, the head, were counted as the intensity. Every population of food-deprived worms (red) was coupled to a control group (black). During the first five hours of food deprivation there is no reduction in fat storage. After ten hours in the absence of food there is a reduced amount of fat droplets and an even further decrease after 24 hours of food withdrawal ($P < 0.001$).

Performed by Sarah Luedtke.

7.2.2 Metabolomic approach in *C. elegans* by Nuclear Magnetic Resonance showed a marked reduction of lipid stores after 2 hours of food deprivation

Histological approaches are widely used but may not provide information on dynamic effects. Recent use of label-free techniques permitted to further investigate worms' nutritional status (Yen *et al.*, 2010). First, a metabolomic approach based on a ¹H high resolution magic angle spinning (HRMAS), a whole-organism nuclear magnetic resonance (NMR) method that permits the characterisation of different metabolites within the worms (Blaise *et al.*, 2007), has been undertaken. Metabolomic is the study of the metabolome, the complete set of metabolites (small molecules intermediates and products of metabolism) (Oliver *et al.*, 1998). Therefore this assay permits the investigation of all metabolites (including lipids) level in whole worms during food-deprivation.

Proton NMR spectra were gathered and data were processed and analysed by Dr. Philip Williamson. The proton spectra of both N2 and *egl-3(ok979)* worms were similar with resonances from both carbohydrates and the fatty acids present in the spectra (**Figure 75A**). L4+1 worms were used and either kept well-fed or food-deprived for 4 or 24 hours, harvested and fixed with formalin. The envelope corresponding to the carbohydrate resonances, although low intensity is observed in the un-starved worms, disappears within 4 hours, whilst resonances assignable to fatty acids decreased to ~40% of the levels seen in the fed worms within the first 4 hours, decreasing by a further ~10% over the following 20 hours (**Figure 75B**). This suggests that fatty acids start to be consumed within the first four hours of food deprivation, an observation contrasting with previous results obtained with the Sudan black staining. Furthermore, the signals associated to glycerol also decrease after 4 hours of food deprivation indicating that TAGs (**Figure 75D**), and therefore lipid stores, are consumed. These results correlate with the general appearance of worms following the use of the magnet, with the 24 hours food-deprived worms appearing paler (**Figure 75C**).

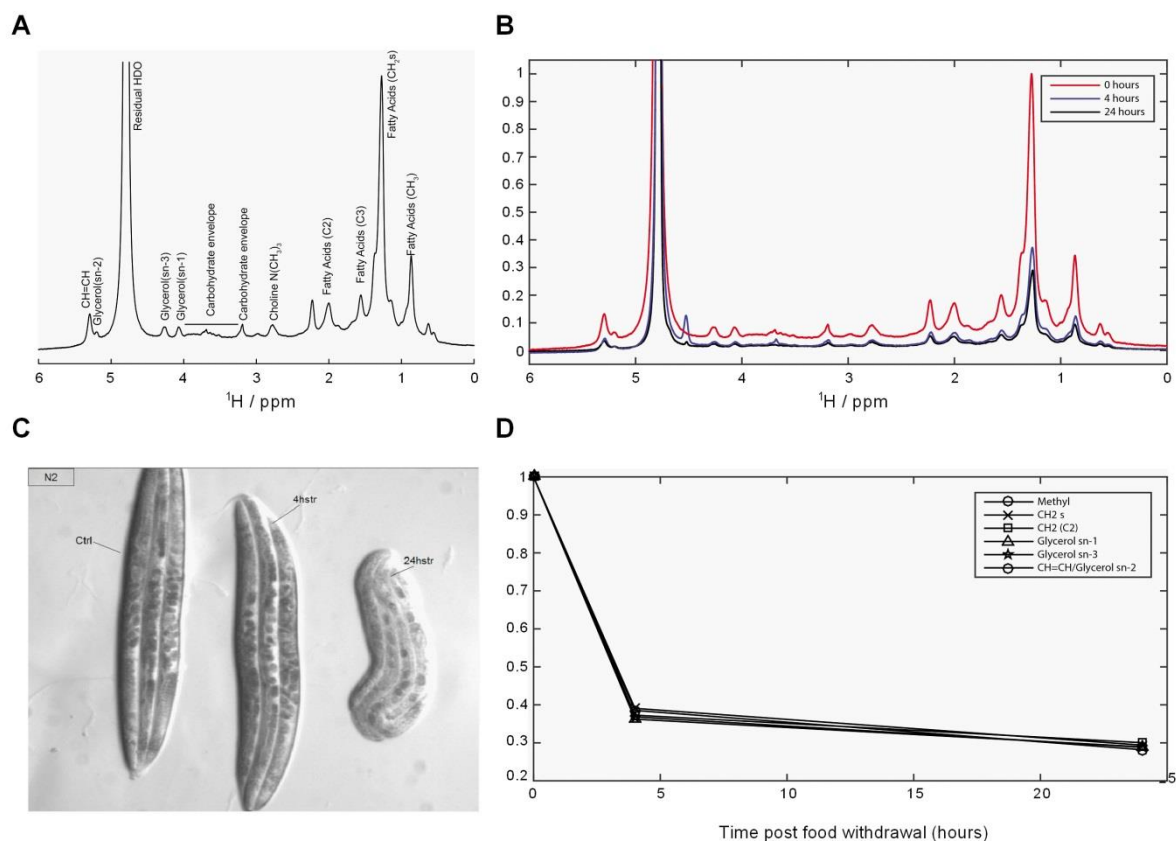


Figure 75: ^1H high resolution magic angle spinning whole-organism nuclear magnetic resonance (^1H HRMAS-NMR) of wild type worms, well-fed or food deprived for 4 and 24 hours.

A. Annotated proton spectra of a N2 well-fed worm with each peak assigned with the represented metabolite.

B. Spectra of wild type worms well-fed or food deprived for 4 or 24 hours. The high peak on left hand side of the graph represents the residual HDO water resonance. Estimated number of worms per condition: well-fed (0h) = 220; food-deprived for: 4h = 300; 24 h = 350

C. Picture of worm sample after going through the magnet.

D. Individual metabolite reduction over extended periods of food deprivation.

Chapter 7

A second experiment was conducted in parallel using a mutant deficient in the pumping behaviour in absence of food, *egl-3(ok979)*. As presented in **chapters 3** and **Chapter 5**, *egl-3* mutants displayed almost no pump motions when placed of food, during both phases. This mutant was then assessed to test whether this absence of normal pumping behaviour was due to a defect in metabolism.

egl-3(ok979) mutants were harvested, fixed and processed as described above. However, one extra time point, two hours of food deprivation, was available here. As previously mentioned, the proton spectra of *egl-3* mutant were similar to N2's spectra, however, a reduced intensity associated to FAs was observed in the *egl-3* mutant (data not shown). Similar to that observed with N2 worms, the resonance associated to FAs was markedly reduced after 4 hours of food deprivation to around ~45% of well-fed's one, and further reduced after 24h (~25%) (**Figure 76A, B**). Interestingly, a reduction was also observed after 2 hours of food deprivation, although less marked than after 4 hours (**Figure 76A, B**). This suggests, at least in *egl-3(ok979)* mutants, that the FAs start to be consumed within the first two hours following the removal of food. Moreover, the decay observed in *egl-3(ok979)* mutants was quantitatively similar to that observed in N2, suggesting that the absence of temporal pumping phases in this mutant is unlikely to be due to a defect in metabolism.

Carbohydrates appeared to be reduced in worms which have been food deprived for 2 hours, and about the same level in worms placed in absence of food for 4 hours. However, opposite to the results observed in wild type worms, the carbohydrates were not completely depleted after 4 hours of food deprivation.

Overall, these results reveal a potential reduction of the FA stores during the first 2 hours of food deprivation, which could therefore be correlated with the first phase of the pumping 'off' food behaviour.

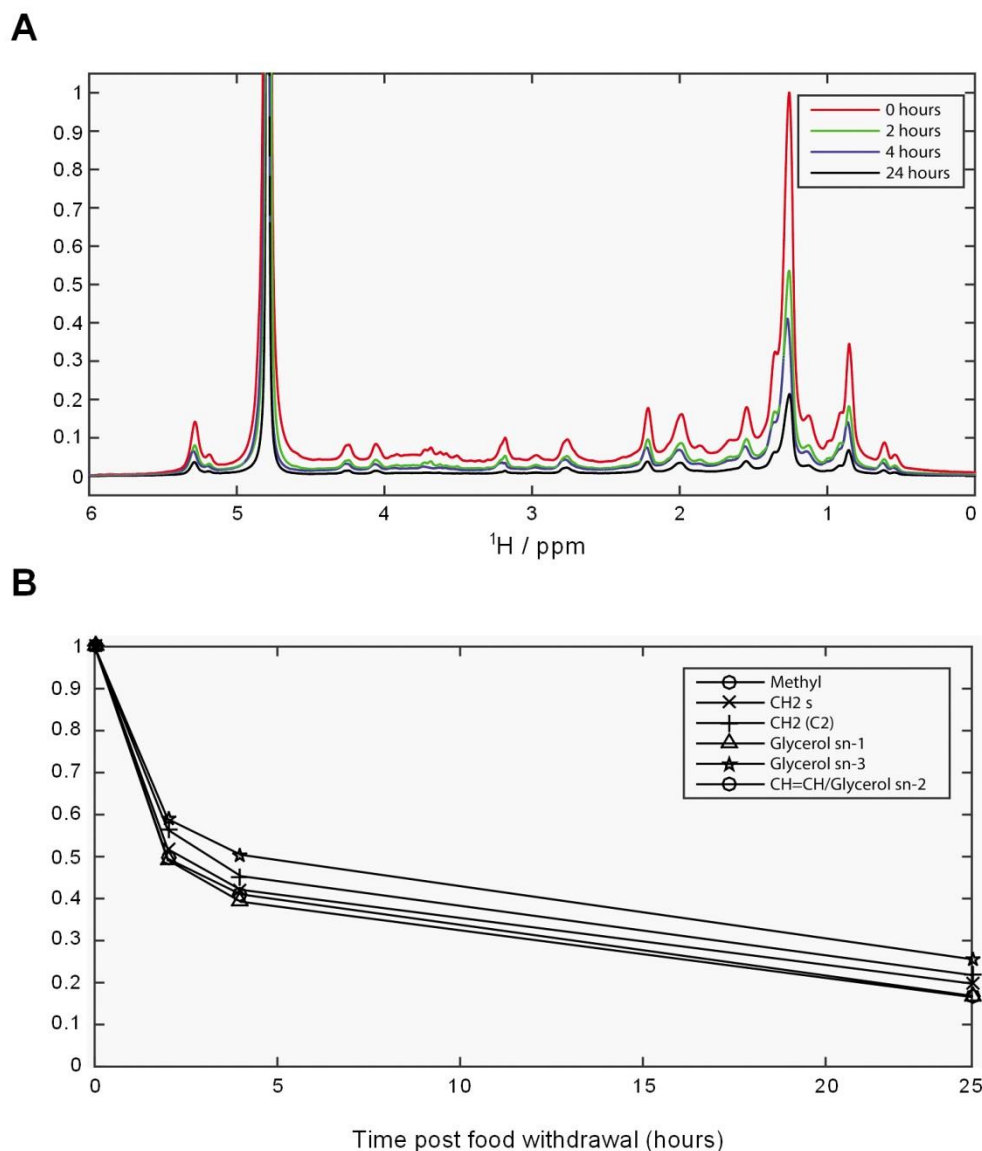


Figure 76: ^1H high resolution magic angle spinning whole-organism nuclear magnetic resonance (^1H HRMAS-NMR) of *egl-3(ok979)* worms, well-fed or food deprived for 2, 4 and 24 hours.

A. Spectra of *egl-3(ok979)* worms well-fed or food deprived for 4 or 24 hours.

The high peak on left hand side of the graph represents the residual water signal. Estimated number of worms per condition: well-fed (0h) = 617; food-deprived for: 2h: 812, 4h = 933; 24 h = 1517

B. Individual metabolites reduction over extended periods of food deprivation.

7.2.3 Coherent anti-Stokes Raman scattering (CARS) imaging of *C. elegans* lipid stores

The NMR approach described above showed a reduction of signals associated to FAs after 4 hours of food deprivation, and potentially after 2 hours, although the latter has only been observed in the mutant *egl-3(ok979)*. NMR is quite time demanding and requires a large number of worms. Therefore, another approach was taken to refine the understanding of how lipid stores are used up during food deprivation, based on the Coherent anti-Stokes Raman spectroscopy (CARS) imaging technique. CARS is a Dye-free microscopy sensitive to vibrational C-H bond signature of molecules (excited by two lasers) (Evans and Xie, 2008) and imaging can be made on individual worms. Each molecule has a distinct fingerprint spectrum. This allows the experiment to be tuned to resolve major biomolecules associated with metabolism. In particular it has been identified as a technology that can resolve lipids and monitor dynamic changes associated with them (Yen *et al.*, 2010). In CARS, two laser beams (pump and Stokes beam) are used. Lasers are tuned to specific vibrations present in the sample and are spatially overlapped, which means that the signal is greatly enhanced, comparing to traditional Raman signals (Chien *et al.*, 2011). One of the advantages of this method is the detection of intestine fat droplets, but also of the ones localised in the hypodermis. The absence of staining makes the sample preparation more straightforward and only a few worms are required per experiment as the results are quite reproducible (Hellerer *et al.*, 2007). At the particular frequency of 2845 cm^{-1} CH₂ bonds are observed so each molecule that is rich in these bonds will appear, i.e. both TAGs and free FAs.

Images of whole worms showed that the strongest lipid droplet signals are localised in the tail region at the terminal end of the intestine. A substantial amount of intestinal lipids are also present in the middle abdominal part of the body, on the dorsal side surrounding the hermaphrodite's vulva. Finally, hypodermal lipid signals are also visible in the head region surrounding the pharynx (**Figure 77A**). Based on this signal distribution, three regions of interest were selected, defined here by land marks (highlighted in **Figure 77A**),

to serve as reference point for comparison between different conditions. Further observation and quantification of lipid droplets were then conducted.

In order to better define when the lipid stores start to be used and how fast they are depleted, well fed worms were compared to 6 different food deprivation time points: 0.5, 1, 1.5, 2, 4 and 24 hours post-food removal. 3 worms were imaged per time point. Images have been processed by adjusting threshold so that signal associated to lipid stores (TAGs + free FAs) appear in white while the rest of the image remained black (**Figure 77B-G**).

A

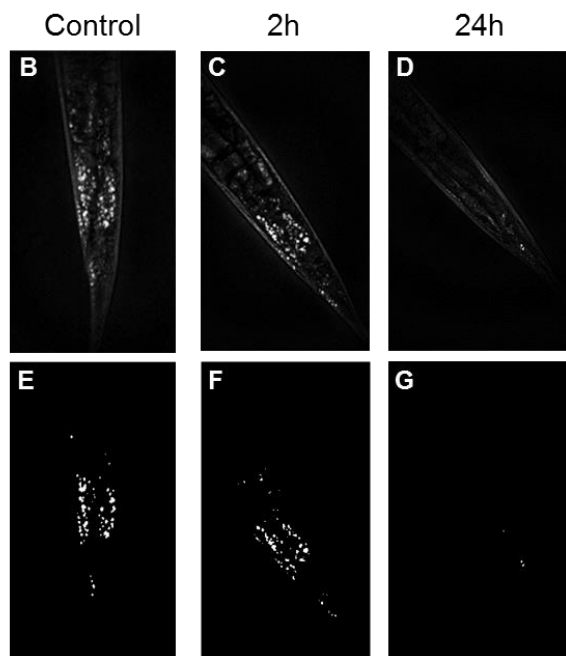
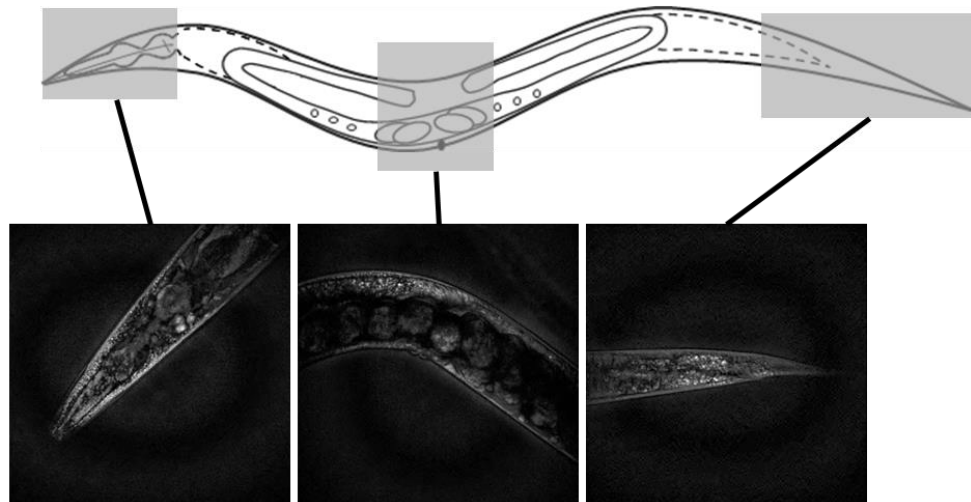


Figure 77: Illustration of the 3 regions of the worm imaged with CARS.

A. CARS images correspond to 3 distinct regions of the worm schematically represented in the top panel with the head, the vulva surrounding region and the tail. CARS images have been obtained from well-fed L4+1 by tuning to the CH_2 stretching frequency at 2850 cm^{-1} for lipids. Lipid rich areas (lipid stores) appear bright in the images.

B-D. CARS images of the tail of a well-fed (**B**) or food deprived worm for 2 (**C**) and 24 (**D**) hours.

E-F. Processed images with adjusted threshold to highlight lipid stores in well-fed

Images taken and processed by Justyna Smus.

An area of interest has been drawn on each image, and the number of pixels corresponding to the area has been determined using ImageJ. Microscopy and image processing were performed by Justyna Smus. Representative images indicate that the lipid stores appeared reduced after only 30 min of food deprivation (**Figure 78**). Indeed, a significant ~30% decrease was observed in the vulva region and a ~40% in the tail (**Figure 78C, D**). The lipid stores in the head region also appeared reduced (~25%) however the difference was not significant (**Figure 78B**).

The signal associated with lipids appeared to gradually decrease overtime to reach around 40% of the initial signal left after 4h of food deprivation in all regions imaged (**Figure 78**). Remarkably, in the middle region of the worm the signal reduction appeared less gradual with an important drop of around 25% observed between 1h and 1.5h post food withdrawal (**Figure 78C**). Finally, the signal associated to lipids was almost completely depleted after 24 hours of food deprivation in all three regions, with on average less than 10% of the initial signal remaining.

Altogether, the results described here indicate a rapid decrease of signal associated with lipids upon food deprivation, suggesting that lipid stores rapidly start to be used up in the absence of food. For instance, a 30% reduction of the initial lipid stores is observed after only 30 min of food deprivation. Therefore it is possible that the nutritional status of the worm affects the pumping rate off food, and could therefore account for, or contribute to, the adaptive pumping behaviour in the absence of food and its distinct phases.

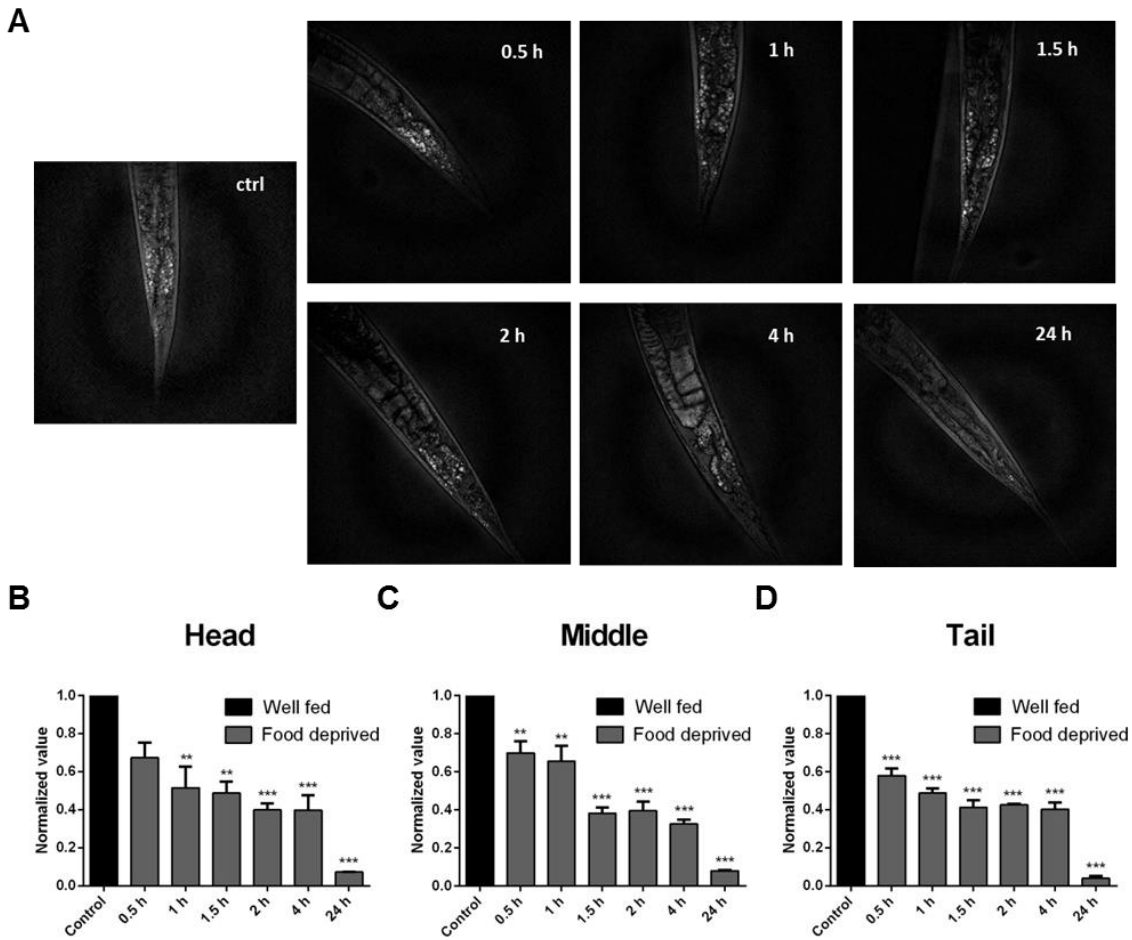


Figure 78: Analysis of lipid stores in *C. elegans* during food deprivation using CARS shows significant decrease over time.

A. Representative images of the tail region of N2 L4 + 1 worms after different time of food deprivation.

B. C. D. Quantitative analysis of the lipid stores during food deprivation from images taken using the CARS method. Values have been normalized to control and averaged from 3 data sets. Stars above bars and lines indicate significant multiple comparisons one-way ANOVA results vs. control and other groups.

* ($p < 0.05$), ** ($p < 0.01$) and *** ($p < 0.001$) compared to paired N2.

Images taken and processed by Justyna Smus.

7.3 Discussion

The nutritional status of *C. elegans* during food deprivation changes over time. In order to determine whether or not these changes correlate with the adaptive changes of pumping behaviour observed during food deprivation, 3 different methods have been performed.

Sudan Black was chosen for this preliminary experiment as the assay has to be performed on food-deprived worms and the vital Nile Red protocol involves feeding the worm with bacteria mixed with the dye. Although it is possible to supply Nile red without bacteria (O'Rourke *et al.*, 2009), the marked reduction of pumping observed in absence of food may significantly reduce the dye uptake. Furthermore, the signal from vital Nile red staining does not decrease upon food deprivation (O'Rourke *et al.*, 2009).

The preliminary results obtained using the Sudan Black lipid staining method showed that a reduction of the lipid stores only occurs between 5 and 10 hours of food deprivation. This result is in broad agreement with previous studies showing a marked decrease of Sudan Black staining after 8 hours of food deprivation (McKay *et al.*, 2003a) and a clear reduction of Oil Red O lipophilic dye in animal fasted for 4 to 6 hours (Lee *et al.*, 2014; Srinivasan, 2014).

7.3.1 NMR-based metabolomic analysis revealed potential reduction of carbohydrates and lipids during the first 2 hours of food-deprivation

The results obtained with Sudan Black staining suggest behavioural modulation of pumping before any change in lipid. However, Sudan Black staining intensity was shown to be highly variable in adult worms due to the final destaining wash with ethanol which is required with its protocol in which slight variation in timing may greatly affect the staining intensity (O'Rourke *et al.*, 2009).

Label-free techniques have been developed more recently to assess the worm fat stores, and two of them were used in this chapter. Firstly, ¹H high

Chapter 7

resolution magic angle spinning (HRMAS), a whole-organism nuclear magnetic resonance (NMR) method permits the detection and quantification of individual metabolites, including fatty acids, in whole fixed worms (Pontoizeau *et al.*, 2014). The results obtained with this method suggest that significant changes may occur within the first 2 hours of food deprivation. Indeed, analysis of food deprived N2 worms' proton spectra showed a marked reduction in lipid-associated resonance after 4 hours without food, indicating food-deprived worms start using up their lipids stores within the first 4 hours. Furthermore, the NMR profile of the neuropeptide processing deficient mutant *egl-3(ok979)* also showed a reduction of the resonance associated with lipids after only 2 hours of food deprivation followed by a further decrease after 4 and 24 hours (**Figure 76**). This suggests lipid stores may start being used during the first 2 hours following food removal, which would correlate with changes in the pumping behaviour off food. However, it is possible this result accounts for the *egl-3(ok979)* mutation itself and an additional 2 hours time point in N2 background would be required to validate this finding. *egl-3* mutant was initially used to investigate potential changes in fat usage in a mutant deficient for the pumping behaviour off food. In this regards, *egl-3* mutant, although known to have a reduced fat content (Husson *et al.*, 2007), appears to use up its lipid stores in a similar fashion to N2 worms as suggested by the marked 60% decrease observed after 4 hours of food deprivation.

This NMR-based experiment is also able to detect the level of carbohydrates. Worms mainly store carbohydrate in the form of glycogen (Frazier and Roth, 2009). In wild type worms, glycogen stores appeared to be almost completely consumed after 4 hours of food deprivation as resonance associated with carbohydrates is markedly reduced and carbohydrates do not appear to further decrease after 24 hours in absence of food. Similarly, carbohydrate associated resonance is reduced in the *egl-3* mutant after 2 and 4 hours of food deprivation, however, a further decrease was observed after 24 hours, suggesting that glycogen stores were not completely depleted after 4 hours off food. The resonance associated with carbohydrates is quite low intensity in this experiment, and it is therefore possible the differences observed are only representing small variation between conditions. However, one explanation for this could be that the absence of pumping off food in the *egl-3* mutant (see **Chapter 3 and 5**) may permit the worms to conserve energy

stores for a bit longer when food is missing by not using energy for pumping. Alternatively, the *egl-3* mutant defect in locomotion in which *egl-3* mutant displays a sluggish locomotion and tends to show a coiled posture (Jacob and Kaplan, 2003), or a combination of both can explain why this mutant consumes its glycogen stores less quickly.

7.3.2 CARS-based lipid imaging validates and refines previous findings to show significant reduction of lipid stores after 30 min off food

Finally, a third method was used taking advantage of Raman technology: Coherent anti-Stokes Raman spectroscopy (CARS). CARS microscopy allows quantitative measurement of fat stores by revealing fat droplets (Yen *et al.*, 2010). Furthermore, the signal associated with lipid droplets observed by CARS was further analysed and revealed strong chemical signatures typical of TAGs (Le *et al.*, 2010).

More time points and shorter time of food deprivation were conducted using this method. Remarkably, a reduction 25% to 40% of the signal associated with lipids was observed after only 30 min of food deprivation depending on the worm region. The lipid stores in food deprived worms then gradually decrease with only ~40% of the initial signal left after 4 hours and less than 10% after 24 hours off food. These results indicate that lipid stores are depleted early during food deprivation. Indeed, a third of the stores appeared used up after 30 min, and only half of the initial stores are remaining after 2 hours of food deprivation. This is consistent with the NMR observation where 60% of the lipids stores are depleted after 4 hours off food in N2 and 50% of the well fed worms are remaining in *egl-3* worms food deprived for 2 hours. Unlike the NMR-based technique, the CARS technique permits observation of the lipid stores in different parts of the worm. Interestingly, after 30 min the tail seems to be the region where the lipids are the most reduced while in the vulva region, although also reduced after 30 min, the main drop of lipid stores seems to occur between 1 hour and 1.5 hours of food

deprivation. Lipid stores in the head region appear to be gradually used over time off food.

7.3.3 Correlation between timing of changes in nutritional status and adaptive feeding behaviours

Together, these results reveal that after 2 hours of food deprivation, a marked reduction in lipid and carbohydrate stores occurs. The low intensity of the NMR signal for carbohydrates prevents making precise quantification of what fraction of the initial carbohydrate remains after 2 hours of food-deprivation, however, the signal appears greatly reduced suggesting only a small fraction remains. In addition, only half of the initial lipid stores remain after 2 hours. Remarkably, 2 hours post food removal corresponds to the change of phase, from early to late phase, in the pumping off food behaviour (see **Chapter 3**). This timing correlation between lipids usage and pumping behaviour reinforces the hypothesis that a change in nutritional status drives the different phases of the pumping behaviour in the absence of food. It is possible that reaching a certain threshold, for instance 50% of stores depleted, corresponds to a critical survival situation and triggers a change of behaviour.

This reasoning could be extended to another feeding behaviour involving locomotion. Assuming that lipid stores start being used up rapidly (**Figure 78**) and worms only synthesized 10% of their lipid stores (Perez and Van Gilst, 2008), worms have the necessity to constantly feed to maintain storage. Interestingly, the main known foraging behaviour of *C. elegans* is the local area search behaviour (Gray *et al.*, 2005). Worms placed in the absence of food first display a specific locomotory pattern based on high angled turn and an increased reversal and omega turn rates in order to look for food in a restricted area, potentially near the place they last found food. There is a switch of behaviour after 15 min of food deprivation where worms display long runs and few reversals in order to seek food in new area. Given the CARS results presented in this chapter showing the signal associated with lipid was already reduced within the first 30 min of food deprivation (and carbohydrate likely to be used up in priority before lipids), then one could hypothesize that the switch of behaviour may be due to a change of nutritional status. It would

be interesting to investigate whether this switch of behaviour happens because of depletion of glycogen or lipid stores.

These findings show that the sequence of utilisation of energy stores appears similar to that observed in vertebrates (see **section 1.4.1.1**). Carbohydrates appear to be used up in priority and depleted first. Similarly, lipid signals start to decrease rapidly consistent with an early mobilisation of lipid stores during food deprivation in parallel to carbohydrates. Lipid consumption continues as time of deprivation increases. The next step would be to investigate the protein stores during food deprivation to see whether their consumption follow a similar pattern that observed in vertebrates.

7.4 Conclusion

Regulation of feeding behaviours appears complex even in a simple organism such as *C. elegans*. Numerous studies have shown the adaptability of these behaviours to the environmental context such as the presence or absence of food, but also the behavioural adaptation to sustained periods of favourable or unfavourable conditions. Indeed, both locomotory behaviour and the pumping behaviour described in this thesis show temporal switch of behaviour in response to prolonged food deprivation. In this chapter, the use of three different methods to assess the worm's energy stores during food deprivation permitted a correlation between nutritional status and adaptive behaviour in response to food removal (**Figure 79**).

A reduction of about a third of the initial lipid stores was already observed after 30min of food deprivation and only half of these initial stores were still present after 2 hours. Moreover, glycogen stores also appeared almost completely depleted after 2 hours spent in absence of food. The timing in the decrease of these energy stores not only indicates that worms use energy rapidly when food is missing but also is compatible with the timing of the switch in pumping behaviour off food. A worm when placed in absence of food

Chapter 7

enters the late phase after two hours, which correspond to a 50% reduction of lipids and of most carbohydrates. However, if a correlation can be made, it remains unclear whether the changes in nutritional status are the cause of the change of behavioural phase. But if the causality can be demonstrated, it would be interesting to determine more accurately what percentage of reduction, or threshold, trigger a change of behaviour.

Despite these caveats, this chapter shows the power of a label-free technique to assess the level of fat stores in *C. elegans* and demonstrates that both NMR based metabolomic and CARS microscopy can be used to study the effect of food deprivation on energy stores in the worm.

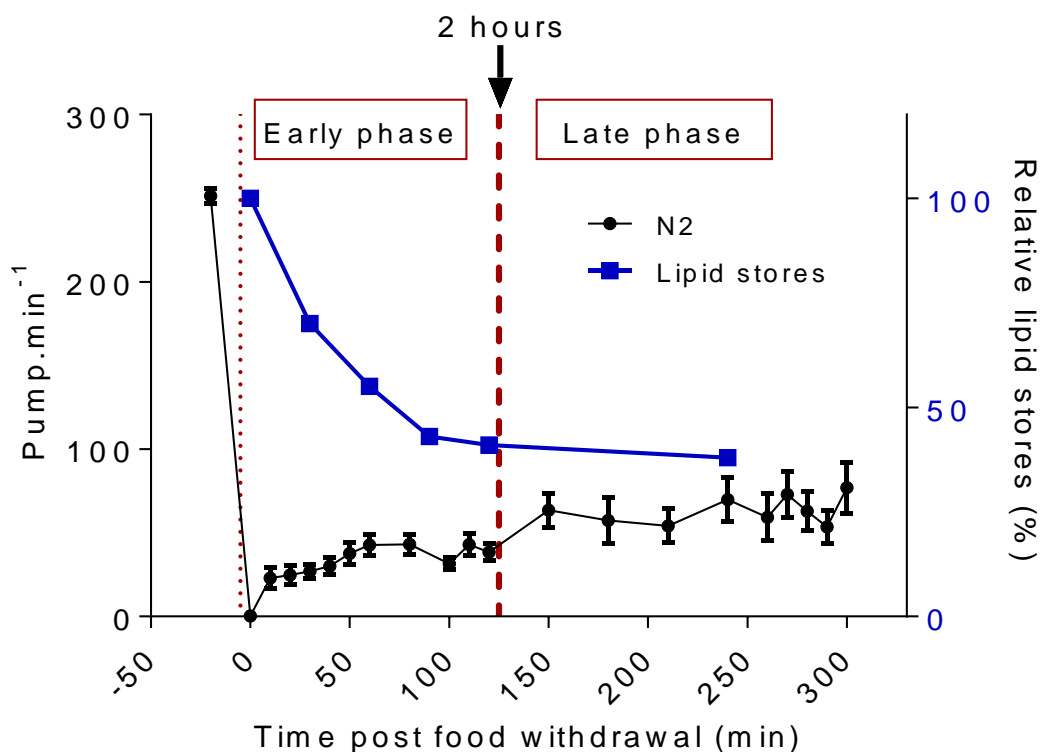


Figure 79: Model representing the correlation between lipid stores consumption and the switch of pumping phases in response to prolonged food-deprivation.

The figure is modified from Figure 26C. The black line (left Y axis) represents the pumping rate of N2 worms over prolonged time of food-deprivation. The blue line (right Y axis) represents the relative lipid stores. During the early

phase of pumping, lipid stores decrease progressively over time while the pumping rate slowly increases. After 2 hours of food-deprivation, the lipid stores are reduced to less than 50% of the initial stores, and the worms enter the late phase of pumping. The pumping rate starts fluctuating, with worms displaying bursts of pumping to optimise their sampling of their environment and conserve energy. Lipid stores keep decreasing until almost complete depletion after 24 hours of food-deprivation (not shown in the graph).

Chapter 8: General discussion

Like many animals, *C. elegans* must feed to maintain a healthy state and a proper energy balance. The nematode's natural feeding behaviour is called pumping behaviour in which bacteria from the environment are pumped into the feeding organ, the pharynx, for grinding and ingestion. In this thesis, I described the neural and molecular mechanisms regulating the pumping behaviours depending on the food context, i.e. with or without food. The high rate of feeding in the presence of food was already well-studied, notably involving key neurons such as M3, MC and ADF (Avery, 1993; Niacaris, 2003; Cunningham et al., 2012). However, findings presented here showed novel components that act to maintain this high pumping rate such as GABA signalling (**Chapter 3**), the thermos/CO₂ sensory neurons AFD (**Chapter 6**), the glutamate receptor GLC-2 (**Chapter 4**) and the neuropeptides FLP-1, FLP-17 and FLP-18 (**Chapter 5**).

Less is known regarding the pumping behaviour when food is lacking. This thesis showed a temporal aspect, describing distinct phases with time of food-deprivation progressing that correlates with the nutritional status of the worm and the reduction of energy stores. Furthermore, the pumping behaviour off food is characterised by marked reduction of pumping, and also by the maintenance of a basal pump rate permitting to sample the environment. Determinants for both aspects were discovered. Notably, the key role of the pharyngeal neurons I2 in both the stimulation and reduction of the pumping rate off food is described. Furthermore, both parts of the nervous system are modulating the pumping behaviour, involving distinct sensory modalities. The absence of olfactory cues perceived by the central nervous system or the removal of mechanosensory and gustatory cues from the enteric system were shown to trigger the activation of key pathways regulating the pumping behaviour off food. The literature and discussion pertaining to specific observations have been covered in individual chapters. In this general discussion, I will attempt to take a wider view of the observations made and provide some schematics detailing the important insights this study has for feeding control in *C. elegans*.

8.1 Conceptually conserved mechanisms regulating feeding behaviours

Observations using the pumping paradigm revealed that the reduced pump rate 'off' food is not a passive loss of stimulatory signals. The absence of food itself is perceived as a signal and triggered active neuronal circuits driving the 'off' food behaviour (**chapter 6** and Chalasani *et al.* 2007). This is conceptually similar to that observed in the mammalian retina where photoreceptors (rods and cones) are hyperpolarised in response to light and are activated in response to the removal of light (Ebrey and Koutalos, 2001).

The regulation of the pumping behaviour depending on the availability of food is therefore more complex than a simple ON/OFF switch. There are distinct circuits acting to regulate the 'on' (**Figure 80**) and 'off' (**Figure 81**) food aspects of the pumping behaviours.

This is similar to the organisation observed in mammalian systems, where two population of neurons localised in the hypothalamic arcuate nucleus, the agouti-related peptide (AGRP) and pro-opiomelanocortin (POMC) expressing neurons, regulate feeding behaviour (Aponte *et al.*, 2011). AGRP neurons activity induces hyperphagia while in contrast, POMC neurons act to reduce food intake. Interestingly, AGRP signalling also inhibits POMC neurons' action on food intake. It is therefore possible that a similar cross-link between excitatory and inhibitory pathways occurs in worms in which the activation of a pathway would lead to the active inhibition of its counterpart. Further investigation is required to determine whether this is the case. However, in *C. elegans*, this kind of counter-regulatory system is found in the control of locomotion where the activation of the neuronal circuit inducing forward movement also represses the circuit mediating backward movements and vice versa (Kawano *et al.*, 2011).

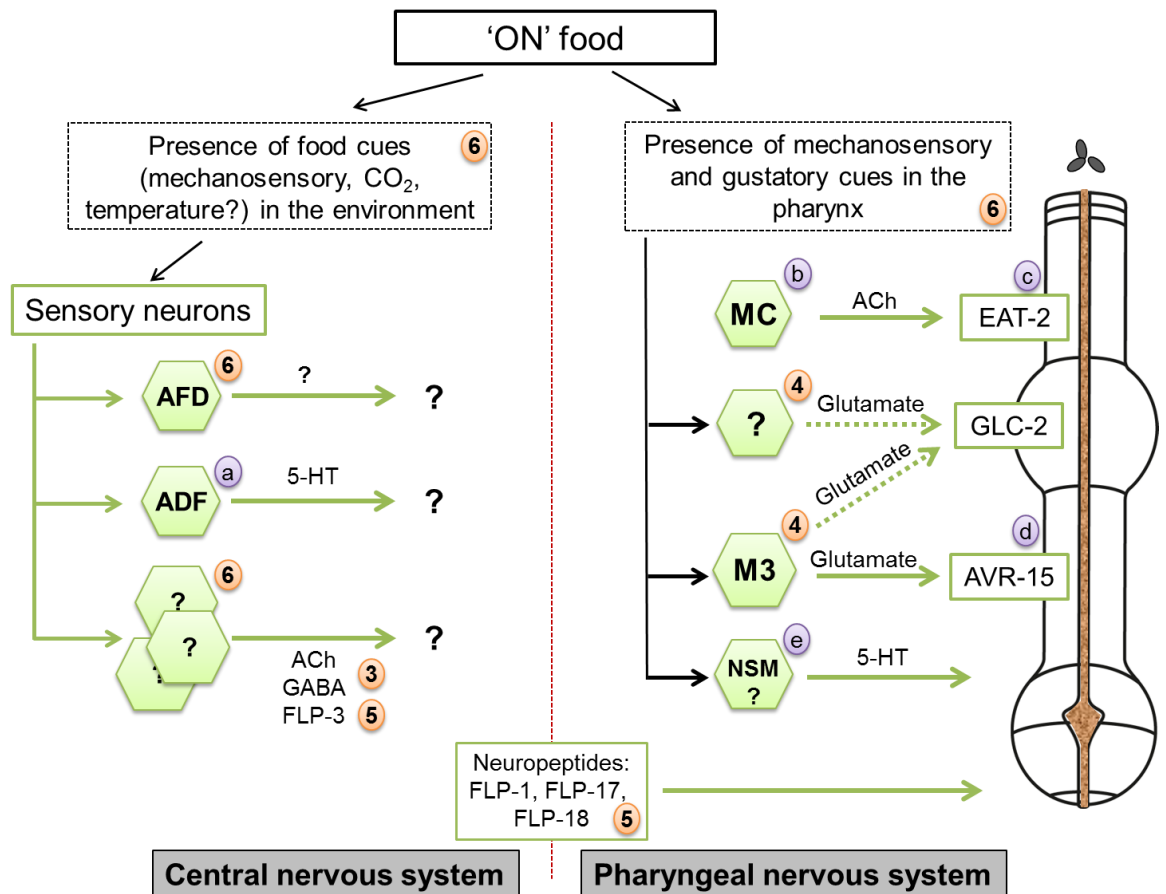


Figure 80: Schematic model of the regulation of the pumping behaviour in the presence of food.

The presence of food cues, most likely mechanosensory or gustatory cues, in the pharynx lumen and from the environment are perceived by sensory neurons from both the central nervous system (on the left hand side) and the pharyngeal nervous system (right hand side). MC and M3 increase the pumping rate controlling the timing and duration of pumping respectively upon 5-HT activation. MC releases acetylcholine (ACh) on the pharynx via the EAT-2 receptor. M3 releases glutamate on the AVR-15 receptor and may also act on GLC-2, however, it is possible that the glutamate acting on GLC-2 receptor is released from another neuron. 5-HT plays an important role in the high pumping rate on food and is released from the ADF and/or NSM neurons. GABA signalling also plays a small part in the pumping behaviour on food, and is only found outside of the pharynx. Finally, neurohormonal signalling plays an important part as there is no cell to cell communication through RIP neurons. FLP-1, FLP-3, FLP-17 and FLP-18 peptides have been shown to stimulate pumping in response to food. It is however not determined where

Chapter 8

they are released from as they are expressed in both parts of the nervous system except for FLP-3 which is only found in the central nervous system. Numbers in orange circles represent the thesis' chapter associated with the observation.

In contrast, blue circles represent information based on literature. (a) Cunningham *et al.* 2012; (b) Avery and Horvitz 1989; (c) McKay *et al.* 2004; (d) Dent *et al.* 1997; (e) Li *et al.* 2012

The data presented in this thesis highlight the multi pathways nature of the signalling controlling feeding in *C. elegans*. There is indeed more than one pathway that leads to the stimulation or reduction of the pumping rate. For instance, I demonstrated distinct circuits that reduce the pumping rate in the absence of food (see **Figure 81** and **section 8.4**). In addition to this complexity, an excitatory peptidergic pathway acts in parallel to maintain a basal pumping rate (**chapter 3** and **Chapter 5**). These show that even the worm's simple feeding is flexible to various environments operating over a range of mixed cues.

This resonates with the neuroendocrine control of mammalian feeding which shows convergent pathways lead to a similar feeding response. Intracranial injection of the neuropeptide NPY has orexigenic effects (Kalra *et al.*, 1999), and chronic treatments lead to obesity (Raposinho *et al.*, 2001). However, mice specifically lacking NPY or AGRP peptides show no eating dysfunction (Palmiter *et al.*, 1998; Qian *et al.*, 2002), suggesting compensatory mechanisms. Mechanisms that could be driven by the neurotransmitter GABA as it was shown to act in the regulation of food intake and energy balance (Wu and Palmiter, 2011).

8.2 Evidence for an autonomic regulation of the pumping behaviours

In mammals, while central drives are critical to higher control of feeding (see **section 8.1**) it is clear that gastrointestinal and gustatory signals are key peripheral determinants of feeding behaviours (Lenard and Berthoud, 2008). Recent studies have shown the potential of gut-brain communication in which gut microbial can communicate directly with the CNS using neural, hormonal and immunological routes (Cryan and Dinan, 2012). Bilateral communication along this axis has been shown to affect distinct behaviours including food intake and satiety (Konturek *et al.*, 2003; Konturek *et al.*, 2004). Therefore both enteric and central drives are critical to feeding behaviours although the latter are less well explored.

In this thesis, the investigation of cellular determinants intervening in the control of pumping behaviours reveals that both extrapharyngeal and pharyngeal nervous systems are involved (**Figure 80** and **Figure 81**). In the case of *C. elegans*, the pharyngeal nervous system can be considered as a correlate of the mammalian enteric system, the pharyngeal nervous system is composed of 20 of the 302 neurons and has a complex and mixed neurochemistry (see **section 1.2.2.2**) which resonates with the 500 million neurons of the enteric nervous system relative to the trillion in the brain (Young, 2012). This suggests an autonomic regulation of the pumping behaviour both in the presence (M3s) and in the absence of food (I2s) (see **chapter 4**).

Ciliated chemosensory neurons of the worm's central nervous system were shown to play a crucial role in the regulation of the pumping behaviour 'off' food, indicating that the absence of chemosensory cues from food triggers the activation of pathways that reduce the pumping rate and that the central nervous system is responsible for the majority of the reduction effect (**Figure 82**). However, a modest reduction of the pumping rate can still be observed when worms deficient for these ciliated chemosensory neurons (*osm-6* mutants) are removed from food. Together with the observed role of the pharyngeal neurons I2 (**Figure 81**), this indicates the central nervous system is accounting for most but not all the pumping reduction observed off food.

Chapter 8

Therefore, it is likely that the reduction of the pumping rate is mediated by at least two distinct circuits, one involving detection and integration of cues, or absence of cues, in the central nervous system (ciliated neurons), and one perceiving the absence of food directly in the pharynx (I2 neurons) (**Figure 82**).

The mechanisms underpinning the communication between these two parts of the worm's nervous system are not determined. However, the non-involvement of RIPs in pumping behaviours indicates a neurohormonal communication and several molecular determinants were discovered during the course of this thesis (**Figure 80** and **Figure 81**). This is notably the case of neuropeptide-Y-like receptors and their ligands (**Chapter 5**), however, their cellular release site and where they act remain to be determined. For this purpose, rescue experiments by specific expression of these molecular determinants need to be performed.

As shown in the diagram the chemical determinants of the neuropeptide-dependent maintenance of pumping off food makes an important case for a complex peptide release - cognate receptor relationship involving both paracrine and volume transmission throughout the pseudocoelomic fluid (see **section 1.1.2.4**).

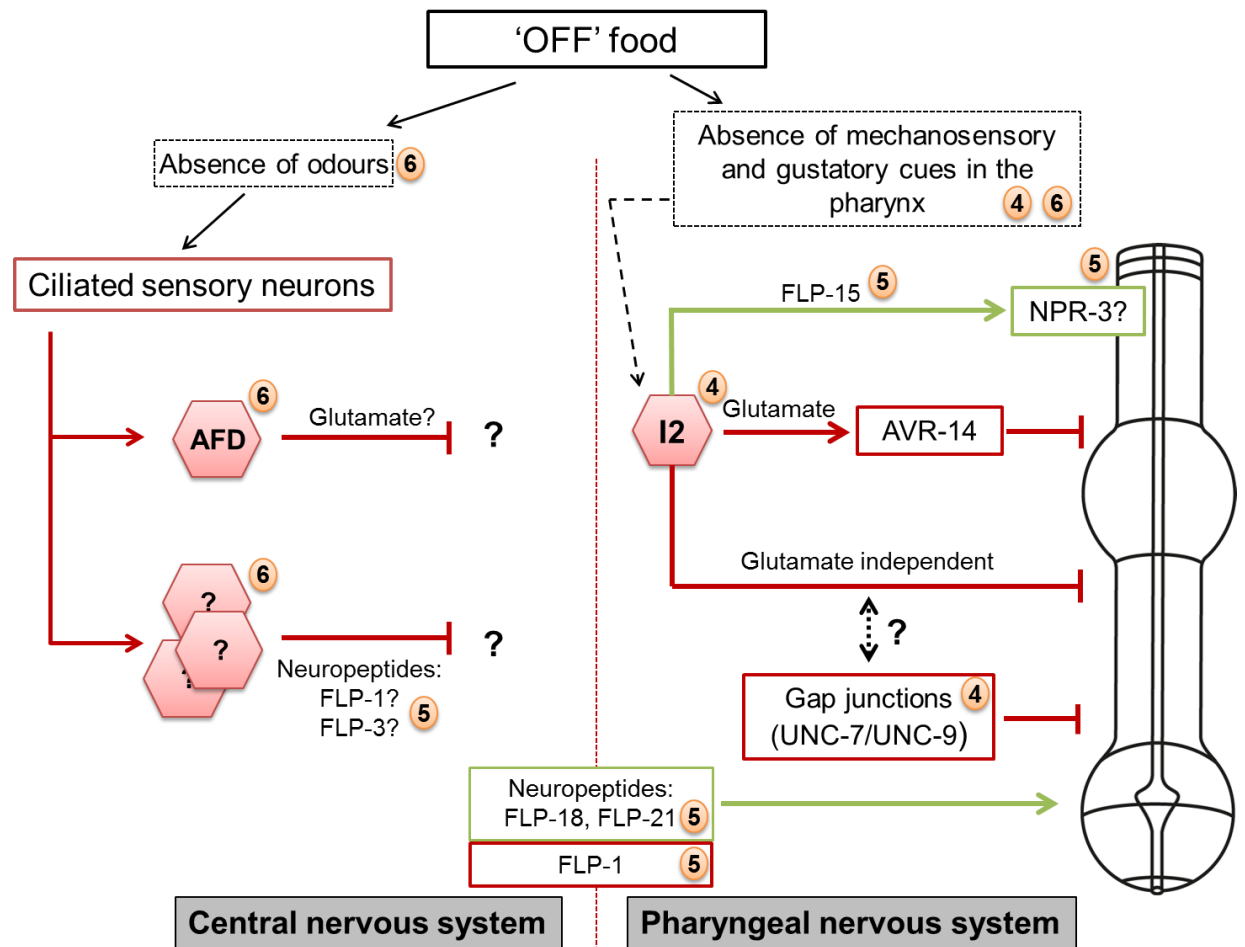


Figure 81: Schematic model of the pumping off food behaviour regulation.

In the absence of food, ciliated sensory neurons perceive the absence of odours from food and in turn act to reduce the pumping rate. The thermo/CO₂ sensory glutamatergic neurons AFD are the only identified ciliated neurons so far investigated that are shown to take part in this pumping reduction. However, it has not been determined whether AFDs' action on the pumping rate is mediated by glutamate or other peptidergic transmitters. Neuropeptides FLP-1 and FLP-3 act to reduce the pumping rate and are expressed in the central nervous system. FLP-1 is also expressed in the pharyngeal nervous system. In parallel, I speculate that the absence of mechanosensory and gustatory cues in the pharynx lumen triggers the activation of the glutamatergic pharyngeal neuron I2. In turn, this leads to the reduction of the pumping rate via two pathways; a glutamate-dependent pathway in which glutamate acts on an *avr-14* expressing neuron and a glutamate-independent pathway which may involve gap junctions.

Chapter 8

In response to food removal, a basal pumping rate is also maintained. I2s activation also leads to the release of FLP-15 peptides which act to stimulate pumping through NPR-3. It is not clear where NPR-3 is localised but preliminary results suggest it may be expressed on the pharynx muscle. In addition, FLP-18 and FLP-21 peptides also stimulate pumping in response to food removal and are predicted to underpin the neuropeptide dependence of the basal off food pump rate at about 30ppm.

Numbers in orange circles represent the thesis' chapter associated with the observation.

8.3 Pumping behaviours are polymodal

Both the presence and the absence of food are perceived as cues by the worm's nervous system. However, the sensory modalities by which these cues are detected, eventually leading to a pumping response, are still ill-defined.

Detection of olfactory cues appears not important to trigger the high pumping rate observed 'on' food as suggested as olfactory deficient *osm-6* mutants pump normally on food. This genetic evidence is reinforced by the observation that increased pumping to food requires proximal contact with food as worms touch the bacterial food lawn with the tip of their mouth (**Chapter 6**). Indeed, the most potent volatile chemo-attractants, that mimic food exert no effect on the OFF food pump rate (Samah Zarroug personal communication). This suggests that gustatory and/or mechanosensory modalities drive the pumping rate 'on' food. There is the possibility that food may be pumped in the pharynx where it would be detected and triggers an increase in pumping. This hypothesis is reinforced by the observation that in the absence of food but in the presence of polystyrene microspheres (beads) small enough to be ingested, worms displayed an elevation of the pumping rate (**Chapter 6**), showing the ability of mechanical stimulus to drive an elevation of pumping. In mammals, nutrients stored in the stomach can be perceived by vagal stretch and tension sensors (Page *et al.*, 2005). Furthermore, this would explain the reason why worms keep displaying pumping motion, although at a low frequency, in the absence of food; to

sample the environment and to bring food cues inside the pharynx/enteric system where they can be sensed and trigger an appropriate pumping response. However, the utilisation of beads showed that mechanical stimulus is not sufficient to drive the entire high pumping rate observed on food, reinforcing the possibility of a role for gustatory modality which would be interesting to investigate. In addition, the neurons and receptors which are required for the detection of these food cues are still not determined.

In contrast to the 'on' food context, ciliated chemosensory neurons from the central nervous system play a critical role in the reduction of the pumping rate 'off' food. The absence of olfactory cues from food indeed appears to play a major role as shown by the *osm-6* mutant's deficiency in the pumping behaviour 'off' food. The neurons responsible for this remain unknown. The neurons AWC were previously shown to respond to the removal of odours (Chalasan *et al.*, 2007) and are therefore a good candidate for a role in pumping behaviour 'off' food, and ablation experiments would be required to assess their role. Among the ciliated neurons, only AFDs were shown to act to reduce the pumping rate. However, whether AFDs have a role as a sensory or interneuron in this neuronal circuit is not known. This could be assessed by restoring *osm-6* cDNA expression specifically in AFD neurons to selectively rescue its sensory capability.

Furthermore, the circuit involving I2 neurons suggests that food removal in the pharynx can be perceived to drive the pumping behaviour 'off' food. I2s possess subcuticular endings around the worm's lips that make them good candidates for a proprioceptive function (Albertson and Thomson, 1976). One possibility could be that I2s perceive the absence of mechanosensory and/or gustatory cues in the pharynx lumen upon food removal. In this case, one hypothesis would be to have a tonic activation of I2 when no food is present and in contrast, mechanical stimulus when food is present in the pharynx could activate ion channels triggering hyperpolarisation, an hypothesis supported by the increased Ca^{2+} activity in I2 during food-deprivation (see **section 4.2.9**).

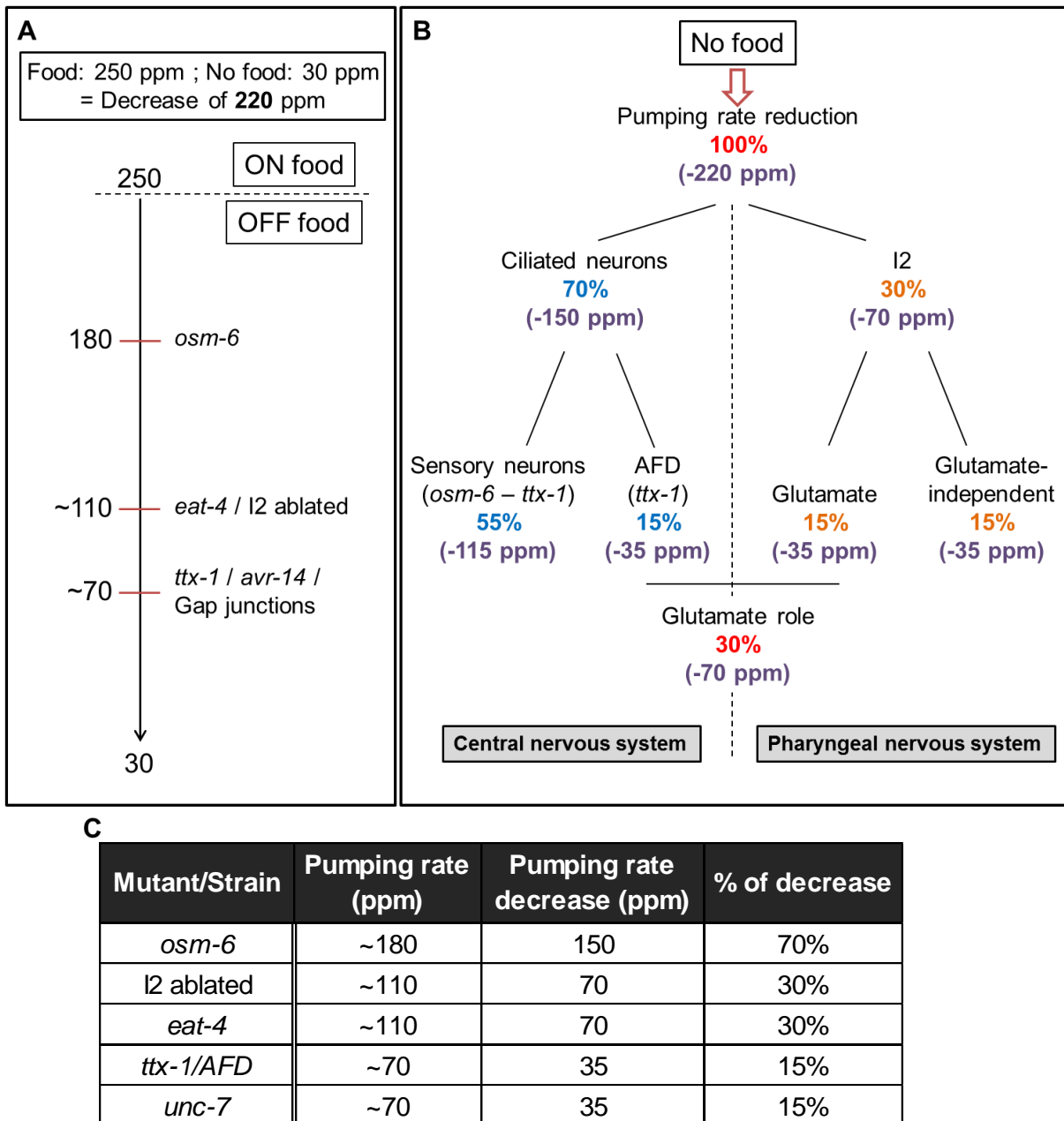


Figure 82: Simplistic representation of the quantitative effects of the main pathways modulating the reduction of the pumping rate observed in response to food removal.

A. Schematic representation of the pumping rate off food of different mutants/strains compared to N2 ‘on’ and ‘off’ food pumping rate. In my hands, the wild-type pumping rate on food is 250 ppm and off food is 30 ppm then there is a decrease of 220 ppm from the ‘on’ to ‘off’ context.

B. Schematic diagram representing the involvement of the different parts of the nervous system (NS) and their cellular and molecular components. 100% corresponds to the total pumping reduction when placed off food (220 ppm).

70% of the total reduction accounts for the central NS involving the ciliated sensory neurons. Part of this 70% is due to the AFD neurons (15% of the total reduction). The remaining 30% accounts for the pharyngeal NS via the neurons I2. I2s reduce the pumping rate via two pathways, one involves glutamate, and one doesn't. Each of these pathways accounts for half of the reduction effect of I2, i.e. 15% of the total reduction. Glutamate net role accounts for 30% of the total reduction, with one part acting in the central NS (AFDs) and the other in the pharyngeal NS (I2s).

C. Table summarising the pumping behaviour off food of the different mutants/strains, their reduction effect on the pumping rate and the percentage of reduction they account for.

8.4 Chain of event: Transition from no food to food

Findings presented in this thesis obtained using a simple paradigm informed us on the transition from an environment where food is abundant to a no food environment. A summary of the main findings integrated as a simple chain of events model, a worm transiting from a no food to food environment, can be presented as followed.

In response to food removal, a worm first displays a local search area (LSA) (see **section 1.2.1.2**) behaviour and in parallel displays a very low pumping rate to sample its environment for food, fined-tuned by the action of ciliated sensory cilia and pharyngeal I2 neurons (**Figure 81**). After 15min of food-deprivation, the worm starts exploring other areas by changing its locomotion pattern increasing long runs forward (Gray *et al.*, 2005). As time of food-deprivation increases, the pumping rate slowly increases up to 30-40 ppm while the worm's nutritional status progressively changes, with the consumption of carbohydrates and fat stores (see **Chapter 7**). After, two hours of food-deprivation, the energy stores may have passed a threshold and trigger a behavioural switch, leading to the late phase of the pumping behaviour off food as the need for food to replenish the energy stores becomes more urgent. The worm displays bursts of pumping separated by low pumping periods

Chapter 8

indicating a trade-off between increasing the chances of finding food (high rates) and saving more energy (low rates). This could permit the worm to sample more areas in a more efficient manner on the following pattern; burst of pumping in one area, long run without pumping while changing area, new burst of pumping to sample the new area...

Detections of volatiles from food do not modify pumping but direct the worm toward the source of food (chemotaxis). Upon contact with the food source, the basal pumping rate permits to pump food in the pharynx which is detected by mechanosensory and gustatory neurons. The presence of food in the pharynx is also believed to promote dwelling through release of 5-HT by NSMs (Flavell *et al.*, 2013), while extrapharyngeal food detection triggers a release of dopamine from the mechanosensory neurons of the central nervous system (ADE, CEP, PDE) leading to a slowing response (Sawin *et al.*, 2000). In parallel, 5-HT from ADF and/or NSM, glutamate from M3 and potentially AFD, acetylcholine from MC, neuropeptides and GABA are released to increase and maintain a high frequency pumping rate (**Figure 80**). Upon feeding, the worm can refill its energy stores in preparation for the next food-deprivation period.

These findings made by using a simple paradigm informed us on the transition from an environment where food is abundant to a no food environment. In its natural habitat, however, it is likely that worms also encounter intermediate environments with various gradient and density of food. It will be interesting to investigate the worm's behaviours in response to various amount and/or quality of food.

The experimental design used favours observation of the transition from an 'on' to an 'off' food context. However, assays performed with protracted periods of time hint at a behavioural plasticity with time, as suggested by the distinct pumping behaviour phases observed in a food-deprived worm. Interestingly, it is possible to establish a correlation between the behavioural switches and the nutritional status of the worm (see **chapter 7**), suggesting that adaptability on longer periods of food-deprivation might be driven by changes in nutritional status. Future prospect in this area would focus on

establishing a more precise and detailed connection between pumping and nutritional status. Furthermore, the mechanisms by which changes of nutritional status are perceived and drive behavioural changes need to be investigated.

Thus even a simple animal like *C. elegans*, with a network of just 302 neurons, engages a complex framework for regulating feeding which has organisational similarities to inform on circuit organization that controls mammalian feeding in which multiple converging signals act to finely titrate context-dependent feeding behaviour (Aponte et al., 2011).

List of References

- **Akerboom, J., Chen, T.W., Wardill, T.J., Tian, L., Marvin, J.S., Mutlu, S., Calderon, N.C., Esposti, F., Borghuis, B.G., Sun, X.R., et al.** (2012). Optimization of a GCaMP calcium indicator for neural activity imaging. *The Journal of neuroscience : the official journal of the Society for Neuroscience* **32**, 13819-13840.
- **Albertson, D.G., and Thomson, J.N.** (1976). The pharynx of *Caenorhabditis elegans*. *Philosophical transactions of the Royal Society of London Series B, Biological sciences* **275**, 299-325.
- **Alfonso, A., Grundahl, K., Duerr, J.S., Han, H.P., and Rand, J.B.** (1993). The *Caenorhabditis elegans* unc-17 gene: a putative vesicular acetylcholine transporter. *Science* **261**, 617-619.
- **Alkema, M.J., Hunter-Ensor, M., Ringstad, N., and Horvitz, H.R.** (2005). Tyramine Functions independently of octopamine in the *Caenorhabditis elegans* nervous system. *Neuron* **46**, 247-260.
- **Altun, Z.F., Chen, B., Wang, Z.W., and Hall, D.H.** (2009). High resolution map of *Caenorhabditis elegans* gap junction proteins. *Developmental dynamics : an official publication of the American Association of Anatomists* **238**, 1936-1950.
- **Alvarado, F., Lherminier, M., and Phan, H.H.** (1984). Hamster intestinal disaccharide absorption: extracellular hydrolysis precedes transport of the monosaccharide products. *The Journal of physiology* **355**, 493-507.
- **An, J.H., and Blackwell, T.K.** (2003). SKN-1 links *C. elegans* mesendodermal specification to a conserved oxidative stress response. *Genes & development* **17**, 1882-1893.
- **Andriamampandry, M.D., Bnouham, M., Michard, D., Gutbier, G., Le Maho, Y., and Leray, C.** (1996). Food deprivation modifies fatty acid partitioning and beta-oxidation capacity in rat liver. *The Journal of nutrition* **126**, 2020-2027.
- **Ann, K., Kowalchuk, J.A., Loyet, K.M., and Martin, T.F.** (1997). Novel Ca²⁺-binding protein (CAPS) related to UNC-31 required for Ca²⁺-activated exocytosis. *The Journal of biological chemistry* **272**, 19637-19640.
- **Antin, J., Gibbs, J., Holt, J., Young, R.C., and Smith, G.P.** (1975). Cholecystokinin elicits the complete behavioral sequence of satiety in rats. *Journal of comparative and physiological psychology* **89**, 784-790.
- **Aponte, Y., Atasoy, D., and Sternson, S.M.** (2011). AGRP neurons are sufficient to orchestrate feeding behavior rapidly and without training. *Nature neuroscience* **14**, 351-355.
- **Ashrafi, K.** (2007). Obesity and the regulation of fat metabolism. *WormBook : the online review of C elegans biology*, 1-20.
- **Ashrafi, K., Chang, F.Y., Watts, J.L., Fraser, A.G., Kamath, R.S., Ahringer, J., and Ruvkun, G.** (2003). Genome-wide RNAi analysis of *Caenorhabditis elegans* fat regulatory genes. *Nature* **421**, 268-272.
- **Aspöck, G.** (2003). The *Caenorhabditis elegans* ems class homeobox gene *ceh-2* is required for M3 pharynx motoneuron function. *Development* **130**, 3369-3378.
- **Avery, L.** (1993). Motor neuron M3 controls pharyngeal muscle relaxation timing in *Caenorhabditis elegans*. *The Journal of experimental biology* **175**, 283-297.

Bibliography

- **Avery, L.** (2003). Food transport in the *C. elegans* pharynx. *Journal of Experimental Biology* 206, 2441-2457.
- **Avery, L.** (2010). *Caenorhabditis elegans* behavioral genetics: where are the knobs? *BMC biology* 8, 69.
- **Avery, L., Bargmann, C.I., and Horvitz, H.R.** (1993). The *Caenorhabditis elegans unc-31* gene affects multiple nervous system-controlled functions. *Genetics* 134, 455-464.
- **Avery, L., and Horvitz, H.R.** (1987). A Cell That Dies during Wild-Type *C. elegans* Development Can Function as a Neuron in a Ced-3 Mutant. *Cell* 51, 1071-1078.
- **Avery, L., and Horvitz, H.R.** (1989). Pharyngeal pumping continues after laser killing of the pharyngeal nervous system of *C. elegans*. *Neuron* 3, 473-485.
- **Avery, L., and Horvitz, H.R.** (1990). Effects of starvation and neuroactive drugs on feeding in *Caenorhabditis elegans*. *The Journal of experimental zoology* 253, 263-270.
- **Avery, L., and Shtonda, B.B.** (2003). Food transport in the *C. elegans* pharynx. *The Journal of experimental biology* 206, 2441-2457.
- **Avery, L., and Thomas, J.H.** (1997). Feeding and Defecation. In *C elegans II*, D.L. Riddle, T. Blumenthal, B.J. Meyer, and J.R. Priess, eds. (Cold Spring Harbor (NY)).
- **Avery, L., and You, Y.J.** (2012). *C. elegans* feeding. *WormBook : the online review of C elegans biology*, 1-23.
- **Axang, C., Rauthan, M., Hall, D.H., and Pilon, M.** (2008). Developmental genetics of the *C. elegans* pharyngeal neurons NSML and NSMR. *BMC developmental biology* 8, 38.
- **Bargmann, C.I.** (1998). Neurobiology of the *Caenorhabditis elegans* Genome. *Science* 282, 2028-2033.
- **Bargmann, C.I.** (2006). Chemosensation in *C. elegans*. *WormBook : the online review of C elegans biology*, 1-29.
- **Bargmann, C.I., Hartwig, E., and Horvitz, H.R.** (1993). Odorant-selective genes and neurons mediate olfaction in *C. elegans*. *Cell* 74, 515-527.
- **Bargmann, C.I., and Horvitz, H.R.** (1991). Chemosensory neurons with overlapping functions direct chemotaxis to multiple chemicals in *C. elegans*. *Neuron* 7, 729-742.
- **Beaudoin, F., Michaelson, L.V., Hey, S.J., Lewis, M.J., Shewry, P.R., Sayanova, O., and Napier, J.A.** (2000). Heterologous reconstitution in yeast of the polyunsaturated fatty acid biosynthetic pathway. *Proceedings of the National Academy of Sciences of the United States of America* 97, 6421-6426.
- **Beck, B., Burlet, A., Bazin, R., Nicolas, J.P., and Burlet, C.** (1993). Elevated neuropeptide Y in the arcuate nucleus of young obese Zucker rats may contribute to the development of their overeating. *The Journal of nutrition* 123, 1168-1172.
- **Beck, B., Burlet, A., Nicolas, J.P., and Burlet, C.** (1990). Hyperphagia in obesity is associated with a central peptidergic dysregulation in rats. *The Journal of nutrition* 120, 806-811.
- **Beets, I., Janssen, T., Meelkop, E., Temmerman, L., Suetens, N., Rademakers, S., Jansen, G., and Schoofs, L.** (2012). Vasopressin/oxytocin-related signaling regulates gustatory associative learning in *C. elegans*. *Science* 338, 543-545.
- **Beets, I., Lindemans, M., Janssen, T., and Verleyen, P.** (2011). Deorphanizing G protein-coupled receptors by a calcium mobilization assay. *Methods in molecular biology* 789, 377-391.

- **Behm, C.A.** (1997). The role of trehalose in the physiology of nematodes. *Int J Parasitol* *27*, 215-229.
- **Belkhou, R., Cherel, Y., Heitz, A., Robin, J.P., and Lemaho, Y.** (1991). Energy Contribution of Proteins and Lipids during Prolonged Fasting in the Rat. *Nutr Res* *11*, 365-374.
- **Ben Arous, J., Laffont, S., and Chatenay, D.** (2009). Molecular and sensory basis of a food related two-state behavior in *C. elegans*. *PloS one* *4*, e7584.
- **Bendena, W.G., Boudreau, J.R., Papanicolaou, T., Maltby, M., Tobe, S.S., and Chin-Sang, I.D.** (2008). A *Caenorhabditis elegans* allatostatin/galanin-like receptor NPR-9 inhibits local search behavior in response to feeding cues. *Proceedings of the National Academy of Sciences of the United States of America* *105*, 1339-1342.
- **Bendesky, A., Tsunozaki, M., Rockman, M.V., Kruglyak, L., and Bargmann, C.I.** (2011). Catecholamine receptor polymorphisms affect decision-making in *C. elegans*. *Nature* *472*, 313-318.
- **Berg, J.M., Tymoczko, J.L., and Stryer, L.** (2002). Chapter 21 Glycogen Metabolism. In *Biochemistry* (New York: W. H. Freeman and Company).
- **Bertile, F., Oudart, H., Criscuolo, F., Maho, Y.L., and Raclot, T.** (2003). Hypothalamic gene expression in long-term fasted rats: relationship with body fat. *Biochemical and biophysical research communications* *303*, 1106-1113.
- **Betz, A., Ashery, U., Rickmann, M., Augustin, I., Neher, E., Sudhof, T.C., Rettig, J., and Brose, N.** (1998). Munc13-1 is a presynaptic phorbol ester receptor that enhances neurotransmitter release. *Neuron* *21*, 123-136.
- **Bhatla, N., Droste, R., Sando, S.R., Huang, A., and Horvitz, H.R.** (2015). Distinct Neural Circuits Control Rhythm Inhibition and Spitting by the Myogenic Pharynx of *C. elegans*. *Current biology : CB*.
- **Bhatla, N., and Horvitz, H.R.** (2015). Light and hydrogen peroxide inhibit *C. elegans* Feeding through gustatory receptor orthologs and pharyngeal neurons. *Neuron* *85*, 804-818.
- **Blaise, B.J., Giacomotto, J., Elena, B., Dumas, M.E., Toulhoat, P., Segalat, L., and Emsley, L.** (2007). Metabotyping of *Caenorhabditis elegans* reveals latent phenotypes. *Proceedings of the National Academy of Sciences of the United States of America* *104*, 19808-19812.
- **Boender, A.J., Roubos, E.W., and van der Velde, G.** (2011). Together or alone?: foraging strategies in *Caenorhabditis elegans*. *Biological reviews of the Cambridge Philosophical Society* *86*, 853-862.
- **Bradbury, M.J., Campbell, U., Giracello, D., Chapman, D., King, C., Tehrani, L., Cosford, N.D., Anderson, J., Varney, M.A., and Strack, A.M.** (2005). Metabotropic glutamate receptor *mGlu5* is a mediator of appetite and energy balance in rats and mice. *The Journal of pharmacology and experimental therapeutics* *313*, 395-402.
- **Brenner, S.** (1974). The genetics of *Caenorhabditis elegans*. *Genetics* *77*, 71-94.
- **Bretscher, A.J., Busch, K.E., and de Bono, M.** (2008). A carbon dioxide avoidance behavior is integrated with responses to ambient oxygen and food in *Caenorhabditis elegans*. *Proceedings of the National Academy of Sciences of the United States of America* *105*, 8044-8049.
- **Bretscher, A.J., Kodama-Namba, E., Busch, K.E., Murphy, R.J., Soltesz, Z., Laurent, P., and de Bono, M.** (2011). Temperature, oxygen, and salt-sensing neurons in *C. elegans* are carbon dioxide sensors that control avoidance behavior. *Neuron* *69*, 1099-1113.
- **Brockie, P.J., Madsen, D.M., Zheng, Y., Mellem, J., and Maricq, A.V.** (2001a). Differential expression of glutamate receptor subunits in the nervous

Bibliography

system of *Caenorhabditis elegans* and their regulation by the homeodomain protein UNC-42. *The Journal of neuroscience : the official journal of the Society for Neuroscience* 21, 1510-1522.

- **Brockie, P.J., and Maricq, A.V.** (2003). Ionotropic glutamate receptors in *Caenorhabditis elegans*. *Neuro-Signals* 12, 108-125.
- **Brockie, P.J., and Maricq, A.V.** (2006). Ionotropic glutamate receptors: genetics, behavior and electrophysiology. *WormBook : the online review of C elegans biology*, 1-16.
- **Brockie, P.J., Mellem, J.E., Hills, T., Madsen, D.M., and Maricq, A.V.** (2001b). The *C. elegans* glutamate receptor subunit NMR-1 is required for slow NMDA-activated currents that regulate reversal frequency during locomotion. *Neuron* 31, 617-630.
- **Brooks, K.K., Liang, B., and Watts, J.L.** (2009). The influence of bacterial diet on fat storage in *C. elegans*. *PloS one* 4, e7545.
- **Brosnan, J.T.** (2003). Interorgan amino acid transport and its regulation. *The Journal of nutrition* 133, 2068S-2072S.
- **Bumbarger, D.J., Riebesell, M., Rodelsperger, C., and Sommer, R.J.** (2013). System-wide rewiring underlies behavioral differences in predatory and bacterial-feeding nematodes. *Cell* 152, 109-119.
- **Burdon, K.L., Stokes, J.C., and Kimbrough, C.E.** (1942). Studies of the Common Aerobic Spore-forming Bacilli: I. Staining for Fat with Sudan Black B-safranin. *Journal of bacteriology* 43, 717-724.
- **Byerly, L., and Masuda, M.O.** (1979). Voltage-clamp analysis of the potassium current that produces a negative-going action potential in *Ascaris* muscle. *The Journal of physiology* 288, 263-284.
- **Cahill, G.F., Jr.** (1971). The Banting Memorial Lecture 1971. Physiology of insulin in man. *Diabetes* 20, 785-799.
- **Cahill, G.F., Jr.** (1976). Starvation in man. *Clinics in endocrinology and metabolism* 5, 397-415.
- **Cahill, G.F., Jr., Herrera, M.G., Morgan, A.P., Soeldner, J.S., Steinke, J., Levy, P.L., Reichard, G.A., Jr., and Kipnis, D.M.** (1966). Hormone-fuel interrelationships during fasting. *The Journal of clinical investigation* 45, 1751-1769.
- **Calvo, A.C., Pey, A.L., Miranda-Vizuete, A., Doskeland, A.P., and Martinez, A.** (2011). Divergence in enzyme regulation between *Caenorhabditis elegans* and human tyrosine hydroxylase, the key enzyme in the synthesis of dopamine. *The Biochemical journal* 434, 133-141.
- **Carre-Pierrat, M., Baillie, D., Johnsen, R., Hyde, R., Hart, A., Granger, L., and Segalat, L.** (2006). Characterization of the *Caenorhabditis elegans* G protein-coupled serotonin receptors. *Invertebrate neuroscience : IN* 6, 189-205.
- **Chalasanani, S.H., Chronis, N., Tsunozaki, M., Gray, J.M., Ramot, D., Goodman, M.B., and Bargmann, C.I.** (2007). Dissecting a circuit for olfactory behaviour in *Caenorhabditis elegans*. *Nature* 450, 63-70.
- **Chalasanani, S.H., Kato, S., Albrecht, D.R., Nakagawa, T., Abbott, L.F., and Bargmann, C.I.** (2010). Neuropeptide feedback modifies odor-evoked dynamics in *Caenorhabditis elegans* olfactory neurons. *Nature neuroscience* 13, 615-621.
- **Chalfie, M., and Sulston, J.** (1981). Developmental genetics of the mechanosensory neurons of *Caenorhabditis elegans*. *Dev Biol* 82, 358-370.
- **Chalfie, M., Sulston, J.E., White, J.G., Southgate, E., Thomson, J.N., and Brenner, S.** (1985). The neural circuit for touch sensitivity in *Caenorhabditis elegans*. *The Journal of neuroscience : the official journal of the Society for Neuroscience* 5, 956-964.

- **Champe, P.C., and Harvey, R.A.** (1994). Biochemistry (J.B. Lippincott).
- **Chao, M.Y., Komatsu, H., Fukuto, H.S., Dionne, H.M., and Hart, A.C.** (2004). Feeding status and serotonin rapidly and reversibly modulate a *Caenorhabditis elegans* chemosensory circuit. Proceedings of the National Academy of Sciences of the United States of America *101*, 15512-15517.
- **Charlie, N.K., Schade, M.A., Thomure, A.M., and Miller, K.G.** (2006). Presynaptic UNC-31 (CAPS) is required to activate the G alpha(s) pathway of the *Caenorhabditis elegans* synaptic signaling network. Genetics *172*, 943-961.
- **Chase, D.L., and Koelle, M.R.** (2007). Biogenic amine neurotransmitters in *C. elegans*. WormBook : the online review of *C. elegans* biology, 1-15.
- **Chen, Y.A., and Scheller, R.H.** (2001). SNARE-mediated membrane fusion. Nature reviews Molecular cell biology *2*, 98-106.
- **Cheong, M.C., Artyukhin, A.B., You, Y.J., and Avery, L.** (2015). An opioid-like system regulating feeding behavior in *C. elegans*. eLife *4*.
- **Cheung, B.H., Arellano-Carbajal, F., Rybicki, I., and de Bono, M.** (2004). Soluble guanylate cyclases act in neurons exposed to the body fluid to promote *C. elegans* aggregation behavior. Current biology : CB *14*, 1105-1111.
- **Chien, C.H., Chen, W.W., Wu, J.T., and Chang, T.C.** (2011). Label-free imaging of *Drosophila* in vivo by coherent anti-Stokes Raman scattering and two-photon excitation autofluorescence microscopy. Journal of biomedical optics *16*, 016012.
- **Chitwood, D.J.** (1999). Biochemistry and function of nematode steroids. Critical reviews in biochemistry and molecular biology *34*, 273-284.
- **Coates, J.C., and de Bono, M.** (2002). Antagonistic pathways in neurons exposed to body fluid regulate social feeding in *Caenorhabditis elegans*. Nature *419*, 925-929.
- **Cohen, M., Reale, V., Olofsson, B., Knights, A., Evans, P., and de Bono, M.** (2009). Coordinated regulation of foraging and metabolism in *C. elegans* by RFamide neuropeptide signaling. Cell metabolism *9*, 375-385.
- **Collet, J., Spike, C.A., Lundquist, E.A., Shaw, J.E., and Herman, R.K.** (1998). Analysis of *osm-6*, a gene that affects sensory cilium structure and sensory neuron function in *Caenorhabditis elegans*. Genetics *148*, 187-200.
- **Consortium, C.e.S.** (1998). Genome sequence of the nematode *C. elegans*: a platform for investigating biology. Science *282*, 2012-2018.
- **Cooper, A.F., and Van Gundy, S.D.** (1970). Metabolism of Glycogen and Neutral Lipids by *Aphelenchus avenae* and *Caenorhabditis sp.* in Aerobic, Microaerobic and Anaerobic Environments. Journal of nematology *2*, 305-315.
- **Couillault, C., Pujol, N., Reboul, J., Sabatier, L., Guichou, J.F., Kohara, Y., and Ewbank, J.J.** (2004). TLR-independent control of innate immunity in *Caenorhabditis elegans* by the TIR domain adaptor protein TIR-1, an ortholog of human SARM. Nature immunology *5*, 488-494.
- **Croll, N.A.** (1975). Components and patterns in the behaviour of the nematode *Caenorhabditis elegans*. Journal of Zoology *176*, 159-176.
- **Crook, R.J., and Walters, E.T.** (2011). Nociceptive behavior and physiology of molluscs: animal welfare implications. ILAR journal / National Research Council, Institute of Laboratory Animal Resources *52*, 185-195.
- **Cryan, J.F., and Dinan, T.G.** (2012). Mind-altering microorganisms: the impact of the gut microbiota on brain and behaviour. Nature reviews Neuroscience *13*, 701-712.
- **Culetto, E., and Sattelle, D.B.** (2000). A role for *Caenorhabditis elegans* in understanding the function and interactions of human disease genes. Human molecular genetics *9*, 869-877.

Bibliography

- **Cully, D.F., Vassilatis, D.K., Liu, K.K., Paress, P.S., Van der Ploeg, L.H., Schaeffer, J.M., and Arena, J.P.** (1994). Cloning of an avermectin-sensitive glutamate-gated chloride channel from *Caenorhabditis elegans*. *Nature* 371, 707-711.
- **Cunningham, K.A., Hua, Z., Srinivasan, S., Liu, J., Lee, B.H., Edwards, R.H., and Ashrafi, K.** (2012). AMP-activated kinase links serotonergic signaling to glutamate release for regulation of feeding behavior in *C. elegans*. *Cell metabolism* 16, 113-121.
- **Davis, J.F., Choi, D.L., and Benoit, S.C.** (2011). Orexigenic Hypothalamic Peptides Behavior and Feeding. *Handbook of Behavior, Food and Nutrition*, 355-369.
- **de Bono, M., and Bargmann, C.I.** (1998). Natural variation in a neuropeptide Y receptor homolog modifies social behavior and food response in *C. elegans*. *Cell* 94, 679-689.
- **de Bono, M., and Maricq, A.V.** (2005). Neuronal substrates of complex behaviors in *C. elegans*. *Annual review of neuroscience* 28, 451-501.
- **de Bono, M., Tobin, D.M., Davis, M.W., Avery, L., and Bargmann, C.I.** (2002). Social feeding in *Caenorhabditis elegans* is induced by neurons that detect aversive stimuli. *Nature* 419, 899-903.
- **de la Fuente-Fernandez, R., Phillips, A.G., Zamburlini, M., Sossi, V., Calne, D.B., Ruth, T.J., and Stoessl, A.J.** (2002). Dopamine release in human ventral striatum and expectation of reward. *Behavioural brain research* 136, 359-363.
- **Denning, D.P., Hatch, V., and Horvitz, H.R.** (2013). Both the caspase CSP-1 and a caspase-independent pathway promote programmed cell death in parallel to the canonical pathway for apoptosis in *Caenorhabditis elegans*. *PLoS Genet* 9, e1003341.
- **Dent, J.A., Davis, M.W., and Avery, L.** (1997). *avr-15* encodes a chloride channel subunit that mediates inhibitory glutamatergic neurotransmission and ivermectin sensitivity in *Caenorhabditis elegans*. *The EMBO journal* 16, 5867-5879.
- **Dent, J.A., Smith, M.M., Vassilatis, D.K., and Avery, L.** (2000). The genetics of ivermectin resistance in *Caenorhabditis elegans*. *Proceedings of the National Academy of Sciences of the United States of America* 97, 2674-2679.
- **Derjean, D., Bertrand, S., Nagy, F., and Shefchyk, S.J.** (2005). Plateau potentials and membrane oscillations in parasympathetic preganglionic neurones and intermediolateral neurones in the rat lumbosacral spinal cord. *The Journal of physiology* 563, 583-596.
- **Di Chiara, G., and Bassareo, V.** (2007). Reward system and addiction: what dopamine does and doesn't do. *Current Opinion in Pharmacology* 7, 69-76.
- **Di Prisco, G.V., Pearlstein, E., Robitaille, R., and Dubuc, R.** (1997). Role of sensory-evoked NMDA plateau potentials in the initiation of locomotion. *Science* 278, 1122-1125.
- **Dillon, J., Franks, C.J., Murray, C., Edwards, R.J., Calahorra, F., Ishihara, T., Katsura, I., Holden-Dye, L., and O'Connor, V.** (2015). Metabotropic glutamate receptors: modulators of context-dependent feeding behaviour in *C. elegans*. *The Journal of biological chemistry*, 15052-15065.
- **Dillon, J., Hopper, N.A., Holden-Dye, L., and O'Connor, V.** (2006). Molecular characterization of the metabotropic glutamate receptor family in *Caenorhabditis elegans*. *Biochemical Society transactions* 34, 942-948.
- **Dittman, J.** (2009). Chapter 2 Worm Watching: Imaging Nervous System Structure and Function in *Caenorhabditis elegans*. In *Advances in Genetics* (Academic Press), pp. 39-78.

- **Doi, M., and Iwasaki, K.** (2002). Regulation of retrograde signaling at neuromuscular junctions by the novel C2 domain protein AEX-1. *Neuron* *33*, 249-259.
- **Dong, W., Fricker, L.D., and Day, R.** (1999). Carboxypeptidase D is a potential candidate to carry out redundant processing functions of carboxypeptidase E based on comparative distribution studies in the rat central nervous system. *Neuroscience* *89*, 1301-1317.
- **Donnelly, J.L., Clark, C.M., Leifer, A.M., Pirri, J.K., Haburcak, M., Francis, M.M., Samuel, A.D., and Alkema, M.J.** (2013). Monoaminergic orchestration of motor programs in a complex *C. elegans* behavior. *PLoS biology* *11*, e1001529.
- **Drozdowski, L.A., and Thomson, A.B.** (2006). Intestinal sugar transport. *World journal of gastroenterology : WJG* *12*, 1657-1670.
- **Durbin, R.M.** (1987). Studies on the development and organisation of the nervous system of *C. elegans* (University of Cambridge, UK).
- **Dwyer, D.S., and Aamodt, E.J.** (2013). Insulin/IGF-1 signaling, including class II/III PI3Ks, beta-arrestin and SGK-1, is required in *C. elegans* to maintain pharyngeal muscle performance during starvation. *PloS one* *8*, e63851.
- **Ebrey, T., and Koutalos, Y.** (2001). Vertebrate photoreceptors. *Progress in retinal and eye research* *20*, 49-94.
- **Edwards, S.L., Charlie, N.K., Richmond, J.E., Hegermann, J., Eimer, S., and Miller, K.G.** (2009). Impaired dense core vesicle maturation in *Caenorhabditis elegans* mutants lacking Rab2. *The Journal of cell biology* *186*, 881-895.
- **Erkut, C., Penkov, S., Khesbak, H., Vorkel, D., Verbavatz, J.M., Fahmy, K., and Kurzchalia, T.V.** (2011). Trehalose renders the dauer larva of *Caenorhabditis elegans* resistant to extreme desiccation. *Current biology : CB* *21*, 1331-1336.
- **Estevez, M., Attisano, L., Wrana, J.L., Albert, P.S., Massague, J., and Riddle, D.L.** (1993). The *daf-4* gene encodes a bone morphogenetic protein receptor controlling *C. elegans* dauer larva development. *Nature* *365*, 644-649.
- **Evans, C.L., and Xie, X.S.** (2008). Coherent anti-stokes Raman scattering microscopy: chemical imaging for biology and medicine. *Annual review of analytical chemistry* *1*, 883-909.
- **Fang-Yen, C., Avery, L., and Samuel, A.D.** (2009). Two size-selective mechanisms specifically trap bacteria-sized food particles in *Caenorhabditis elegans*. *Proceedings of the National Academy of Sciences of the United States of America* *106*, 20093-20096.
- **Fang-Yen, C., Gabel, C.V., Samuel, A.D., Bargmann, C.I., and Avery, L.** (2012a). Laser microsurgery in *Caenorhabditis elegans*. *Methods in cell biology* *107*, 177-206.
- **Fang-Yen, C., Gabel, C.V., Samuel, A.D.T., Bargmann, C.I., and Avery, L.** (2012b). Laser microsurgery in *Caenorhabditis elegans*. In *Meth Cell Biol*, H.R. Joel, and S. Andrew, eds. (Academic Press), pp. 177-206.
- **Fares, H., and Greenwald, I.** (2001). Genetic analysis of endocytosis in *Caenorhabditis elegans*: coelomocyte uptake defective mutants. *Genetics* *159*, 133-145.
- **Felix, M.A., and Duveau, F.** (2012). Population dynamics and habitat sharing of natural populations of *Caenorhabditis elegans* and *C. briggsae*. *BMC biology* *10*, 59.
- **Fenno, L., Yizhar, O., and Deisseroth, K.** (2011). The development and application of optogenetics. *Annual review of neuroscience* *34*, 389-412.
- **Ferraguti, F., and Shigemoto, R.** (2006). Metabotropic glutamate receptors. *Cell and tissue research* *326*, 483-504.

Bibliography

- **Fire, A., Xu, S., Montgomery, M.K., Kostas, S.A., Driver, S.E., and Mello, C.C.** (1998). Potent and specific genetic interference by double-stranded RNA in *Caenorhabditis elegans*. *Nature* *391*, 806-811.
- **Flavell, S.W., Pokala, N., Macosko, E.Z., Albrecht, D.R., Larsch, J., and Bargmann, C.I.** (2013). Serotonin and the Neuropeptide PDF Initiate and Extend Opposing Behavioral States in *C. elegans*. *Cell*, 1023-1035.
- **Franks, C.J., Holden-Dye, L., Bull, K., Luedtke, S., and Walker, R.J.** (2006). Anatomy, physiology and pharmacology of *Caenorhabditis elegans* pharynx: a model to define gene function in a simple neural system. *Invertebrate neuroscience : IN* *6*, 105-122.
- **Frazier, H.N., 3rd, and Roth, M.B.** (2009). Adaptive sugar provisioning controls survival of *C. elegans* embryos in adverse environments. *Current biology : CB* *19*, 859-863.
- **Fredriksson, R., and Schiöth, H.B.** (2005). The repertoire of G-protein-coupled receptors in fully sequenced genomes. *Molecular pharmacology* *67*, 1414-1425.
- **Friedman, J.M.** (2002). The function of leptin in nutrition, weight, and physiology. *Nutrition reviews* *60*, S1-14; discussion S68-84, 85-17.
- **Frooninckx, L., Van Rompay, L., Temmerman, L., Van Sinay, E., Beets, I., Janssen, T., Husson, S.J., and Schoofs, L.** (2012). Neuropeptide GPCRs in *C. elegans*. *Frontiers in endocrinology* *3*, 167.
- **Fuller, R.S., Brake, A.J., and Thorner, J.** (1989). Intracellular targeting and structural conservation of a prohormone-processing endoprotease. *Science* *246*, 482-486.
- **Gannon, M.C., Khan, M.A., and Nuttall, F.Q.** (2001). Glucose appearance rate after the ingestion of galactose. *Metabolism: clinical and experimental* *50*, 93-98.
- **Gao, S., and Zhen, M.** (2011). Action potentials drive body wall muscle contractions in *Caenorhabditis elegans*. *Proceedings of the National Academy of Sciences of the United States of America* *108*, 2557-2562.
- **Garrison, J.L., Macosko, E.Z., Bernstein, S., Pokala, N., Albrecht, D.R., and Bargmann, C.I.** (2012). Oxytocin/vasopressin-related peptides have an ancient role in reproductive behavior. *Science* *338*, 540-543.
- **Gehlert, D.R.** (1999). Role of hypothalamic neuropeptide Y in feeding and obesity. *Neuropeptides* *33*, 329-338.
- **Gems, D., Sutton, A.J., Sundermeyer, M.L., Albert, P.S., King, K.V., Edgley, M.L., Larsen, P.L., and Riddle, D.L.** (1998). Two pleiotropic classes of *daf-2* mutation affect larval arrest, adult behavior, reproduction and longevity in *Caenorhabditis elegans*. *Genetics* *150*, 129-155.
- **Georgi, L.L., Albert, P.S., and Riddle, D.L.** (1990). *daf-1*, a *C. elegans* gene controlling dauer larva development, encodes a novel receptor protein kinase. *Cell* *61*, 635-645.
- **Ghosh, R., Andersen, E.C., Shapiro, J.A., Gerke, J.P., and Kruglyak, L.** (2012). Natural variation in a chloride channel subunit confers avermectin resistance in *C. elegans*. *Science* *335*, 574-578.
- **Giles, A.C., Rose, J.K., and Rankin, C.H.** (2006). Investigations of learning and memory in *Caenorhabditis elegans*. *International review of neurobiology* *69*, 37-71.
- **Glew, R.H.** (2010). You can get there from here: acetone, anionic ketones and even-carbon fatty acids can provide substrates for gluconeogenesis. *Nigerian journal of physiological sciences : official publication of the Physiological Society of Nigeria* *25*, 2-4.

- **Gloria-Soria, A., and Azevedo, R.B.** (2008). *npr-1* Regulates foraging and dispersal strategies in *Caenorhabditis elegans*. *Current biology* : CB *18*, 1694-1699.
- **Gomez-Saladin, E., Luebke, A.E., Wilson, D.L., and Dickerson, I.M.** (1997). Isolation of a cDNA encoding a Kex2-like endoprotease with homology to furin from the nematode *Caenorhabditis elegans*. *DNA and cell biology* *16*, 663-669.
- **Goodman, M.B., Hall, D.H., Avery, L., and Lockery, S.R.** (1998). Active currents regulate sensitivity and dynamic range in *C. elegans* neurons. *Neuron* *20*, 763-772.
- **Gray, J.M., Hill, J.J., and Bargmann, C.I.** (2005). A circuit for navigation in *Caenorhabditis elegans*. *Proceedings of the National Academy of Sciences of the United States of America* *102*, 3184-3191.
- **Gray, J.M., Karow, D.S., Lu, H., Chang, A.J., Chang, J.S., Ellis, R.E., Marletta, M.A., and Bargmann, C.I.** (2004). Oxygen sensation and social feeding mediated by a *C. elegans* guanylate cyclase homologue. *Nature* *430*, 317-322.
- **Greenspan, P., Mayer, E.P., and Fowler, S.D.** (1985). Nile red: a selective fluorescent stain for intracellular lipid droplets. *The Journal of cell biology* *100*, 965-973.
- **Greer, E.R., Perez, C.L., Van Gilst, M.R., Lee, B.H., and Ashrafi, K.** (2008). Neural and molecular dissection of a *C. elegans* sensory circuit that regulates fat and feeding. *Cell metabolism* *8*, 118-131.
- **Grewal, P.S., and Wright, D.J.** (1992). Migration of *Caenorhabditis elegans* (Nematoda : *Rhabditidae*) larvae towards bacteria and the nature of the bacterial stimulus. *Fundam Appl Nematol* *15*, 159-166.
- **Grishanin, R.N., Kowalchuk, J.A., Klenchin, V.A., Ann, K., Earles, C.A., Chapman, E.R., Gerona, R.R., and Martin, T.F.** (2004). CAPS acts at a pre-fusion step in dense-core vesicle exocytosis as a PIP2 binding protein. *Neuron* *43*, 551-562.
- **Gross, D.A., and Silver, D.L.** (2014). Cytosolic lipid droplets: from mechanisms of fat storage to disease. *Critical reviews in biochemistry and molecular biology* *49*, 304-326.
- **Gunther, C.V., Georgi, L.L., and Riddle, D.L.** (2000). A *Caenorhabditis elegans* type I TGF beta receptor can function in the absence of type II kinase to promote larval development. *Development* *127*, 3337-3347.
- **Hall, D.H., and Russell, R.L.** (1991). The posterior nervous system of the nematode *Caenorhabditis elegans*: serial reconstruction of identified neurons and complete pattern of synaptic interactions. *The Journal of neuroscience : the official journal of the Society for Neuroscience* *11*, 1-22.
- **Hammarlund, M., Watanabe, S., Schuske, K., and Jorgensen, E.M.** (2008). CAPS and syntaxin dock dense core vesicles to the plasma membrane in neurons. *The Journal of cell biology* *180*, 483-491.
- **Hashmi, S., Ji, Q., Zhang, J., Parhar, R.S., Huang, C.H., Brey, C., and Gaugler, R.** (2008). A Kruppel-like factor in *Caenorhabditis elegans* with essential roles in fat regulation, cell death, and phagocytosis. *DNA and cell biology* *27*, 545-551.
- **Hashmi, S., Wang, Y., Parhar, R.S., Collison, K.S., Conca, W., Al-Mohanna, F., and Gaugler, R.** (2013). A *C. elegans* model to study human metabolic regulation. *Nutrition & metabolism* *10*, 31.
- **Hashmi, S., Zhang, J., Siddiqui, S.S., Parhar, R.S., Bakheet, R., and Al-Mohanna, F.** (2011). Partner in fat metabolism: role of KLFs in fat burning and reproductive behavior. *3 Biotech* *1*, 59-72.

Bibliography

- **Haycraft, C.J., Schafer, J.C., Zhang, Q., Taulman, P.D., and Yoder, B.K.** (2003). Identification of CHE-13, a novel intraflagellar transport protein required for cilia formation. *Experimental cell research* 284, 251-263.
- **He, L., Vasiliou, K., and Nebert, D.W.** (2009). Analysis and update of the human solute carrier (SLC) gene superfamily. *Human genomics* 3, 195-206.
- **Hedgecock, E.M., and Russell, R.L.** (1975). Normal and mutant thermotaxis in the nematode *Caenorhabditis elegans*. *Proceedings of the National Academy of Sciences of the United States of America* 72, 4061-4065.
- **Hellerer, T., Axang, C., Brackmann, C., Hillertz, P., Pilon, M., and Enejder, A.** (2007). Monitoring of lipid storage in *Caenorhabditis elegans* using coherent anti-Stokes Raman scattering (CARS) microscopy. *Proceedings of the National Academy of Sciences of the United States of America* 104, 14658-14663.
- **Herculano-Houzel, S.** (2012). The remarkable, yet not extraordinary, human brain as a scaled-up primate brain and its associated cost. *Proceedings of the National Academy of Sciences* 109, 10661-10668.
- **Herman, R.K.** (1984). Analysis of genetic mosaics of the nematode *Caenorhabditis elegans*. *Genetics* 108, 165-180.
- **Hetherington, A.W., and Ranson, S.W.** (1940). Hypothalamic Lesions and Adiposity in the Rat, Vol 41.
- **Hieb, W.F., and Rothstein, M.** (1968). Sterol requirement for reproduction of a free-living nematode. *Science* 160, 778-780.
- **Hilliard, M.A., Bargmann, C.I., and Bazzicalupo, P.** (2002). *C. elegans* responds to chemical repellents by integrating sensory inputs from the head and the tail. *Current biology : CB* 12, 730-734.
- **Hills, T., Brockie, P.J., and Maricq, A.V.** (2004). Dopamine and glutamate control area-restricted search behavior in *Caenorhabditis elegans*. *The Journal of neuroscience : the official journal of the Society for Neuroscience* 24, 1217-1225.
- **Hobert, O.** (2013). The neuronal genome of *Caenorhabditis elegans*. *WormBook : the online review of C elegans biology*, 1-106.
- **Hobson, R.J., Geng, J., Gray, A.D., and Komuniecki, R.W.** (2003). SER-7b, a constitutively active Galphas coupled 5-HT7-like receptor expressed in the *Caenorhabditis elegans* M4 pharyngeal motorneuron. *Journal of neurochemistry* 87, 22-29.
- **Hobson, R.J., Hapiak, V.M., Xiao, H., Buehrer, K.L., Komuniecki, P.R., and Komuniecki, R.W.** (2006). SER-7, a *Caenorhabditis elegans* 5-HT7-like receptor, is essential for the 5-HT stimulation of pharyngeal pumping and egg laying. *Genetics* 172, 159-169.
- **Holden-Dye, L., and Walker, R.J.** (2013). The roles of neuropeptides in *Caenorhabditis elegans* including their importance in the regulation of feeding and metabolism. *Protein and peptide letters* 20, 636-646.
- **Horvitz, H.R.** (2003). Worms, life, and death (Nobel lecture). *Chembiochem : a European journal of chemical biology* 4, 697-711.
- **Horvitz, H.R., Chalfie, M., Trent, C., Sulston, J.E., and Evans, P.D.** (1982). Serotonin and octopamine in the nematode *Caenorhabditis elegans*. *Science* 216, 1012-1014.
- **Hu, C., Dillon, J., Kearn, J., Murray, C., O'Connor, V., Holden-Dye, L., and Morgan, H.** (2013). NeuroChip: a microfluidic electrophysiological device for genetic and chemical biology screening of *Caenorhabditis elegans* adult and larvae. *PloS one* 8, e64297.
- **Hu, P.J.** (2007). Dauer. *WormBook : the online review of C elegans biology*, 1-19.

- **Hu, Z., Pym, E.C., Babu, K., Vashlishan Murray, A.B., and Kaplan, J.M.** (2011). A neuropeptide-mediated stretch response links muscle contraction to changes in neurotransmitter release. *Neuron* *71*, 92-102.
- **Hukema, R.K., Rademakers, S., and Jansen, G.** (2008). Gustatory plasticity in *C. elegans* involves integration of negative cues and NaCl taste mediated by serotonin, dopamine, and glutamate. *Learning & memory* *15*, 829-836.
- **Hung, W.L., Hwang, C., Gao, S., Liao, E.H., Chitturi, J., Wang, Y., Li, H., Stigloher, C., Bessereau, J.L., and Zhen, M.** (2013). Attenuation of insulin signalling contributes to FSN-1-mediated regulation of synapse development. *The EMBO journal* *32*, 1745-1760.
- **Husson, S.J., Clynen, E., Baggerman, G., Janssen, T., and Schoofs, L.** (2006). Defective processing of neuropeptide precursors in *Caenorhabditis elegans* lacking proprotein convertase 2 (KPC-2/EGL-3): mutant analysis by mass spectrometry. *Journal of neurochemistry* *98*, 1999-2012.
- **Husson, S.J., Janssen, T., Baggerman, G., Bogert, B., Kahn-Kirby, A.H., Ashrafi, K., and Schoofs, L.** (2007). Impaired processing of FLP and NLP peptides in carboxypeptidase E (EGL-21)-deficient *Caenorhabditis elegans* as analyzed by mass spectrometry. *Journal of neurochemistry* *102*, 246-260.
- **Husson, S.J., Lindemans, M., Janssen, T., and Schoofs, L.** (2009). Comparison of *Caenorhabditis elegans* NLP peptides with arthropod neuropeptides. *Trends in parasitology* *25*, 171-181.
- **Iino, Y., and Yoshida, K.** (2009). Parallel Use of Two Behavioral Mechanisms for Chemotaxis in *Caenorhabditis elegans*. *Journal of Neuroscience* *29*, 5370-5380.
- **Jacob, T.C., and Kaplan, J.M.** (2003). The EGL-21 carboxypeptidase E facilitates acetylcholine release at *Caenorhabditis elegans* neuromuscular junctions. *The Journal of neuroscience : the official journal of the Society for Neuroscience* *23*, 2122-2130.
- **Jafari, G., Xie, Y., Kullyev, A., Liang, B., and Sze, J.Y.** (2011). Regulation of extrasynaptic 5-HT by serotonin reuptake transporter function in 5-HT-absorbing neurons underscores adaptation behavior in *Caenorhabditis elegans*. *The Journal of neuroscience : the official journal of the Society for Neuroscience* *31*, 8948-8957.
- **Jagannathan, S., Loughton, D.L., Critten, C.L., Skinner, T.M., Horoszok, L., and Wolstenholme, A.J.** (1999). Ligand-gated chloride channel subunits encoded by the *Haemonchus contortus* and *Ascaris suum* orthologues of the *Caenorhabditis elegans* *gbr-2 (avr-14)* gene. *Molecular and biochemical parasitology* *103*, 129-140.
- **Jansen, G., Thijssen, K.L., Werner, P., van der Horst, M., Hazendonk, E., and Plasterk, R.H.** (1999). The complete family of genes encoding G proteins of *Caenorhabditis elegans*. *Nature genetics* *21*, 414-419.
- **Janssen, T., Lindemans, M., Meelkop, E., Temmerman, L., and Schoofs, L.** (2010). Coevolution of neuropeptidergic signaling systems: from worm to man. *Annals of the New York Academy of Sciences* *1200*, 1-14.
- **Janssen, T., Meelkop, E., Lindemans, M., Verstraelen, K., Husson, S.J., Temmerman, L., Nachman, R.J., and Schoofs, L.** (2008). Discovery of a cholecystokinin-gastrin-like signaling system in nematodes. *Endocrinology* *149*, 2826-2839.
- **Janssen, T., Meelkop, E., Nachman, R.J., and Schoofs, L.** (2009). Evolutionary conservation of the cholecystokinin/gastrin signaling system in nematodes. *Annals of the New York Academy of Sciences* *1163*, 428-432.
- **Jee, C., Lee, J., Lim, J.P., Parry, D., Messing, R.O., and McIntire, S.L.** (2013). SEB-3, a CRF receptor-like GPCR, regulates locomotor activity states, stress

Bibliography

responses and ethanol tolerance in *Caenorhabditis elegans*. *Genes, brain, and behavior* 12, 250-262.

- **Jeong, P.Y., Jung, M., Yim, Y.H., Kim, H., Park, M., Hong, E., Lee, W., Kim, Y.H., Kim, K., and Paik, Y.K.** (2005). Chemical structure and biological activity of the *Caenorhabditis elegans* dauer-inducing pheromone. *Nature* 433, 541-545.
- **Jimerson, D.C., Wolfe, B.E., Carroll, D.P., and Keel, P.K.** (2010). Psychobiology of purging disorder: reduction in circulating leptin levels in purging disorder in comparison with controls. *The International journal of eating disorders* 43, 584-588.
- **Jo, H., Shim, J., Lee, J.H., Lee, J., and Kim, J.B.** (2009). IRE-1 and HSP-4 contribute to energy homeostasis via fasting-induced lipases in *C. elegans*. *Cell metabolism* 9, 440-448.
- **Jockusch, W.J., Speidel, D., Sigler, A., Sorensen, J.B., Varoqueaux, F., Rhee, J.S., and Brose, N.** (2007). CAPS-1 and CAPS-2 are essential synaptic vesicle priming proteins. *Cell* 131, 796-808.
- **Johnstone, I.L.** (1994). The cuticle of the nematode *Caenorhabditis elegans*: a complex collagen structure. *BioEssays : news and reviews in molecular, cellular and developmental biology* 16, 171-178.
- **Jones, K.T., and Ashrafi, K.** (2009). *Caenorhabditis elegans* as an emerging model for studying the basic biology of obesity. *Disease models & mechanisms* 2, 224-229.
- **Jorgensen, E.M.** (2005). GABA. *WormBook : the online review of C elegans biology*, 1-13.
- **Kaga, T., Inui, A., Okita, M., Asakawa, A., Ueno, N., Kasuga, M., Fujimiya, M., Nishimura, N., Dobashi, R., Morimoto, Y., et al.** (2001). Modest overexpression of neuropeptide Y in the brain leads to obesity after high-sucrose feeding. *Diabetes* 50, 1206-1210.
- **Kahn, F.R., and McFadden, B.A.** (1980). Embryogenesis and the glyoxylate cycle. *FEBS letters* 115, 312-314.
- **Kaletta, T., and Hengartner, M.O.** (2006). Finding function in novel targets: *C. elegans* as a model organism. *Nature reviews Drug discovery* 5, 387-398.
- **Kalivas, P.W., and Nakamura, M.** (1999). Neural systems for behavioral activation and reward. *Current opinion in neurobiology* 9, 223-227.
- **Kalra, S.P., Dube, M.G., Pu, S., Xu, B., Horvath, T.L., and Kalra, P.S.** (1999). Interacting appetite-regulating pathways in the hypothalamic regulation of body weight. *Endocrine reviews* 20, 68-100.
- **Kamath, R.S., and Ahringer, J.** (2003). Genome-wide RNAi screening in *Caenorhabditis elegans*. *Methods* 30, 313-321.
- **Kano, T., Brockie, P.J., Sassa, T., Fujimoto, H., Kawahara, Y., Iino, Y., Mellem, J.E., Madsen, D.M., Hosono, R., and Maricq, A.V.** (2008). Memory in *Caenorhabditis elegans* is mediated by NMDA-type ionotropic glutamate receptors. *Current biology : CB* 18, 1010-1015.
- **Kaplan, J.M., and Horvitz, H.R.** (1993). A dual mechanosensory and chemosensory neuron in *Caenorhabditis elegans*. *Proceedings of the National Academy of Sciences of the United States of America* 90, 2227-2231.
- **Kass, J., Jacob, T.C., Kim, P., and Kaplan, J.M.** (2001). The EGL-3 proprotein convertase regulates mechanosensory responses of *Caenorhabditis elegans*. *The Journal of neuroscience : the official journal of the Society for Neuroscience* 21, 9265-9272.
- **Kawano, T., Po, M.D., Gao, S., Leung, G., Ryu, W.S., and Zhen, M.** (2011). An imbalancing act: gap junctions reduce the backward motor circuit activity to bias *C. elegans* for forward locomotion. *Neuron* 72, 572-586.

- **Keane, J., and Avery, L.** (2003). Mechanosensory inputs influence *Caenorhabditis elegans* pharyngeal activity via ivermectin sensitivity genes. *Genetics* 164, 153-162.
- **Keating, C.D., Kriek, N., Daniels, M., Ashcroft, N.R., Hopper, N.A., Siney, E.J., Holden-Dye, L., and Burke, J.F.** (2003). Whole-Genome Analysis of 60 G Protein-Coupled Receptors in *Caenorhabditis elegans* by Gene Knockout with RNAi. *Current Biology* 13, 1715-1720.
- **Keen-Rhinehart, E., Ondek, K., and Schneider, J.E.** (2013). Neuroendocrine regulation of appetitive ingestive behavior. *Frontiers in neuroscience* 7, 213.
- **Kenyon, C., Chang, J., Gensch, E., Rudner, A., and Tabtiang, R.** (1993). A *C. elegans* mutant that lives twice as long as wild type. *Nature* 366, 461-464.
- **Kim, E., Sun, L., Gabel, C.V., and Fang-Yen, C.** (2013). Long-term imaging of *Caenorhabditis elegans* using nanoparticle-mediated immobilization. *PloS one* 8, e53419.
- **Kim, H., Ishidate, T., Ghanta, K.S., Seth, M., Conte, D., Jr., Shirayama, M., and Mello, C.C.** (2014). A co-CRISPR strategy for efficient genome editing in *Caenorhabditis elegans*. *Genetics* 197, 1069-1080.
- **Kim, K., and Li, C.** (2004). Expression and regulation of an FMRFamide-related neuropeptide gene family in *Caenorhabditis elegans*. *The Journal of comparative neurology* 475, 540-550.
- **Kimura, K.D., Tissenbaum, H.A., Liu, Y., and Ruvkun, G.** (1997). *daf-2*, an insulin receptor-like gene that regulates longevity and diapause in *Caenorhabditis elegans*. *Science* 277, 942-946.
- **Kiyama, Y., Miyahara, K., and Ohshima, Y.** (2012). Active uptake of artificial particles in the nematode *Caenorhabditis elegans*. *The Journal of experimental biology* 215, 1178-1183.
- **Klapper, M., Ehmke, M., Palgunow, D., Bohme, M., Matthaus, C., Bergner, G., Dietzek, B., Popp, J., and Doring, F.** (2011). Fluorescence-based fixative and vital staining of lipid droplets in *Caenorhabditis elegans* reveal fat stores using microscopy and flow cytometry approaches. *Journal of lipid research* 52, 1281-1293.
- **Knowles, J.R.** (1980). Enzyme-catalyzed phosphoryl transfer reactions. *Annual review of biochemistry* 49, 877-919.
- **Kohn, R.E., Duerr, J.S., McManus, J.R., Duke, A., Rakow, T.L., Maruyama, H., Moulder, G., Maruyama, I.N., Barstead, R.J., and Rand, J.B.** (2000). Expression of multiple UNC-13 proteins in the *Caenorhabditis elegans* nervous system. *Molecular biology of the cell* 11, 3441-3452.
- **Kolhekar, A.S., Roberts, M.S., Jiang, N., Johnson, R.C., Mains, R.E., Eipper, B.A., and Taghert, P.H.** (1997). Neuropeptide amidation in *Drosophila*: separate genes encode the two enzymes catalyzing amidation. *The Journal of neuroscience : the official journal of the Society for Neuroscience* 17, 1363-1376.
- **Komatsu, H., Mori, I., Rhee, J.S., Akaike, N., and Ohshima, Y.** (1996). Mutations in a cyclic nucleotide-gated channel lead to abnormal thermosensation and chemosensation in *C. elegans*. *Neuron* 17, 707-718.
- **Komuniecki, R.W., Hobson, R.J., Rex, E.B., Hapiak, V.M., and Komuniecki, P.R.** (2004). Biogenic amine receptors in parasitic nematodes: what can be learned from *Caenorhabditis elegans*? *Molecular and biochemical parasitology* 137, 1-11.
- **Konturek, S.J., Konturek, J.W., Pawlik, T., and Brzozowski, T.** (2004). Brain-gut axis and its role in the control of food intake. *Journal of physiology and pharmacology : an official journal of the Polish Physiological Society* 55, 137-154.

Bibliography

- **Konturek, S.J., Pepera, J., Zabielski, K., Konturek, P.C., Pawlik, T., Szlachcic, A., and Hahn, E.G.** (2003). Brain-gut axis in pancreatic secretion and appetite control. *Journal of physiology and pharmacology : an official journal of the Polish Physiological Society* *54*, 293-317.
- **Kramer, J.M.** (1994). Structures and functions of collagens in *Caenorhabditis elegans*. *FASEB journal : official publication of the Federation of American Societies for Experimental Biology* *8*, 329-336.
- **Kubiak, T.M., Larsen, M.J., Zantello, M.R., Bowman, J.W., Nulf, S.C., and Lowery, D.E.** (2003). Functional annotation of the putative orphan *Caenorhabditis elegans* G-protein-coupled receptor C10C6.2 as a FLP15 peptide receptor. *The Journal of biological chemistry* *278*, 42115-42120.
- **Kurzchalia, T.V., and Ward, S.** (2003). Why do worms need cholesterol? *Nature cell biology* *5*, 684-688.
- **Laffel, L.** (1999). Ketone bodies: a review of physiology, pathophysiology and application of monitoring to diabetes. *Diabetes/metabolism research and reviews* *15*, 412-426.
- **Lau, H.E., and Chalasani, S.H.** (2014). Divergent and convergent roles for insulin-like peptides in the worm, fly and mammalian nervous systems. *Invertebrate neuroscience : IN* *14*, 71-78.
- **Laughton, D.L., Lunt, G.G., and Wolstenholme, A.J.** (1997). Reporter gene constructs suggest that the *Caenorhabditis elegans* avermectin receptor beta-subunit is expressed solely in the pharynx. *The Journal of experimental biology* *200*, 1509-1514.
- **Le, T.T., Duren, H.M., Slipchenko, M.N., Hu, C.D., and Cheng, J.X.** (2010). Label-free quantitative analysis of lipid metabolism in living *Caenorhabditis elegans*. *Journal of lipid research* *51*, 672-677.
- **Lee, B.H., Liu, J., Wong, D., Srinivasan, S., and Ashrafi, K.** (2011). Hyperactive neuroendocrine secretion causes size, feeding, and metabolic defects of *C. elegans* Bardet-Biedl syndrome mutants. *PLoS biology* *9*, e1001219.
- **Lee, D., Jung, S., Ryu, J., Ahnn, J., and Ha, I.** (2008). Human vesicular glutamate transporters functionally complement EAT-4 in *C. elegans*. *Molecules and cells* *25*, 50-54.
- **Lee, H., Choi, M.K., Lee, D., Kim, H.S., Hwang, H., Kim, H., Park, S., Paik, Y.K., and Lee, J.** (2012). Nictation, a dispersal behavior of the nematode *Caenorhabditis elegans*, is regulated by IL2 neurons. *Nature neuroscience* *15*, 107-112.
- **Lee, J.H., Kong, J., Jang, J.Y., Han, J.S., Ji, Y., Lee, J., and Kim, J.B.** (2014). Lipid Droplet Protein LID-1 Mediates ATGL-1-Dependent Lipolysis during Fasting in *Caenorhabditis elegans*. *Molecular and cellular biology* *34*, 4165-4176.
- **Lee, R.Y., Hench, J., and Ruvkun, G.** (2001). Regulation of *C. elegans* DAF-16 and its human ortholog FKHRL1 by the *daf-2* insulin-like signaling pathway. *Current biology : CB* *11*, 1950-1957.
- **Lee, R.Y., Lobel, L., Hengartner, M., Horvitz, H.R., and Avery, L.** (1997). Mutations in the alpha1 subunit of an L-type voltage-activated Ca²⁺ channel cause myotonia in *Caenorhabditis elegans*. *The EMBO journal* *16*, 6066-6076.
- **Lee, R.Y., Sawin, E.R., Chalfie, M., Horvitz, H.R., and Avery, L.** (1999). EAT-4, a homolog of a mammalian sodium-dependent inorganic phosphate cotransporter, is necessary for glutamatergic neurotransmission in *caenorhabditis elegans*. *The Journal of Neuroscience* *19*, 159-167.

- **Leinwand, S.G., and Chalasani, S.H.** (2013). Neuropeptide signaling remodels chemosensory circuit composition in *Caenorhabditis elegans*. *Nature neuroscience* *16*, 1461-1467.
- **Lemieux, G.A., Cunningham, K.A., Lin, L., Mayer, F., Werb, Z., and Ashrafi, K.** (2015). Kynurenic acid is a nutritional cue that enables behavioral plasticity. *Cell* *160*, 119-131.
- **Lenard, N.R., and Berthoud, H.R.** (2008). Central and peripheral regulation of food intake and physical activity: pathways and genes. *Obesity* *16 Suppl 3*, S11-22.
- **Li, C.** (2005). The ever-expanding neuropeptide gene families in the nematode *Caenorhabditis elegans*. *Parasitology* *131 Suppl*, S109-127.
- **Li, C., and Kim, K.** (2008). Neuropeptides. *WormBook : the online review of C elegans biology*, 1-36.
- **Li, C., and Kim, K.** (2010). Neuropeptide gene families in *Caenorhabditis elegans*. *Advances in experimental medicine and biology* *692*, 98-137.
- **Li, C., and Kim, K.** (2014). Family of FLP Peptides in *Caenorhabditis elegans* and Related Nematodes. *Frontiers in endocrinology* *5*, 150-166.
- **Li, C., Kim, K., and Nelson, L.S.** (1999a). FMRFamide-related neuropeptide gene family in *Caenorhabditis elegans*. *Brain research* *848*, 26-34.
- **Li, C., Nelson, L.S., Kim, K., Nathoo, A., and Hart, A.C.** (1999b). Neuropeptide gene families in the nematode *Caenorhabditis elegans*. *Annals of the New York Academy of Sciences* *897*, 239-252.
- **Li, S., Dent, J.A., and Roy, R.** (2003). Regulation of intermuscular electrical coupling by the *Caenorhabditis elegans* innexin *inx-6*. *Molecular biology of the cell* *14*, 2630-2644.
- **Li, Z., Li, Y., Yi, Y., Huang, W., Yang, S., Niu, W., Zhang, L., Xu, Z., Qu, A., Wu, Z., et al.** (2012). Dissecting a central flip-flop circuit that integrates contradictory sensory cues in *C. elegans* feeding regulation. *Nature communications* *3*, 776.
- **Lindemans, M., Janssen, T., Husson, S.J., Meelkop, E., Temmerman, L., Clynen, E., Mertens, I., and Schoofs, L.** (2009). A neuromedin-pyrokinin-like neuropeptide signaling system in *Caenorhabditis elegans*. *Biochemical and biophysical research communications* *379*, 760-764.
- **Lindsay, T.H., Thiele, T.R., and Lockery, S.R.** (2011). Optogenetic analysis of synaptic transmission in the central nervous system of the nematode *Caenorhabditis elegans*. *Nature communications* *2*, 306.
- **Lints, R., and Emmons, S.W.** (1999). Patterning of dopaminergic neurotransmitter identity among *Caenorhabditis elegans* ray sensory neurons by a TGFbeta family signaling pathway and a Hox gene. *Development* *126*, 5819-5831.
- **Lipton, J., Kleemann, G., Ghosh, R., Lints, R., and Emmons, S.W.** (2004). Mate searching in *Caenorhabditis elegans*: a genetic model for sex drive in a simple invertebrate. *The Journal of neuroscience : the official journal of the Society for Neuroscience* *24*, 7427-7434.
- **Liu, F., Thatcher, J.D., Barral, J.M., and Epstein, H.F.** (1995). Bifunctional glyoxylate cycle protein of *Caenorhabditis elegans*: a developmentally regulated protein of intestine and muscle. *Dev Biol* *169*, 399-414.
- **Liu, F., Thatcher, J.D., and Epstein, H.F.** (1997). Induction of glyoxylate cycle expression in *Caenorhabditis elegans*: a fasting response throughout larval development. *Biochemistry* *36*, 255-260.
- **Liu, Q., Hollopeter, G., and Jorgensen, E.M.** (2009). Graded synaptic transmission at the *Caenorhabditis elegans* neuromuscular junction.

Bibliography

Proceedings of the National Academy of Sciences of the United States of America *106*, 10823-10828.

- **Liu, T., Kim, K., Li, C., and Barr, M.M.** (2007). FMRFamide-like neuropeptides and mechanosensory touch receptor neurons regulate male sexual turning behavior in *Caenorhabditis elegans*. *The Journal of neuroscience : the official journal of the Society for Neuroscience* *27*, 7174-7182.
- **Lockery, S.R., and Goodman, M.B.** (2009). The quest for action potentials in *C. elegans* neurons hits a plateau. *Nature neuroscience* *12*, 377-378.
- **Lodish, H., Berk, A., Zipursky, S.L., Matsudaira, P., Baltimore, D., and Darnell, J.** (2000). Section 21.5 Neurotransmitter Receptors. In *Molecular Cell Biology* 4th edition, W.H. Freeman, ed.
- **Lowery, D.E., Geary, T.G., Kubiak, T.M., and Larsen, M.J.** (2003). *G Protein-Coupled Receptor-like Receptors and Modulators Thereof* (Pharmacia and Upjohn Company).
- **Lutter, M., and Nestler, E.J.** (2009). Homeostatic and hedonic signals interact in the regulation of food intake. *The Journal of nutrition* *139*, 629-632.
- **MacNeil, L.T., Watson, E., Arda, H.E., Zhu, L.J., and Walhout, A.J.** (2013). Diet-induced developmental acceleration independent of TOR and insulin in *C. elegans*. *Cell* *153*, 240-252.
- **Mahoney, T.R., Luo, S., Round, E.K., Brauner, M., Gottschalk, A., Thomas, J.H., and Nonet, M.L.** (2008). Intestinal signaling to GABAergic neurons regulates a rhythmic behavior in *Caenorhabditis elegans*. *Proceedings of the National Academy of Sciences of the United States of America* *105*, 16350-16355.
- **Mangahas, P.M., Yu, X., Miller, K.G., and Zhou, Z.** (2008). The small GTPase Rab2 functions in the removal of apoptotic cells in *Caenorhabditis elegans*. *The Journal of cell biology* *180*, 357-373.
- **Mano, I., Straud, S., and Driscoll, M.** (2007). *Caenorhabditis elegans* glutamate transporters influence synaptic function and behavior at sites distant from the synapse. *Journal of Biological Chemistry* *282*, 34412-34419.
- **Maricq, A.V., Peckol, E., Driscoll, M., and Bargmann, C.I.** (1995). Mechanosensory signalling in *C. elegans* mediated by the GLR-1 glutamate receptor. *Nature* *378*, 78-81.
- **Marks, M.S., Heijnen, H.F., and Raposo, G.** (2013). Lysosome-related organelles: unusual compartments become mainstream. *Current opinion in cell biology* *25*, 495-505.
- **McElwee, J.J., Schuster, E., Blanc, E., Thornton, J., and Gems, D.** (2006). Diapause-associated metabolic traits reiterated in long-lived *daf-2* mutants in the nematode *Caenorhabditis elegans*. *Mechanisms of ageing and development* *127*, 458-472.
- **McIntire, S.L., Jorgensen, E., Kaplan, J., and Horvitz, H.R.** (1993). The GABAergic nervous system of *Caenorhabditis elegans*. *Nature* *364*, 337-341.
- **McKay, J.P., Raizen, D.M., Gottschalk, A., Schafer, W.R., and Avery, L.** (2004). *eat-2* and *eat-18* are required for nicotinic neurotransmission in the *Caenorhabditis elegans* pharynx. *Genetics* *166*, 161-169.
- **McKay, R.M., McKay, J.P., Avery, L., and Graff, J.M.** (2003a). *C. elegans*: a model for exploring the genetics of fat storage. *Developmental cell* *4*, 131-142.
- **McKay, S.J., Johnsen, R., Khattra, J., Asano, J., Baillie, D.L., Chan, S., Dube, N., Fang, L., Goszczynski, B., Ha, E., et al.** (2003b). Gene expression profiling of cells, tissues, and developmental stages of the nematode *C. elegans*. *Cold Spring Harbor symposia on quantitative biology* *68*, 159-169.
- **Meelkop, E., Temmerman, L., Janssen, T., Suetens, N., Beets, I., Van Rompay, L., Shanmugam, N., Husson, S.J., and Schoofs, L.** (2012). PDF

- receptor signaling in *Caenorhabditis elegans* modulates locomotion and egg-laying. *Molecular and cellular endocrinology* 361, 232-240.
- **Mellem, J.E., Brockie, P.J., Zheng, Y., Madsen, D.M., and Maricq, A.V.** (2002). Decoding of polymodal sensory stimuli by postsynaptic glutamate receptors in *C. elegans*. *Neuron* 36, 933-944.
 - **Mello, C.C., Kramer, J.M., Stinchcomb, D., and Ambros, V.** (1991). Efficient gene transfer in *C. elegans*: extrachromosomal maintenance and integration of transforming sequences. *The EMBO journal* 10, 3959-3970.
 - **Mercer, A.R., Kloppenburg, P., and Hildebrand, J.G.** (2005). Plateau potentials in developing antennal-lobe neurons of the moth, *Manduca sexta*. *Journal of neurophysiology* 93, 1949-1958.
 - **Merris, M., Wadsworth, W.G., Khamrai, U., Bittman, R., Chitwood, D.J., and Lenard, J.** (2003). Sterol effects and sites of sterol accumulation in *Caenorhabditis elegans*: developmental requirement for 4 α -methyl sterols. *Journal of lipid research* 44, 172-181.
 - **Meyer-Lindenberg, A., Domes, G., Kirsch, P., and Heinrichs, M.** (2011). Oxytocin and vasopressin in the human brain: social neuropeptides for translational medicine. *Nature reviews Neuroscience* 12, 524-538.
 - **Miller, K.G., Alfonso, A., Nguyen, M., Crowell, J.A., Johnson, C.D., and Rand, J.B.** (1996). A genetic selection for *Caenorhabditis elegans* synaptic transmission mutants. *Proceedings of the National Academy of Sciences of the United States of America* 93, 12593-12598.
 - **Mills, H., Wragg, R., Hapiak, V., Castelletto, M., Zahratka, J., Harris, G., Summers, P., Korchnak, A., Law, W., Bamber, B., et al.** (2012). Monoamines and neuropeptides interact to inhibit aversive behaviour in *Caenorhabditis elegans*. *EMBO J* 31, 667-678.
 - **Milward, K., Busch, K.E., Murphy, R.J., de Bono, M., and Olofsson, B.** (2011). Neuronal and molecular substrates for optimal foraging in *Caenorhabditis elegans*. *Proceedings of the National Academy of Sciences of the United States of America* 108, 20672-20677.
 - **Mitchell, P., Mould, R., Dillon, J., Glautier, S., Andrianakis, I., James, C., Pugh, A., Holden-Dye, L., and O'Connor, V.** (2010). A differential role for neuropeptides in acute and chronic adaptive responses to alcohol: behavioural and genetic analysis in *Caenorhabditis elegans*. *PloS one* 5, e10422.
 - **Mori, I., and Ohshima, Y.** (1995). Neural regulation of thermotaxis in *Caenorhabditis elegans*. *Nature* 376, 344-348.
 - **Morley, J.E., Hernandez, E.N., and Flood, J.F.** (1987). Neuropeptide Y increases food intake in mice. *The American journal of physiology* 253, R516-522.
 - **Mueller, G.P., Husten, E.J., Mains, R.E., and Eipper, B.A.** (1993). Peptide alpha-amidation and peptidylglycine alpha-hydroxylating monooxygenase: control by disulfiram. *Molecular pharmacology* 44, 972-980.
 - **Mukhopadhyay, A., Deplancke, B., Walhout, A.J., and Tissenbaum, H.A.** (2005). *C. elegans* tubby regulates life span and fat storage by two independent mechanisms. *Cell metabolism* 2, 35-42.
 - **Mulcahy, B., Holden-Dye, L., and O'Connor, V.** (2013). Pharmacological assays reveal age-related changes in synaptic transmission at the *Caenorhabditis elegans* neuromuscular junction that are modified by reduced insulin signalling. *The Journal of experimental biology* 216, 492-501.
 - **Mullaney, B.C., and Ashrafi, K.** (2009). *C. elegans* fat storage and metabolic regulation. *Biochimica et biophysica acta* 1791, 474-478.
 - **Murphy, C.T., Lee, S.J., and Kenyon, C.** (2007). Tissue entrainment by feedback regulation of insulin gene expression in the endoderm of

Bibliography

- Caenorhabditis elegans*. Proceedings of the National Academy of Sciences of the United States of America *104*, 19046-19050.
- **Nakanishi, S., Nakajima, Y., Masu, M., Ueda, Y., Nakahara, K., Watanabe, D., Yamaguchi, S., Kawabata, S., and Okada, M.** (1998). Glutamate receptors: brain function and signal transduction. *Brain research Brain research reviews* *26*, 230-235.
 - **Nakayama, K.** (1997). Furin: a mammalian subtilisin/Kex2p-like endoprotease involved in processing of a wide variety of precursor proteins. *The Biochemical journal* *327 (Pt 3)*, 625-635.
 - **Nathoo, A.N., Moeller, R.A., Westlund, B.A., and Hart, A.C.** (2001). Identification of neuropeptide-like protein gene families in *Caenorhabditiselegans* and other species. *Proceedings of the National Academy of Sciences of the United States of America* *98*, 14000-14005.
 - **Nehlig, A.** (2004). Brain uptake and metabolism of ketone bodies in animal models. *Prostag Leukotr Ess* *70*, 265-275.
 - **Nelson, L.S.** (1998). Disruption of a Neuropeptide Gene, *flp-1*, Causes Multiple Behavioral Defects in *Caenorhabditis elegans*. *Science* *281*, 1686-1690.
 - **Nestler, E.J.** (2001). Molecular basis of long-term plasticity underlying addiction. *Nature reviews Neuroscience* *2*, 119-128.
 - **Niacaris, T.** (2003). Serotonin regulates repolarization of the *C. elegans* pharyngeal muscle. *Journal of Experimental Biology* *206*, 223-231.
 - **Niswender, C.M., and Conn, P.J.** (2010). Metabotropic glutamate receptors: physiology, pharmacology, and disease. *Annual review of pharmacology and toxicology* *50*, 295-322.
 - **Nonet, M.L., Grundahl, K., Meyer, B.J., and Rand, J.B.** (1993). Synaptic function is impaired but not eliminated in *C. elegans* mutants lacking synaptotagmin. *Cell* *73*, 1291-1305.
 - **O'Rahilly, S., and Farooqi, I.S.** (2008). Human obesity as a heritable disorder of the central control of energy balance. *Int J Obes (Lond)* *32 Suppl 7*, S55-61.
 - **O'Riordan, V.B., and Burnell, A.M.** (1990). Intermediary metabolism in the dauer larva of the nematode *Caenorhabditis elegans*—II. The glyoxylate cycle and fatty-acid oxidation. *Comparative Biochemistry and Physiology Part B: Comparative Biochemistry* *95*, 125-130.
 - **O'Rourke, E.J., Soukas, A.A., Carr, C.E., and Ruvkun, G.** (2009). *C. elegans* major fats are stored in vesicles distinct from lysosome-related organelles. *Cell metabolism* *10*, 430-435.
 - **Ogg, S., Paradis, S., Gottlieb, S., Patterson, G.I., Lee, L., Tissenbaum, H.A., and Ruvkun, G.** (1997). The Fork head transcription factor DAF-16 transduces insulin-like metabolic and longevity signals in *C. elegans*. *Nature* *389*, 994-999.
 - **Oliver, S.G., Winson, M.K., Kell, D.B., and Baganz, F.** (1998). Systematic functional analysis of the yeast genome. *Trends in biotechnology* *16*, 373-378.
 - **Owen, O.E., Reichard, G.A., Jr., Patel, M.S., and Boden, G.** (1979). Energy metabolism in feasting and fasting. *Advances in experimental medicine and biology* *111*, 169-188.
 - **Packham, R., Walker, R.J., and Holden-Dye, L.** (2010). The effect of a selective octopamine antagonist, epinastine, on pharyngeal pumping in *Caenorhabditis elegans*. *Invertebrate neuroscience : IN* *10*, 47-52.
 - **Page, A.J., Brierley, S.M., Martin, C.M., Price, M.P., Symonds, E., Butler, R., Wemmie, J.A., and Blackshaw, L.A.** (2005). Different contributions of ASIC channels 1a, 2, and 3 in gastrointestinal mechanosensory function. *Gut* *54*, 1408-1415.

- **Palmiter, R.D., Erickson, J.C., Hollopeter, G., Baraban, S.C., and Schwartz, M.W.** (1998). Life without neuropeptide Y. Recent progress in hormone research *53*, 163-199.
- **Papaioannou, S., Holden-Dye, L., and Walker, R.J.** (2008a). The actions of *Caenorhabditis elegans* neuropeptide-like peptides (NLPs) on body wall muscle of *Ascaris suum* and pharyngeal muscle of *C. elegans*. *Acta biologica Hungarica 59 Suppl*, 189-197.
- **Papaioannou, S., Holden-Dye, L., and Walker, R.J.** (2008b). Evidence for a role for cyclic AMP in modulating the action of 5-HT and an excitatory neuropeptide, FLP17A, in the pharyngeal muscle of *Caenorhabditis elegans*. *Invertebrate neuroscience : IN 8*, 91-100.
- **Papaioannou, S., Marsden, D., Franks, C.J., Walker, R.J., and Holden-Dye, L.** (2005). Role of a FMRFamide-like family of neuropeptides in the pharyngeal nervous system of *Caenorhabditis elegans*. *Journal of neurobiology 65*, 304-319.
- **Pellerone, F.I., Archer, S.K., Behm, C.A., Grant, W.N., Lacey, M.J., and Somerville, A.C.** (2003). Trehalose metabolism genes in *Caenorhabditis elegans* and filarial nematodes. *Int J Parasitol 33*, 1195-1206.
- **Perez, C.L., and Van Gilst, M.R.** (2008). A ¹³C isotope labeling strategy reveals the influence of insulin signaling on lipogenesis in *C. elegans*. *Cell metabolism 8*, 266-274.
- **Perkins, L.A., Hedgecock, E.M., Thomson, J.N., and Culotti, J.G.** (1986). Mutant sensory cilia in the nematode *Caenorhabditis elegans*. *Dev Biol 117*, 456-487.
- **Peymen, K., Watteyne, J., Froninckx, L., Schoofs, L., and Beets, I.** (2014). The FMRFamide-Like Peptide Family in Nematodes. *Frontiers in endocrinology 5*, 90.
- **Phelan, P., Bacon, J.P., Davies, J.A., Stebbings, L.A., Todman, M.G., Avery, L., Baines, R.A., Barnes, T.M., Ford, C., Hekimi, S., et al.** (1998). Innexins: a family of invertebrate gap-junction proteins. *Trends in genetics : TIG 14*, 348-349.
- **Pierce-Shimomura, J.T., Morse, T.M., and Lockery, S.R.** (1999). The fundamental role of pirouettes in *Caenorhabditis elegans* chemotaxis. *The Journal of neuroscience : the official journal of the Society for Neuroscience 19*, 9557-9569.
- **Pierce, S.B., Costa, M., Wisotzkey, R., Devadhar, S., Homburger, S.A., Buchman, A.R., Ferguson, K.C., Heller, J., Platt, D.M., Pasquinelli, A.A., et al.** (2001). Regulation of DAF-2 receptor signaling by human insulin and *ins-1*, a member of the unusually large and diverse *C. elegans* insulin gene family. *Genes & development 15*, 672-686.
- **Piggott, B.J., Liu, J., Feng, Z., Wescott, S.A., and Xu, X.Z.** (2011). The neural circuits and synaptic mechanisms underlying motor initiation in *C. elegans*. *Cell 147*, 922-933.
- **Pontoizeau, C., Mouchiroud, L., Molin, L., Mergoud-Dit-Lamarque, A., Dalli re, N., Toulhoat, P., Elena-Herrmann, B., and Solari, F.** (2014). Metabolomics analysis uncovers that dietary restriction buffers metabolic changes associated with aging in *Caenorhabditis elegans*. *Journal of proteome research 13*, 2910-2919.
- **Portillo, V., Jagannathan, S., and Wolstenholme, A.J.** (2003). Distribution of glutamate-gated chloride channel subunits in the parasitic nematode *Haemonchus contortus*. *The Journal of comparative neurology 462*, 213-222.

Bibliography

- **Prigge, S.T., Mains, R.E., Eipper, B.A., and Amzel, L.M.** (2000). New insights into copper monooxygenases and peptide amidation: structure, mechanism and function. *Cellular and molecular life sciences* : CMLS 57, 1236-1259.
- **Qian, S., Chen, H., Weingarth, D., Trumbauer, M.E., Novi, D.E., Guan, X., Yu, H., Shen, Z., Feng, Y., Frazier, E., et al.** (2002). Neither agouti-related protein nor neuropeptide Y is critically required for the regulation of energy homeostasis in mice. *Molecular and cellular biology* 22, 5027-5035.
- **Qu, W., Ren, C., Li, Y., Shi, J., Zhang, J., Wang, X., Hang, X., Lu, Y., Zhao, D., and Zhang, C.** (2011). Reliability analysis of the Ahringer *Caenorhabditis elegans* RNAi feeding library: a guide for genome-wide screens. *BMC genomics* 12, 170.
- **Raizen, D.M., and Avery, L.** (1994). Electrical activity and behavior in the pharynx of *Caenorhabditis elegans*. *Neuron* 12, 483-495.
- **Raizen, D.M., Lee, R.Y., and Avery, L.** (1995). Interacting genes required for pharyngeal excitation by motor neuron MC in *Caenorhabditis elegans*. *Genetics* 141, 1365-1382.
- **Raizen, D.M., Zimmerman, J.E., Maycock, M.H., Ta, U.D., You, Y.J., Sundaram, M.V., and Pack, A.I.** (2008). Lethargus is a *Caenorhabditis elegans* sleep-like state. *Nature* 451, 569-572.
- **Rand, J.B., and Russell, R.L.** (1984). Choline acetyltransferase-deficient mutants of the nematode *Caenorhabditis elegans*. *Genetics* 106, 227-248.
- **Randle, P.J., Newsholme, E.A., and Garland, P.B.** (1964). Regulation of glucose uptake by muscle. 8. Effects of fatty acids, ketone bodies and pyruvate, and of alloxan-diabetes and starvation, on the uptake and metabolic fate of glucose in rat heart and diaphragm muscles. *The Biochemical journal* 93, 652-665.
- **Ranganathan, R., Cannon, S.C., and Horvitz, H.R.** (2000). MOD-1 is a serotonin-gated chloride channel that modulates locomotory behaviour in *C. elegans*. *Nature* 408, 470-475.
- **Raposinho, P.D., Pierroz, D.D., Broqua, P., White, R.B., Pedrazzini, T., and Aubert, M.L.** (2001). Chronic administration of neuropeptide Y into the lateral ventricle of C57BL/6J male mice produces an obesity syndrome including hyperphagia, hyperleptinemia, insulin resistance, and hypogonadism. *Molecular and cellular endocrinology* 185, 195-204.
- **Reboul, J., Vaglio, P., Rual, J.F., Lamesch, P., Martinez, M., Armstrong, C.M., Li, S., Jacotot, L., Bertin, N., Janky, R., et al.** (2003). *C. elegans* ORFeome version 1.1: experimental verification of the genome annotation and resource for proteome-scale protein expression. *Nature genetics* 34, 35-41.
- **Reddy, K.C., Andersen, E.C., Kruglyak, L., and Kim, D.H.** (2009). A polymorphism in *npr-1* is a behavioral determinant of pathogen susceptibility in *C. elegans*. *Science* 323, 382-384.
- **Reece-Hoyes, J.S., Shingles, J., Dupuy, D., Grove, C.A., Walhout, A.J., Vidal, M., and Hope, I.A.** (2007). Insight into transcription factor gene duplication from *Caenorhabditis elegans* Promoterome-driven expression patterns. *BMC genomics* 8, 27.
- **Ren, P., Lim, C.S., Johnsen, R., Albert, P.S., Pilgrim, D., and Riddle, D.L.** (1996). Control of *C. elegans* larval development by neuronal expression of a TGF-beta homolog. *Science* 274, 1389-1391.
- **Rex, E., Hapiak, V., Hobson, R., Smith, K., Xiao, H., and Komuniecki, R.** (2005). TYRA-2 (F01E11.5): a *Caenorhabditis elegans* tyramine receptor expressed in the MC and NSM pharyngeal neurons. *Journal of neurochemistry* 94, 181-191.

- **Rex, E., Molitor, S.C., Hapiak, V., Xiao, H., Henderson, M., and Komuniecki, R.** (2004). Tyramine receptor (SER-2) isoforms are involved in the regulation of pharyngeal pumping and foraging behavior in *Caenorhabditis elegans*. *Journal of neurochemistry* *91*, 1104-1115.
- **Richmond, J.E., Weimer, R.M., and Jorgensen, E.M.** (2001). An open form of syntaxin bypasses the requirement for UNC-13 in vesicle priming. *Nature* *412*, 338-341.
- **Ringstad, N., and Horvitz, H.R.** (2008). FMRFamide neuropeptides and acetylcholine synergistically inhibit egg-laying by *C. elegans*. *Nature neuroscience* *11*, 1168-1176.
- **Robin, J.P., Frain, M., Sardet, C., Groscolas, R., and Le Maho, Y.** (1988). Protein and lipid utilization during long-term fasting in emperor penguins. *The American journal of physiology* *254*, R61-68.
- **Roeder, T., Seifert, M., Kahler, C., and Gewecke, M.** (2003). Tyramine and octopamine: antagonistic modulators of behavior and metabolism. *Archives of insect biochemistry and physiology* *54*, 1-13.
- **Rogers, C., Reale, V., Kim, K., Chatwin, H., Li, C., Evans, P., and de Bono, M.** (2003). Inhibition of *Caenorhabditis elegans* social feeding by FMRFamide-related peptide activation of NPR-1. *Nature neuroscience* *6*, 1178-1185.
- **Rogers, C.M., Franks, C.J., Walker, R.J., Burke, J.F., and Holden-Dye, L.** (2001). Regulation of the pharynx of *Caenorhabditis elegans* by 5-HT, octopamine, and FMRFamide-like neuropeptides. *Journal of neurobiology* *49*, 235-244.
- **Rongo, C., Whitfield, C.W., Rodal, A., Kim, S.K., and Kaplan, J.M.** (1998). LIN-10 is a shared component of the polarized protein localization pathways in neurons and epithelia. *Cell* *94*, 751-759.
- **Rose, J.K., Kaun, K.R., Chen, S.H., and Rankin, C.H.** (2003). GLR-1, a non-NMDA glutamate receptor homolog, is critical for long-term memory in *Caenorhabditis elegans*. *The Journal of neuroscience : the official journal of the Society for Neuroscience* *23*, 9595-9599.
- **Rosen, E.D., Walkey, C.J., Puigserver, P., and Spiegelman, B.M.** (2000). Transcriptional regulation of adipogenesis. *Genes & development* *14*, 1293-1307.
- **Rual, J.F., Ceron, J., Koreth, J., Hao, T., Nicot, A.S., Hirozane-Kishikawa, T., Vandenhaute, J., Orkin, S.H., Hill, D.E., van den Heuvel, S., *et al.*** (2004). Toward improving *Caenorhabditis elegans* phenome mapping with an ORFeome-based RNAi library. *Genome Res* *14*, 2162-2168.
- **Sahu, A., Sninsky, C.A., and Kalra, S.P.** (1997). Evidence that hypothalamic neuropeptide Y gene expression and NPY levels in the paraventricular nucleus increase before the onset of hyperphagia in experimental diabetes. *Brain research* *755*, 339-342.
- **Salio, C., Lossi, L., Ferrini, F., and Merighi, A.** (2006). Neuropeptides as synaptic transmitters. *Cell and tissue research* *326*, 583-598.
- **Salkoff, L., Wei, A.D., Baban, B., Butler, A., Fawcett, G., Ferreira, G., and Santi, C.M.** (2005). Potassium channels in *C. elegans*. *WormBook : the online review of C elegans biology*, 1-15.
- **Sanyal, S., Wintle, R.F., Kindt, K.S., Nuttley, W.M., Arvan, R., Fitzmaurice, P., Bigras, E., Merz, D.C., Hebert, T.E., van der Kooy, D., *et al.*** (2004). Dopamine modulates the plasticity of mechanosensory responses in *Caenorhabditis elegans*. *The EMBO journal* *23*, 473-482.
- **Sarter, M., Parikh, V., and Howe, W.M.** (2009). Phasic acetylcholine release and the volume transmission hypothesis: time to move on. *Nature reviews Neuroscience* *10*, 383-390.

Bibliography

- **Satterlee, J.S., Sasakura, H., Kuhara, A., Berkeley, M., Mori, I., and Sengupta, P.** (2001). Specification of thermosensory neuron fate in *C. elegans* requires *ttx-1*, a homolog of *otd/Otx*. *Neuron* 31, 943-956.
- **Sawin, E.R., Ranganathan, R., and Horvitz, H.R.** (2000). *C. elegans* locomotory rate is modulated by the environment through a dopaminergic pathway and by experience through a serotonergic pathway. *Neuron* 26, 619-631.
- **Schackwitz, W.S., Inoue, T., and Thomas, J.H.** (1996). Chemosensory neurons function in parallel to mediate a pheromone response in *C. elegans*. *Neuron* 17, 719-728.
- **Schaffer, J.E., and Lodish, H.F.** (1994). Expression cloning and characterization of a novel adipocyte long chain fatty acid transport protein. *Cell* 79, 427-436.
- **Schofield, P.R., Darlison, M.G., Fujita, N., Burt, D.R., Stephenson, F.A., Rodriguez, H., Rhee, L.M., Ramachandran, J., Reale, V., Glencorse, T.A., et al.** (1987). Sequence and functional expression of the GABA A receptor shows a ligand-gated receptor super-family. *Nature* 328, 221-227.
- **Schroeder, L.K., Kremer, S., Kramer, M.J., Currie, E., Kwan, E., Watts, J.L., Lawrenson, A.L., and Hermann, G.J.** (2007). Function of the *Caenorhabditis elegans* ABC transporter PGP-2 in the biogenesis of a lysosome-related fat storage organelle. *Molecular biology of the cell* 18, 995-1008.
- **Schuske, K., Beg, A.A., and Jorgensen, E.M.** (2004). The GABA nervous system in *C. elegans*. *Trends in neurosciences* 27, 407-414.
- **Schwartz, M.W., Woods, S.C., Porte, D., Jr., Seeley, R.J., and Baskin, D.G.** (2000). Central nervous system control of food intake. *Nature* 404, 661-671.
- **Scroggs, R.S., and Anderson, E.G.** (1989). Serotonin modulates calcium-dependent plateau of action potentials recorded from bull frog A-type sensory neurons which is omega-conotoxin GVIA-sensitive, but dihydropyridine-insensitive. *Brain research* 485, 391-395.
- **Serrano-Saiz, E., Poole, R.J., Felton, T., Zhang, F., De La Cruz, E.D., and Hobert, O.** (2013). Modular control of glutamatergic neuronal identity in *C. elegans* by distinct homeodomain proteins. *Cell* 155, 659-673.
- **Shaye, D.D., and Greenwald, I.** (2011). OrthoList: a compendium of *C. elegans* genes with human orthologs. *PloS one* 6, e20085.
- **Sherwin, R.S., Hendler, R.G., and Felig, P.** (1975). Effect of ketone infusions on amino acid and nitrogen metabolism in man. *The Journal of clinical investigation* 55, 1382-1390.
- **Shtonda, B.B., and Avery, L.** (2006). Dietary choice behavior in *Caenorhabditis elegans*. *The Journal of experimental biology* 209, 89-102.
- **Sieburth, D., Madison, J.M., and Kaplan, J.M.** (2007). PKC-1 regulates secretion of neuropeptides. *Nature neuroscience* 10, 49-57.
- **Simmer, F., Moorman, C., van der Linden, A.M., Kuijk, E., van den Berghe, P.V., Kamath, R.S., Fraser, A.G., Ahringer, J., and Plasterk, R.H.** (2003). Genome-wide RNAi of *C. elegans* using the hypersensitive *rrf-3* strain reveals novel gene functions. *PLoS biology* 1, E12.
- **Snow, J.J., Ou, G., Gunnarson, A.L., Walker, M.R., Zhou, H.M., Brust-Mascher, I., and Scholey, J.M.** (2004). Two anterograde intraflagellar transport motors cooperate to build sensory cilia on *C. elegans* neurons. *Nature cell biology* 6, 1109-1113.
- **Song, B.M., and Avery, L.** (2012). Serotonin activates overall feeding by activating two separate neural pathways in *Caenorhabditis elegans*. *The Journal of neuroscience : the official journal of the Society for Neuroscience* 32, 1920-1931.

- **Song, B.M., Faumont, S., Lockery, S., and Avery, L.** (2013). Recognition of familiar food activates feeding via an endocrine serotonin signal in *Caenorhabditis elegans*. *eLife* 2, e00329.
- **Soukas, A.A., Kane, E.A., Carr, C.E., Melo, J.A., and Ruvkun, G.** (2009). Rictor/TORC2 regulates fat metabolism, feeding, growth, and life span in *Caenorhabditis elegans*. *Genes & development* 23, 496-511.
- **Speese, S., Petrie, M., Schuske, K., Ailion, M., Ann, K., Iwasaki, K., Jorgensen, E.M., and Martin, T.F.** (2007). UNC-31 (CAPS) is required for dense-core vesicle but not synaptic vesicle exocytosis in *Caenorhabditis elegans*. *The Journal of neuroscience : the official journal of the Society for Neuroscience* 27, 6150-6162.
- **Speidel, D., Bruederle, C.E., Enk, C., Voets, T., Varoqueaux, F., Reim, K., Becherer, U., Fornai, F., Ruggieri, S., Holighaus, Y., et al.** (2005). CAPS1 Regulates Catecholamine Loading of Large Dense-Core Vesicles. *Neuron* 46, 75-88.
- **Srinivasan, S.** (2014). Regulation of Body Fat in *Caenorhabditis elegans*. *Annual review of physiology*.
- **Srinivasan, S., Sadegh, L., Elle, I.C., Christensen, A.G., Faergeman, N.J., and Ashrafi, K.** (2008). Serotonin regulates *C. elegans* fat and feeding through independent molecular mechanisms. *Cell metabolism* 7, 533-544.
- **Stanley, B.G., Anderson, K.C., Grayson, M.H., and Leibowitz, S.F.** (1989). Repeated hypothalamic stimulation with neuropeptide Y increases daily carbohydrate and fat intake and body weight gain in female rats. *Physiology & behavior* 46, 173-177.
- **Stanley, B.G., and Leibowitz, S.F.** (1984). Neuropeptide Y: stimulation of feeding and drinking by injection into the paraventricular nucleus. *Life sciences* 35, 2635-2642.
- **Starich, T.A., Herman, R.K., Kari, C.K., Yeh, W.H., Schackwitz, W.S., Schuyler, M.W., Collet, J., Thomas, J.H., and Riddle, D.L.** (1995). Mutations affecting the chemosensory neurons of *Caenorhabditis elegans*. *Genetics* 139, 171-188.
- **Starich, T.A., Lee, R.Y., Panzarella, C., Avery, L., and Shaw, J.E.** (1996). *eat-5* and *unc-7* represent a multigene family in *Caenorhabditis elegans* involved in cell-cell coupling. *The Journal of cell biology* 134, 537-548.
- **Starich, T.A., Miller, A., Nguyen, R.L., Hall, D.H., and Shaw, J.E.** (2003). The *caenorhabditis elegans* innexin INX-3 is localized to gap junctions and is essential for embryonic development. *Developmental Biology* 256, 403-417.
- **Starich, T.A., Xu, J., Skerrett, I.M., Nicholson, B.J., and Shaw, J.E.** (2009). Interactions between innexins UNC-7 and UNC-9 mediate electrical synapse specificity in the *Caenorhabditis elegans* locomotory nervous system. *Neural development* 4, 16.
- **Steger, K.A., and Avery, L.** (2004). The GAR-3 muscarinic receptor cooperates with calcium signals to regulate muscle contraction in the *Caenorhabditis elegans* pharynx. *Genetics* 167, 633-643.
- **Sterling, P., and Matthews, G.** (2005). Structure and function of ribbon synapses. *Trends in neurosciences* 28, 20-29.
- **Sudhof, T.C.** (2013). A molecular machine for neurotransmitter release: synaptotagmin and beyond. *Nature medicine* 19, 1227-1231.
- **Sugiura, M., Fuke, S., Suo, S., Sasagawa, N., Van Tol, H.H., and Ishiura, S.** (2005). Characterization of a novel D2-like dopamine receptor with a truncated splice variant and a D1-like dopamine receptor unique to invertebrates from *Caenorhabditis elegans*. *Journal of neurochemistry* 94, 1146-1157.

Bibliography

- **Sulston, J., Dew, M., and Brenner, S.** (1975). Dopaminergic neurons in the nematode *Caenorhabditis elegans*. *The Journal of comparative neurology* *163*, 215-226.
- **Sulston, J.E., Albertson, D.G., and Thomson, J.N.** (1980). The *Caenorhabditis elegans* male: postembryonic development of nongonadal structures. *Dev Biol* *78*, 542-576.
- **Sulston, J.E., and Horvitz, H.R.** (1977). Post-embryonic cell lineages of the nematode, *Caenorhabditis elegans*. *Dev Biol* *56*, 110-156.
- **Sulston, J.E., Schierenberg, E., White, J.G., and Thomson, J.N.** (1983). The embryonic cell lineage of the nematode *Caenorhabditis elegans*. *Dev Biol* *100*, 64-119.
- **Suo, S., Kimura, Y., and Van Tol, H.H.** (2006). Starvation induces cAMP response element-binding protein-dependent gene expression through octopamine-Gq signaling in *Caenorhabditis elegans*. *The Journal of neuroscience : the official journal of the Society for Neuroscience* *26*, 10082-10090.
- **Suzuki, H., Thiele, T.R., Faumont, S., Ezcurra, M., Lockery, S.R., and Schafer, W.R.** (2008). Functional asymmetry in *Caenorhabditis elegans* taste neurons and its computational role in chemotaxis. *Nature* *454*, 114-117.
- **Svoboda, J.A., Kaplanis, J.N., Robbins, W.E., and Thompson, M.J.** (1975). Recent developments in insect steroid metabolism. *Annual review of entomology* *20*, 205-220.
- **Sze, J.Y., Victor, M., Loer, C., Shi, Y., and Ruvkun, G.** (2000). Food and metabolic signalling defects in a *Caenorhabditis elegans* serotonin-synthesis mutant. *Nature* *403*, 560-564.
- **Szekeress, P.G.** (2002). Functional assays for identifying ligands at orphan G protein-coupled receptors. *Receptors & channels* *8*, 297-308.
- **Tabish, M., Siddiqui, Z.K., Nishikawa, K., and Siddiqui, S.S.** (1995). Exclusive expression of *C. elegans osm-3* kinesin gene in chemosensory neurons open to the external environment. *Journal of molecular biology* *247*, 377-389.
- **Tan, K.T., Luo, S.C., Ho, W.Z., and Lee, Y.H.** (2011). Insulin/IGF-1 receptor signaling enhances biosynthetic activity and fat mobilization in the initial phase of starvation in adult male *C. elegans*. *Cell metabolism* *14*, 390-402.
- **Tappy, L., and Le, K.A.** (2010). Metabolic effects of fructose and the worldwide increase in obesity. *Physiological reviews* *90*, 23-46.
- **Thacker, C., Peters, K., Srayko, M., and Rose, A.M.** (1995). The *bli-4* locus of *Caenorhabditis elegans* encodes structurally distinct kex2/subtilisin-like endoproteases essential for early development and adult morphology. *Genes & development* *9*, 956-971.
- **Thacker, C., and Rose, A.M.** (2000). A look at the *Caenorhabditis elegans* Kex2/Subtilisin-like proprotein convertase family. *BioEssays : news and reviews in molecular, cellular and developmental biology* *22*, 545-553.
- **Thomas, J.H.** (1990). Genetic analysis of defecation in *Caenorhabditis elegans*. *Genetics* *124*, 855-872.
- **Thouzeau, C., Robin, J.P., Le Maho, Y., and Handrich, Y.** (1999). Body reserve dynamics and energetics of barn owls during fasting in the cold. *J Comp Physiol B* *169*, 612-620.
- **Tian, L., Hires, S.A., Mao, T., Huber, D., Chiappe, M.E., Chalasani, S.H., Petreanu, L., Akerboom, J., McKinney, S.A., Schreiter, E.R., et al.** (2009). Imaging neural activity in worms, flies and mice with improved GCaMP calcium indicators. *Nature methods* *6*, 875-881.

- **Timmons, L., and Fire, A.** (1998). Specific interference by ingested dsRNA. *Nature* 395, 854.
- **Trent, C., Tsuing, N., and Horvitz, H.R.** (1983). Egg-laying defective mutants of the nematode *Caenorhabditis elegans*. *Genetics* 104, 619-647.
- **Tsalik, E.L., and Hobert, O.** (2003). Functional mapping of neurons that control locomotory behavior in *Caenorhabditis elegans*. *Journal of neurobiology* 56, 178-197.
- **Tsalik, E.L., Niacaris, T., Wenick, A.S., Pau, K., Avery, L., and Hobert, O.** (2003). LIM homeobox gene-dependent expression of biogenic amine receptors in restricted regions of the *C. elegans* nervous system. *Developmental Biology* 263, 81-102.
- **van Beek, J.D.** (2007). matNMR: a flexible toolbox for processing, analyzing and visualizing magnetic resonance data in Matlab. *Journal of magnetic resonance* 187, 19-26.
- **Van Gilst, M.R., Hadjivassiliou, H., Jolly, A., and Yamamoto, K.R.** (2005). Nuclear hormone receptor NHR-49 controls fat consumption and fatty acid composition in *C. elegans*. *PLoS biology* 3, e53.
- **Varshney, L.R., Chen, B.L., Paniagua, E., Hall, D.H., and Chklovskii, D.B.** (2011). Structural properties of the *Caenorhabditis elegans* neuronal network. *PLoS computational biology* 7, e1001066.
- **Vassilatis, D.K., Arena, J.P., Plasterk, R.H., Wilkinson, H.A., Schaeffer, J.M., Cully, D.F., and Van der Ploeg, L.H.** (1997). Genetic and biochemical evidence for a novel avermectin-sensitive chloride channel in *Caenorhabditis elegans*. Isolation and characterization. *The Journal of biological chemistry* 272, 33167-33174.
- **Volkman, J.K.** (2003). Sterols in microorganisms. *Applied microbiology and biotechnology* 60, 495-506.
- **von Gersdorff, H.** (2001). Synaptic ribbons: versatile signal transducers. *Neuron* 29, 7-10.
- **Wadsworth, W.G., and Riddle, D.L.** (1989). Developmental regulation of energy metabolism in *Caenorhabditis elegans*. *Dev Biol* 132, 167-173.
- **Wahlby, C., Conery, A.L., Bray, M.A., Kamentsky, L., Larkins-Ford, J., Sokolnicki, K.L., Veneskey, M., Michaels, K., Carpenter, A.E., and O'Rourke, E.J.** (2014). High- and low-throughput scoring of fat mass and body fat distribution in *C. elegans*. *Methods* 68, 492-499.
- **Wakabayashi, T., Kitagawa, I., and Shingai, R.** (2004). Neurons regulating the duration of forward locomotion in *Caenorhabditis elegans*. *Neuroscience research* 50, 103-111.
- **Walker, D.S., Gower, N.J., Ly, S., Bradley, G.L., and Baylis, H.A.** (2002). Regulated disruption of inositol 1,4,5-trisphosphate signaling in *Caenorhabditis elegans* reveals new functions in feeding and embryogenesis. *Molecular biology of the cell* 13, 1329-1337.
- **Wang, M.C., O'Rourke, E.J., and Ruvkun, G.** (2008). Fat metabolism links germline stem cells and longevity in *C. elegans*. *Science* 322, 957-960.
- **Wang, T., Hung, C.C., and Randall, D.J.** (2006). The comparative physiology of food deprivation: from feast to famine. *Annual review of physiology* 68, 223-251.
- **Ward, S.** (1973). Chemotaxis by the nematode *Caenorhabditis elegans*: identification of attractants and analysis of the response by use of mutants. *Proceedings of the National Academy of Sciences of the United States of America* 70, 817-821.

Bibliography

- **Ward, S., Thomson, N., White, J.G., and Brenner, S.** (1975). Electron microscopical reconstruction of the anterior sensory anatomy of the nematode *Caenorhabditis elegans*.? The Journal of comparative neurology 160, 313-337.
- **Watts, J.L., and Browse, J.** (2002). Genetic dissection of polyunsaturated fatty acid synthesis in *Caenorhabditis elegans*. Proceedings of the National Academy of Sciences of the United States of America 99, 5854-5859.
- **Watts, J.L., and Browse, J.** (2006). Dietary manipulation implicates lipid signaling in the regulation of germ cell maintenance in *C. elegans*. Dev Biol 292, 381-392.
- **Wenick, A.S., and Hobert, O.** (2004). Genomic cis-regulatory architecture and trans-acting regulators of a single interneuron-specific gene battery in *C. elegans*. Developmental cell 6, 757-770.
- **Werner, K.M., Perez, L.J., Ghosh, R., Semmelhack, M.F., and Bassler, B.L.** (2014). *Caenorhabditis elegans* Recognizes a Bacterial Quorum-Sensing Signal Molecule Through the AWC^{ON} Neuron. The Journal of biological chemistry.
- **Wes, P.D., and Bargmann, C.I.** (2001). *C. elegans* odour discrimination requires asymmetric diversity in olfactory neurons. Nature 410, 698-701.
- **White, J.G., Southgate, E., Thomson, J.N., and Brenner, S.** (1986). The structure of the nervous system of the nematode *Caenorhabditis elegans*. Philosophical transactions of the Royal Society of London Series B, Biological sciences 314, 1-340.
- **Wicks, S.R., de Vries, C.J., van Luenen, H.G., and Plasterk, R.H.** (2000). CHE-3, a cytosolic dynein heavy chain, is required for sensory cilia structure and function in *Caenorhabditis elegans*. Dev Biol 221, 295-307.
- **Wise, R.A.** (2006). Role of brain dopamine in food reward and reinforcement. Philosophical transactions of the Royal Society of London Series B, Biological sciences 361, 1149-1158.
- **Wolins, N.E., Brasaemle, D.L., and Bickel, P.E.** (2006). A proposed model of fat packaging by exchangeable lipid droplet proteins. FEBS letters 580, 5484-5491.
- **Wood, W.B.** (1988). Introduction to *C. elegans* Biology.
- **Wragg, R.T., Hapiak, V., Miller, S.B., Harris, G.P., Gray, J., Komuniecki, P.R., and Komuniecki, R.W.** (2007). Tyramine and octopamine independently inhibit serotonin-stimulated aversive behaviors in *Caenorhabditis elegans* through two novel amine receptors. The Journal of neuroscience : the official journal of the Society for Neuroscience 27, 13402-13412.
- **Wu, Q., and Palmiter, R.D.** (2011). GABAergic signaling by AgRP neurons prevents anorexia via a melanocortin-independent mechanism. European Journal of Pharmacology 660, 21-27.
- **Wu, Z., and Wang, S.** (2013). Role of kruppel-like transcription factors in adipogenesis. Dev Biol 373, 235-243.
- **Xu, N., Zhang, S.O., Cole, R.A., McKinney, S.A., Guo, F., Haas, J.T., Bobba, S., Farese, R.V., Jr., and Mak, H.Y.** (2012). The FATP1-DGAT2 complex facilitates lipid droplet expansion at the ER-lipid droplet interface. The Journal of cell biology 198, 895-911.
- **Yang, F., Vought, B.W., Satterlee, J.S., Walker, A.K., Jim Sun, Z.Y., Watts, J.L., DeBeaumont, R., Saito, R.M., Hyberts, S.G., Yang, S., et al.** (2006). An ARC/Mediator subunit required for SREBP control of cholesterol and lipid homeostasis. Nature 442, 700-704.
- **Yeh, E., Ng, S., Zhang, M., Bouhours, M., Wang, Y., Wang, M., Hung, W., Aoyagi, K., Melnik-Martinez, K., Li, M., et al.** (2008). A putative cation channel, NCA-1, and a novel protein, UNC-80, transmit neuronal activity in *C. elegans*. PLoS biology 6, e55.

- **Yen, K., Le, T.T., Bansal, A., Narasimhan, S.D., Cheng, J.X., and Tissenbaum, H.A.** (2010). A comparative study of fat storage quantitation in nematode *Caenorhabditis elegans* using label and label-free methods. *PLoS one* 5.
- **You, Y.J., Kim, J., Cobb, M., and Avery, L.** (2006). Starvation activates MAP kinase through the muscarinic acetylcholine pathway in *Caenorhabditis elegans* pharynx. *Cell metabolism* 3, 237-245.
- **You, Y.J., Kim, J., Raizen, D.M., and Avery, L.** (2008). Insulin, cGMP, and TGF-beta signals regulate food intake and quiescence in *C. elegans*: a model for satiety. *Cell metabolism* 7, 249-257.
- **Young, E.** (2012). Gut instincts: The secrets of your second brain. *New Scientist* 216, 38-42.
- **Zhang, J., Yang, C., Brey, C., Rodriguez, M., Oksov, Y., Gaugler, R., Dickstein, E., Huang, C.H., and Hashmi, S.** (2009). Mutation in *Caenorhabditis elegans* Kruppel-like factor, KLF-3 results in fat accumulation and alters fatty acid composition. *Experimental cell research* 315, 2568-2580.
- **Zhang, P., Na, H., Liu, Z., Zhang, S., Xue, P., Chen, Y., Pu, J., Peng, G., Huang, X., Yang, F., et al.** (2012). Proteomic study and marker protein identification of *Caenorhabditis elegans* lipid droplets. *Molecular & cellular proteomics : MCP* 11, 317-328.
- **Zhang, S.O., Box, A.C., Xu, N., Le Men, J., Yu, J., Guo, F., Trimble, R., and Mak, H.Y.** (2010a). Genetic and dietary regulation of lipid droplet expansion in *Caenorhabditis elegans*. *Proceedings of the National Academy of Sciences of the United States of America* 107, 4640-4645.
- **Zhang, S.O., Trimble, R., Guo, F., and Mak, H.Y.** (2010b). Lipid droplets as ubiquitous fat storage organelles in *C. elegans*. *BMC cell biology* 11, 96.
- **Zheng, H., Patterson, L.M., and Berthoud, H.R.** (2007). Orexin signaling in the ventral tegmental area is required for high-fat appetite induced by opioid stimulation of the nucleus accumbens. *The Journal of neuroscience : the official journal of the Society for Neuroscience* 27, 11075-11082.
- **Zhou, A., Martin, S., Lipkind, G., LaMendola, J., and Steiner, D.F.** (1998). Regulatory roles of the P domain of the subtilisin-like prohormone convertases. *The Journal of biological chemistry* 273, 11107-11114.
- **Zinser, E., Paltauf, F., and Daum, G.** (1993). Sterol composition of yeast organelle membranes and subcellular distribution of enzymes involved in sterol metabolism. *Journal of bacteriology* 175, 2853-2858.